STATUS OF THESIS

Title of thesis | Physical Properties and Solubility of CO_2 in Bis(2-Hydroxyethyl) ammonium Acetate ([bheaa]), 1-Butyl-3-Methylimidazolium Tetraflouroborate ([bmim][BF_4]) and Monoethanolamine (MEA)Based Hybrid Solvents

I MALYANAH BINTI MOHD TAIB

hereby allow my thesis to be placed at the Information Resource Center (IRC) of Universiti Teknologi PETRONAS (UTP) with the following conditions:

1. The thesis becomes the property of UTP
2. The IRC of UTP may make copies of the thesis for academic purposes only.
3. This thesis is classified as

☐ Confidential

☐ Non-confidential

If the thesis is confidential, please state the reason:

The contents of the thesis will remain confidential for _____ years.

Remarks on disclosure:

Signature of Author

Permanent address:

No. 1, Jalan Delima 2/8, Taman Delima, 81100 Johor Bahru, Johor

Date: 6 APRIL 2012

Endorsed by

Prof. Dr. T. Murugesan
Chemical Engineering Department
Universiti Teknologi PETRONAS

Signature of Supervisor

Name of Supervisor

Prof. Dr. Thanabalan Murugesan

Date: 06/04/2012

UNIVERSITI TEKNOLOGI PETRONAS

PHYSICAL PROPERTIES AND SOLUBILITY OF CO_2 IN BIS(2-HYDROXYETHYL)AMMONIUM ACETATE ([BHEAA]), 1-BUTYL-3-METHYLIMIDAZOLIUM TETRAFLOUROBORATE ([BMIM][BF_4]) AND MONOETHANOLAMINE (MEA) BASED HYBRID SOLVENTS

by

MALYANAH BINTI MOHD TAIB

The undersigned certify that they have read, and recommend to the Postgraduate Studies Programme for acceptance this thesis for the fulfillment of the requirements for the degree stated.

Signature: _____

Main Supervisor: Prof. Dr. Thanabalan Murugesan

Prof. Dr. T. Murugesan
Chemical Engineering Department
Universiti Teknologi PETRONAS

Signature: _____

Head of Department: Assoc. Prof. Dr. Mohd Azmi Bustam

Assoc. Prof. Dr. Mohamed Azmi Bustam @ Khalil
Head, Chemical Engineering Department
Universiti Teknologi PETRONAS

Date: 6/4/2012

PHYSICAL PROPERTIES AND SOLUBILITY OF CO_2 IN BIS(2-HYDROXYETHYL)AMMONIUM ACETATE ([BHEAA]), 1-BUTYL-3-METHYLIMIDAZOLIUM TETRAFLOUROBORATE ([BMIM][BF_4]) AND MONOETHANOLAMINE (MEA) BASED HYBRID SOLVENTS

by

MALYANAH BINTI MOHD TAIB

A Thesis

Submitted to the Postgraduate Studies Programme

as a Requirement for the Degree of

MASTER OF SCIENCE

CHEMICAL ENGINEERING

UNIVERSITI TEKNOLOGI PETRONAS

BANDAR SERI ISKANDAR,

PERAK

APRIL 2011

DECLARATION OF THESIS

Title of thesis | Physical Properties and Solubility of CO_2 in Bis(2-Hydroxyethyl) ammonium Acetate ([bheaa]), 1-Butyl-3-Methylimidazolium Tetraflouroborate ([bmim][BF_4]) and Monoethanolamine (MEA)Based Hybrid Solvents

I MALYANAH BINTI MOHD TAIB

hereby declare that the thesis is based on my original work except for quotations and citations which have been duly acknowledged. I also declare that it has not been previously or concurrently submitted for any other degree at UTP or other institutions.

Witnessed by

Prof. Dr. T. Murugesan
Chemical Engineering Department
Universiti Teknologi PETRONAS

Signature of Author

Signature of Supervisor

Permanent address:

No. 1, Jalan Delima 2/8, Taman Delima, 81100 Johor Bahru, Johor

Name of Supervisor

Prof. Dr. Thanabalan Murugesan

Date: 6 APRIL 2012

Date: 06/04/2012

To my beloved parents for their unconditional love and support and to my husband who never failed to always be by my side

ACKNOWLEDGEMENTS

It would not have been possible to complete this research project without the help and support of the people around me. It is a pleasure to convey my gratitude to all of them in my humble acknowledgement.

Above all, I would like to thank my parents for their never ending love and for always believe in me and support throughout every decisions that I made. Thank you also for the everyday call that always makes my spirit boost up. I would also like to thank my fiancé who never failed to be by my side during hard times and never failed to encourage me to pursue my dream.

This thesis would not have been possible without the help, support and patience of my supervisor, Prof. Dr. Thanabalan Murugesan, not to mention his advice and guidance as well as his strategic plan that makes this research project ends on time. Thank you also for all his time and effort in making this project a success.

In my daily work, I have been blessed with a kind and friendly group of lab mates who makes the lab a fun and enjoyable place to work. Thank to Sabtanti Harimurti, Annisa Ur Rahmah, and Surya Abadi Ginting, for their jokes and laughter that makes all the hard times seems easy.

My housemates, Wani, Sara, Atilia, and Didi who never fails to make me feels like home and for the time we spend together. I feel blessed to get to know all of you. Also many thanks to Chuya, Ita and Morkge for always be there when I need someone to talk to.

Last but not least, thank you to the Postgraduate Studies Programme, the Chemical Engineering Department and all staffs of Universiti Teknologi PETRONAS for the financial support and all the helps that you gave me.

For any errors or inadequacies in this work, the responsibility is entirely my own.

ABSTRACT

An industrially attractive solvent to capture CO_2, has been developed by incorporating the desirable properties of ionic liquids(ILs) as well as amines through mixing of the targeted ILs with amine to form hybrid solvents for the effective capture of CO_2. In the present work, ILs of two different families namely, bis(2-hydroxyethyl)ammonium acetate ([bheaa]) and 1-butyl-3-methylimidazolium tetraflouroborate ([bmim][BF_4]) have been chosen to form a new binary/ ternary solvents in combination with monoethanolamine (MEA) and water for the solubility of CO_2. In order to establish the physical properties for the new binary [(bheaa + water); (bheaa+ MEA); (bmimBF_4+water); BmimBF_4+MEA) / ternary [(bheaa + MEA + Water) (bmimBF_4 + MEA + Water)] solvents, density, viscosity and refractive index measurements have been made at T = (293.15 to 353.15) K for the whole composition range. Based on the measured values the effects of temperature and concentration of individual spicies have been discussed in detail and suitable correlations have been proposed.

The excess properties, namely, the excess molar volume V^E, viscosity deviation $\Delta\eta$, as well as the refractive index deviation Δn_D, have been deduced from the measured density, viscosity and refractive index values respectively for all the binary and ternary systems studied in the research. The Redlich Kister equation was used to correlate the estimated excess properties for the binary systems while the Cibulka equation was used to correlate the excess properties for the ternary systems.

The CO_2 uptake capabilities of the present developed hybrid binary ([bheaa] + water; [bheaa] + MEA; [bmimBF_4] + water; [bmimBF_4]+MEA) / ternary ([bheaa] + MEA + Water, [bmimBF_4] + MEA + Water) solvents, have been made by using the SOLTEQ High Pressure Gas Solubility Cell (Model: BP-22) and the results are presented and the effect of concentration, pressure and temperature on the CO_2 uptake have been

discussed in detail. The present results indicated that the aqueous solution of [bheaa] + MEA have been found to have better CO_2 loading than the aqueous solution of [bmim][BF_4] + MEA. The combination of these chosen ILs with selective amine solution have proved to have the characteristics for efficent CO_2 capture and seems to be a promising alternative for the aqueous amine solution/absorbents which are currently being used for CO_2 absorption.

ABSTRAK

Projek penyelidikan ini telah menggabungkan sifat- sifat tertentu cecair berion and amina dengan mencampurkan kedua- dua cecair terpilih bagi menghasilkan pelarut hibrid untuk menyerap karbon dioksida (CO_2) dengan efektif. Pelarut yg dihasilkan ini dijangka akan menarik minat industi- industri berkaitan penyerapan CO_2. Dalam penyelidiakan ini, cecair berion daripada dua famili yang berlainan iaitu, imidazolium dan hidrosil ammonia telah dipilih untuk menghasilkan pelarut binari baru hasil penggabungan monoethanolamine (MEA) dan air untuk pehyerapan CO_2. Untuk mengdapatkan sifat- sifat fizikal bagi pelarut binari/ ternari, ketumpatan, kelikatan dan ukuran indeks biasan telah dibuat pada suhu (293.15 hingga 353.15) K bagi julat kesuluruhan komposisi. Berdasarkan nilai- nilai yang diperolehi , kesan suhu dan kepekatan spesis individu telah dibincangkan secara mendalam dan korelasi yang sesuai telah dicadangkan.

Sifat- sifat berlebihan seperti isipadu molar berlebihan, sisihan kelikatan dan sisihan indeks biasan telah disimpulkan daripada ukuran ketumpatan, kelikatan dan indeks biasan pelarut binari dan ternari yang telah diukur. Persamaan Redlick Kister telag digunakan untuk korelasi dan anggaran sifat- sifat lebihan bagi sistem binari manakala persamaan Cibulka pula digunakan untuk korelasi dan anggaran sifat- sifat lebihan bagi sistem ternari.

Keupayaan penyerapan CO_2 oleh sistem- sistem binari ([bheaa] + water; [bheaa] + MEA; [bmimBF_4] + water; [bmimBF_4]+MEA) dan sistem- sistem ternari ([bheaa] + MEA + Water, [bmimBF_4] + MEA + Water) telah dilakukan dengan menggunakan sel pelarutan bertekanan tinggi SOLTEQ (Model: BP-22). Keputusan dan kesan suhu, tekanan dan kepekatan terhadap penyerapan CO_2 telah dibincangkan secara mendalam. Keputusan kajian ini menunjukkan bahawa larutan akues [bheaa] + MEA didapati mempunyai nilai penyerapan CO_2 yang lebih tinggi daripada larutan akues

[bmimBF_4] + MEA. Kombinasi larutan berion dan amina yang telah dipilih terbukti mempunyai sifat- sifat sebagai penyerap CO_2 yang cekap dan boleh menjadi alternatif yang meyakinkan bagi menggantikan larutan akues amina yang digunakan dalam penyerapan CO_2 pada masa kini.

LIST OF TABLES

LIST OF FIGURES

LIST OF ABBREVIATIONS

[Bheaa]	bis(2-hydroxyethyl)ammonium acetate
[Bmim][BF_4]	1-butyl-3-methylimidazolium tetraflouroborate
[Bmim][PF_6]	1-butyl-3-methylimidazolium hexaflourophosphate
[Emim][BF_4]	1-ethyl-3-methylimidazolium tetraflouroborate
[Emim][PF_6]	1-ethyl-3-methylimidazolium hexaflourophosphate
[Emim][Tf_2N]	1-ethyl-3-methylimidazolium bis(triflouromethylsulfonyl)imide
[Hmim] [BF_4]	1-hexyl-3-methylimidazolium tetraflouroborate
[Hmim][Tf_2N]	1-hexyl-3-methylimidazolium bis(triflouromethylsulfonyl)imide
MEA	monoethanolamine
DEA	Diethanolamine
MDEA	N-methyldiethanolamine

CHAPTER 1

INTRODUCTION

1.0 Overview

This chapter deals with the brief discussion on the background and the need for the present research, which includes the origin for CO_2 and its impact on atmosphere, necessity for CO_2 removal and current techniques used for the same. The merits and demerits of the solvents (alkanolamine, ionic liquid etc.,) currently being used for this purpose is elaborated. Based on the details, the objectives for the present research is derived (section 1.3) and the detailed scope (section 1.4) is also presented.

1.1 Research Background

1.1.1 Overview on Natural Gas

Natural gas is used as the raw material for many chemical and petrochemical processes, despite being a major source for power plants to generate electricity and transportation. Natural gas consists of methane (70 to 90%) as major component with other hydrocarbon as well as non-hydrocarbon gases. Natural gas also consists of considerable amounts of carbon dioxide (CO_2), sulfur dioxide (SO_2), hydrogen sulphide (H_2S) and nitrogen oxides (NO_x), etc., along with less quantities of carbon monoxide, and other reactive hydrocarbons. Among all types of fossil fuel, natural

gas can be considered as the cleanest, as evidenced from Environmental Protection Agency's report (Table 1.1).

Table 1.1 Fossil Fuel Emission Levels Pounds per Billion Btu of Energy Input

Pollutant	**Natural Gas**	**Oil**	**Coal**
Carbon Dioxide	117,000	164,000	208,000
Carbon Monoxide	40	33	208
Nitrogen Oxides	92	448	457
Sulfur Dioxide	1	1,122	2,591
Particulates	7	84	2,744
Mercury	0.000	0.007	0.016

Source: EIA - Natural Gas Issues and Trends 1998

The wide application across all sectors and the history of being the cleanest energy source makes the natural gas to play an important role in meeting the global energy demand. In general, there are two primary source that determine the demand for natural gas, namely the short term demand and the long term demand. The short term demand includes the weather, fuel switching as well as the current economy while the long term demand includes the residential, commercial, industrial, electric generation and transportation sector demands. While short term factors can significantly affect the demand for natural gas, it is the long term demand factors that reflect the basic trends for natural gas use for the future. Statistics show that the production of natural gas have been increasing gradually over the years to meet the

global demand for natural gas in various sectors. Figure 1.1 shows the production of natural gas in major countries namely, Middle East, Asia and Oceania.

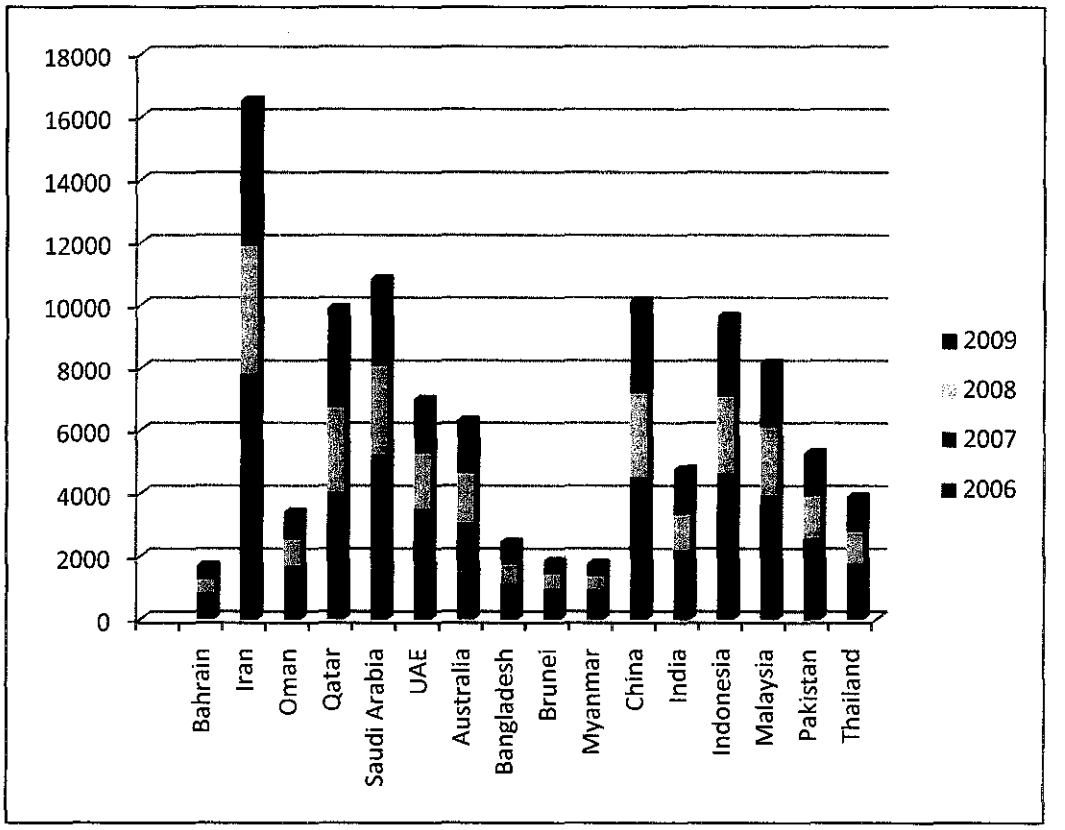

Figure1.1 Dry Natural Gas Production (Billion Cubit Feet) from 2006 to 2009 in Middleeast and Asia & Oceania

An estimate during January 2008 showed that the natural gas reserves in Malaysia were at 88.0 trillion standard cubic feet (tscf) or 14.67 billion barrels of oil equivalent, approximately three times the size of crude oil reserves (5.46 billion barrel). The distribution of gas reserves in Malaysia is shown in Figure 1.2. At the current rate of production, Malaysia's gas reserves are expected to last for another 36 years (approximately) and currently, Malaysia in ranked 14th in the world.

Despite being the cleanest energy source, the production and use of natural gas does contribute substantially to global CO_2 emissions, and this contribution is projected to grow. The presence of CO_2 in natural gas reduces the fuel value of natural gas, whereas the presence of H_2S increases the toxicity. These type of

contaminants are considered as important for deciding the quality of natural gas produced especially for priceing. The presence of these acid gases (CO_2 and H_2S) not only makes the natural gas sour, but also leads to corrosion problem in the pipelines and equipments used for natural gas processing. Since CO_2 is the main product during the combustion of natural gas, it can cause serious environment concern especially the greenhouse effect that can contribute to global warming. Global climate change has a long time issue with implications in different areas, such as, climate, environment, economy, society, politics, technology, institution, etc.

Figure 1.3 shows the distribution of CO_2 emission from natural gas combustion in 2009, in Middle East, Asia and Oceania. With all the concerns and problems caused by fossil fuels, it must undergo effective treatment processes to remove all the unwanted and harmful materials that can cause environment concerns. A global movement towards the generation of renewable energy is under way to help meet the increased energy needs. Research related to the development of an efficient as well as cost effective solvent is of high commercial value since CO_2 removal is energy demanding.

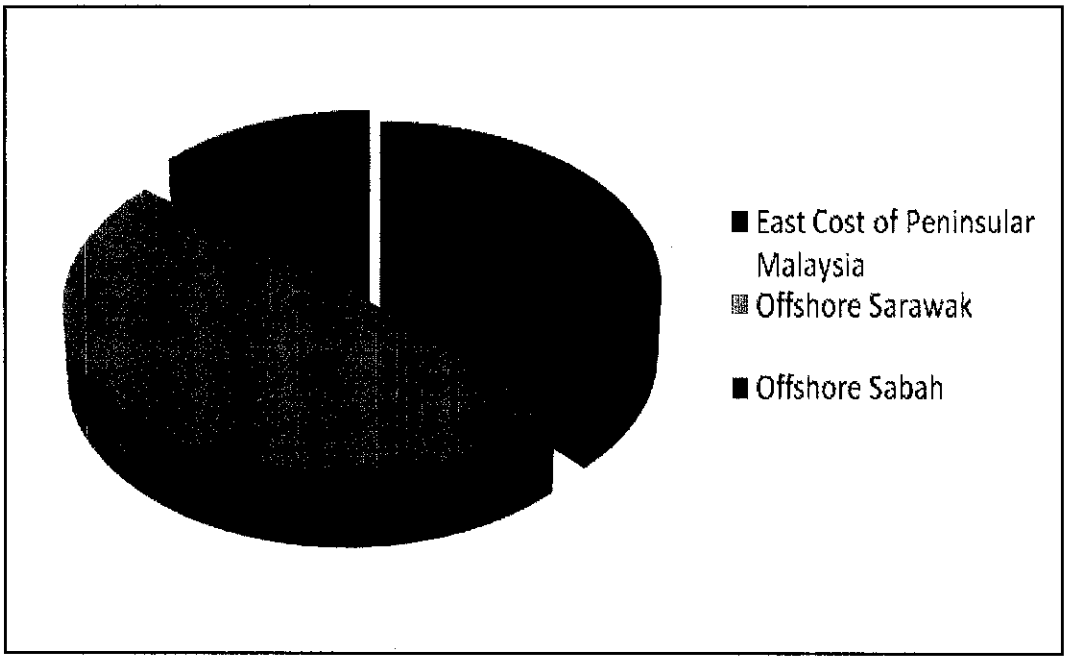

Figure 1.2. Malaysia natural gas reserves. (Source: www.gasmalaysia.com).

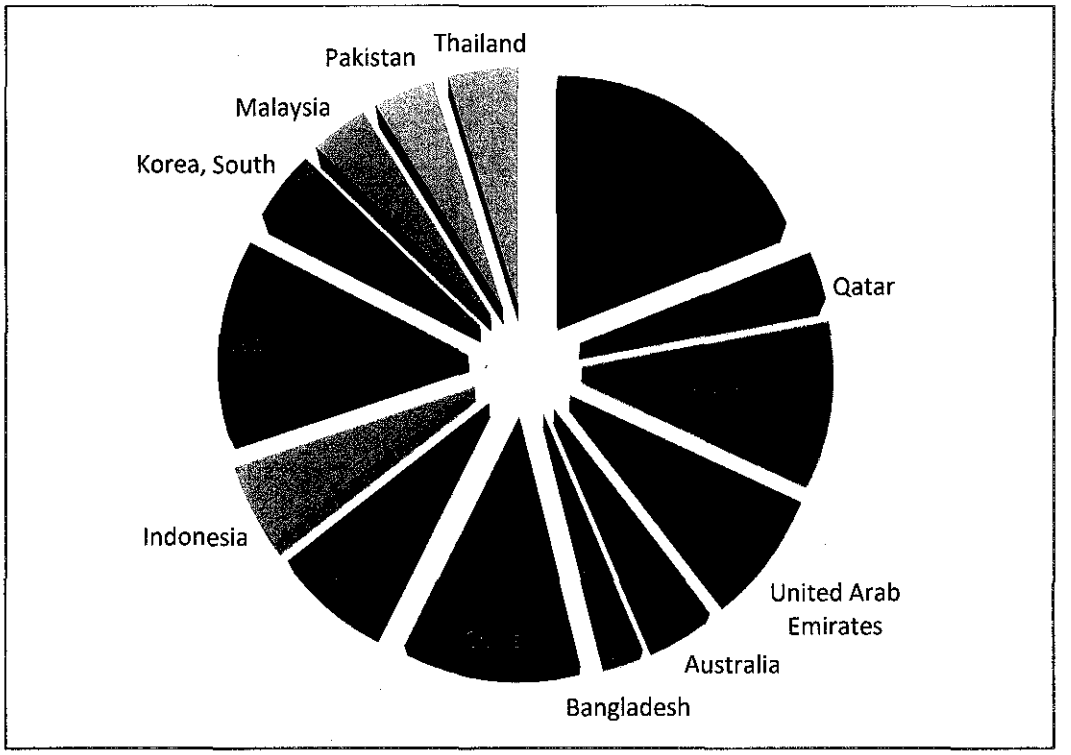

Figure 1.3. CO_2 Emissions from the Consumption and Flaring of Natural Gas (Million Metric Tons) in 2009, in Middle East and Asia & Oceania. (Source: EIA, International Energy Outlook 2011).

1.1.2 CO_2 Removal from Natural Gas

Carbon dioxide (CO_2) is a chemical compound composed of two oxygen atoms covalently bonded to a single carbon atom. It is an inorganic compound, a colorless gas with a faint, sharp odour and a sour taste when dissolved in water. It is the important greenhouse gas produced by human activities, primarily through the combustion of fossil fuels. It is also produced from gas wells, during fermentation process and also as by-product of many chemical processes.

CO_2 when combined with water forms carbonic acid, which causes corrosion problems in pipelines during transmission and also in processing equipments. The presence of CO_2 will lower the heating value of the natural gas and when the concentrations exceed 2% to 3%, its market value reduces. As discussed earlier, burning of natural gas release CO_2 into the atmosphere, which leads to the long- term effects on global climate. Hence, CO_2 must be romoved from the natural gas before its further utilisation.

A wide range of processes are available for the removal of CO_2 from natural gas. Membrane separation technology provide a safe and efficient option for water vapor and carbon dioxide removal from natural gas, especially in remote locations. Membrane systems are adaptable to various gas volumes, CO_2 concentrations, and/or product-gas specifications. Carbon dioxide membranes operate on the principle of selective permeation. Each gas component has a specific permeation rate. The rate of permeation is determined by the rate at which a component dissolves into the membrane surface and the rate at which it diffuses through the membrane. Since CO_2 has higher permeation rate, it permeates faster than other components and separated by the difference in partial pressure of the permeating component. However, the usage of membrane process are restricted as it cannot withstand high temperature and pressure condition.

Adsorption is another process that can also be used for CO_2 removal. Adsorption method is a surface phenomenon whereby the solute accumulates on the surface of the adsorbent. The most common adsorbents used to remove CO_2 includes activated carbon, zeolites, carbon molecular sieves, silica gel and alumina. There are two main sections in adsorption process which are the adsorption of the gas in the adsorbents and the regeneration step to reuse the adsorbents. However, due to their limitating capacity and low CO_2 selectivity of the available adsorbents, the usage of adsorption method in industries is not attractive especially for large-scale CO_2 gas separation.

Cryogenic separation process (based on the difference in freezing points of each constituents) also can be used to remove CO_2 particularly at low temperature conditions. However, the cryogenic separation process is rarely used in commercial process due to its high energy consumption mainly for the refrigerant compressor and also high in overall cost of installation, which is due to the additional separation steps; i.e.; i) to remove water and other condensable gases before the gas is cooled, ii) to remove about 10% of hydrocarbon components that are also present together with CO_2.

Among all the processes, gas absorption is the most common and established process which is currently used in industrial practice. Absorption process is a process where the gases are directly dissolved into liquids phase. It can be classisfied into

physical absorption and chemical absorption. The physical absorption does not involve any reactions while in chemical absorption, the gas molecules undergo chemical reactions (which enhance the CO_2 loadings) but in contrast, it leads to excessive energy consumption for the regenaration of solvents. Irrespective of energy consumption, chemical absorption is more preferable in industrial process, than the physical absorption. In U.S, 95% of natural gas 'sweetening' operations are mainly amine – based absorption, which is a two stage process, namely; i) the absorption of CO_2 by chemical solvents such as alkanolamine at a low temperature (40 – 65 °C); ii) the recovery of CO_2 from chemical solvents at about 100- 150 °C. There are several advantages of using the absorption method, which includes the flexibility of the absorber to handle wide range of feed rates, rapid reaction rate, low cost of the solvent, ease of reclaiming, and reasonable thermal stability, etc. ((Li *et al.*, 1994); (Jou *et al.*, 1995); (Liu *et al.*, 1999)).

1.1.3 Common Solvents for CO_2 Removal

For the capture of CO_2, a wide range of solvents have been used for different separation processes. These solvents can be clasified into physical and the chemical solvents. The physical solvents are suitable mainly for high pressure gas streams. Examples of physical solvent are propylene carbonate, selexol, methanol, and n-methyl-2-pyrrolidone (NMP). Table 1.2 includes some of the solvents (along with their physical properties) that have been used in commercial operations. Eventhough it require less energy for the solvent regenaration, the use of physical solvents are however been restricted since these solvents are considered as highly volatile organic compounds (VOCs). Therefore, there will be quite a good amount of loss of these solvents especially when operating at elevated operating conditions. Moreover, the use of physical solvents alone is ineffective for low-pressure gas streams.

Chemical solvents on the other hand, involve a classical acid-base reaction between the targeted gas and solvent and is commonly used for treating gas streams with low and moderate CO_2 partial pressure (Thitakamol *et al.*, 2007). In this process, high CO_2 loading can be attained even with very low partial pressure of the gas. The most commonly used chemical solvents are the aqueous solutions of alkanolamines which include monoethanolamine (MEA), diethanolamine (DEA), N-

methyldiethanolamine (MDEA), diglycolamine (DGA), diisopropanolamine (DIPA, and 2-amino-2-methyl-1-propanol (AMP). Some of the physical and chemical solvents that are currently used in commercial processes are presented in Table 1.2, along with their vapor pressure data.

1.1.3.1 Alkanolamine

The aqueous solution of alkanolamines are the most common chemical solvents used in the industry. It is a proven technology that removes H_2S and CO_2 from natural gas and liquid hydrocarbon streams through chemical absorption. These alkanolamines can be divided into different groups based on the number of substituent groups in the nitrogen atom of the amines. Each of the amines offer distinct advantages along with their own disadvantages:

- Monoethanolamine (MEA) is a primary alkanolamines in which one hydrogen atom of the ammonia molecule is replaced by an ethanol group. It is used in low pressure natural gas treatment applications which requires stringent outlet gas specifications and in low CO_2 partial pressure.

- Diethanolamine (DEA) is the secondary alkanolamines in which two ethanol groups are present in the molecular backbone. It is used in medium to high pressure treating and does not require reclaiming.

- Methyldiethanolamine (MDEA) is the tertiary alkanolamines in which all hydrogen atoms are replaced by either alkyl or alcohol groups. It has a higher affinity for H_2S than CO_2 which allows some CO_2 to "slip" while retaining H_2S removal capabilities.

Eventhough the process is energy intensive, their effectiveness in capturing CO_2 is relatively high. However, due to their high volatility and corrosiveness, these solvents will develop few problems during long term operation, especially with respect to the corrosion, degradation and volatility of amines. The mass transfer and reaction rates are low at concentrated solutions due to the formation of carbamate,

which is produced by the conversion of free amine, especially with primary and secondary alkanolamines (Aboudheir *et al.*, 2003).

Table 1.2 Physical and Cheemical Solvents Used in Commercial Processes

Chemical	Boiling Point	Vapor pressure (mmHg) at 20°C
Monoethanolamine (MEA)	170.5 °C	1000 (110°C, 30wt%)
Diethanolamine (DEA)	217.0 °C	1000 (110°C, 30wt%)
N - Methyldiethanolamine (MDEA)	247.3 °C	950 (110°C, 50wt%)
Diglycolamine (DGA)	221.0 °C	900 (110°C, 50wt%)
Diisopropanolamine (DIPA)	249.0 °C	900 (110°C, 60wt%)
2-Amino-2-methyl-1-propanol (AMP)	165 °C	<1 (25°C)
Hot potassium carbonate (HPC)	366.5 °C	-
Methanol	64.6 °C	127 (25°C)
n-Methyl-2-pyrrolidone (NMP)	202.0 °C	0.5 (25°C)
Selexol (Dimethyl ethers of polyethylene glycol- DMPEG)	N/A	-
Sulphinol-D and Sulphinol-M (mixture of DIPA or MDEA, water and sulpholane)	N/A	-

Ref: (Thitakamol, 2007)

The tertiary alkanolamines did not form carbamates and therefore, these solvents have received a great attention from many researchers as it can be mixed with the primary and secondary alkanolamines. These mixture of amines are advantegeous in terms of their selectivity for H_2S and has low enthalphy of reaction with the acidic gases which leads to low energy consumption for regeneration. MDEA has better thermal and chemical stability and also less corrosive. The vapor pressure is also relatively low. But the usage of the tertiary alkanolamine have its own limitations in terms of the slower reaction rate with CO_2 and a lower absorption capacity at low concentrations of CO_2 ((Jou *et al.*, 1993); (Rou *et al.*, 1997)). Many industrial processes that previously used the conventional solvents have now shifted to the mixed solvents to increase CO_2 loading. However, the use of alternative mixed solvents that can avoid the corrosion problem and reduce the energy consumption, apart from an effective and high capability for CO_2 capture could be advantageous.

1.1.3.2 Ionic Liquids

Ionic liquids (ILs) are a relatively new family of substances constituted entirely by ions and exist as a liquid over a wide temperature range especially below 100^0C and even at room temperature (room temperature ionic liquids, RTILs). Due to its low melting point, high solubility with both polar and non-polar substances, negligible vapor pressure, and high thermal stability, ILs have been now preferred for few of the commercial processes. ILs are considered as green solvent and they are the potential environmental friendly replacement for the conventional volatile organic solvents. These properties make the ILs a specific choice of solvent for gas separation by absorption technique.

A wide range of ILs can be produced by varying their combinations of cations and anions since ILs solely comprised of ions i.e., organic cations and organic/ inorganic anions (Wilkes, 2002). Some of the common cations that have been found by the researchers include imidazolium, pyrrolidinium, quaternary ammonium, and pyridium, etc. Among the available ionic liquids, the one with imidazolium type of cations are found to be more suitable for CO_2 removal ((Kamps *et al.*, 2003); (Finatello *et al.*, 2008); (Lee *et al.*, 2006)). While for anion, tetraflouroborate [BF_4], hexaflourophosphate [PF_6] and bis(triflouromethylsulfonyl) imide [Tf_2N] are often

used among various other anions namely triflate [CF_3SO_3], acetate [CH_3CO_3], dicyanamide [(CN)2N], nitrate [NO_3], chloride [Cl], bromide [br] or iodide [I] ((Husson-Borg *et al.*, 2003); Byung- Chul and Outcalt, 2006); Shiflett and Yokozeki, 2007); Shin *et. al.*, 2008)).

Recently many researchers reported that few types of ILs have a high capacity for effective CO_2 capture and have several advantages over other molecular solvents used for the same purpose ((Kamps *et al.*, 2003); (Finatello *et al.*, 2008); (Lee *et al.*, 2006)). These ionic liquids have negligible vapor pressure and significant thermal stability which reduces the risk of solvent loss during the regeneration process and thus makes them a most suitable alternative solvent for the removal of CO_2.

ILs can be catogarized as room-temperature ILs (RTILs) and task-spesific ILs (TSILs). The first study reported on the solubility of CO_2 by using RTILs was by a research group from Notre Dame University (Anthony *et al.*, 2002) who reported that CO_2 is highly soluble in 1-butyl-3-methylimidazolium hexaflourophosphate ([bmim][PF_6] with highest mole fraction of 0.6 at pressure up to 8Mpa. TSILs are also found to be capable of capturing CO_2, by the combination of the desirable properties of RTILs with the reactivity of amines (Bates *et al.*, 2002; Ohno *et al.*, 2005; Zhang *et al.*, 2006; Kagimoto *et al.*, 2006). However, TSILs did have certain limitations such as high viscosity in their unreacted states, thus the utility of TSILs as solvents for CO_2 capture is limited (Camper *et al.*, 2008; Bates *et al.*, 2002). In addition, the synthesis of most ILs require several synthetic and purification steps and thus, is not cost-competitive with commercial chemicals such as MEA (Dean *et al.*, 2008).

1.2 Problem Statement

Natural gas is of great importance, not only as a primary energy source, but also as a raw material for many chemical and petrochemical industries. It consist of hydrocarbon and non-hydrocarbon gases primarily, methane. Natural gas also consists of other hydrocarbon molecules such as ethane, propane, butane, pentane and hexane and also some inorganic compounds as impurities such as CO_2, H_2S and nitrogen (N_2). The presence of these acid gases (CO_2 and H_2S) makes the natural gas sour. The presence of CO_2 content in natural gas not only decrease the value of the

fuel, but also leads to the corrosion problem in pipelines and equipments. The emission of CO_2 (greeanhouse gas) to the atmosphere, through the burning of natural gas can cause serious environment concerns.

Amine based solvents are the most common solvents used for the commercial removal of CO_2. However, the use of amines is energy-intensive and causes environmental concerns in the form of degradation during absorption/ regenaration. Therefore a solvent that could absorb CO_2 while being non-volatile and non-corrosive could be advantageous in order to improve the energy efficiency of CO_2 absorption. ILs with the properties such as low melting point, high solubility with both polar and non-polar substances, negligible vapor pressure, and high thermal stability that avoid loss of absorbents, are believed to be a more suitable alternative for the amine solutions. However, the application of ILs do not appear to be viable for industrial processes due to some disadvantages especially their high viscosity that can hinder their application in the separation process. Theoretically, the absorption of CO_2 is highly affected by the viscosity of the absorbent. The lower the viscosity, the higher the absorption will be and faster the rate of absorption.

While ILs can be dissolved in other solvents to offset their limitation due to their viscosity, there are simpler ways to achieve efficient CO_2 capture in IL solvents. Most of the previous studies involving carbon dioxide absorption were mainly focused either on ionic liquid or amines individually, but the literature pertaining to the studies on the combination of amines with ionic liquids either as binary or ternary mixture with water for CO_2 removal is not readily available. Since the application of both amine and ILs individually has been proven for the absorption of CO_2, the combination of these two solutions is believe can give better efficiency in the absorption of CO_2 than in these individual solutions. Compared to the aqueous amine solutions, addition of ILs to the former solutions provides: 1) reduce the possibility of chemical absoprtion by reducing the amine solutions; 2) reduce the loss of solvents due to degradation and volatility by limitating the usage of amine; 3) less viscosity to the pure ILs. With the facts that most of the inexpensive and commercially available amines or their aqueous solutions are readily soluble in most of ILs in the manner of which this mixtures act is similar to their aqueous counterparts. Hence, in this work, it

is proposed to develop an industrially attractive tunable hybrid solvent to capture carbon dioxide. It is expected that the mixtures will maintain the performance of amine in absorbing CO_2 while utilizing the desirable properties of ILs.

Since the basic physical properties are essential for the design, scale up and sizing of the equipments for commercial applications, the physical properties of the binary/ ternary mixturs as well as the solubility of CO_2 in these mixture of ILs and alkanolamine solutions, will be measured.

1.3 Research Objectives

The aim of the present study is to establish the physical properties as well as the CO_2 loading in the aqueous ionic liquid and amine based binary/ ternary mixtures. The following are the spesific objectives:

1. To determine the physical properties, namely, density, viscosity and refractive index and further to calculate the excess properties of the binary and ternary solutions of ILs and aqueous alkanolamine mixtures.

2. To measure the CO_2 loading in the hybrid mixed solvents for different conditions (pressure and temperature) using pressure drop method.

3. To analyze the effect of variables namely the temperature, pressure and concentrations on the rate and amount of absorption by using the chosen solvents and to understand CO_2 absorption process on the particular solvents.

1.4 The Scope of Studies

The overall scope of the present research is to systematically identify the suitable combination of ionic liquids and amines to form hybrid solvents for the effective capture of CO_2. The scope also includes the measurement of their physical properties and hence to deduce their excess properties, for a fundamental understanding between them and their affinity for CO_2 on the basis of the experimental outcome.

For this purpose, two ILs namely bis(2-hydroxyethyl)ammonium acetate [bheaa] from hydroxyl ammonium type ILs and 1-butyl-3-methylimidazolium tetrafluoroborate [bmim][BF_4] from imidazolium type ILs have been chosen to form binary/ ternary mixtures with monoethanolamine and water.

The physical properties namely, density, viscosity and refractive index for pure ([bheaa] and [bmim][BF_4]), binary mixtures ([bheaa] + water, [bheaa] + MEA, [bmim][BF_4] + water, [bmim][BF_4] + MEA) and ternary mixtures ([bheaa] + MEA + water and [bmim][BF_4] + MEA + water) have been measured and the excess properties namely excess molar volume, viscosity and refractive index deviations have also been deduced from the experimental measurements and correlated using Redlich-Kister (binary mixtures) and Cibulka equation (ternary mixtures). The performance of the present developed hybrid solvent for CO_2 capture have been carried out systematically by using binary and ternary combinations of ILs, MEA and water. The CO_2 uptake at three different temperatures (298.15, 308.15 and 313.15 K) has been measured to study the temperature effect.

CHAPTER 2

LITERATURE REVIEW

2.0 Overview

In this chapter, the literature survey pertaining to the present research work, in terms of the application of binary and ternary mixtures as well as the importance of the measurement of thermophysical properties of the solvent used and their applications with a focus on CO_2 loading are discussed in detail. Binary and ternary mixtures have been widely used in various chemical processes. The advantages in using the binary and ternary mixtures cannot be denied since it has been proved since ages. Despite reducing the energy consumption, the usage of binary and ternary mixtures can also reduce the viscosity of some higly viscous pure solvents. An appropriate combination of a mixture is also advantageous, since it can fully utilize the advantages of the specific properties of both the solvents used for effective chemical processes. The information on the physical properties such as density, viscosity and refractive index is important in understanding the basic principles and the nature of the operation involved. This knowledge is also essential in designing the process for both pilot and industrial scale. The details of the methods used for CO_2 absorption in commercial practice is discussed in this chapter. Alkanoloamines (including the primary, secondary and ternary alkanolamines) are considered as the most common solvents used for the removal of CO_2 in commercial processes. The solubility of CO_2 using various types of alkanolamines and their mixtures with other solvents has been

discussed. Since the usage of alkanolamine has caused great environmental concern, more work have been done in order to find alternative sovents to replace/ reduce the usage of alkanolamines. Recently, researchers found that ionic liquids (ILs) possess a good physicochemical properties that allow them to play the key role in improving chemical processes. Despite their unique properties such as negligible vapor pressure, low melting point, low volatility and high thermal stability, the chemical structure of ILs can be tuned so that their properties can be designed to meet the requirements of a specific process (Alberto *et al.*, 2009). Therefore, the literature review on the applications of ILs in the absorption of CO_2 has also been discussed in detail. There are various types of ILs available for research purposes. However, the imidazolium based ILs are the most common among all types of ILs since it can dissolve high amount of CO_2. But the high viscosity of this type of ILs has hindered many of their application for commercial processes. Therefore, the hydroxyl ammonium based ILs has also been discused together with other ILs with different anions and cations at various temperatures and pressures to study their potential application for CO_2 removal.

2.1 Binary and Ternary Mixtures

Binary and ternary mixture is a substance/ solvent that consists of exactly two or three different compounds respectively, that are mixed together but not in fixed proportions and they are not chemically united. It refers to a physical combination of the substances in which their identity are retained and are mixed in the form of alloys, solutions, suspensions and colloids. Since there is neither chemical bonding nor chemical changes, each compound retains its own chemical properties and make up. But the physical properties of the mixtures may differ depending upon the individual pure compounds.

Binary mixtures have been applied in most chemical processes either in industry or for research purposes, especially in the separation process. For instance, Li *et al.* (2009) used the binary mixtures involving diethylene glycol monobutyl ether (DEGMBE) with water as scrubbing liquid for the absorption of carbonyl sulfide from H_2S. Wang *et al.* (2009) on the other hand, used binary mixtures in the crystallization process to purify deflazacort for the medication purposes. Xia *et al.* (2008)

investigated the usage of binary mixtures of water and alcohol to purify sebacic acid from the caustic fusion of custor oil. Alberto *et al.* (2005) investigated the binary and ternary mixtures of alcohol and ether which are used as the octane-enhancing components in gasoline. Binary and ternary mixtures of diisopropyl ether + 2,2,2-trifluoroethanol + ethanol were also being used as the working fluids in Rankine engines for terrestrial and space application (Atik *et al.*, 2007). Binary liquid mixtures containing monodisperse glycols and poly(ethylene glycol)s on the other hand are being used in the pharmaceutical, chemical, cosmetics, and food industries, for the purification of biological materials and also as an additive for the production of coating films for food materials (Francesconi *et al.*, 2004).

The usage of binary mixture is more favourable rather than the pure component, since it is believed that by using the binary mixture, more potential advantages can be exploited. The advantages of binary mixture that has been proved so far is their ability to decrease energy requirement in contacting equipments such as condenser, turbine and heat exchanger, thus, decrease the overall process cost. A research group from, University of Oklahoma, Oklahoma (1976), has investigated the advantages of using the mixtures as working fluids in geothermal binary cycles. They found that, by using the mixtures, even with unoptimized conditions, the turbine throughput was increased and the condenser duty as well as cooling water requirement was decreased, despite the potential cascade system of binary cycles in which the work obtained from the coupled cycles could be maximized.

The advantage of using the mixtures of the pure components, is to utilize the unique qualities of each components and combine them in such a way that it cannot be extracted by using a single component system. Since no chemical changes involved during mixing the components, their chemical properties can be maintained, thus make it possible to tune the physical properties, resulting in a highly effective new solvent with better properties. This criteria is believed to be valuable, especially for the absorption of CO_2. Camper *et al.* (2008), in their research demonstrated that the ILs and amines can be combined for an efficient and effective absorption of CO_2. By combining both solvents, the desirable and valuable properties of ILs can be fully utilized without neglecting the high efficiency of the conventional amine solutions for

CO_2 absorption. These combinations are also believed to reduce the corrosion problems, caused by amines and the high viscosity of pure ILs while increasing the solubility of CO_2. They also claimed that the IL + amine solutions behave similar to the conventional solvents used and despite that, the mixtures are also believed to have offered significant advantages especially in terms of energy consumption. Most research regarding the absorption of CO_2, involved the use of the binary mixtures of various solvents. For instance, Tan and Chen (2006) used the binary mixtures of piperazine with monoethanolamine (MEA), N-methyldiethanolamine (MDEA), and also 2-amino-2-methyl-1-propanol (AMP) for the absorption of CO_2. Ma'mun *et al.* (2005) used aqueous mixtures of MEA while Song *et al.* (1997) used the ternary mixtures of MEA + Ethylene Glycol/ poly(ethylene glycol) + water. Binary and ternary mixtures were also being used by many other researchers for CO_2 absorption (Zhang *et al.*, 2005; Kumelan *et al.*, 2006; Jou and Mather, 2005; Kundu and Bandyopadhyay, 2006; Feng *et al.*, 2010; Sairi *et al.*, 2011). Commercial CO_2 scrubbing process also does not involve pure alkanolamine, instead aqueous solution of amines with water are used since it is believed that by adding water, the rate of CO_2 absorption could be increased and at the same time, the time to attain equilbrium could be reduced.

2.2 Physical Properties of Solvents Used

The knowledge of physical properties including density, viscosity and refractive index is important in all steps of design and development of contacting equipments (Alberto *et al.*, 2009). The thermophysical properties are also essential for the simulation, optimization and analysis of the behaviour of these components for the development of the thermodynamic modelling. It is useful in performing engineering calculations typically for sizing the column diameter, velocities, pressure drop in a column, (Eckert *et al.*, 1970) and also for the prediction of mass transfer behaviour (Wang *et al.*, 2005).

Despite the physical properties of pure component, the physical properties of the binary and ternary mixtures is also required. Since there are no chemical changes to its constituents, the physical properties of a mixtures especially their density, viscosity and refractive index may differ from those of the pure components. It is known that

the thermodynamic properties of liquid mixtures depend on the way in which the molecules of pure solvents are associated during the mixing process. Therefore, it is important to establish the physical properties of these mixtures before their application. Hence, the measurement of physical properties and to derive the excess properties from it, is an important task. The characteristics and properties of a solvent varies depending on the amount and concentration of the solvent in its natural state. Therefore, the measurement of the properties of the solvent before it is being used in the CO_2 solubility should be advantegous. In addition to that, the behavior of CO_2 absorption using mixtures can also be discussed and justified by using their physical properties and characteristics. For instance, density measurement is useful for the conversion of weight to volume, and conversion of kinematic viscosity to dynamic viscosity of a sample for practical/ analytical engineering calculations. But the most important advantage of using weight basis is that for a given mixture it neither change with temperature, pressure nor on mixing the components (Tseng et l., 1963). The information on the viscosity is also essentials in the CO_2 solubility measurement since it is believed that the CO_2 solubility can also be affected by the viscosity of the solvent used.

The importance of measuring the physical properties mentioned above has influenced many researchers to investigate the physical properties of various solvents used for different purposes. But even so, the information regarding the physical properties of binary and ternary mixtures involving various type of ILs with alkanolamine for the absorption of CO_2 is still limited. Only a very few data have been found on the physical properties of these mixtures for a very limited range of temperatures. Therefore, there is a need to establish their physical as well as the excess properties, before their application for CO_2 absorption.

2.2.1 Density

Density 'ρ'of a substance is defined as the mass per unit volume under fixed conditions. The term is applicable for solids, liquids and gases and it depends on the temperature and pressure. The unit for density measurement is $kg \cdot m^{-3}$. The measurement of density can be considered as a must in any chemical processes since it is useful in many engineering calculations. Density values can also be used to

calculate many other properties such as the excess molar volume, partial molar volume and the thermal expansion coefficient and these properties can be correlated using various emphirical correlation such as the Redlich-Kister polynomial equation which describes the functionality of both concentration (mole fraction) and temperature (Aguila- Hernandez *et al.*, 2001).

There are many instruments for measuring density with wide range of uncertainties. The density values are affected by the impurities and moisture content in the solvent. Since in many processes, density is taken as the controlling parameter for the rest of the operations, an accurate system with a reliable uncertainties that can give accurate mesurements are necessary. A vibrating U tube density meter is preferred since it gives a good accuracy in both the density measurement and temperature controlling system. Density in liquid solutions of monoethanolamine (MEA) and water both before and after CO_2 absorption were measured using an Anton Paar density meter (DMA 4500) with an estimated uncertainties of ±0.00005 $g \cdot cm^{-3}$ (Trine *et al.*, 2009). The density of binary mixtures of MEA with water at 303.15, 308.15, 313.15 and 318.15 K has been investigated using a vibrating tube density meter (Anton Paar Model DMA 5000) with a reproducibility of $1 \cdot 10^{-5}$ $g \cdot cm^{-3}$ (U.R. Kapadi *et al.*, 2002). Song *et al.* (1996) reported the densities of the mixtures of MEA with ethylene glycol and water while Geng *et al.* (2008) reported the densities of MEA with 1-butyl-3-methylimidazolium hexafluorophosphate and *N,N*-dimethylethanolamine mixtures. Ayyaz *et al.* (2008) also used the Anton Paar vibrating tube density meter (model DMA 5000) for their measurement of the densities for water, MDEA, and (MDEA + water). From the literature review on the density of MEA, a decreasing trend has been observed with an increase in temperature. It can also been observed in aqueous mixtures of MEA and water that the density increase with an increase in MEA concentration in the mixtures. Although there are many data on the density of MEA, at its pure state, in aqueous mixture or mixtures with other organic or inorganic solvents, there is still a lack in density data especially at low temperature (room temperature and below), since at these particular temperatures any measurement done is not very accurate and reproducible.

Tariq *et al.* (2009) reported the effect of temperature, alkyl chain and anion on the densities of imidazolium- and phosphonium- based ionic liquids using Anton Paar vibrating tube density meter (model DMA 5000). They used 17 room temperature ILs involving 1-alkyl-3-methylimidazolium- and trihexyl(tetradecyl)phosphonium- based cations coupled with six different anions such as acetate, [O*Ac*], triflate, [OT*f*], tetraflouroborate, [BF_4], and bis(trifluoromethylsulfonyl)imide, [NTf_2], methysulfate, [*Me*SO_4], and hexaflourophosphate, [PF_6] for density measurements at atmospheric pressure and at four different temperatures (293 to 333) K. The results showed a linear increase in density with decreasing temperature and decreasing alkyl chain length. On the other hand, Kurnia *et al.* (2009) who also used the Anton Paar vibrating tube density meter (model DMA 5000) and reported the density of six hydroxyl ammonium ILs at temperature from 293.15 to 353.15 K. It was also found that density of the ILs decreased with increasing temperature. Figure 2.1 shows the sample data on the density of 2-hydroxyethylammonium acetate (HEA) against temperature.

A similar type of equipment was also used by Gao *et al.* (2009) except that they used Anton Paar model DMA 4500 for measuring the densities of the binary mixtures formed by 1-butyl-3-methylimidazolium tetraflouroborate [bmim][BF_4] with aromatic compound (benzaldehyde) over the full range of compositions at the temperature range from (298.15 to 313.15) K at atmospheric pressure.

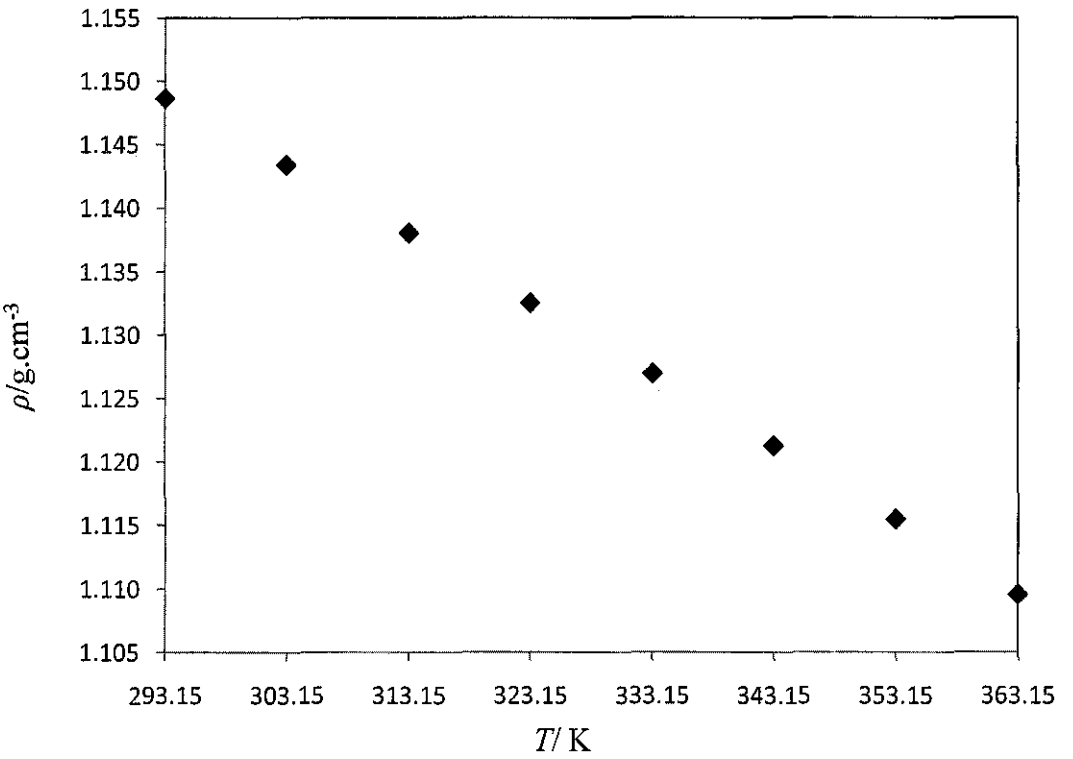

Figure 2.1. Density of 2-hydroxyethylammonium acetate (HEA) against temperature. (Kurnia *et al.*, 2009)

2.2.2 Viscosity

Viscosity 'η' is a measure of the resistance of a fluid which is being deformed by either shear stress or tensile stress. In everyday terms, viscosity can also be known as the thickness or internal friction of the fluid to flow. Besides density, viscosity is another important property of a fluid since it helps in fixing the optimum conditions for the processes and operations as well as in the power requirements for the unit operations such as mixing, pipeline design, pump characteristics, atomization, , injection, and transportation etc. (Viswanath *et al.*, 2007). The SI unit of dynamic viscosity is the pascal-second (Pa.s) while the SI unit for the kinematic viscosity is $m^2.s^{-1}$. Viscosities are usually measured with various types of viscometers and rheometers. Close temperature control of the fluids is essential for accurate measurements. One of the most common instruments for measuring kinematic vsicosity is the glass capillary viscometer in which the efflux time for a liquid to flow through a U-shaped glass capillary are measured. The dinamic viscosity (η) can be

calculated from the mesured kinemtic viscosity (v) using the density (ρ) of the fluid at that particular condition:

$$\eta = \rho.v \tag{2.1}$$

Direct measurement of the dynamic viscosities of the fluids can also be done using a cone and plate viscometer (Brookfield) or rotational type viscometer (Anton Paar SVM 3000, Stabinger).

Aguila-Hernandez *et al.* (2008) used five different size of Cannon Fenske routine capillary viscometer to determine the viscosity of the binary systems composed of N-methylpyrrolidone + MEA and N-methylpyrrolidone + DEA throughout the concentration range but the measurement did not cover low temperatures ($\leq 25^0$C). The dynamic viscosities of the aqueous MEA solutions were measured by Trine *et al.* at temperatures ranging from 25 to 80 ^{0}C using ZIDIN viscometer with an estimated measurement uncertainty of ±0.03 mpa·s. They found that the viscosity of these solutions increase with an increase in MEA concentration and decrease in temperature. Malham *et al.* (2008) reported the viscosity measurements for the pure and binary mixtures of 1-butyl-3-methylimidazolium tetraflouroborate and 1-butyl-2,3-dimethylimidazolium tetraflouroborate with water at 298.15K using an Ubbelohde suspended level viscometer that was dipped in a water bath thermostat at 298.15 K. The results obtained were in good agreement with the reported data (Hunt, 2007). It is often sufficient to know the viscosity of liquids at atmospheric pressure as a function of temperature. For example, the viscosity of 1-butyl-2-methylimidazolium nitrate [Bmim][NO_3] decrease with increasing temperature as shown in Figure 2.2 (Mokhtarani *et al.*, 2009).

The viscosity of ILs are high when compared with the viscosity of the pure amine or aqueous amine solution. Huddleston *et al.* (2001) reported that the viscosities of ILs are two or more orders of magnitude greater than most of the traditional organic solvents and are more comparable to the viscosity values of typical oils. This high viscosity of ILs have somewhat hindered their application in many chemical processes. For effective usage of ILs in industry, it needs to be diluted or being

operated at higher temperature since increasing temperature will decrease the viscosity value in a rapid and non linear fashion and is not significantly dependent on pressures up to several atmospheric pressures (Azevedo *et al.*, 2005) due to the diminishing effect on the strength of interactions between their cations and anions. Therefore, the studies on the viscosity is required for every solvent before further being used in any chemical process.

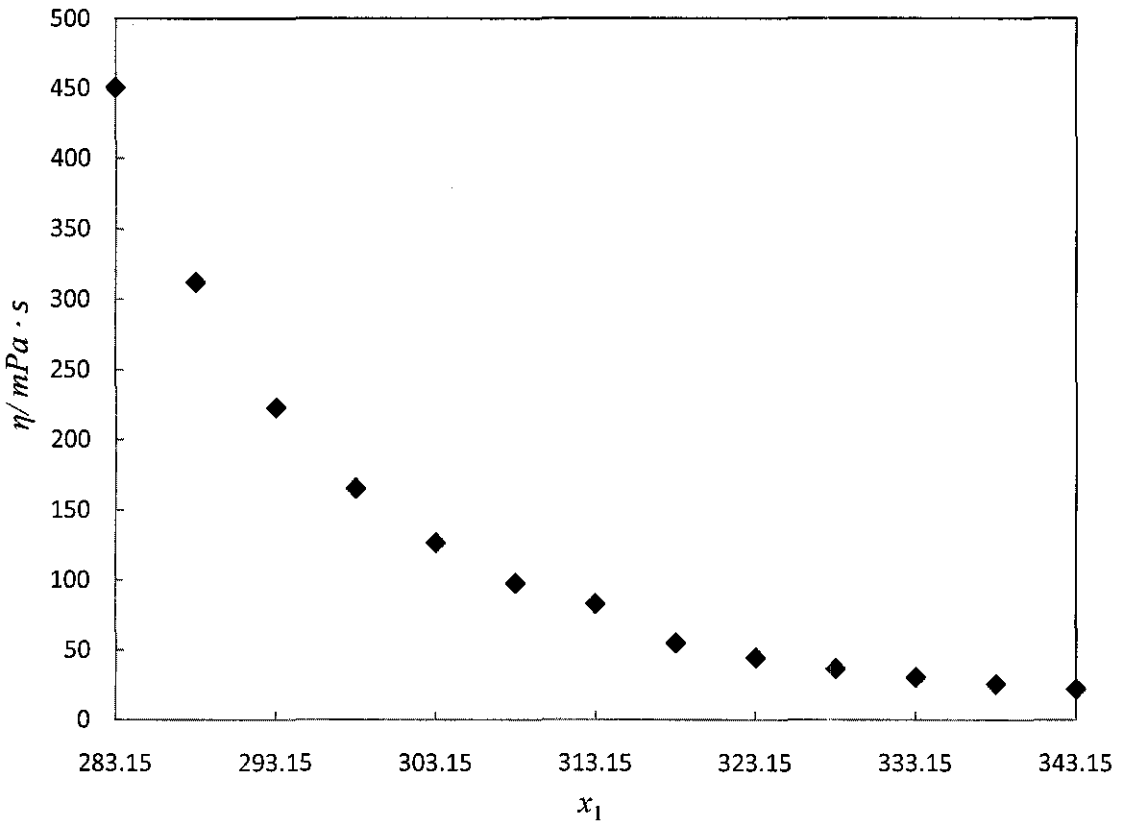

Figure 2.2. Viscosity of 1-butyl-2-methylimidazolium nitrate [Bmim][NO_3] (Mokhtarani *et al.*, 2009)

2.2.3 Refractive Index

Refractive index of a substance is defined as a measure of the speed of light in that substance. It is expressed as the ratio of the velocity of light in vacuum relative to that in the considered medium. Mathematically, refractive index can be described as follows:

n=velocity of light in vacuum / velocity of light in medium (2.2)

Refractive index is a fundamental optical property of a substance and it is often used to identify a particular substance, confirm its purity, or measure its concentration. Most common use of refractive index is to measure/ calibrate the concentration of a solute in an aqueous solution. The measurement of refractive index value of used solutions are expected can help researchers in determining the types of components and the component's concentration especially using back calibration and benefits them in many ways. Refractive index of a compound depends on its operating temperature whereby the value of refractive index decrease with increasing temperature. Figure 2.3 shows the trend of refractive index against temperature for 1-butylpyridinium bis(trifluoromethylsulfonyl) imide [C_4py][Tf_2N] (Yunus *et al.*, 2010).

Tseng *et al.* (1963) reported the refractive index for aqueous solutions of MEA, DEA and TEA at 20, 25 and 30^{0}C by using an improved Precision Valentine refractometer. A discussion of the advantages of plotting the refractive index data against either volume % or weight % is included. The values of the refractivity intercept, [n_D – (d/2)], at 25^{0}C plotted by both methods (weight% and volume%) show a nearly linear relationship for all amines investigated.

Soriano *et al.*, 2009 measured the refractive index of four 1-n-butyl-3-imidazolium-based ILs at atmospheric pressure and temperature up to 353.2 K using the commercial refractometer (ATAGO (model PAL-RI)) with an uncertainty of ±0.0003 with water at 298.15 K as reference. The results showed a linear relation with temperature and their temperature-dependence were anologous. They correlated their data using several empirical equation such as Lorentz Lorentz (Soriano *et al.*, 2009), Dale- Gladstone (Soriano *et al.*, 2010), Ekyman and Newton equation (Soriano *et al.*, 2009), as well as the modified Eykman equation (Pineiro *et al.*, 1999) and a satisfactory predictions (AAD% ≤ 0.07%) were reported. Iglesias-Otero *et al.* (2008) on the other hand reported the refractive index of the mixtures of 1-butyl-3-methylimidazolium tetarflouroborate and 1-butyl-3-methylimidazolium methylsulfate with organic solvents measured using a Mettler Toledo RE 50 refractometer. Lorentz-

Lorentz equation was used to correlate the refractive index data and reported that the agreement was satisfactory for all the studied systems (RMS ≤ 0.001).

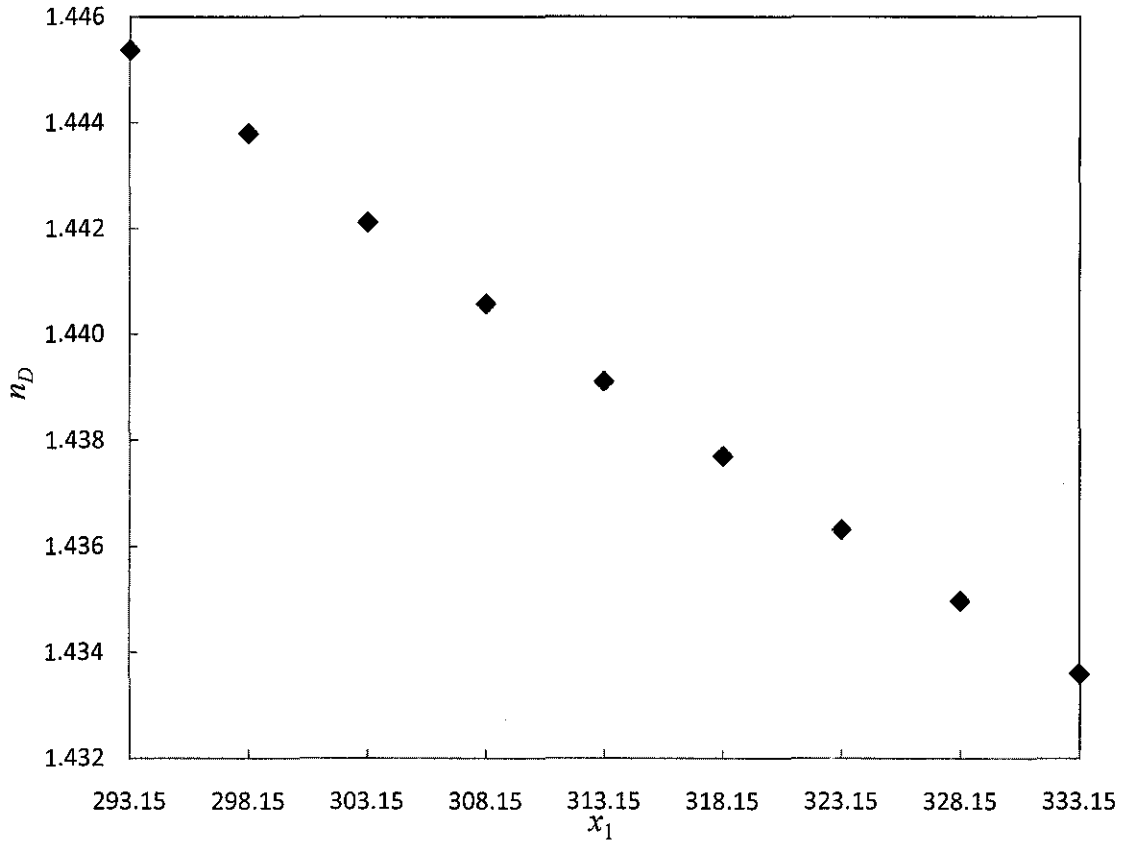

Figure 2.3. Refractive index of 1-butylpyridinium bis(trifluoromethylsulfonyl) imide [C_4py][Tf_2N] (Yunus *et al.*, 2010).

2.2.4 Excess Properties

Excess thermodynamic properties of liquid mixtures are receiving great interest in understanding the behaviour of the solution/ solvents involved in the chemical processes. The knowledge of the excess properties helps us to understand the interactions that determine the physical properties, making it easier to search for the optimal conditions of the solvents for the specific application (Tian *et al.*, 2008). The excess thermodynamic properties and their deviations of binary and ternary liquid mixtures over the whole composition range at various temperatures are essential for engineering design with subsequent operations and for testing molecular theories and models of solution to extend the understanding about interparticle (mainly hydrophilic and hydrophobic) interactions between the components (Ivanov *et al.* 2010). It can

also be used as the qualitative and quantitative guide to predict the extent of complex formation in the mixtures (Battino, 1971; Prigogine, 1969; Astarita *et al.*,1957). The excess properties of the solvent used can be calculated from the measured experimental values. The investigation on the excess and deviation properties of binary and ternary mixtures should be considered imporant, since they not only depend on solute- solute, solvent- solvent, and solute- solvent interactions, but also on the structural effects arising from interstitial accommodation (Almasi and Iloukhani, 2010).

The effect of excess molar volumes have been widely studied since it describes the interactions in the binary and ternary mixtures. The excess molar volumes of the binary and ternary mixtures involving alkanolamines have been studied by Maham *et al.* (2002), Trine *et al.* (2009), Chan *et al.* (2002), Valtz *et al.* (2006), Aguila-Hernandez *et al.* (2008), Hafaiedh *et al.* (2009) and Kapadi *et al.* (2002), while the excess molar volume of the binary and ternary mixtures involving various type of ILs have been studied by Arce *et al.* (2009), Gonzalez *et al.* (2007), Tian *et al.* (2008), Anouti *et al.* (2010), Rodriguez and Brennecke (2006), and Deenadayalu *et al.* (2010).

The excess molar volume for the binary mixtures are normally correlated using the Redlich-Kister polynomial equation

$$V_m^E = x_i x_j \sum_{i=0}^{n} A_k \left(x_i - x_j\right)^k \tag{2.3}$$

where V_m^E and x are the excess properties and the mole fraction respectively. The order (k) and the coefficients (A_k) of the Redlich-Kister polynomial equation can be obtained using the method of least squares. Figure 2.4 shows the reported excess molar volume for the binary mixtures of water and 1-ethyl-3-methylimidazolium trifluoroacetate [emim][TFA] at 298.15 K (Rodriguez and Brennecke, 2006)

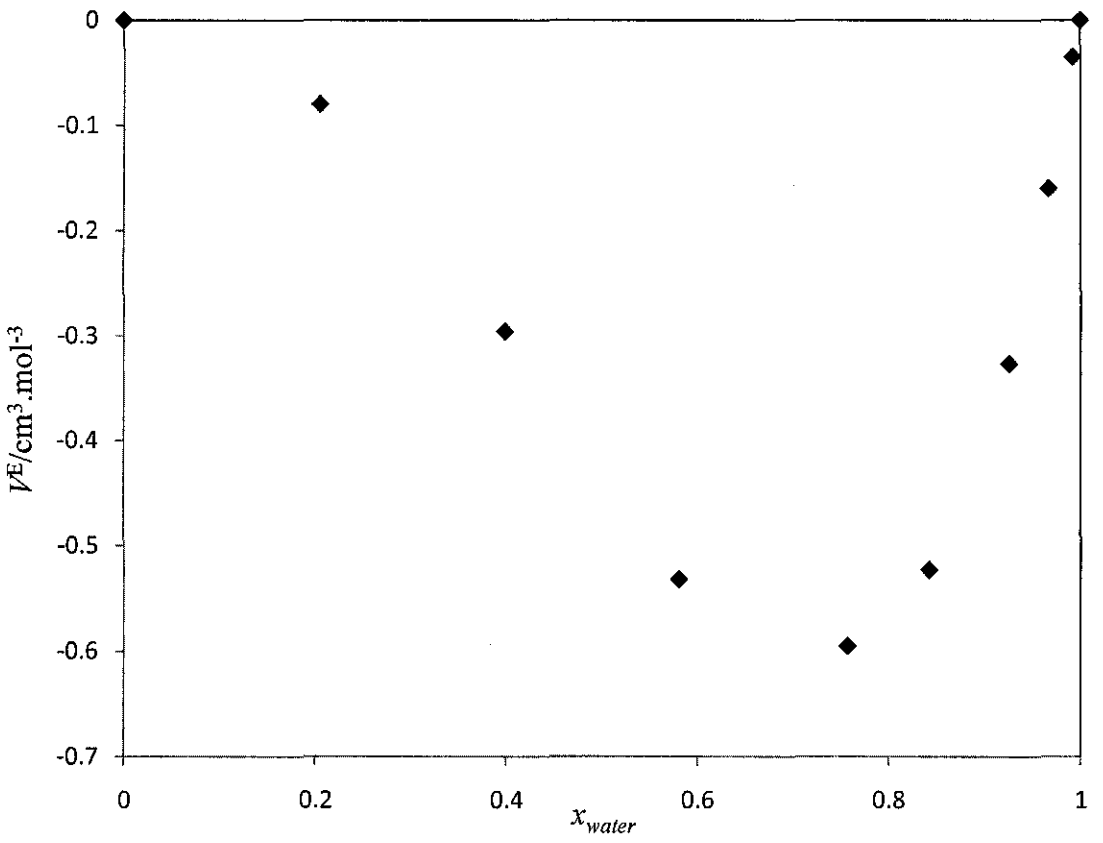

Figure 2.4. The excess molar volume for the binary mixtures of water and 1-ethyl-3-methylimidazolium trifluoroacetate [emim][TFA] at 298.15 K (Rodriguez and Brennecke, 2006).

Figure 2.4 shows that the mixtures of [emim][TFA] and water exhibit mostly negative deviations from ideality. This indicates that the [emim][TFA] have stronger interactions with water, that resulting in the negative excess volumes.

The excess molar volume for the ternary mixtures on the other hand can be correlated by using Cibulka equation

$$Y_{123}^{E} = Y_{bin}^{E} + x_1 x_2 (1 - x_1 - x_2)(B_0 + B_1 x_1 + B_2 x_2) \qquad (2.4)$$

where $Y_{bin}^{E} = Y_{12}^{E} + Y_{13}^{E} + Y_{23}^{E}$, which is the binary mixtures of the components involved, Y is the excess molar volume, x_1 and x_2 are the mole fraction of components 1 and 2,

respectively, B_0, B_1 and B_2 are the correction over the three binary contributions for each ternary systems. Figure 2.5 shows the excess molar volume for the ternary mixtures of methyltrioctylammonium bis(triflouromethylsulfonyl)imide [MOA][Tf_2N] + ethanol + methyl acetate at 298.15 K (Deenadayalu *et al.* (2010).

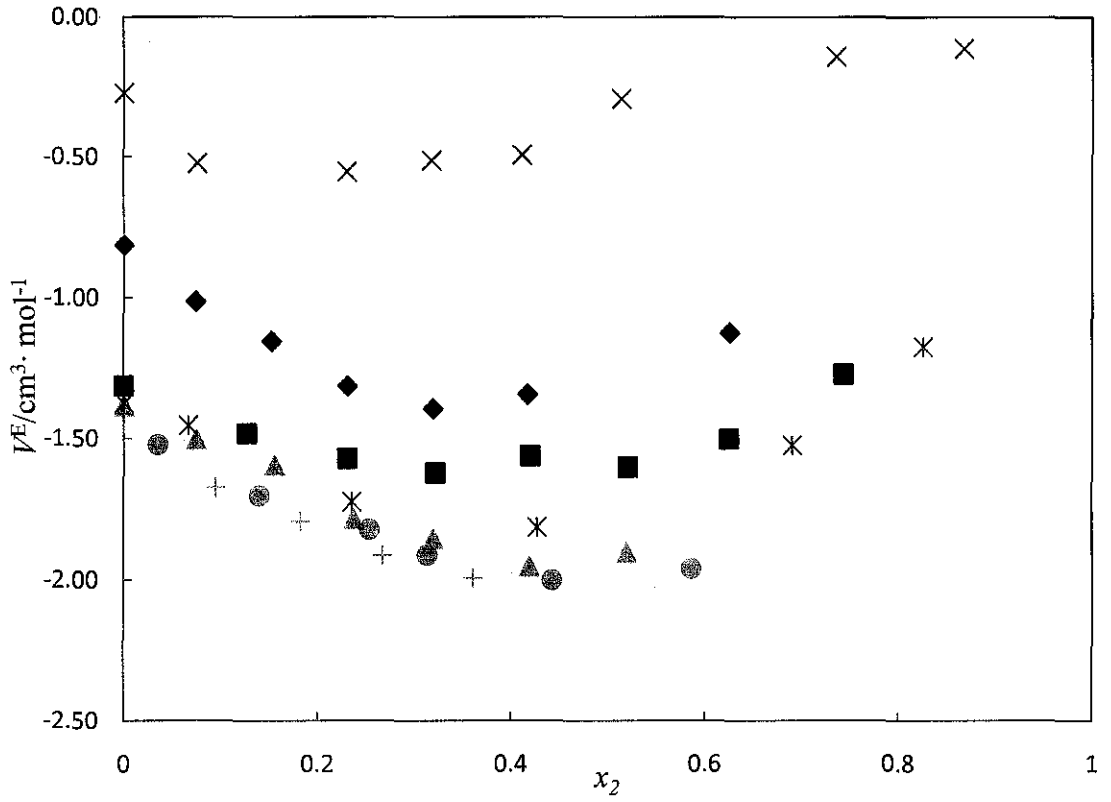

Figure 2.5. The excess molar volume for the ternary mixtures of methyltrioctylammonium bis(triflouromethylsulfonyl)imide [MOA][Tf_2N (x_1) + ethanol (x_2) + methyl acetate (x_3) against mole fraction ethanol at T = 298.15 K at constant z = x_3/ x_1. The symbols represent experimental results: ●, z = 0.10; +, z = 0.20; ▲, z = 0.50; ✳, z = 1.00; ■, z = 1.50; ◆, z = 4.00; X, z = 9.00. (Deenadayalu *et al.*, 2010).

Figure 2.5 shows that the excess molar volumes of the mixtures of [MOA][Tf_2N] + ethanol + methyl acetate are negative for all the ternary compositions. The negative values for the ternary mixtures of the corresponding IL + ethanol + methyl acetate indicate that the ion-dipole interactions between ethanol, methyl acetate and IL, as

well as the accommodation of the smaller (ethanol) molecules into the interstices of the IL, which is the packing effect, dominate over the dissociation of the self-associated ethanol and methyl acetate molecules (Deenadayalu *et al.*, 2010).

The viscosity of ILs at its pure state are higher when compared with any other conventional pure solvents. By adding the pure ILs with other solvent either to form a binary or a ternary mixtures, can result in a dramatic change, particularly a decrease in the viscosity of the ILs. The viscosity of the resulting mixtures by adding two liquids may not be equal to the summation of the viscosity of the pure constituents. It may be positive or negative depending on the interactions of the components involved. The deviation of the viscosity of the binary and ternary mixtures from its pure constituents may be calculated by the following expression

$$\Delta\eta = \eta - \sum x_i \eta_i \tag{2.5}$$

where η is the viscosity of the mixture, and η_i refer to the viscosity of the pure component *i*. The viscosity deviation of the binary mixtures can also be correlated by using the Redlich-Kister equation

$$\Delta\eta = x_i x_j \sum_{i-0}^{n} A_k \left(x_i - x_j\right)^k \tag{2.6}$$

On the other hand, the viscosity deviation for the ternary mixtures can be correlated by using Cibulka equation (equation 2.4). The viscosity deviation of the binary and ternary mixtures involving ILs and alkanolamine has been studied by various researchers including Arce *et al.* (2008), Bou Malham and Turmine (2008), Rodriguez and Brennecke (2006), Gonazalez *et al.* (2007), Anaouti *et al.* (2010), Kapadi *et al.* (2002), Hafaeidh *et al.* (2009), Deenadayalu *et al.*(2010), Fattahi and

Iloukhani (2010). Figure 2.6 shows the sample data on the viscosity deviation of the binary mixtures of water and 1-ethyl-3-methylimidazolium triflouroacetate [emim][TFA] that are fully dissociated at 298.15 K (Rodriguez and Brennecke, 2006).

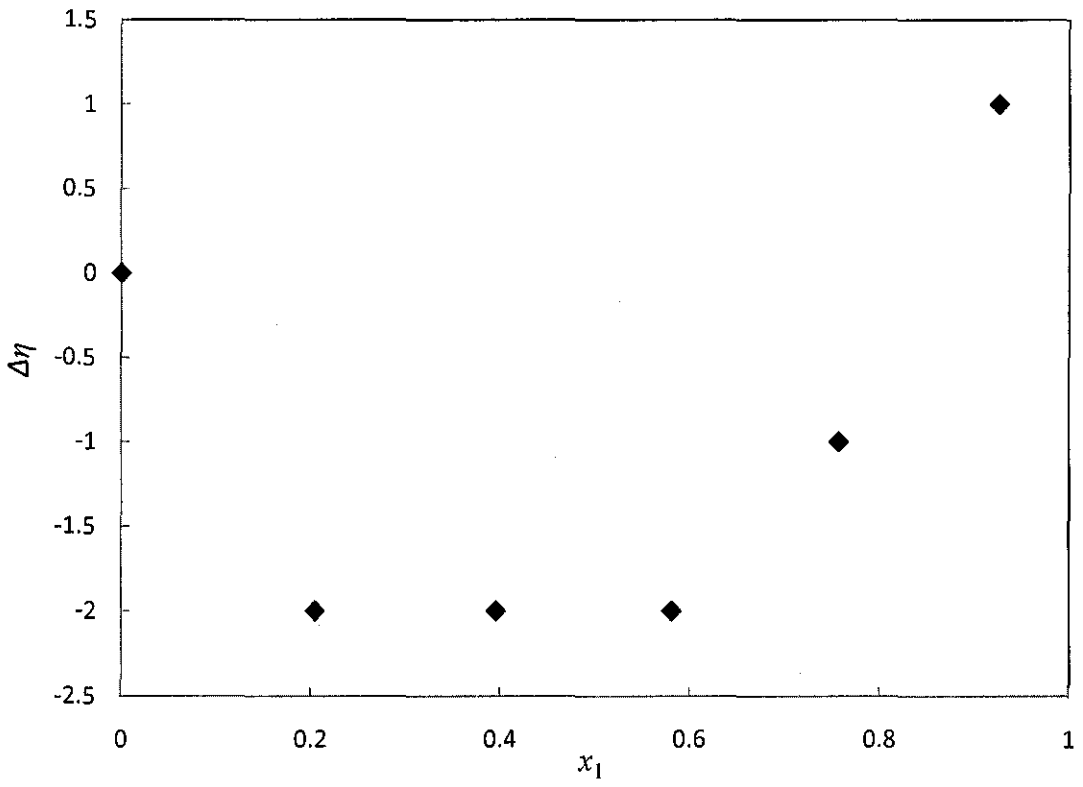

Figure 2.6. The viscosity deviation for the binary mixtures of water and 1-ethyl-3-methylimidazolium trifluoroacetate [emim][TFA] (x_1) at 298.15 K (Rodriguez and Brennecke, 2006).

Figure 2.6 shows that the mixtures of [emim][TFA] and water exhibit mostly negative deviation and the magnitude is decreasing and even reach slightly positive values at the higher concentration of water. The negative deviation indicates the predominance of specific hydrogen bonding/ interaction between like molecules compared to unlike molecules. Figure 2.7 on the other hand, shows the negative viscosity deviation for the ternary mixtures of 2-methyl-2-butanol + tetrahydrofuran (THF) + propylamine at 298.15 K over the whole composition range that indicates the

characteristic of systems where dispersion forces predominated (Fattahi and Iloukhani, 2010).

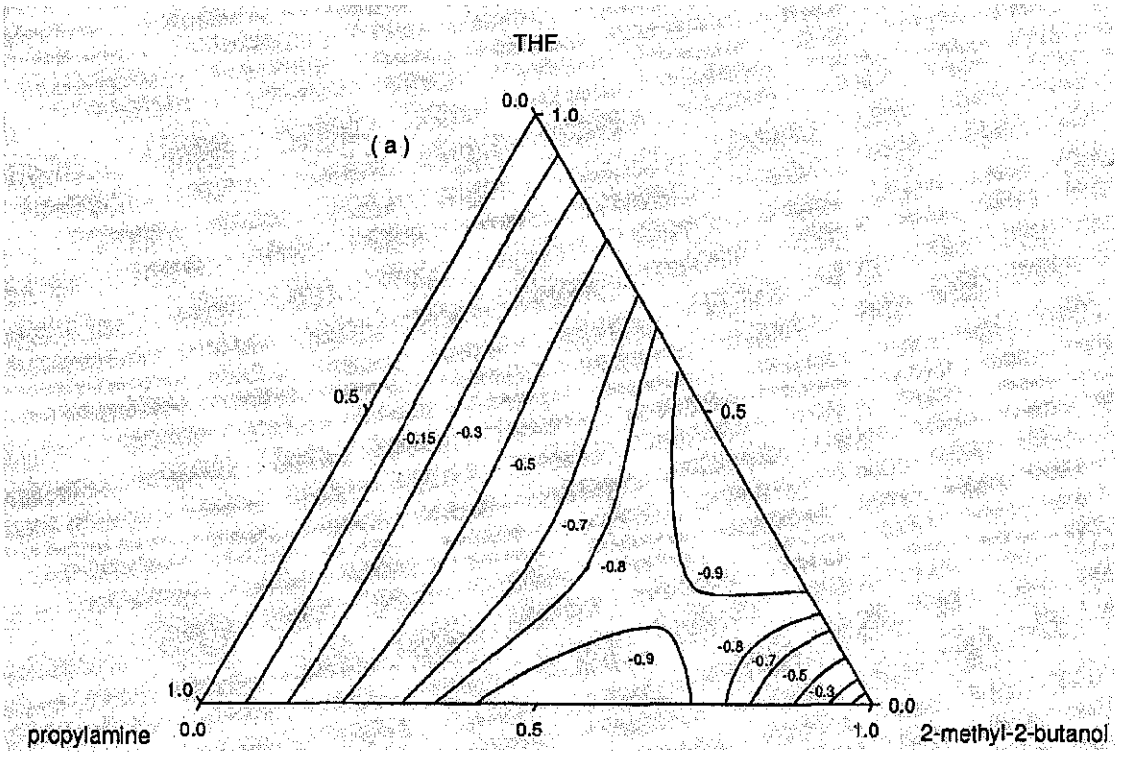

Figure 2.7. The viscosity deviation for the ternary mixtures of 2-methyl-2-butanol + tetrahydrofuran (THF) + propylamine at 298.15 K (Fattahi and Iloukhani, 2010).

Similar to the density and viscosity, the refractive index of a mixture can be more or less than the refractive index of the individual components involved. Therefore, the deviation of the refractive index of the mixtures relative to the refractive index of the individual component can be calculated

$$\Delta n_D = n_D - \sum x_i n_{Di} \qquad (2.7)$$

where n_D are the refractive index of the solutions while n_{Di} refer to the refractive index of the pure component *i*. The refractive index deviation of the binary mixtures can be correlated by using Redlich Kister form of polynomial equation

$$\Delta n_D = x_i x_j \sum_{i=0}^{n} A_k \left(x_i - x_j\right)^k \tag{2.8}$$

On the other hand, the refractive index deviation for the ternary mixtures can be correlated by using Cibulka equation (equation 2.4). Refractive index deviation of binary and ternary mixtures involving ILs and alkanolamine have been studied by Gomez *et al.* (2008), Gonzales *et al.* (2008), Gonzalez *et al.* (2007), Arce *et al.* (2009), Singh and Kumar (2007), Arce *et al.* (2008), and Anouti *et al.* (2009). Figure 2.8 shows the negative refractive index deviation of the binary mixtures of tetrahydrofuran (THF) + propylamine at 298.15 K over the whole composition range (Fattahi and Iloukhani, 2010).

The refractive index deviations for the ternary mixtures of 2-methyl-2-butanol + tetrahydrofuran (THF) + propylamine at 298.15 K are shown in Figure 2.9 (Fattahi and Iloukhani, 2010). The refractive index deviations for the ternary mixtures of the stated components show a positive deviation over the whole composition range.

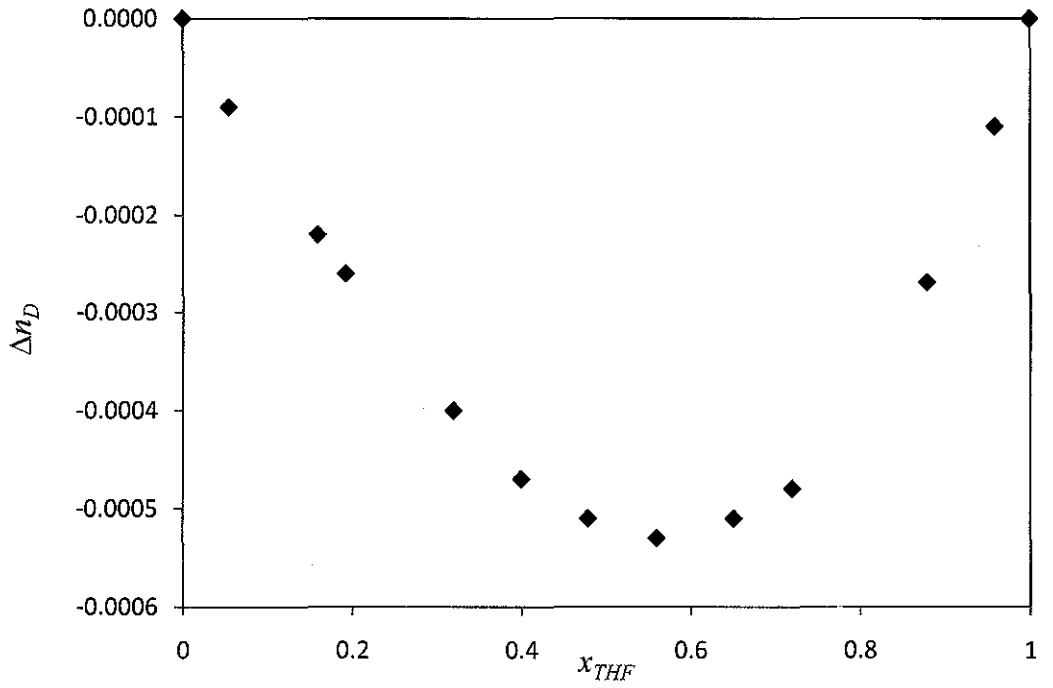

Figure 2.8. The refractive index deviation for the binary mixtures of tetrahydrofuran (THF) + propylamine at 298.15 K (Fattahi and Iloukhani, 2010).

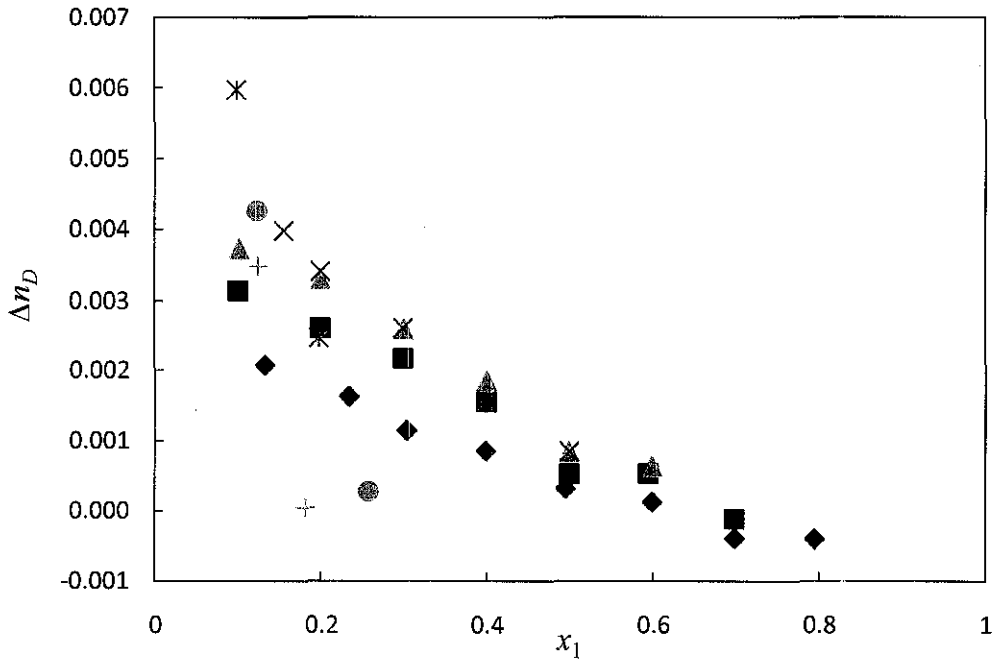

Figure 2.9. The refractive index deviation for the ternary mixtures of 2-methyl-2-butanol + tetrahydrofuran (THF) + propylamine at 298.15 K (Fattahi and Iloukhani, 2010).

2.3 Carbon Dioxide Solubility

2.3.1 Introduction

The combustion of natural gas produce gases namely vapors of methane (CH_4), sulfur dioxide (SO_2), hydrogen sulphide (H_2S), nitrogen oxides (NO_2) and also carbon dioxide (CO_2) which is the major greenhouse gas that contribute to the climate change. The increasing utilization of natural gas has increased the emission of CO_2 (from combustion of natural gas) thus leads to many environmental problems (Armstrong *et al.*, 2006, Mira *et al.*, 2006). Therefore removal of CO_2 is one of the most important topics to be discussed and further to be investigated in order to protect the environment from the effect of greenhouse gases. It is also important to remove CO_2 from natural gas in order to maintain the quality of these clean-burning, efficient fuel sources. Currently stringent regulations have been created to enforce the reduction of greenhouse gas emissions. For instance, Kyoto Protocol was established in December 1997 at the United Nations Framework Convention on Climate Change with a global reduction target of at least 5% below 1990 levels by the period of 2008-2012. The protocol was signed by 162 countries from all over the world, including United States and Canada, who are expected to contribute about 17.8% and 1.4%, respectively, of the world CO_2 emissions in 2030 (Energy Information Administration, 2006). Therefore, in order to help all the countries to achieve the protocol target, a process that can capture CO_2 from the combustion of fossil fuels despite ensuring the continuation of fossil fuels utilization in an environmentally benign and sustainable manner is needed without affecting the effiency and operating cost of the process.

Among all the available gas separation process for capturing CO_2, gas absorption into liquid solvent is the most attractive because of its process maturity in gas treating services (Thitakamol, 2007). Gas absorption process involves two major sections that is the absorption section where CO_2 in the flue gas is absorbed into the liquid solvent and a regeneration section where the absorbed CO_2 is stripped out by means of heat pressure. The crucial part of gas absorption is the development of more efficient solvents for increased rate of absorption and at the same time reducing the cost. Different factors that affect the efficiency of the solvent for carbon dioxide absorption

includes: solubility, vapor pressure, molecular weight, foaming tendency, corrosion properties and also degradation during regenaration process, apart from reaction kinetics, heat of reaction and energy requirements for their recycling (Aronu *et al*, 2009). Alkanolamines such as monoethanolamine (MEA), diethanolamine (DEA), N-methyldiethanolamine (MDEA), and diisopropanolamine (DIPA), have been used as common solvents for the absorption of CO_2. The merits and the disadvantages are discussed in the following section.

2.3.2 Solubility of CO_2 in Alkanolamines

Alkanolamines such as monoethanolamine (MEA), diethanolamine (DEA), N-methyldiethanolamine (MDEA), and diisopropanolamine (DIPA) are the common solvents used in gas absorption process for the removal of CO_2 in industries. Table 2.1 shows the common alkanolamines used for CO_2 capture. An example of the existing power plant with an amine absorption- based CO_2 capture unit is the Warrior Run Power station in Cumberland, USA which has a capacity of 150 tonnes/ day of CO_2 captured (Davison *et al*, 2001). This process involves two major sections which is basically the absorption of CO_2 in the liquid solvent using counter current mode and the regenaration of CO_2. The treated gas with low CO_2 content passing out from the top of the absorber and a CO_2 – rich solvent leaving the absorber at the bottom. The CO_2 – rich solvent is then heated in a heat exchanger before going to the regeneration section where it is being heated to its boiling point by a hot stream reboiler, to release the captured CO_2 from the solvent.

During the recent two decades, many reports have been published with respect to the application of alkanolamines for CO_2 absorption at various conditions. For instance, Palmeri *et al.* (2008), investigated the absorption of CO_2 by aqueous solution of monoethanolamine (MEA) (12 mass%) using a bubble column reactor at atmospheric pressure and reflux time of 3hours with reactor temperature from 283 to 353 K. They concluded that monoethanolamine (MEA) solutions could be recycled at 374K for 3 hours even though this will leads to a partial loss of absorbent power with respect to fresh solutions. They also developed a simplified semi-emphirical model (first- order in MEA concentration) that can describe the absorption of CO_2 in MEA as a function of temperature, flow rate of CO_2 and time.

Table 2.1. Common alkanolamines for the solubility of CO_2.

Alkanolamine	**Reference**
Monoethanolamine (MEA)	Boudheir *et al.*, 2003; Ma'mun *et al.*, 2005; Palmeri *et al.*, 2008; Gaur *et al.*,2010
Diethanolamine (DEA)	Kundu *et al.*, 2006
N-methyldiethanolamine (MDEA)	Jou *et al.*, 1993; Xu *et al.*, 1998; Lemoine *et al.*,.2000; Park and Sandall, 2001; Ermatchkov *et al.*, 2006
2-amino-2-methyl-1-propanol (AMP)	Silkenbaumer *et al.*, 1998; Murrieta-Guevara *et al.*, 1998; Samanta *et al.*, 2009

Boudheir *et al.* (2003) investigated the kinetics of the reactive absorption of carbon dioxide in MEA (3 M to 9 M) with CO_2- loading of 0.1 to 0.49 mol/ mol over the temperature range from 293 to 333 K. They reported that both kinetic model with an aid of numerically solved absorption model have been used to accurately predict, the CO_2 absorption for the high CO_2 loaded and highly concentrated MEA solutions. Gaur *et al* (2010) investigated the landfill gas (LFG) processing via adsorption and alkanolamine absorption for the removal of CO_2. They found that the maximum loading of CO_2 was obtained at 30wt% of monoethanolamine (MEA) rather than 30wt% of diethanolamine (DEA) due to the structure and size of MEA which is smaller than DEA. But no appreciable difference was observed in the loading of CO_2 or the rate of absorption between 20wt% and 30wt% MEA. Besides MEA, other types of alkanolamines have also been used for the absorption of CO_2 by various reseachers (Arcis, H., 2009; Jou *et al*, 1993; Xu *et al*, 1998; Lemoine *et al.* 2000; Park and Sandall, 2001; Ermatchkov *et al.* 2006). Solubility of CO_2 in aqueous solution of alkanolamine can be clearly analyzed based on the plot of CO_2 loading (mol of CO_2/ mol alkanolamine), molarity (mol of CO_2/ kg of alkanolamine), or molality (mol of CO_2/ L of alkanolamine), against the CO_2 partial pressure. With the various references on the usage of MEA, it supported the facts that MEA has been used extensively for the purpose of removing CO2 from natural gas since MEA has a high enthalpy of

solution with CO2, which tends to drive the dissolution process at high rates (GCEP Energy Assessment Analysis, 2005). A sample plot of CO_2 loading in MEA solution against pressure is shown in Figure 2.10.

Despite the establishment of using various type of alkanolamines for CO_2 capture in industry, the application of these solvents have their own limitations. For instance, highly concentrated MEA solutions could not be used for the removal of acid gases, since they can also react with unrelated materials such as reactor vessels, tubing lines, and several process compartments. Depending on the operationg conditions of the process, namely , operating temperature, amine concentration, dissolved CO_2 and some degradation products (Veawab *et al.*, 1999), there could be major drawbacks associated with corrosion in certain sections of CO_2 plant (Kladkaew *et al.*, 2011). Corrosion seems to take place in several plant locations including the bottom portion of the absorber, the heat exchanger, the regenerator, and the reboiler (Veawab *et al.*, 1999) with different types of corrosions depending on the ways in which the process equipment was designed, fabricated, installed and operated.

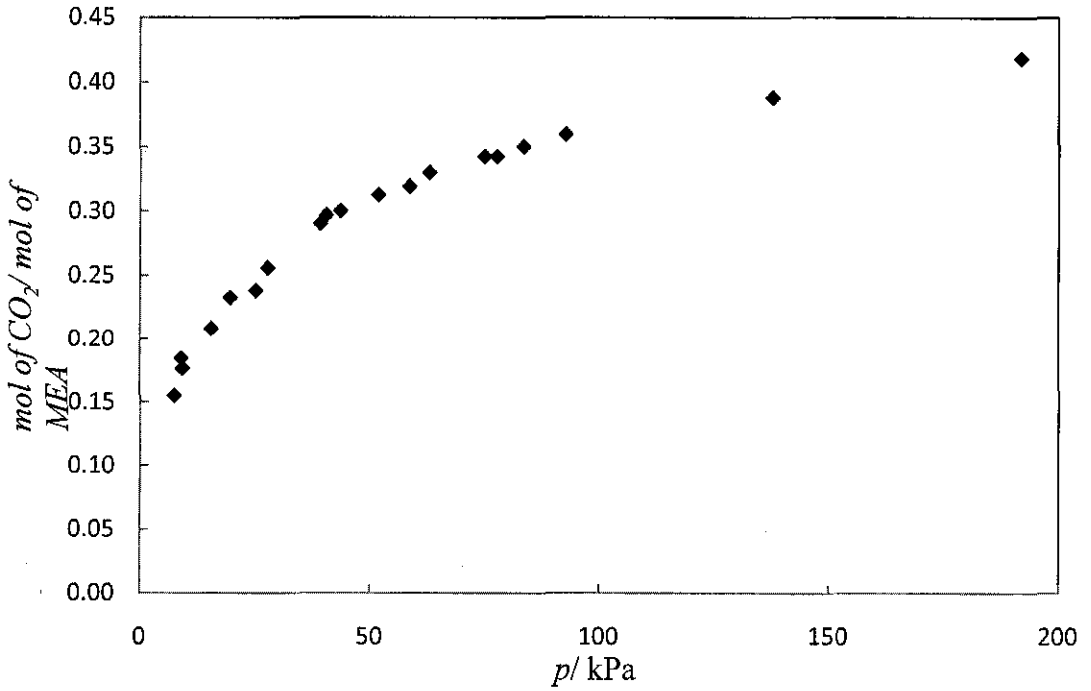

Figure 2.10. Experimental results for the solubility of CO_2 in MEA solution (30 mass%) at 120^0C (Ma'mun *et al.*, 2005)

The corrosion in CO_2 plants can lead to an economical impact, since it results in the lose of production, reduced equipment life, unplanned plant shutdown and limiting the operating ranges that makes a reduction in the production capacity of existing plant, which could not be easily increased at reasonable cost. In 1998, CC Technologies & NACE International in the United States (Koch *et al.*, 2001), reported that the plant expenditure due to corrosion was estimated to be US$276 billions. On safety basis, corrosion also has adverse effects on plant personnel. In a refinery at Romeoville (United States), the amine absorber pressure vessel got ruptured and a large amount of flammable gases and vapors were released and later it was found that the accident was due to the corrosion in amine treating units (Soosaiprakasam and Veawab, 2008). There are several ways to control the corrosion effects including the usage of proper materials for the equipments, the usage of higly resistant materials and also the use of alternative solvent which could reduce the corrosion rate in the processing equipments. However, the usage of properly designed and highly resistant materials for the equipment, increased the operating cost to reasonably high. Veawab *et al.* (1999) reported that MEA had the highest corrosion rate followed by AMP and DEA while MDEA is the least corrosive. Even though the aqueous MDEA is better than any other alkanolamine, the slow reactivity of MDEA solutions with CO_2 limits their use (Yoon *et al.*, 2003). But even so, on the basis of experience, all types of alkanolamines can generate corrosion problems due to the presence of bicarbonate ion that react with iron. Hence, to reduce the corrosion problems despite maintaining the capability of capturing CO_2, alkanolamines should be blended with other solvents (without/ less corrosion problems) that is also capable of capturing CO_2.

2.3.3 Solubility of CO_2 in Ionic Liquids

Recently, ILs have drawn great attention due to its advantageous properties and identified as potential solvents to replace the conventional organic solvents. Some researchers reported that ionic liquids (ILs) pose an effective and high capability for CO_2 capture and have several advantages over other molecular solvents used for the purpose [Alvaro *et al.*, 2003; Finotello *et al.*, 2008; ; Finotello *et al.*, 2008; Lee *et al.*, 2006]. Moreover, the important properties of ILs such as its wide liquid range, low melting point, high solubility with both polar and non-polar substances apart from its

negligible vapor pressure, and high thermal stability, which avoid loss of absorbents during regeneration process. These properties are expected to enhance the efficiency of the CO_2 absorption process. Considering these favorable properties of ILs and the disadvantages of the conventional organic solvents used for CO_2 capture, the former has attracted the attention of the researchers [Li *et al.*, 2006; Wang *et al.*, 2003; Zhang *et al.*, 2004].

There are millions of combinations of cations and anions of ILs which makes them one of the largest known compounds in chemistry (Brennecke and Maginn, 2001). The unique properties of ILs have increased their application in various fields namely: hydrogenation (Fonseca *et al.*, 2006), oxidation (Jukabiak, 2005) and also in gas separation process. Some of the common ILs used for CO_2 absorption are listed in Table 2.2.

The are several factors that has to be consider in choosing the ILs for the CO_2 absorption. One of the important factor is the knowledge of its viscosity especially at its pure state. Viscosity of the pure ILs is relatively high, about 5-fold higher than that of a traditional aqueous solution of MEA (Meidersma, 2007) and increase with CO_2 loading, leading to an additional energy penalty in pumping the solvents. The ILs that has lower viscosity are more favor since the high viscosity can hindered and lowering the CO_2 loading by the solvents despite high energy requirement.

Since there are millions of ILs, the combination of certain cation with certain types of anion also plays an important role in CO_2 absorption. The gas absorption capacity of ILs, depends on the chemical and molecular structure of the ILs, especially the anions (Tang *et al.*, 2005). Jalili *et al.* (2010) investigated the solubility of CO_2 in 1-(2-hydroxyethyl)-3-methylimidazolium ILs with different anions, *viz.* hexaflourophosphate ($[PF_6]^-$), trifluoromethanesulfonate ([OTF]$^-$) and bis-(trifluoromethyl)sulfonylimide ($[Tf_2N]^-$). They reported that the solubility of CO_2 is the highest in [hemim][Tf_2N] and the lowest in [hemim][PF_6] and they concluded that the ILs containing anions with flouroalkyl groups, *i.e.* $[Tf_2N]^-$ and [OTF]$^-$, have higher affinities for CO_2 than those other anions.

Camper *et al.* (2004, 2005) measured the solubility of CO_2 and other hydrocarbons in imidazolium based ILs with anions $[BF_4]$, $[PF_6]$ and $[NO_3]$ at atmospheric pressure. Based on their experiments, they also concluded that the type of anion has significant effect on the solubility and that CO_2 solubility in all the studied ILs is much higher compared with other hydrocarbons. Amine functioanlized ILs were recently reported to be capable of capturing CO_2, by incorporating the desirable properties of ILs and the reactivity of amines. Amine functionalized ILs have been synthesized by Bates *et al.* (2007) and they found that the molar uptake of CO_2 per mole of IL approached to the theoretical maximum under atmospheric pressure and temperature. Feng *et al.* (2010) also synthesized tetramethylammonium ($[N_{1111}]^+$) and tetraethylammonium ($[N_{2222}]^+$) based ILs as the cation and glycinate and lysinate as the anion which contained the amine groups for the solubility of CO_2. Figure 2.11 shows the structure of $[N_{1111}]^+$ and $[N_{2222}]^+$ as cation and lysine and glysine as anion.

Most researchers focussed their studies on the solubility of CO_2 in pure ILs with various combinations of anion and cations. Chen *et al.* (2006) investigated the imidazolium type of ILs with anion $[BF_4]$ and 1-n-3- methylimidazolium with n= 4, 6, 8 as cation at temperatures between 307 to 322 K. They reported that the CO_2 solubility increase slightly with an increase in alkyl chain length of cations due to the availability of more free space within ILs. Chen et al. (2012) also reported that the chain length plays an important role in governing the absorption properties of ILs, including the free energies of absorption, equlibrium constants, desorption temperature, absorption rate constants, diffusion coefficients, and organizations of CO_2 around cations and anions. However, the mechanisms for selectively capturing CO_2 by ionic liquids are unclear. Aki et al. (2004) on the other hand reported the solubility of CO_2 in 1-butyl-3- methylimidazolium cation with different anions ($[BF_4]$, $[NO_3]$, $[PF_6]$, [TfO] and $[Tf_2N]$. Figure 2.12 shows the plot of CO_2 uptake in pure 1-butyl-3-methylimidazolium trifluoromethanesulfonate [Bmim][triflate] (Soriano et al., 2009).

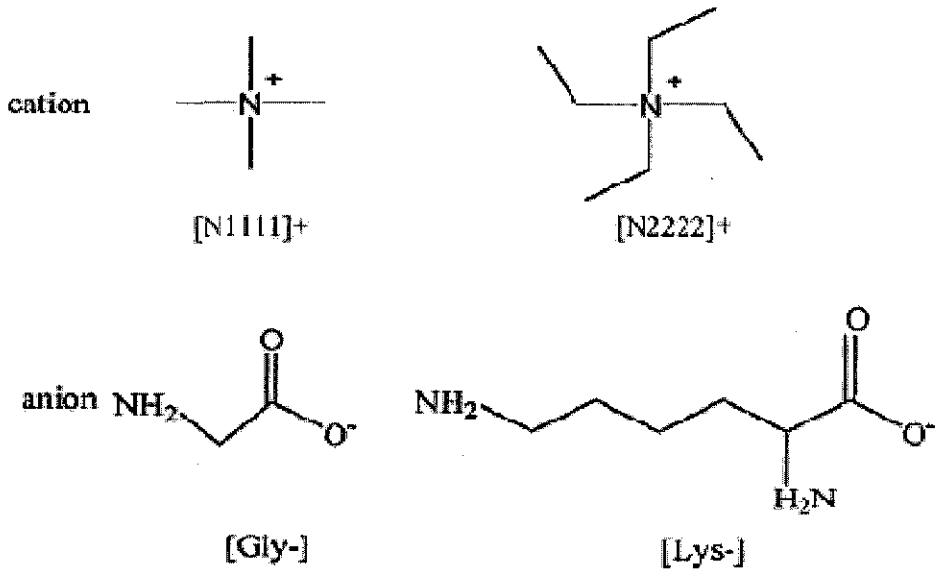

Figure 2.11. Cation and Anion of amino acid ionic liquids (Feng *et al.*, 2010)

Table 2.2. Common ILs used for the solubility CO_2 absorption

Ionic Liquids	Reference	Temperature Range	Pressure Range
1-butyl-3-methylimidazolium tetraflouroborate [Bmim][BF_4]	Shiflett and Yokozeki, 2005	(293.15 to 348.15) K	≤ 2 MPa
	Jacquemin *et al.*; 2006;		
	Aki *et al.*, 2004	(298.15, 313.15, 333.15) K	≤ 150 bar
	Kroon *et al.*, 2005	(278.47 to 368.22) K	≤ 70 MPa
1-butyl-3-methylimidazolium hexaflourophosphate [Bmim][PF_6]	Anthony *et al.*, 2002	(283.15 to 323.15) K;	≤ 1 atm;
	Aki *et al.*, 2004	(298.15, 313.15, 333.15) K	≤ 150 bar
	Zhang *et al.*, 2005	(297 to 328) K	0 to 11 Mpa
	Kamps *et al.*, 2003	(293.15 to 393.15) K	≤ 9.7 MPa
	Shiflett and Yokozeki, 2005	(293.15 to 348.15) K	≤ 2 MPa
1-ethyl-3-methylimidazolium tetraflouroborate [Emim][BF_4]	Finotello *et al.*, 2008	(293.15, 313.15 328.15, 343.15) K	≤ 1 atm
	Kuhne *et al.*, 2006	(343.15 to 443.15) K	1 to 14 MPa
	Soriano *et al.*, 2008	(303.2 to 343.2) K	≤ 5 MPa
	Lei *et al.*, 2010	(298.2 and 313.2)K	≤ 8 MPa

contd...

Ionic Liquids	Reference	Temperature Range	Pressure Range
1-ethyl-3-methylimidazolium hexaflourophosphate [Emim][PF_6]	Schilderman *et al.*, 2007;	(298.15 to 333.15) K	≤ 9 MPa
	Shariati and Peters, 2004	(308.14 to 366.03) K	1.49 to 97.10 Mpa
1-ethyl-3-methylimidazolium bis(triflouromethylsulfonyl)imide [Emim][Tf_2N]	Camper *et al.*, 2006;	(303.15 to 343.15) K	0.32 - 0.76 psi
	Finotello *et al.*, 2008	(293.15, 313.15 328.15, 343.15)	≤ 1 atm
	Ren et al., 2009	(298.15, 323.15, 343.15)	≤ bar
	Carvalho *et al.*, 2009	(293 to 363) K	≤ 50 MPa
1-hexyl-3-methylimidazolium tetraflouroborate [Hmim] [BF_4]	Chen *et al.*, 2006	(293.15, 313.15 328.15, 343.15) K	≤ 1 atm
	Zhang *et al.*, 2006	(305 to 325) K	1 to 9 MP
	Kroon *et al.*, 2010	(254.64 to 348.17) K	2.102 to 13.189 MPa
1-hexyl-3-methylimidazolium bis(triflouromethylsulfonyl)imide [Hmim][Tf_2N]	Kumelan *et al.*, 2006;	(293.2 to 413.1) K	≤ 10 MPa
	Ren *et al.*, 2009	(298.15, 323.15, 343.15) K	≤ bar
	Finotello *et al.*, 2008	(293.15, 313.15 328.15, 343.15) K	≤ 1 atm
	Shin *et al.*, 2008	(298.15 to 343.15) K	≤ 45 MPa
	Kumelan *et al.*, 2011	(293 to 373) K	≤ 9.2 MPa

Anthony *et al.* (2002) found that CO_2 has the highest solubilty in 1-butyl-3-methylimidazolium hexaflourophosphate [bmim][PF6] among other gases (ethane,ethylene, methane, argon, oxygen, carbon monoxide, hydrogen and nitrogen) and also reported the vapor-liquid equilibrium of water with butyl methyl

imidazolium hexaflourophosphate ([bmim][PF_6]), octyl methly imidazolium hexaflourophosphate ([C_8mim][PF_6]) and octyl methly imidazolium tetraflouroborate ([C_8mim][BF_4]). Kumelan *et al.* (2006) reported the solubility of CO_2 in 1-hexyl-3-methylimidazolium bis(trifluoromethylsulfonyl)imide ([hmim][Tf_2N]). On the other hand, Yuan *et al.* (2007) studied the solubility of CO_2 in hydroxyl ammonium ionic liquids and concluded that the solubility of CO_2 in these ionic liquids increase with an increase in pressure and the trend was reverse for the case of temperature.

The solubilities of CO_2 at high pressures have been investigated by various researchers (Liu *et al.* (2003); Kamps *et al.* (2003); Kim *et al.* (2005) and Chen *et al.* (2006)). Most of them concluded that the CO_2 solubility in ILs increase almost linearly with an increase in gas pressure and decreasing with increasing temperature. The trends observed on the CO_2 solubility in ILs with pressure is the characteristic of physical solubility. While the solubility of CO_2 at high pressures have received great attention, solubility of CO_2 at low pressure conditions using ILs received least attention. However, in fully utilizing the properties of ILs, it would also be useful to study their ability towards the solubility of gases at lower pressure.

Pure ILs are highly viscous in their natural/ unreacted states which makes it difficult for transferring/ pumping them for continous/ batch operations, which requires high energy input. Therefore, ILs have to be heated before pumping process which is time/ energy consuming or the pure ILs must be diluted before further use. The solubility of CO_2 in aqueous solution of ILs have not received great attention from the researchers, which might be due to the facts that not all ILs are soluble in water. The data on the physical properties and the solubility of CO_2 in aqueous solution of ILs are not readily available. Feng *et al.* [2010] studied the aqueous solutions of four types of Task Specific Ionic Liquid (TSIL) that is fully dissociated in CO_2 namely tetramethylammonium glycinate ([N_{1111}][Gly]), tetraethylammonium glycinate ([N_{2222}][Gly]), tetramethylammonium lysinate ([N_{1111}][Lys]) and tetraethylammonium lysinate ([N_{2222}][Lys]) for CO_2 absorption. The results obtained by Feng *et al.* for the ([N_{1111}][Gly]) are shown in Table 2.3. With a brief literature review, it can be concluded that not much data on the solubility of CO_2 in aqueous solution are available for other ILs, except that have been discussed

above. Therefore, more research is needed for the selection of suitable types of ILs that can be dissolved in water or in any molecular solvents, before it can be used further for the studies on the solubility of CO_2.

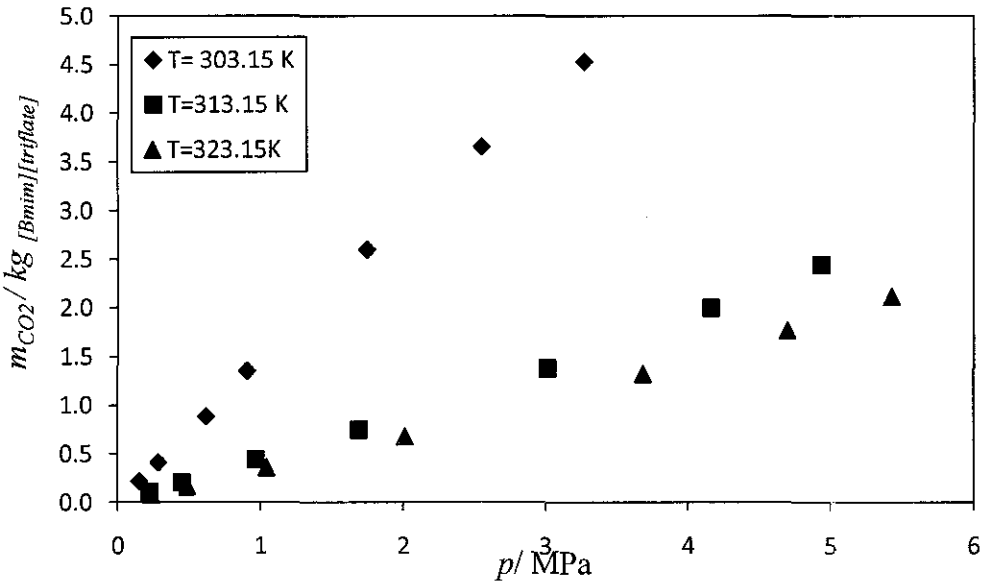

Figure 2.12. Experimental results for the solubility of carbon dioxide in 1-butyl-3-methylimidazolium trifluoromethanesulfonate [Bmim][triflate] at 303.15, 313.15 and 323.15 K (Soriano et al., 2009).

Table 2.3. Absorption amount of CO_2 in aqueous solutions of ($[N_{1111}][Gly]$) at room temperature (feng et al., 2010).

IL (wt%)	mol CO_2/ mol IL
30	0.169
50	0.253
65	0.311
80	0.402
100	0.601

2.4 Solubility of CO_2 in mixtures of amines and ILs

Some researchers have found that blending the physical and chemical solvents could improve their efficiency for CO_2 capture. For instance, blends of physical and chemical solvents such as sulphinol-D (sulpholane and DIPA) and sulphinol- M (sulpholane and MDEA) are found effective for the removal of CO_2 and sulphur compound from gas streams (Gupta *et al.* 2003). In their work, sulpholane works as a large storage species for capturing CO_2 while DIPA and MDEA work as the reactive species for capture activities. The main advantage of these blended solvents are the reduction in corrosion rates and also the foaming problems.

By considering the demerits of amines and the high viscosity of ILs, researchers have attempeted to achieve efficient CO_2 capture by combining a physical and a chemical solvent. With the knowledge that the commercially available and inexpensive organic amines, such as MEA, is readily soluble in normal solvents, it could be blended with various types of solvents especially in ILs at room temperature, thus maintaining the performance of MEA and fully utilizing the desirable properties of ILs. The viscosity of ILs is at least one to three orders of magnitude higher than any other conventional solvents. Therefore, the mixing of ILs with alkanolamine, can lower the viscosity of the pure ILs while enhancing the performance of the system. In addition, since ILs are considered as the physical solvent, less heat is required for regenaration, thus makes it a very potential solvent (Sairi *et al.*, 2011)

Zhang *et al.* (2010) have synthesized four functionalized ILs and mixed with water or MDEA aqueous solutions to form a new type of solvent for the absorption of CO_2. They found that the functionalized ILs have greatly enhanced the absorption rate of CO_2 in MDEA aqueous solutions and the highest CO_2 uptake was reported at 15% IL + 15% MDEA aqueous solutions. Functionalized ILs are usually synthesized with amine group in the molecule since it can quickly react with CO_2. The ability to tune the solubility and compatibility properties of ILs with amine are the powerful tools for the optimization process for CO_2 solubility. Therefore, instead of using the functionalized ILs, room temperature ILs are more favoured when blending with amine for the same purposes.

Recently, researchers found that mixtures of room temperature IL (RTIL) and amines can be used for CO_2 capture in a manner similar to their aqueous counterparts. A research group from the University of Colorado, U.S.A was the first group that pioneered the idea of mixing the RTILs and amines. The research group lead by Professor R. D. Noble found that the mixtures of RTILs and amines exhibit a rapid and reversible CO_2 uptake, in which they are capable of capturing 1 mol of CO_2 per 2 moles of dissolved amine (Camper *et al.,* 2008). They claimed that ILs- amine solutions may also offer significant advantages especially in terms of energy requirements based on the facts that ILs have less than one- third of the heat capacity of water, or less than one half on a volume basis. Since the decomplexation of CO_2 from aqueous carbamates require heating the solution to elevated temperature, thus vaporising water and amine, that must be condensed or replenished to the process. The mixtures of ILs and amines has also received a great attention from the industry due to its advantages and its capability in solving or reducing the problem raised by the conventional amine solutions is really promising. ION ENGINEERING is the first company to successfully commerciallize the solutions of ILs and amine for the CO_2 capture. They claimed that the solvent and process solution are capable of significantly reducing the capital and operating costs, increasing gas output, minimizing corrosion and shrinking unit footprints. The ILs – amines solutions also offer dramatically increased cost advantages compared to the conventional aqueous amine solutions which are currently being used in over 95% of U.S. natural gas sweetening operations.

2.5 Summary

Based on the brief literature review on the physical properties of binary and ternary mixtures and the absorption of CO_2 in alkanolamines and ILs, it can be observed that the knowledge of physical properties of any new solvents is important for understanding their behaviour and potential applications in many commercial processes, and gas absorption in particular. The physical properties of aqueous solution of MEA and various ILs individually have been measured by various researchers for a wide range of operation conditions. However, not much

measurement of physical properties have been reported for the IL + MEA mixture. The available data on the excess properties of the mixed solvents are also limited.

Room- temperature ILs + amine solutions behave similar to the aqueous amine solutions that are being currently used, and it is believed that they are capable of delivering significant advantages in terms of energy consumption and reduction in corrosion problems. ILs are known for their high viscosity in nature even though their desirable properties are believed to enhance the solubility of CO_2. Thus, by mixing ILs with amine, the problem regarding high viscosity of ILs can be encountered without disturbing their potential for CO_2 capture. A novel class of solvent such as the aqueous solution of ILs + amine has attracted various researchers in the field of selective separation of gases. The unique properties of ILs favours as potential solvents for CO_2 while solving the problems caused by the alkanolamine solutions.

From the foregoing literature review, it is very clear that there is a need to develop a new combination of IL with amines solvents and to esablish their physical as well as excess properties for their application towards the CO_2 capture. The imidazolium type ILs is a very common ILs used in the absorption of CO_2. Based on the literature survey, the most common ILs from the imidazolium family that are usually used and has proved to posses high efficiency in the absorption of CO_2 including [bmim][BF_4], [bmim][PF_6], [bmim][Tf_2N], [emim][BF_4], [hmim][[BF_4], [hmim][PF_6] and [hmim][Tf_2N]. From the experimental work on investigating the the behaviour of the ILs in water (dissolve or not dissolve), it was found that among the common ILs for the imidazolium family, [bmim][BF_4] was found to dissolve in both water and MEA. Meanwhile, the hydroxyl ammonium ILs, which can be considered as a new type of ILs has increasingly receive great attention due to the capibility of the ILs to capture CO_2. But the literature pertaining the properties as well as the solubility of the ILs from the mentioned family are very scarce. Studies on the hydroxyl ammonium ILs was only reported by Yuan *et al.* (2007) and Kurnia *et al.* (2009, 2010). Therefore, this type of IL was considered as uncommon ILs and further investigation has to be done in order to establish and to prove the efficiency of the ILs.

Therefore, with good history of CO_2 absorption and having good solubility with water and MEA, as well as affordable price and availability, [bmim][BF_4] from the commonly imidazolium type ILs was chose to be use in this work and the effect of temperature and composition on the physical properties and the solubility of CO_2 was also been measured. The results on the physical properties and solubility of CO_2 of the former ILs was being compared with the results on the physical properties and solubility of CO_2 by using the uncommon ILs from the hydroxyl ammonium type IL namely bis(2-hydroxyethyl)ammonium acetate ([bheaa]). The comparison will be made in terms of its variation on temperature and composition with physical properties (density, viscosity, and refractive index) and their behaviour in CO_2 solubility in term of the effects of temperatures, pressures and ILs concentration as well as the effect on the anion and cation of both ILs.

Meanwhile, the amine used in this present study is the primary amine namely monoethanolamine (MEA). From the literature survey, MEA has been used widely for the absorption of CO_2 since its high efficiency as well as high rate of absorption cannot be denied. The usual concentration of MEA used in industry are below 30wt% since highly concentrated MEA can react with the unreacted material such as the vessels and tubelines and can cause corrosion. Therefore, in this work, the concentration of MEA used will be retained accordingly so as to ensure that the concentration doesnt't exceed the concentration used in the industry and in the dsame time, still remained its high efficiency in the CO_2 absorption.

CHAPTER 3

MATERIALS AND METHODS

3.0 Overview

In the present chapter, the details of the materials, experimental setup and the details of the experimental procedures are discussed in detail. This chapter is divided into four sections. Section 3.1 and 3.2 deals with the materials used for the present studies and the preparation of binary and ternary mixtures respectively. The details of the measurement of physical properties namely density, viscosity and refractive index are discussed in section 3.3, whereas the experiments on CO_2 solubility measurement are explained in section 3.4.

3.1 Materials

In the present study, two different types of ILs namely bis(2-hydroxyethyl)ammonium acetate ([bheaa]) and 1-butyl-3-methylimidazolium tetraflouroborate ([Bmim][BF_4]) and monoethanolamine (MEA) were used. The structure of the solvents used is shown in Table 3.1, while the molecular weight and the physical properties, namely density, viscosity and refractive index are presented in Table 3.2. The details of the supplier,

the purity and the specification of the chemicals have been included in this section. The details of the preparation of the binary and ternary mixtures are also discussed in detail.

Table 3.1. The structure of the chemicals used in the present study.

Components	Structure
[bheaa]	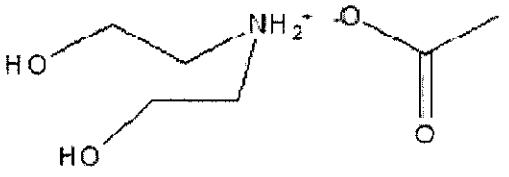
[bmim][BF_4]	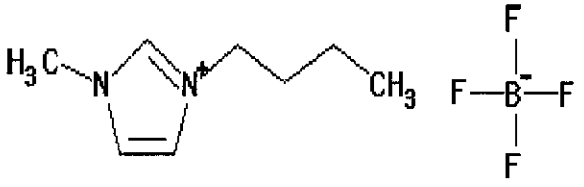
MEA	

Table 3.2. The properties of the pure chemicals used in the present study at T = 298.15 K.

Components	Molecular weight ($g.mol^{-1}$)	Density ($g.cm^{-3}$)	Viscosity (mPa.s)	Refractive Index
[Bheaa]	165.20	1.17172	560.23	1.48113
[Bmim][BF4]	226.02	1.20057	111.92	1.42425
MEA	61.08	1.01251	17.44	1.45432

3.1.1 Ionic Liquids

For the present study the IL bis(2-hydroxyethyl)ammonium acetate ([bheaa]) was synthesized in our laboratory, while 1-butyl-3-methylimidazolium tetrafluoroborate ([Bmim][BF4]) was purchased from Merck Sdn Bhd, Malaysia with purity < 99%. Prior to its use, both ILs were dried for 24h under vacuum at temperatures 373.15K to remove any possible traces of water and impurities. The water contents were determined using a coulometer Karl Fischer titrator, DL 39 (Mettler Toledo) using the Hydranal coulomat AG reagent (Riedel-de Haen). The estimated water content of [bheaa] was 166 ppm while the water content for [Bmim][BF_4] was 320 ppm.

3.1.2 Monoethanolamine (MEA)

MEA was obtained from Aldrich (AR grade) with a purity of ≤ 99% and was used without further purification.

3.2 Preparation of samples

The experimental set up and procedures used for the present research are presented in this section which include:

1. The preparation of the samples

2. Measurement of physical properties

3. Solubility of carbon dioxide.

3.2.1 Preparation of Binary and Ternary Mixtures for Physical Properties Measurement

All samples were prepared freshly and retained at room temperature for 24h, to ensure their solubility at the desired temperature. The samples were prepared based on mass fraction using an analytical balance (model AS120S, Mettler Toledo) with a precision of ±0.0001 g. All samples were kept in airtight glass vials and sealed with parafilm to prevent any possible humid effects on the samples.

3.2.1.1 Preparation of Binary Mixtures

Four binary mixtures involving IL+water ([bheaa] + water; [bmim][BF_4] + water) and IL+MEA ([bheaa] + MEA; [bmim][BF_4] + MEA) were used in the present study. The mixtures were prepared based on mass and later were converted to mole fraction. The range of mole fraction varies from 0.1 to 0.9 and the possible error in the mole fraction calculations was estimated to be around ± 0.0001.

3.2.1.2 Preparation of Ternary Mixtures

Two ternary mixture of IL+ MEA+ Water system ([bheaa] + MEA + water; [bmim][BF_4] + MEA + water) were prepared based on three constant ratio of $z = x_3/x_1$, whereby x_1 is the mole fraction of ILs and x_3 is the mole fraction of water, with varying mole fraction of MEA (x_2). The ratio of ILs over water were chosen in such a way that the mole fraction of all components involved must have the possible highest and lowest values. The ratio of both ILs over water (z), used in the present study are shown in Table 3.3.

3.2.2 Preparation of Samples for CO_2 Solubility Measurement.

The samples were prepared based on the mass fraction. For the CO_2 solubility measurements, the following three solvents were prepared:

(1) pure ILs;

(2) ILs aqueous solutions (20wt% to 80wt%);

(3) ILs + MEA aqueous solutions.

Table 3.3. The ratio of [bheaa] and [Bmim][BF4] over water for the preparation of ternary mixtures

Ternary Systems	Ratio '*z*' (molse of ILs/ moles of water
[Bheaa] + MEA + water	0.11
	0.62
	4.03
[Bmim][BF4] + MEA + water	0.08
	0.32
	5.03

3.3 Measurement of Physical Properties

The density, viscosity and refractive index for both binary and ternary system were measured at temperature from 293.15 K to 353.15 K at atmospheric pressure for the whole range of composition.

3.3.1 Density

The density of the binary and ternary mixture including the pure MEA, [bheaa] and [Bmim][BF_4] were measured using an oscillating U-tube density meter (model DMA-5000 M, Anton Paar) at temperatures from (293.15 to 353.15) K with a built-in platinum resistance thermometer with an uncertainty of ± 0.01 K . Figure 3.1 shows

the density meter used for the present studies. The apparatus was calibrated frequently, by measuring the density of milipore quality water and dry air at regular intervals as instructed by the supplier and validated using several established data of pure organic and ionic liquids of known densities. The apparatus is precise to within $1 \cdot 10^{-5}$ g·cm^{-3} and the uncertainty of the measurements was better than $4 \cdot 10^{-5}$ g·cm^{-3}. The density measurements for all samples were made in triplicate and the average values were considered for further analysis.

Figure 3.1. The Oscillating U- Tube density meter (Anton Paar model DMA-5000M).

3.3.2 Viscosity

The viscosity of all the binary and ternary mixtures including the pure MEA, [bheaa] and [Bmim][BF_4] were measured using Ubbelohde viscometer. Suitable capillary size was selected based on their viscosity value. Four different size of capillaries (1, 1B, 2B and 2C) were used in the present study (Table 3.4). The viscometer was immersed in a thermostatic water bath with an accuracy of $\pm$ 0.01 K. The samples were maintained at the required temperature for a minimum of 1 hour to ensure thermal stability. The efflux time of the samples through the capillary was measured manually using a digital stopwatch with an accuracy of 0.01 seconds. The viscometers used were initially calibrated using distilled water and further validated using several established data of pure organic and ionic liquids. The experiments were repeated

atleast three times for all compositions and temperatures and the average values were considered for futher calculations. The kinematic viscosities were obtained using the following equation:

$$v = k(t - \upsilon) \tag{3.1}$$

where k is the capillary constant of the viscometer, t, is the efflux time and υ is the hagenbach correction. The dynamic viscosities were estimated using the following equation:

$$\eta = \rho \cdot v \tag{3.2}$$

where ρ is the measured density (g/cm^{-3}) of the sample.

Table 3.4. The range of viscosity for different capillary size

Size	Kinematic Viscosity Range (mm^2/s)
1C	6 to 30
1B	10 to 50
2C	60 to 300
2B	100 to 500

3.3.3 Refractive Index

The refractive indices of all the binary and ternary mixtures including the pure MEA, [bheaa] and [bmim][BF_4] were measured using the digital refractometer (ATAGO model RX-5000) with a measuring accuracy of ±4.10^{-5} in the temperature range of (293.15 to 353.15) K and the equipment is shown in Figure 3.2. The temperature of

the apparatus was controlled to within ±0.05 ^{0}C. The apparatus was calibrated by measuring the refractive index of milipore quality water and again validated using several established data of pure organic liquids. All the measurements were made in triplicate and the average values were used for further analysis.

Figure 3.2. The Digital Refractometer (ATAGO model RX-5000)

3.4 Measurement of Solubility of Carbon Dioxide

The SOLTEQ High Pressure Gas Solubility Cell (Model: BP-22) was used for the gas solubility measurements. The schematic diagram of the apparatus used in the present study is shown in Figure 3.3. The SOLTEQ High Pressure Gas Solubility Cell consists of a jacketed storage vessel and a jacketed absorption cell, for maintaining the temperature in both cells. Other supporting components include the magnetic stirrer, circulation pumps, vacuum pump, thermostat heating bath, liquid feed pump, liquid degassing unit and instrumentations such as mass flow controllers, pressure and temperature indicators. The unit has the provision to accommodate a mixture of 12 possible types of gases namely, carbon dioxide, hydrogen sulfide, sulfur dioxide, nitrogen dioxide, oxygen, methane, ethane, propane, n-butane, iso-butane, n-pentane and iso-pentane.

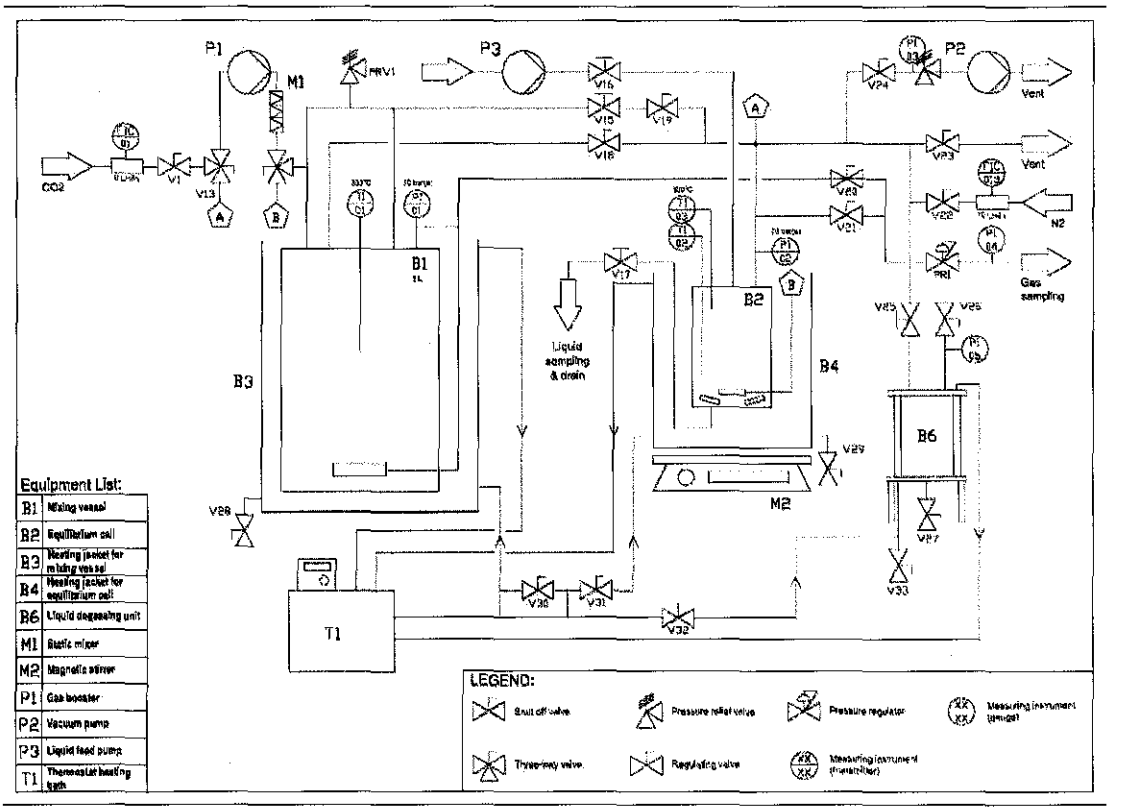

Figure 3.3. Schematic Diagram of High Pressure Gas Solubility Equipment (SOLTEQ, model BP-22).

3.4.1 Procedure for Measuring CO_2 Solubility in Solvents

The pressure drop method was used for the CO_2 solubility in the hybrid solvents whereby the volume was maintained as constant, while the change in pressure drop in the equilibrium cell was monitored during the absorption of gas by the solvents. Before operating the unit, both gas mixing vessel and equilibrium cell (50ml) were evacuated using the turbomolecular vacuum pump. After achieving a specific level of vacuum, the pure CO_2 gas was initially charged into the mixing vessel. Pressurized CO_2 in the mixing vessel (P_0) was then charged into the equilibrium cell where desired pressure and temperature were maintained. A known weight of absorbent was then fed into the equilibrium cell. Initially, the equilibrium cell was purged with nitrogen and evacuated to a pressure of < 5kPa. The equilibrium cell consists of a magnetic stirring bar and was seated on top of a magnetic stirrer for enhancing the contact between the gas and liquid mixture. Furthermore, a circulation pump was attached to the equilibrium cell, for the circulation of gases from the top of the cell

into the liquid at the bottom to enhance the contact between the two phases. Both mixing vessel and equilibrium cell were immersed in a circulating bath inside individual heating jackets, which were connected to a thermostat heating bath to maintain constant temperature throughout the unit. The water circulator (JULABO) was used to maintain the temperature within ±0.1 K.

As CO_2 in the equilibrium cell dissolved in the liquid, pressure inside the cell started to decrease. The pressure drop in the equilibrium cell was recorded for every one minute. Once the pressure is constant, the solubility process has reached a steady state level. Analysis of both gas and liquid samples were carried out to determine the solubility of gases in the liquid. The pressure of the system was recorded by a digital pressure indicator (Druck DPI 150) with a precision of ±0.1 kPa for a range of (0 to 7000) kPa. Temperature of the equilibrium cell was measured using a digital thermometer (YOKOGAWA 7653) with a precision of ±0.01 K. When the pressure in the equilibrium cell (P) reaches a constant value and retained for at least 2h, the equilibrium was assumed and the final values were noted.

The amount of gas absorbed were calculated based on the measured pressure drop in the equilibrium cell using the following equation:

$$n_{CO_2} = \frac{((P_0/Z_0)-(P/Z))(V_M + V_E + V_L) + P_V V_L}{RT} \tag{3.3}$$

where n_{CO_2} is the mole of CO_2, V_M and V_E are the volumes of mixing vessel and equilibrium cell, respectively. V_L represents volume of liquids (absorbents), Z is compressibility factor and P_v is the saturated vapor pressure of liquid.

The experiments were conducted to study the effect of the nature of pure ionic liquids, their combinations with amine and water, on the rate as well as on CO_2 loading. The effect of temperature and pressure on CO_2 loading were also studied. The experiments were performed in three stages: i) the absorption of CO_2 by using the

aqueous [bheaa] and [bmim][BF_4] solutions (20 to 100 wt%) at 5 different pressures ($\leq$ 1600kPa); ii) the absorption of CO_2 by using aqueous [bheaa] and [bmim][BF_4] solutions with highest CO_2 loading (stage i) that are mixed with several fractions of aqueous alkanolamine (MEA) at 5 different pressures ($\leq$ 1600kPa); iii) the absorption of CO_2 by using [bheaa] + MEA + water and [bmim][BF_4] + MEA + water solution with highest CO_2 loading (from stage (ii)) at 3 different temperatures (298.15, 308.15 and 313.15 K) and at fixed pressure to study the effect of temperature.

CHAPTER 4

RESULTS AND DISCUSSION

4.0 Introduction

The knowledge of thermophysical properties of solvents used in any chemical process is important in order to understand the nature of their fundamental behaviour. It is also essential to establish these fundamental properties for the design, scale-up and sizing of the equipments for commercial applications of the solvent. Besides the physical behaviour, the knowledge of thermophysical properties will also provide an insight about their chemical behaviour such as van der waals forces, hydrogen bonding, intramolecular bonding and also the interactions between solute - solvent and solvent - solvent. The understanding of the stated behaviour will also help in determining the optimal properties of the solvents for further application. Therefore, in order to understand the physical and chemical behaviour of the mixed solvents used, the present chapter discuss the thermophysical properties namely density, viscosity and refractive index for pure, binary and ternary mixtures of both ILs (namely bis(2-hydroxyethyl)ammonium acetate, [bheaa] and 1-butyl-3-methylimidazolium tetraflouroborate, [bmim][BF_4]) with monoethanolamine (MEA) and water. The details of the estimated excess properties namely excess molar volume V^E, viscosity deviation $\Delta\mu$ and refractive index deviation Δn_D are also discussed in details. All properties were measured at atmospheric pressure and at temperatures from 293.15 K to 353.15 K. The binary mixtures involved were [bheaa]

+ water and [bheaa] + MEA, and [bmim][BF_4] + water and [bmim][BF_4] + MEA at all composition ranges while the ternary mixtures were [bheaa] + MEA + water and [bmim][BF_4] + MEA + water. Since there are no reference available on the density, viscosity and refractive index of the mentioned binary and ternary system, therefore for validation purposes, comparison of the measured data with literature were only made for pure components at various temperatures. The measured value of densities, viscosities, refractive indices and the estimated excess properties are presented in tables in Appendix A- F and the details are discussed below. This chapter also discuss about the results on CO_2 solubility in present developed hybrid binary and ternary solvents, and also the effect of varies parameters on CO_2 loading.

4.1 Density

The density of the binary mixtures at all compositions including the pure MEA, [bheaa] and [bmim][BF_4] were measured using an oscillating U-tube density meter (model DMA-5000 M, Anton Paar) at temperatures from (293.15 to 353.15) K with a built-in platinum resistance thermometer with an uncertainty of ± 0.01 K. The apparatus is precise to within $1 \cdot 10^{-5}$ g·cm^{-3} and the uncertainity of the measurements was better than $3 \cdot 10^{-5}$ g.cm^{-3}. The complete description of the apparatus used have been discussed in section 3.3.1. Before and during the actual measurements, the apparatus was calibrated by measuring the density of milipore quality water and dry air at regular intervals as instructed by the supplier and validated using several established data of pure organic liquids of known densities.

The measured densities of pure components involved in this research are presented in Table 4.1. The comparison of densities between the experimental data and published literature data for pure solvents namely MEA, [bheaa] and [bmim][BF_4] is shown in Figure 4.1. The calculated deviation of measurement values from the reported data at all temperatures are found to be ≤ 0.2% for [bheaa], ≤ 0.1% for [bmim][BF_4] and ≤ 0.3% for MEA. It proves that the results obtained are in good agreement with the literature.

It can be seen from the table that the density of pure [bmim][BF_4] is higher than the density of pure [bheaa] and pure MEA. This shows that the molecule of pure

[bmim][BF_4] is heavier than the molecule of [bheaa] and MEA. The molecular weight are in the order of: [bmim][BF_4] (MW: 226.02 g.mol^{-1}) ≥ [bheaa] (MW: 165.20 g.mol^{-1}) ≥ MEA (MW: 61.08 g.mol^{-1}).

Table 4.1. The measured densities of pure components at temperature from (303.15 to 353.15) K

T/ K	ρ (g·cm^{-3})		
	MEA	[bheaa]	[bmim][BF_4]
303.15	1.01067	1.16862	1.19698
313.15	1.00277	1.16229	1.18986
323.15	0.99480	1.15584	1.18281
333.15	0.98675	1.14928	1.17583
343.15	0.97862	1.14276	1.16890
353.15	0.97040	1.13612	1.16204

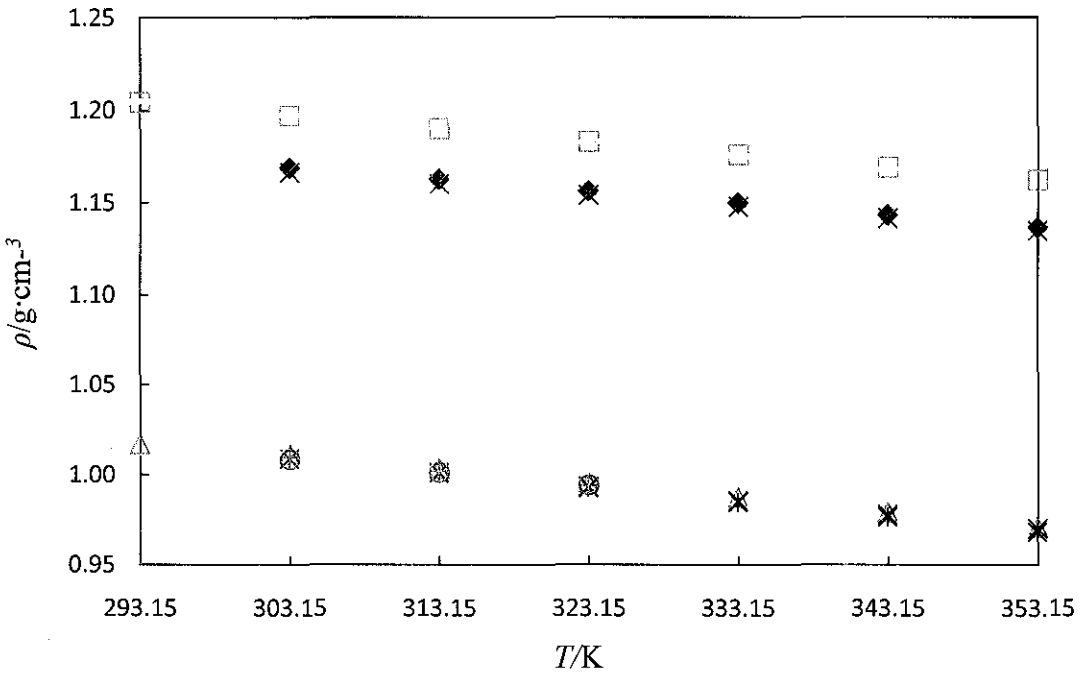

Figure 4.1. Comparison of experimental densities data with literature: ◆, [bheaa] this work; X, kurnia *et al.* (2009); △ , MEA this work; X , Jacinto *et al.* (2008); ✳ , Alain *et al.* (2005); ○, Geng *et al.* (2008); +, Song *et al.* (1996); □ ,[bmim][BF_4] this work; , Jacquemin *et al.* (2008).

4.1.1 Binary mixtures

[bheaa] system

The present experimental values of density of [bheaa] – water and [bheaa] – MEA system at temperature range (303.15 to 353.15) K are presented in Table A-1 of Appendix A. From the analysis of data, it was found that the densities are more dependent on the mole fraction of [bheaa] or MEA in the solution. But the trend for all the two systems are similar where the density values decreased with increasing temperature. On the other hand, density for [bheaa]-water system were found to increase with increasing [bheaa] composition up to $x_{BHEAA} \approx 0.5$. The increment for the density value above the stated [bheaa] composition were also found to be very small and becomes nearly constant. In contrast with [bheaa]-water system, the density values for [bheaa] -MEA system increased with [bheaa]composition. The increasing behaviour of the density with respect to [bheaa] composition is due to the fact that the density of pure [bheaa] are 1.2 times higher that the density of water and MEA.

The variation of density with temperatures, for the whole range of compositions are shown in Figure 4.2 and 4.3 respectively.

As can be seen from both figures, the value for densities are found to decrease with increasing temperature eventhough the variation is very small. The obtained results on the behaviour of density as a function of temperature are found to be similar with few literatures who also used binary mixtures involving similar ILs (Zhou *et.al.*,2010; Pereiro *et.al*, 2009; Anouti *et al.*, 2009).

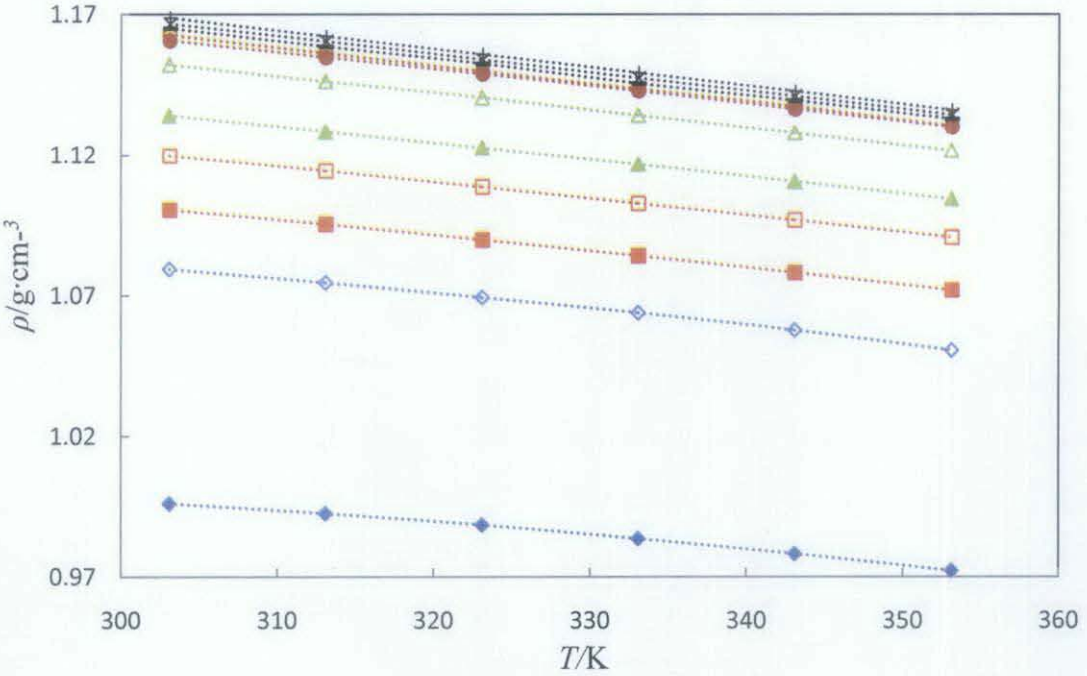

Figure 4.2. Plot of experimental values of density ρ against temperature T and fitted curve (----) for [bheaa] (1) + water (2) binary mixture: ◆ , 0.0000; ◇ , 0.0678; ■ , 0.0995; □, 0.1432; ▲ , 0.2005; △ , 0.3159; ● , 0.4659; ○ ,0.6045; —, 0.7465; X , 0.8700; + , 1.0000.

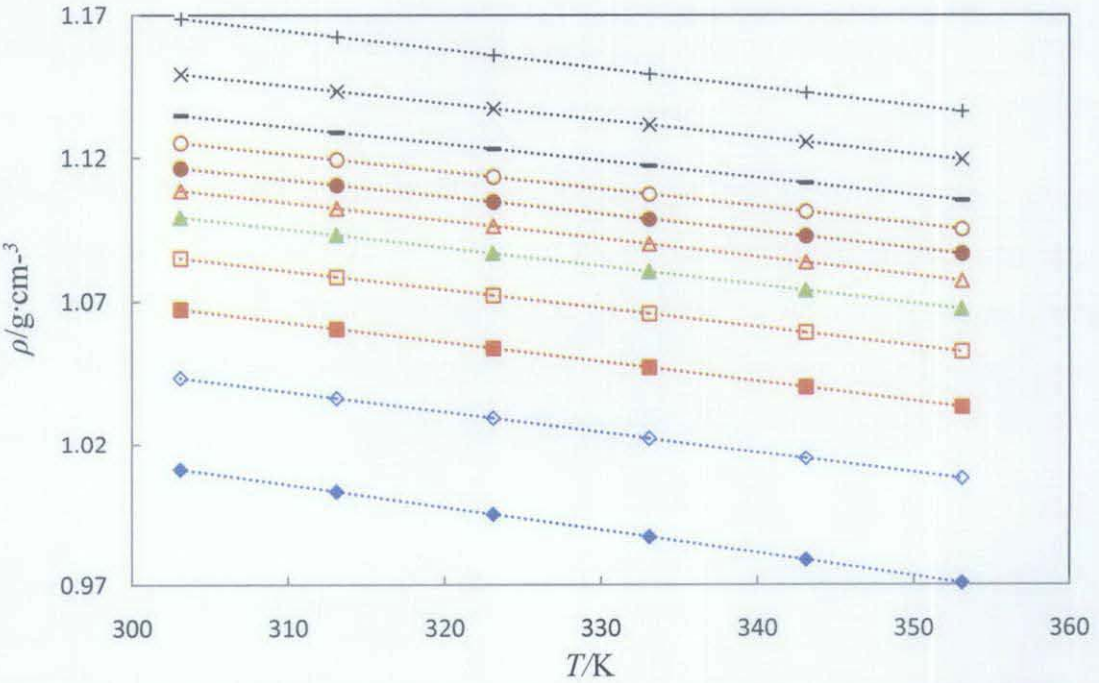

Figure 4.3. Plot of experimental values of density ρ against temperature T and fitted curve (----) for [bheaa] (1) + MEA (2) binary mixture: ◆ , 0.0000; ◇ , 0.1000; ■ , 0.2028; □, 0.3000; ▲ , 0.4000; △ , 0.5000; ● , 0.5998; ○ ,0.7001; —, 0.8004; X , 0.9000; + , 1.0000.

[bmim][BF4] system

The densities of [bmim][BF_4] - water and [bmim][BF_4] - MEA have been measured over the temperature range from T = (293.15 to 353.15) K and are presented in Table A-2 of Appendix A. It can be seen that the density values decrease with decreasing mole fraction of [bmim][BF_4]. The density of pure [bmim][BF_4] was found to be 1.2 times higher than the density of pure water and MEA.the density of the binary mixtures of [bmim][BF_4] was also found to has higher value than the binary mixtures of [bheaa] due to the higher density of [bmim][BF_4] at its pure state. It can also be seen that the densities of the binary systems decrease with increasing temperature, similar to those for [bheaa] systems. The variation of density with respect to temperature for both the mixtures are shown in Figure 4.4 and 4.5.

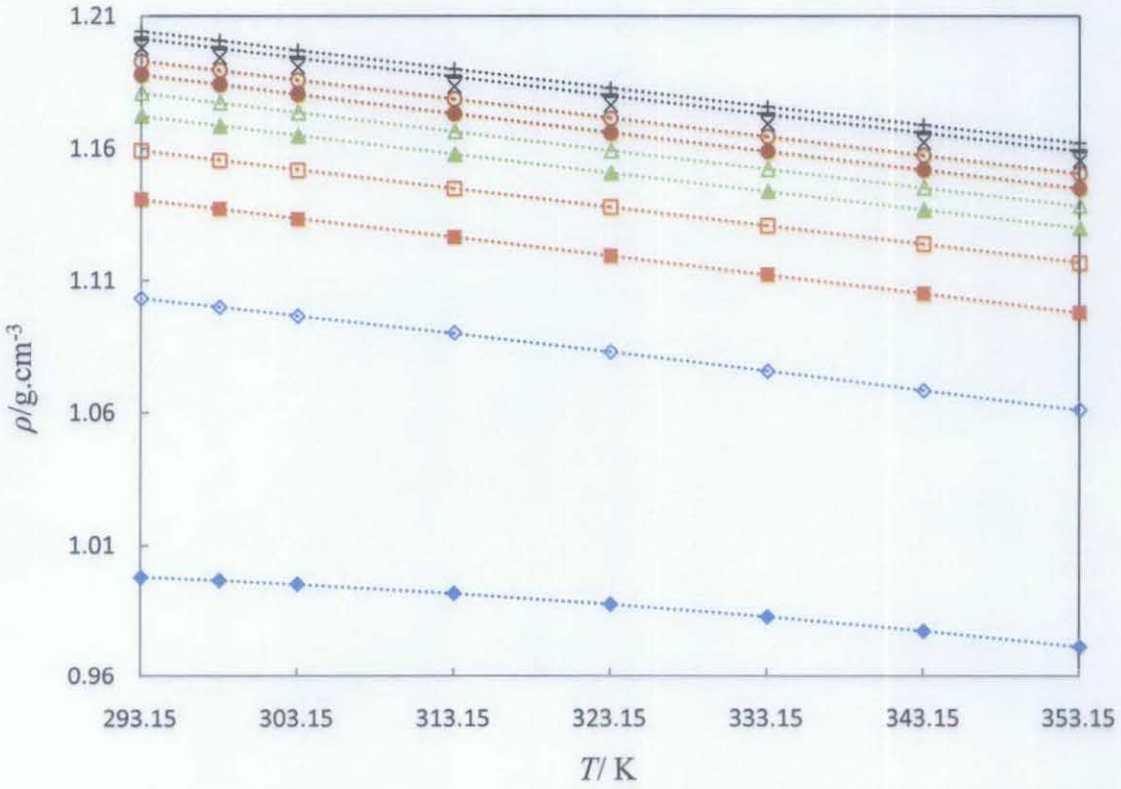

Figure 4.4. Plot of experimental values of density ρ against temperature T and fitted curve (----) for [bmim][BF_4] (1) + water (2) binary mixture: ◆, 0.0000; ◇, 0.1000; ■, 0.2000; □, 0.2950; ▲, 0.4016; △, 0.5002; ●, 0.5963; ○,0.6997; X, 0.8014; —, 0.8988 ; +, 1.000

Correlation of density data for binary systems.

Based on the results obtained for all binary systems, it is observed that densities can be analysed as the function of composition and temperature. Since the dependency of density with composition is predominance than the temperature, an attempt has been made to correlate the measured density data as a function of composition using the following form of polynomial equation:

$$\rho = A_0 + A_1 x + A_2 x^2 + A_3 x^3 + A_n x^4 \qquad (4.1)$$

where ρ is the density, A_0, A_1, A_2, A_3 and A_4 are the correlation coefficients and x is the mole fraction of ILs.

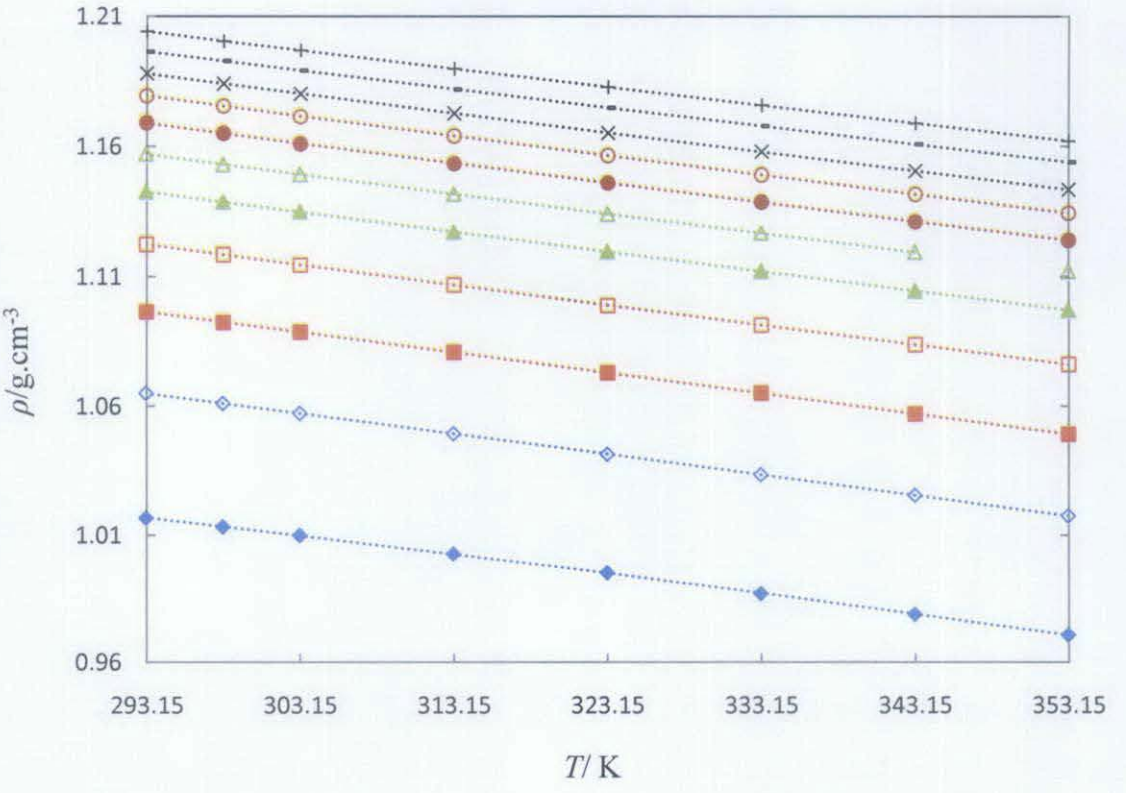

Figure 4.5. Plot of experimental values of density ρ against temperature T and fitted curve (----) for [bmim][BF_4] (1) + MEA (2) binary mixture: ◆, 0.0000; ◇ , 0.0999; ■, 0.2001; □, 0.2994; ▲ , 0.4004; △ , 0.4999; ● , 0.5994; ○, 0.7005; X , 0.7992; — , 0.9002 ; + , 1.000

The estimated correlation coefficient of equation (4.1) are found to be a function of temperature. Hence, the coefficients are also being correlated with the temperature using the following form of equation:

$$A_n = B_0 + B_1 T + B_2 T^2 + B_3 T^3 + B_k T^k \tag{4.2}$$

where A_n is the correlation coefficients obtained using equation 4.1, B_0, B_1, B_2, B_3 and B_k are the correlation coefficients (for equation (4.2)) as the function of temperature and T is the experimental temperature (K). The standard deviations (σ) are calculated using the following equation

$$\sigma = \left[\frac{\sum (Z_{\exp} - Z_{cal})^2}{n} \right]^{\frac{1}{2}} \tag{4.3}$$

where n is the number of experimental points, Z_{exp} and Z_{cal} are experimental and calculated values, respectively.

All the correlation coefficients for both the binary systems involving [bheaa] ([bheaa] + water, [bheaa] + MEA) and [bmim][BF_4] ([bmim][BF_4] + water, [bmim][BF_4] + MEA) were estimated using least square method, and the values for the coefficients are presented in Table A-3and A-4 of Appendix A respectively.

The thermal expansion coefficients α_p is a measure of volume changes in the mixture with temperature. It can be calculated from the measured densities using the following equation:

$$\alpha_p / \left(K^{-1}\right) = -\frac{1}{\rho}\left(\frac{\partial \rho}{\partial T}\right)_P \tag{4.4}$$

where α_p is the thermal expansion coefficient, ρ is the density and T is the temperature while subscript P indicates constant pressure. A careful examination on the measured values of densities reveal that the densities do not increase linearly with temperature eventhough to the eye, it looks linear. By increasing the composition of either water or MEA in the systems, the temperature dependence becomes distinctly nonlinear. A second order polynomial of the following form was used to represent the density data as a function of temperature, for different concentrations.

$$\rho = C_0 + C_1 T + C_2 T^2 \tag{4.5}$$

where T is the temperature and C_0, C_1 and C_2 are correlation coefficients. A similar type of polynomial equation was also used by Rodriguez and Brennecke (2006) to estimate the thermal expansion coefficients for ILs – water systems. The correlation coefficients were estimated using least square method, and the values of the coefficients (equation 4.5) are listed in Table A-5 and A-6 of Appendix A for [bheaa] binary systems and [bmim][BF_4] binary systems respectively. The partial derivative of the right hand side of equation (4.5) was used to estimate the thermal expansion coefficient (equation 4.4) and the estimated coefficients are summarized in Table A-7 for [bheaa] binary systems and A-8 of Appendix A for [bmim][BF_4] binary systems.

From the table, it can be seen that the thermal expansion coefficient of the binary mixture [bheaa] – water and [bheaa] – MEA system increase with increasing temperature. The thermal expansion coefficient also varies with mole fraction. For [bheaa] – water system, the thermal expansion coefficient increase with increasing mole fraction of [bheaa] particularly at lower temperature while for [bheaa] – MEA system, it decrease with an increase in [bheaa] mole fraction. However, this trend also shows that the change in the thermal expansion coefficient with temperature for both systems is not as significant as compared to the change with mole fraction, which are in good agreement with most of literature data (Kurnia et al., 2011; Ziyada *et al.*, 2010; Iglesias *et al.*, 2010).

On the other hand, for [bmim][BF_4] – water system the variation of thermal expansion coefficients is significant with increasing temperature and it increases with increasing mole fraction of [bmim][BF_4]. But for the case of [bmim][BF_4] - MEA binary mixtures, the variation with temperature is not significant and it decreases with increasing mole fraction of [bmim][BF_4].

4.1.2 Ternary Mixtures

The measured density values of ternary system involving [bheaa] + MEA + water at temperature ranging from 303.15 to 353.15 K are presented in Tables A-9 of Appendix A. From the analysis of the data, it was found that the density values increased with increasing ratio of 'z', mole fraction of [bheaa] over mole fractions of water. Figure 4.6 shows the variation of density for all ratios at different temperatures studied.

a)

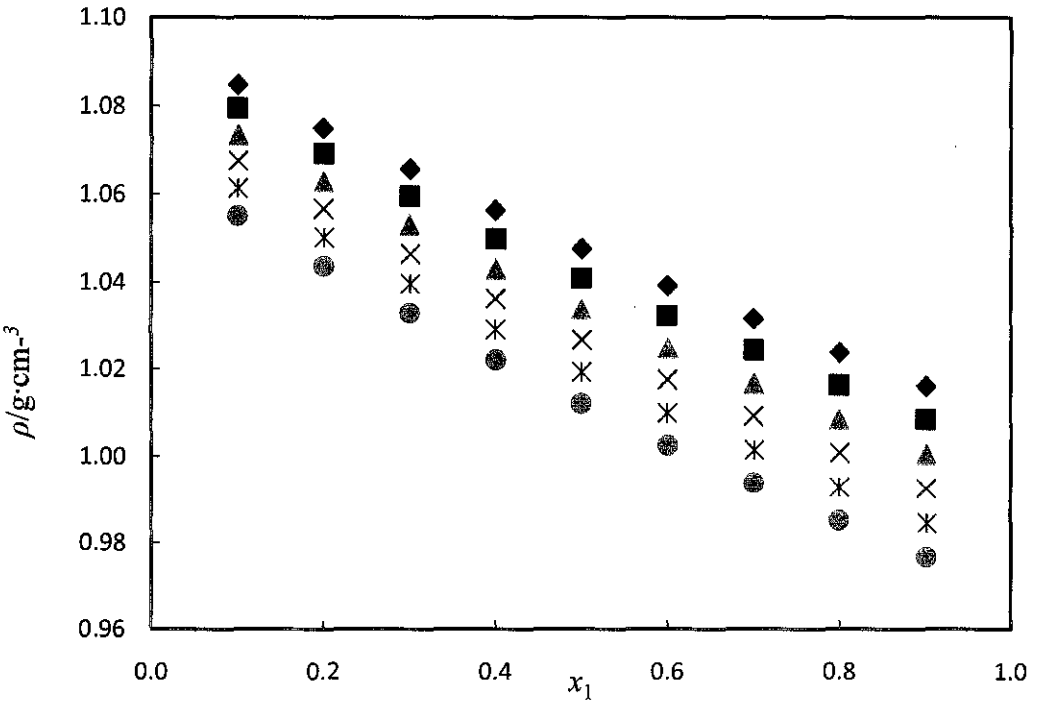

b)

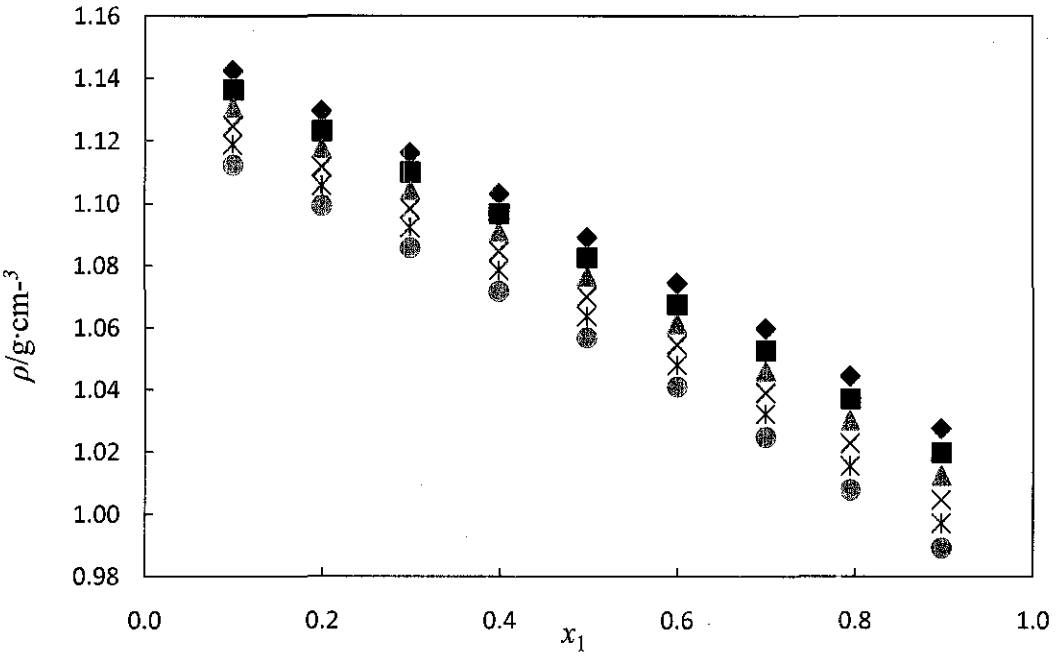

c)

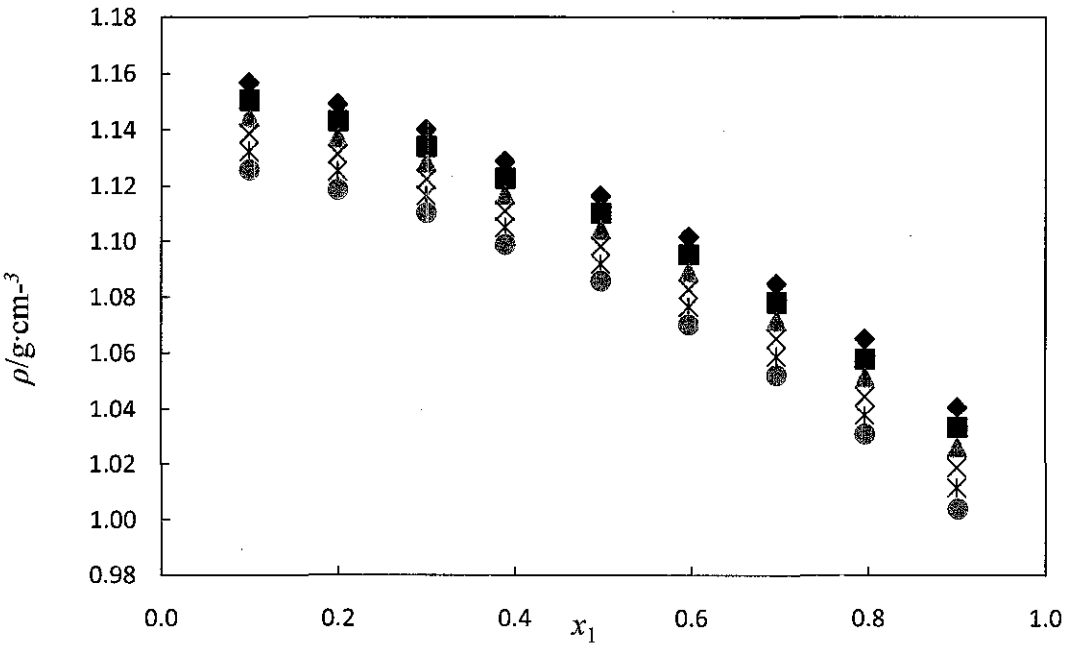

Figure 4.6. Plot of experimental values of density, ρ, of the ternary mixtures for [bheaa] (x_1) + MEA (x_2) water (x_3) against mole fraction of MEA at constant: a) z = 0.11; b) z = 0.62; c) z = 4.03 at temperatures: ◆ , 303.15 K; ■ , 313.15 K; ▲, 323.15 K; X, 333.15 K; ✳ , 343.15 K; ● , 353.15 K.

From the figures, it can be seen that the density values of the ternary mixtures behave similarly for all '*z*' with decreasing value when the temperatures are increasing and also with increasing mole fraction of MEA.

On the other hand, the experimental density values of ternary system involving [bmim][BF_4] + MEA + water at temperature ranging from 293.15 to 353.15 K are presented in Tables A-10 of Appendix A. It can also be seen that the trends for density values of [bmim][BF_4] ternary system is similar to the trends for the density values of [bheaa] ternary system whereby the density values increased with increasing ratio of mole fraction of [bmim][BF_4] over mole fractions of water, '*z*' and decreased with increasing temperature and increasing mole fraction of MEA for all value of *z*. The variation of density for all ratios at different temperatures studied are shown in Figure 4.7.

a)

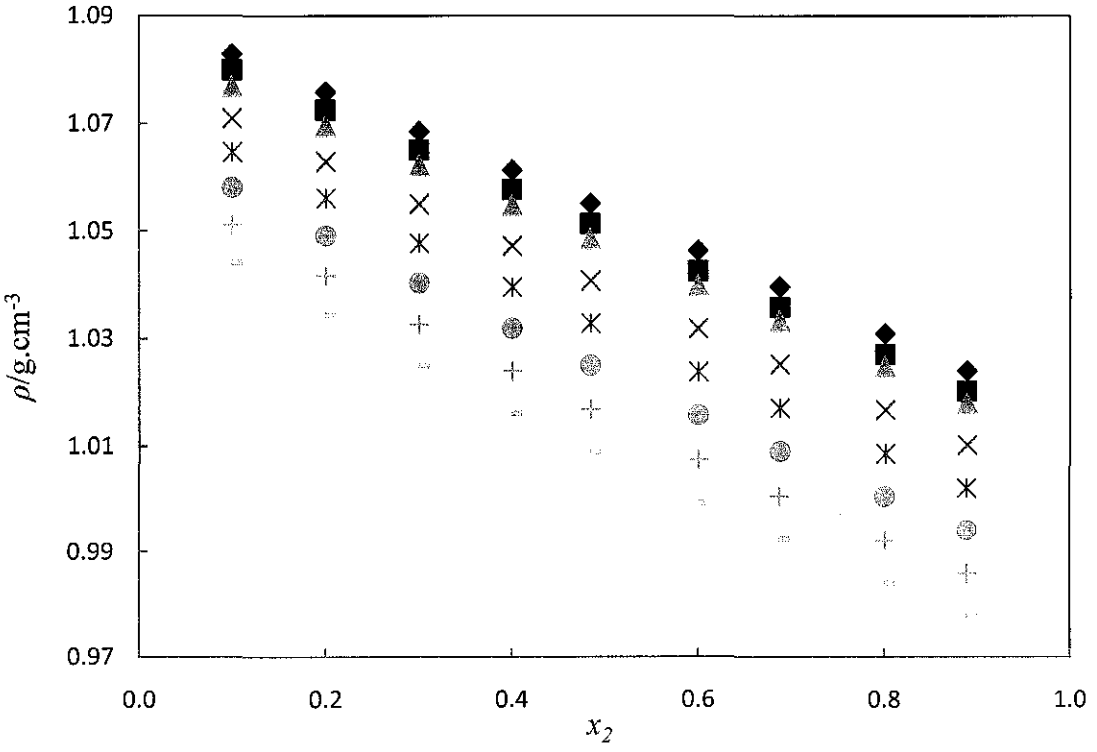

b)

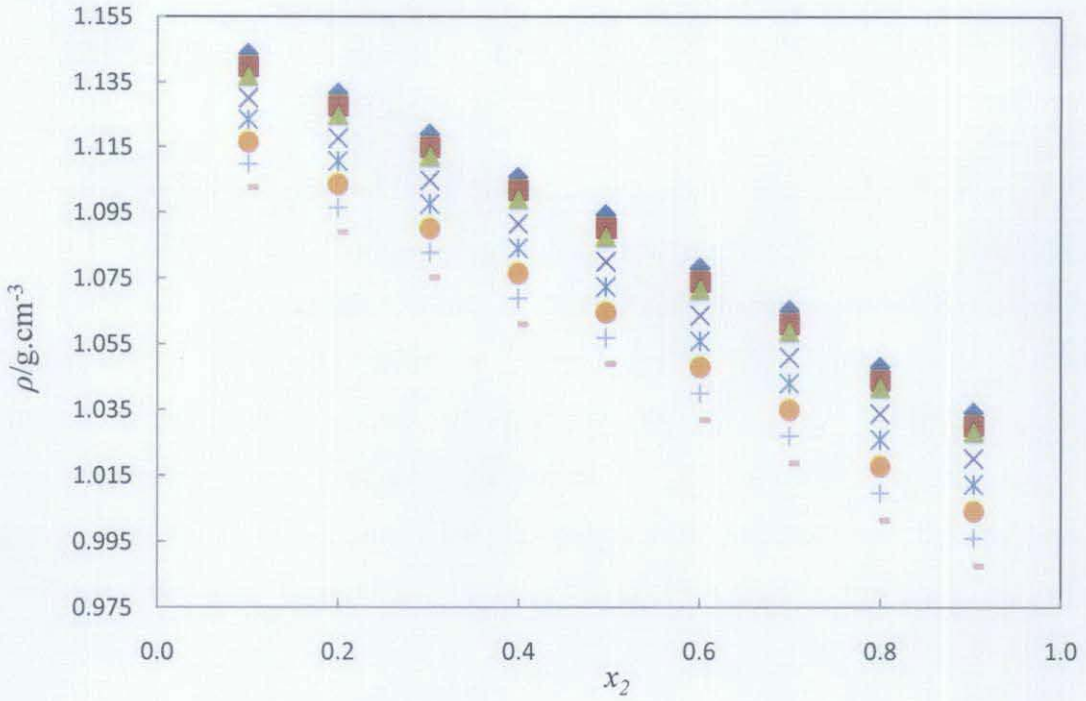

c)

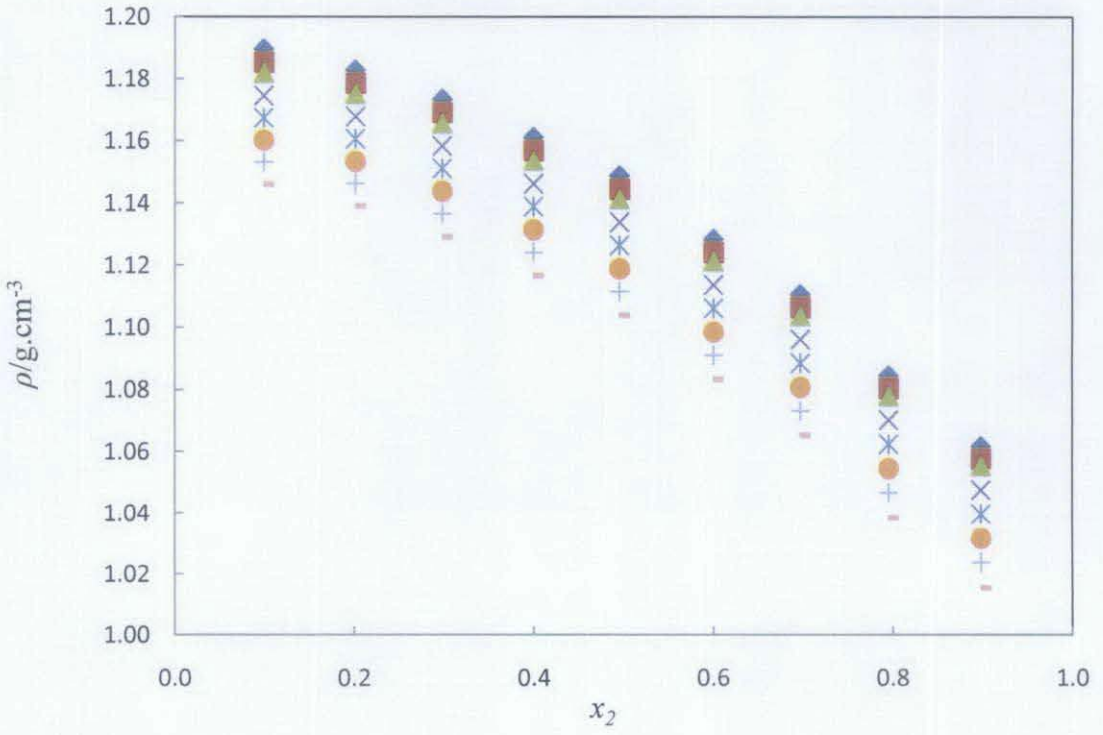

Figure 4.7. Plot of experimental values of density, ρ, of the ternary mixtures for [bmim][BF_4] (x_1) + MEA (x_2) water (x_3) against mole fraction of MEA at constant: a) $z = 0.08$; b) $z = 0.32$; c) $z = 5.03$ at temperatures: ◆, 293.15 K; ■, 298.15 K; ▲, 303.15 K; X, 313.15 K; ✳, 323.15 K; ●, 333.15 K; +, 343.15 K; —, 353.15 K.

Correlation of density data for ternary systems.

The results obtained for both ternary mixtures ([bheaa] + MEA + water and [bmim][BF_4] + MEA + water) show that density of the ternary mixtures varies with mole fractions of MEA (x_2), since 'z' is kept constant. Hence, a correlation as a function of mole fractions of MEA (x_2) have been made using the following equations:

$$\rho = A_0 + A_1 x_2 + A_2 x_2^{\,2} + A_3 x_2^{\,3} + A_n x_2^{\,4} \qquad (4.6)$$

where ρ is the density, A_0, A_1, A_2, A_3 and A_n are the correlation coefficients and x_2 is the mole fraction of MEA. The coefficients for both correlations are estimated using least square method, and the values are presented in Table A-11 and Table A-12 of Appendix A together with the standard deviation (σ) for [bheaa] + MEA + water and [bmim][BF_4] + MEA + water system respectively. It can be seen that a second order polynomial fits well for all ratios 'z' in [bheaa] + MEA + water systems while for [bmim][BF_4] + MEA + water systems, a second and third order polynomial was found to fits well with the density data.

The thermal expansion coefficients for both ternary mixtures were also estimated using equation 4.4 and 4.5 and the correlation constant are presented in Table A-13 and A-14 of Appendix A respectively. The partial derivative of the right hand side of the equation 4.5, using the estimated constant gave the thermal expansion coefficients for the ([bheaa] + MEA + water) and ([bmim][BF_4] + MEA + water) system and the α_p values are presented in Table A-15 and A-16 respectively.

From the estimated thermal expansion coefficients for [bheaa] + MEA + water system, it was found that the values are increasing with an increase in temperature and an increase in mole fractions of [bheaa] for all ratios 'z' (mole fractions of IL/ mole fractions of water). A similar observations were also found for [bmim][BF_4] + MEA + water system.

4.2 Viscosity

The viscosity of all the pure, binary, and ternary mixtures involving the pure MEA, [bheaa] and [bmim][BF_4] were measured using selected size of Ubbelohde viscometer at temperatures from 293.15 to 353.15 K. The complete description of apparatus setup and viscosity measurements were discussed in the earlier section (3.3.2). The viscometers used were initially calibrated using distilled water and further validated using several established data of pure organic liquids. The experiments were repeated for at least three times for all compositions and temperatures and the average values were considered for futher calculations. The estimated uncertainty in calculating the dynamic viscosities were found to be within ± 0.4 mPa.s.

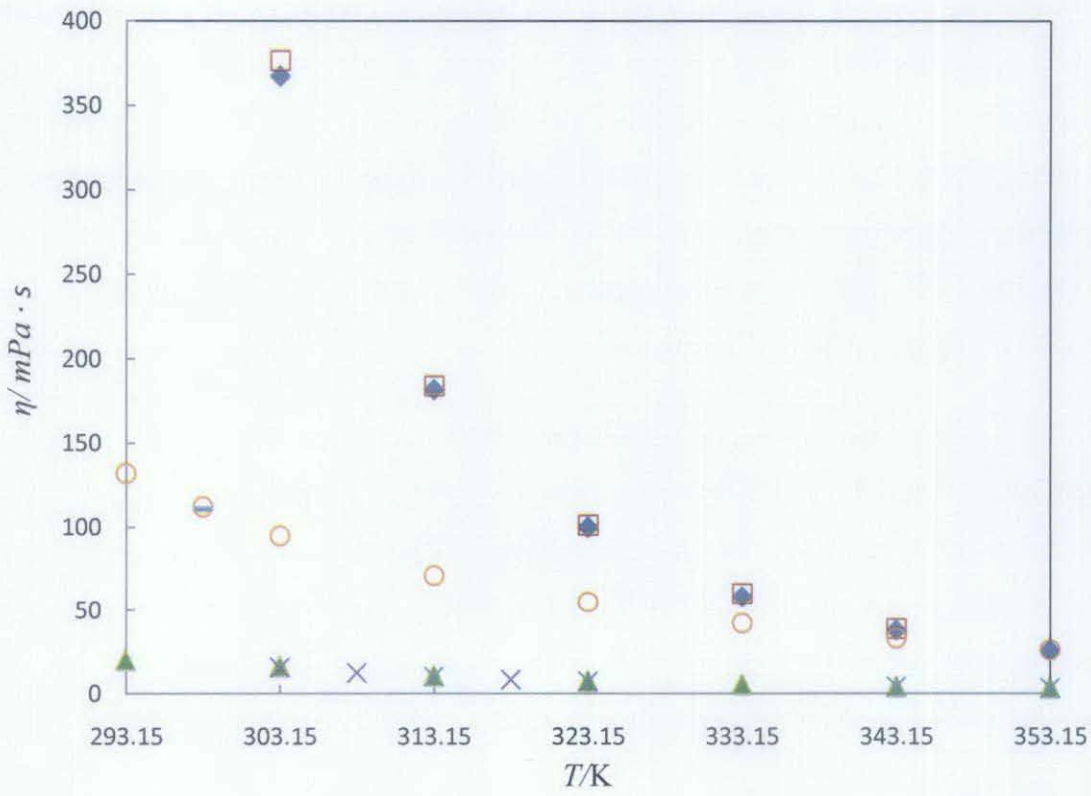

Figure 4.8. Comparison of experimental viscosities data with literature: ◆, [bheaa] this work; □, kurnia *et al.* (2009); ▲, MEA this work; X, Kapadi *et al.* (2002); ✳, trine *et al.* (2009); ○, [bmim][BF_4] this work; —, Tian *et al.* (2008).

The comparison of viscosities between the experimental data and published literature data for pure solvents namely MEA, [bheaa] and [bmim][BF_4] is shown in Figure 4.8. The calculated errors were found to be $\leq 4.0\%$ for [bheaa] and MEA, and $\leq 2.0\%$ for [bmim][BF_4], which shows that the results obtained are in good agreement with the literature.

The measured viscosities of MEA, [bheaa] and [bmim][BF_4] are presented in Table 4.2. It can be seen that the viscosity of pure [bheaa] (MW: 165.20 $g.mol^{-1}$) is higher than the viscosity of pure [bmim][BF_4] (MW: 226.02 $g.mol^{-1}$) and MEA (MW: 61.08 $g.mol^{-1}$), significantly at higher temperature. Since viscosity does depend on hydrogen bonding, therefore it can be said that hydrogen bonding of [bheaa] is higher than that of pure [bmim][BF_4] (Welton *et al.*, 2003).

Table 4.2. Measured viscosities of pure ILs and MEA at temperature from (303.15 to 353.15)K.

T/ K		η/ mPa·s	
	[Bheaa]	[bmim][BF_4]	MEA
303.15	366.90	94.70	15.40
313.15	181.36	71.00	9.96
323.15	99.57	54.91	6.65
333.15	58.03	41.90	4.79
343.15	37.50	32.77	3.63
353.15	25.27	25.72	2.82

4.2.1 Binary mixtures

[bheaa] system

Viscosities of both [bheaa] – water system and [bheaa] – MEA system are presented in Table B-1 of Appendix B. Both the systems showed a quite similar trend whereby viscosity decrease with an increase in temperature and decrease in mole fractions of [bheaa]. Figures 4.9 and 4.10 show the plot of viscosity against composition of ILs at different temperatures of [bheaa]- water and [bheaa]– MEA system, respectively. A very steep curve has been observed from both figures due the large difference between the viscosity of pure [bheaa] with viscosity of water and pure MEA.

The higher viscosity of pure [bheaa] and pure [bmim][BF_4] was expected when compared with water and pure MEA since it has been reported that viscosities of ILs can be as high as 5 orders of magnitude greater than most of the traditional organic solvents (Huddleston *et al.*, 2001). The viscosities are in the following order: MEA (MW:61.08 $g.mol^{-1}$) < [bheaa] (MW: 165.20 $g.mol^{-1}$) < [bmim][BF_4] (MW: 226.02 $g.mol^{-1}$).

[bmim][BF_4] system

The viscosities of [bmim][BF_4] - water and [bmim][BF_4] - MEA binary mixtures were measured over the range from T = (293.15 to 353.15) K. The experimental data are reported in Table B-2 of Appendix B and the effect of temperature and composition on viscosity are demonstrated in Figure 4.11 and 4.12 for bmim][BF_4] - water and [bmim][BF_4] - MEA, respectively. The viscosity value of the binary mixtures involving [bmim][BF_4] are more stable since the observation on Figure 4.11 and Figure 4.12 shows a contiually decrease values with increasing temperature compare to the steep curve of [bheaa] binary systems.

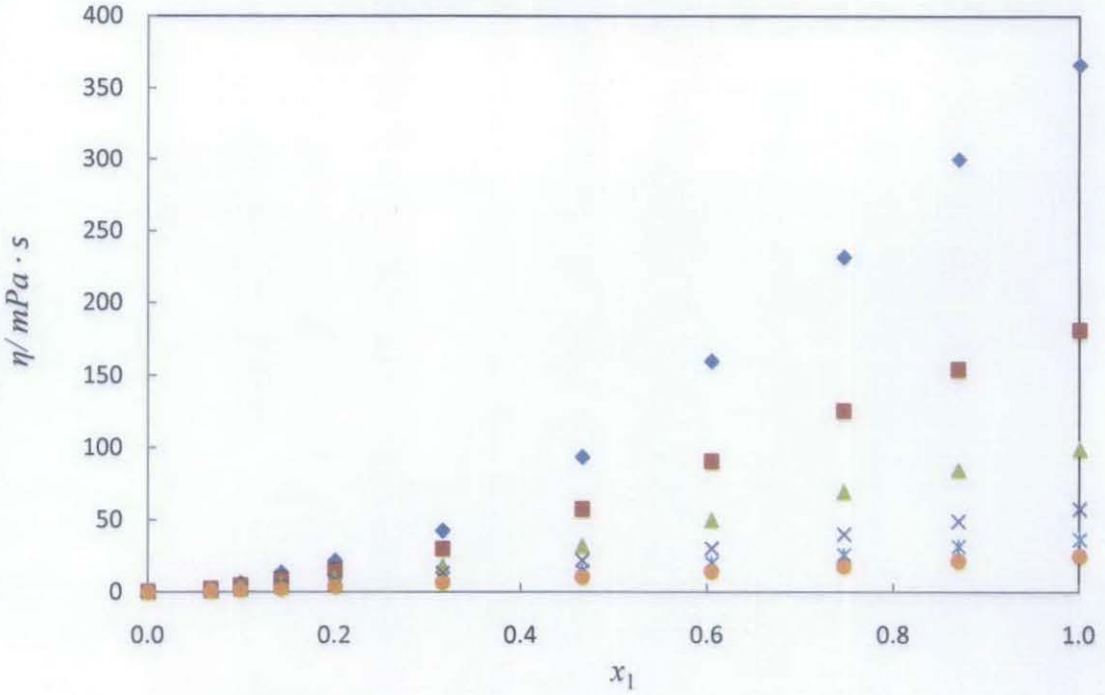

Figure 4.9. Plot of experimental values of viscosity η against x_1 for [bheaa] (1) + water (2) binary mixture: ◆, 303.15 K; ■, 313.15 K; ▲, 323.15 K; X, 333.15 K; ✳, 343.15 K; ●, 353.15

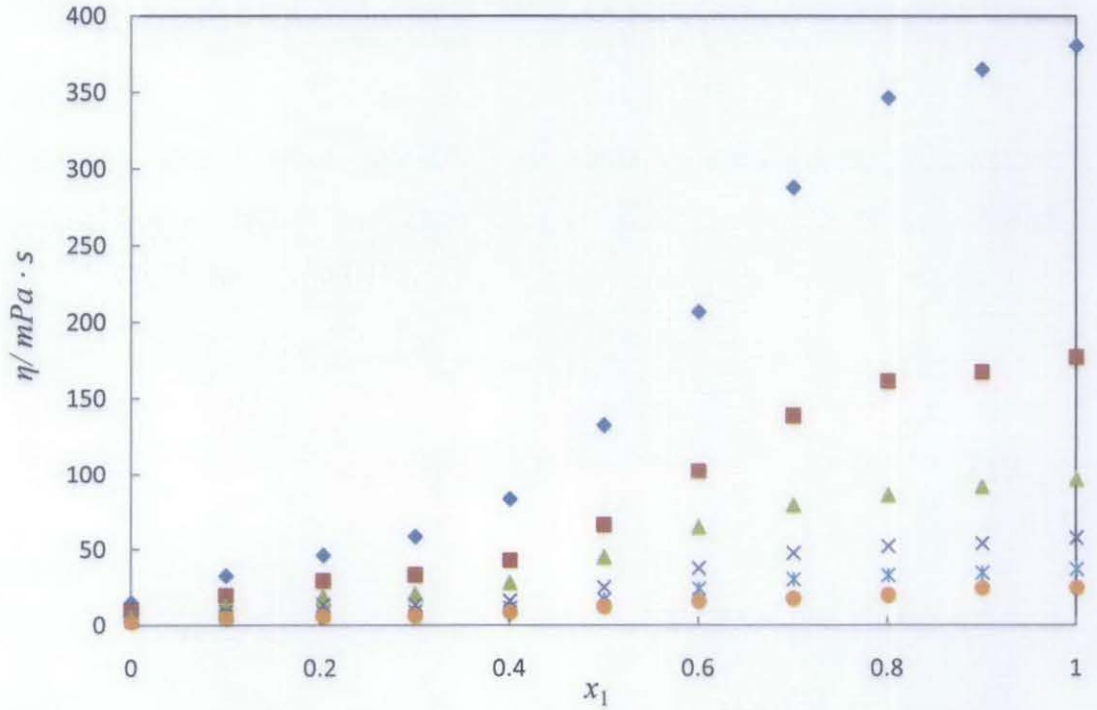

Figure 4.10. Plot of experimental values of viscosity η against x_1 for [bheaa] (1) + MEA (2) binary mixture: ◆, 303.15 K; ■, 313.15 K; ▲, 323.15 K; X, 333.15 K; ✳, 343.15 K; ●, 353.15 K.

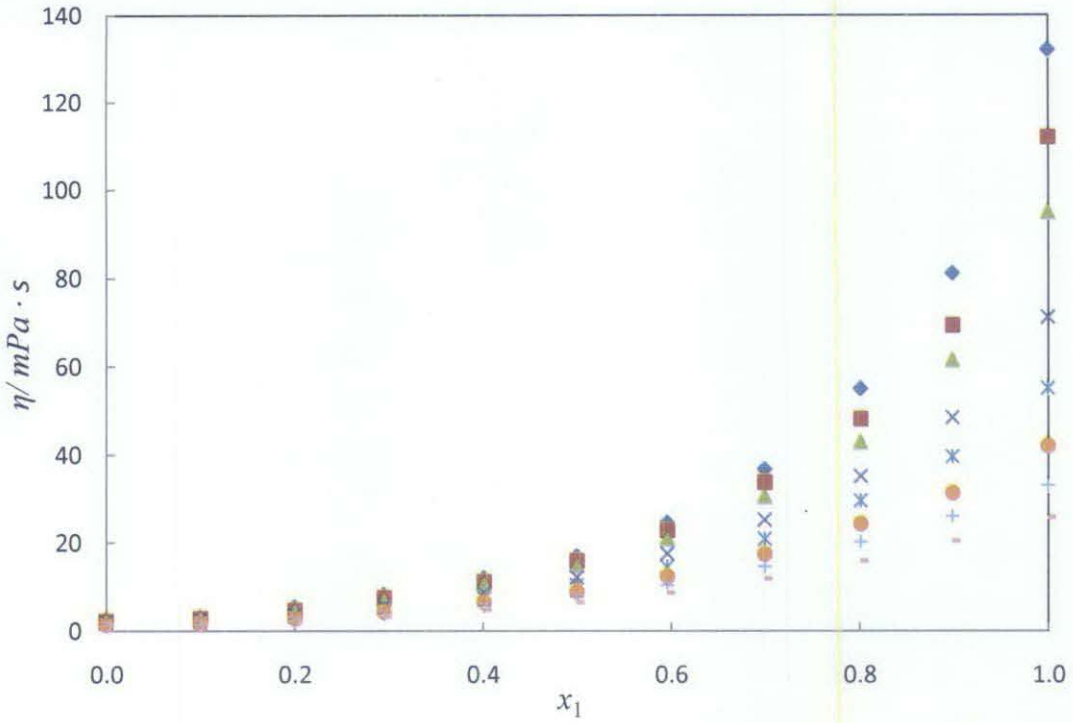

Figure 4.11. Plot of experimental values of viscosity η against x_1 for [bmim][BF_4] (1) + water (2) binary mixture: ◆ , 293.15 K; ■ , 298.15 K; ▲, 303.15 K; X, 313.15 K; ✳ , 323.15 K; ● , 333.15 K; + , 343.15 K; , —, 353.15 K

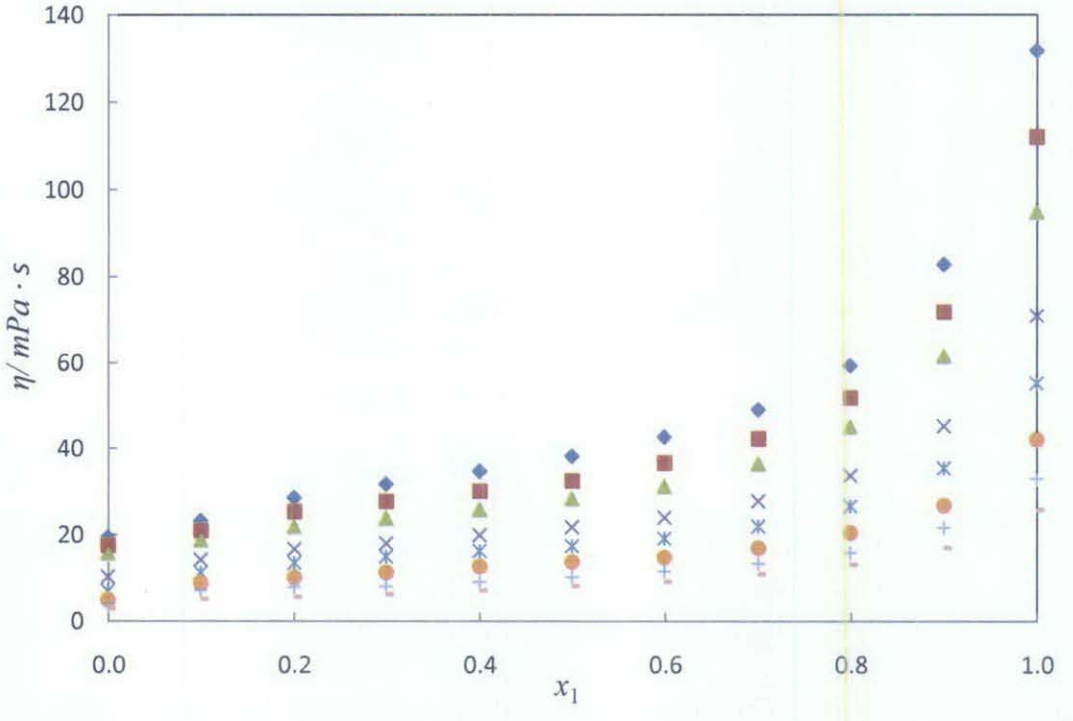

Figure 4.12. Plot of experimental values of viscosity η against x_1 for [bmim][BF_4] (1) + MEA (2) binary mixture: ◆ , 293.15 K; ■ , 298.15 K; ▲, 303.15 K; X, 313.15 K; ✳ , 323.15 K; ● , 333.15 K; + , 343.15 K; , —, 353.15 K

Correlation of viscosity data for binary systems.

Both systems show a decrease in viscosity with a decrease in mole fractions of [bmim][BF_4]. It also show a decrease in viscosity with an increase in temperature. Similar with densities, the measured viscosity data are also more dependent on the composition, than the temperature. Hence, the viscosity results are also correlated as the function of composition using the following form of polynomial equation

$$\eta = A_0 + A_1 x + A_2 x^2 + A_3 x^3 + A_n x^4 \tag{4.7}$$

where η is the viscosity, A_0, A_1, A_2, A_3 and A_n are the correlation coefficients and x is the mole fraction of ILs. The correlation coefficients (equation 4.7) are further correlated with the temperature using the following form of equation:

$$A_n = B_0 + B_1 T + B_2 T^2 + B_3 T^3 + B_k T^k \tag{4.8}$$

where A_n is the correlation coefficients obtained using equation (4.7), B_0, B_1, B_2, B_3 and B_k are the correlation coefficients (for equation (4.8)) as the function of temperature and T is the experimental temperature (K). Both correlation coefficients are estimated using least square method, and the values of the coefficients for [bheaa] systems ([bheaa] + water, [bheaa] + MEA) and [bmim][BF_4] systems ([bmim][BF_4] + water, [bmim][BF_4] + MEA) are shown in Table B-3 and Table B -4 of Appendix B respectively, together with the estimated standard deviations (σ).

4.2.2 Ternary Mixtures

The experimental viscosity values of the ternary system involving [bheaa] + MEA + water at temperature ranging from 303.15 to 353.15 K are presented in Table B-5 of Appendix B and the variation of viscosity for all ratios 'z' at different temperatures studied are shown in Figure 4.13.

a)

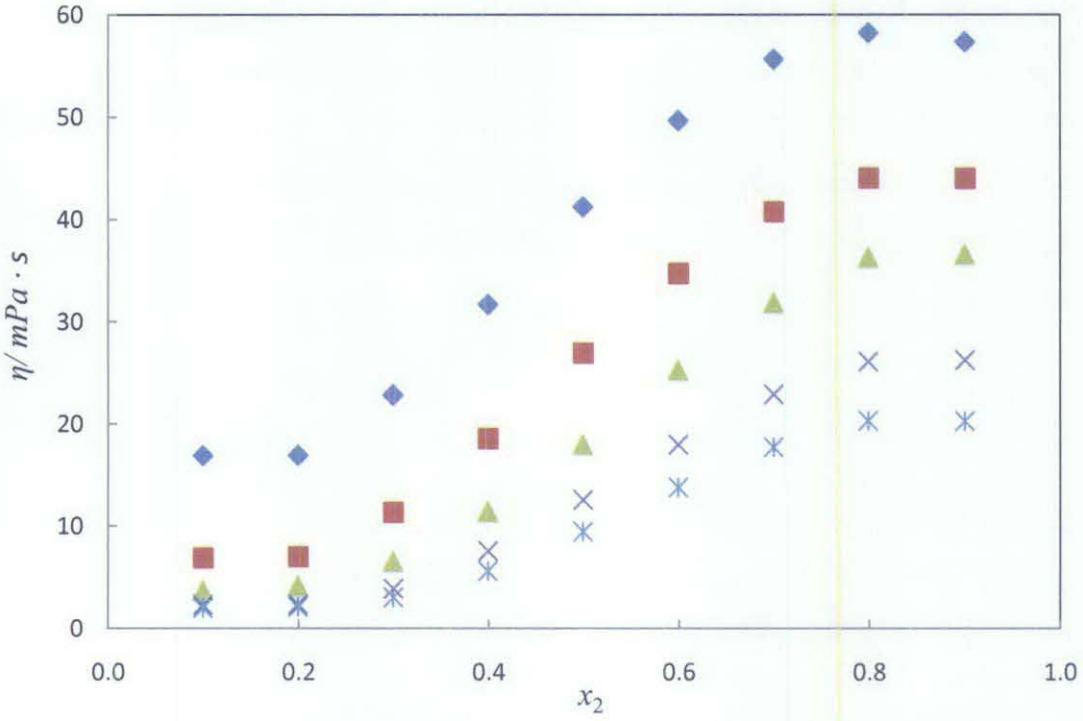
60
50
40
30
20
10
0
0.0
0.2
0.4
0.6
0.8
1.0
$\eta / mPa \cdot s$
x_2

b)

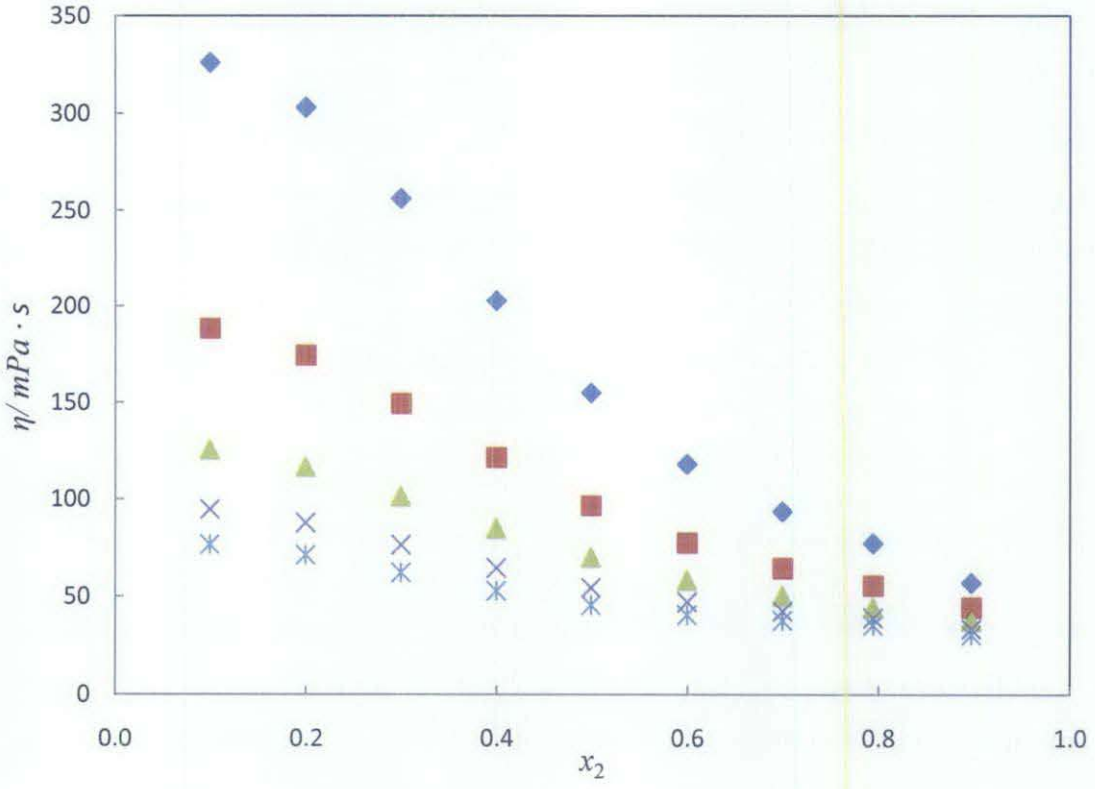
350
300
250
200
150
100
50
0
0.0
0.2
0.4
0.6
0.8
1.0
$\eta / mPa \cdot s$
x_2

c)

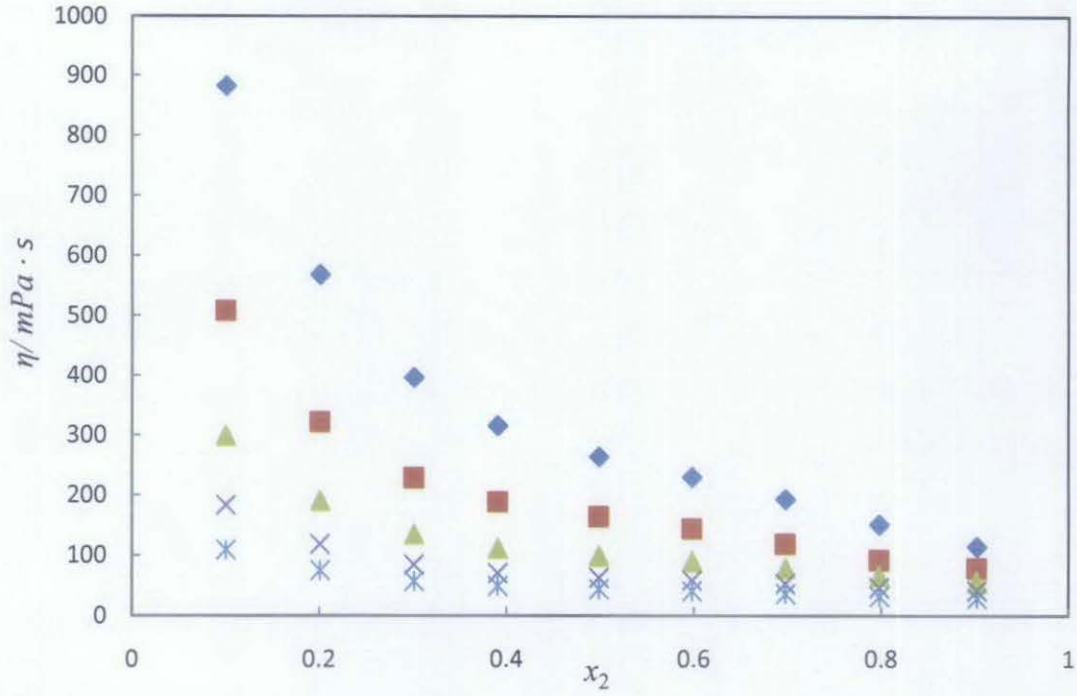

Figure 4.13. Plot of experimental values of viscosity, η, of the ternary mixtures for [bheaa] (x_1) + MEA (x_2) water (x_3) against mole fraction of MEA at constant: a) z = 0.11; b) z = 0.62; c) z = 4.03 at temperatures: ◆ , 303.15 K; ■ , 313.15 K; ▲, 323.15 K; X, 333.15 K; ✳ , 343.15 K

It can be seen from Figure 4.13 that the viscosity values show different trend for every ratio studied. For z = 0.11, the viscosity values increase with the increasing mole fraction of MEA. The viscosity value at $x_2 \approx 0.1$ and $x_2 \approx 0.2$ did not show any significant difference since the compositions of [bheaa], water and MEA at that particular points are not much difference. On the other hand, for z = 0.62 and z = 4.03, the trends are almost similar whereby the viscosity values are found to decrease with an increase in the mole fraction of MEA but the values were found to be higher at z = 4.03 due to the higher ILs amount at that particular z. It can also be seen that the viscosity values decrease with increasing temperatures at all values of z. The viscosity measurement for this ternary system has been done only until T = 343.15 K since the measurement at higher temperature gave high fluctuation in the results.

The viscosity results of the [bmim][BF_4] + MEA + water system are presented in Table B-6 of Appendix B at temperature ranging from 293.15 to 353.15 K and the

effect of temperature on viscosiy of the ternary system for all ratios 'z' are shown plotted in Figure 4.14. It can be seen that the variation of viscosity against temperature still follow a usual behaviour whereby the viscosity values decreased with increasing temperatures for all values of z. For z = 0.08 and 0.32, a similar trends were observed whereby the viscosity increase with an increase in mole fraction of MEA except at $x_{MEA} \geq 0.8$, where the viscosity value decrease slightly. In contrast with that, for z = 5.03, the viscosity value show an increasing trend until x_{MEA} = 0.2980, that it starts to decrease continually. From the observed behaviour, it can be said that the viscosity of ILs plays a major role in detemining the viscosity of the ternary system.

a)

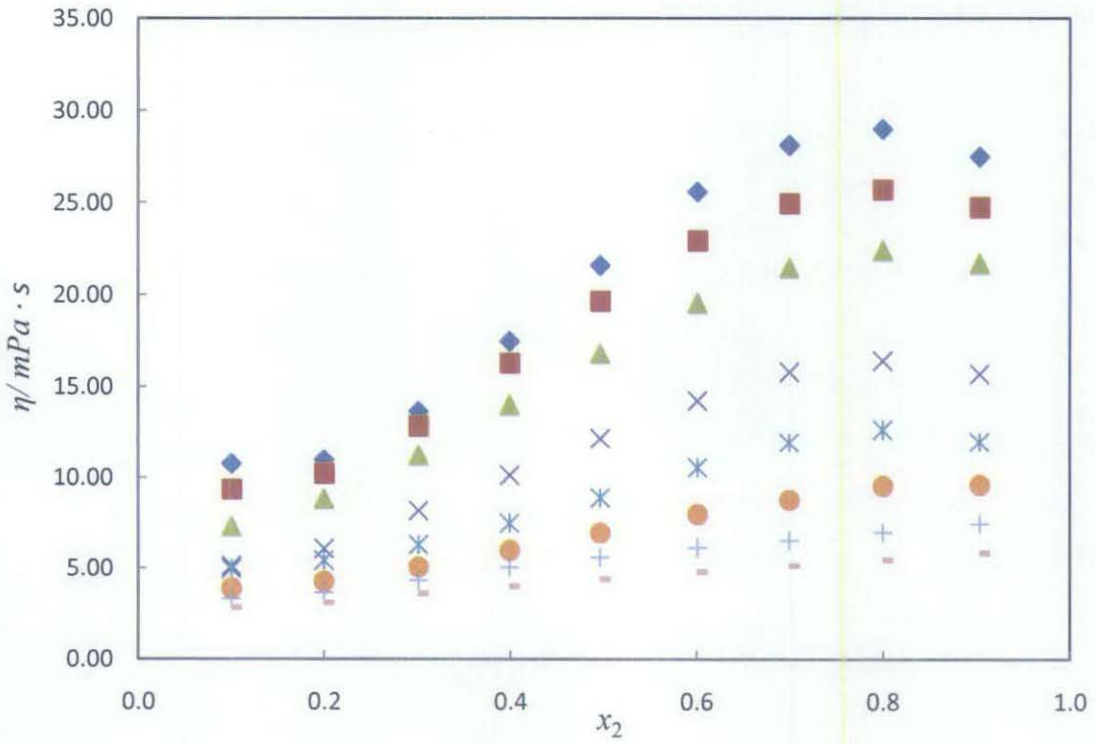

b)

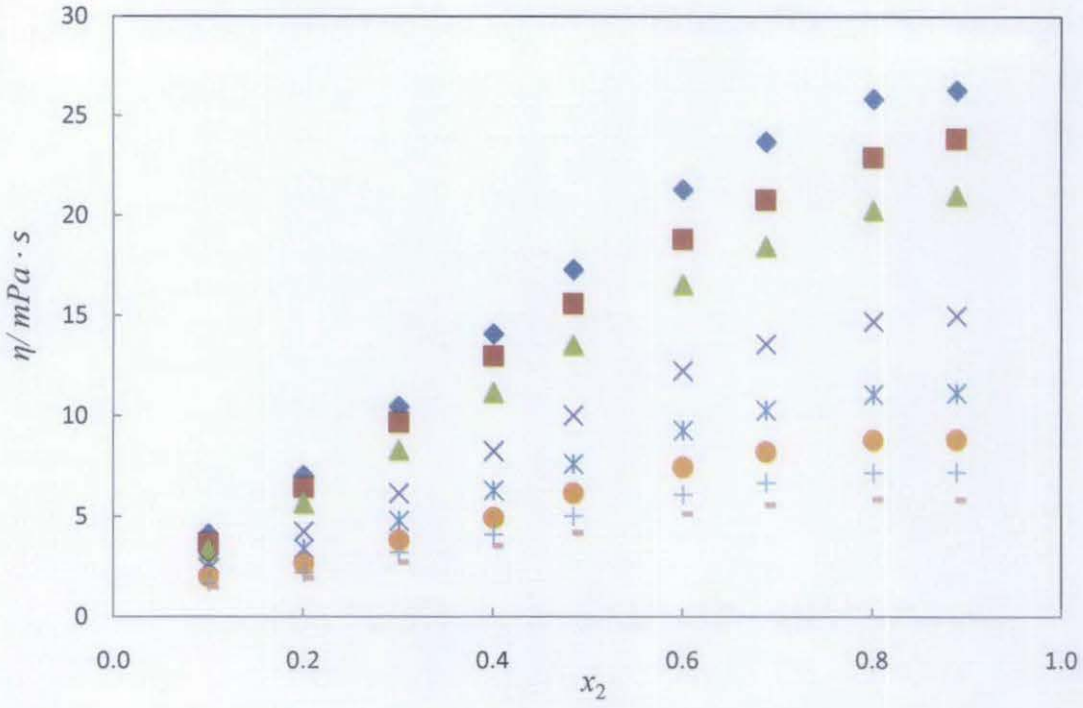

c)

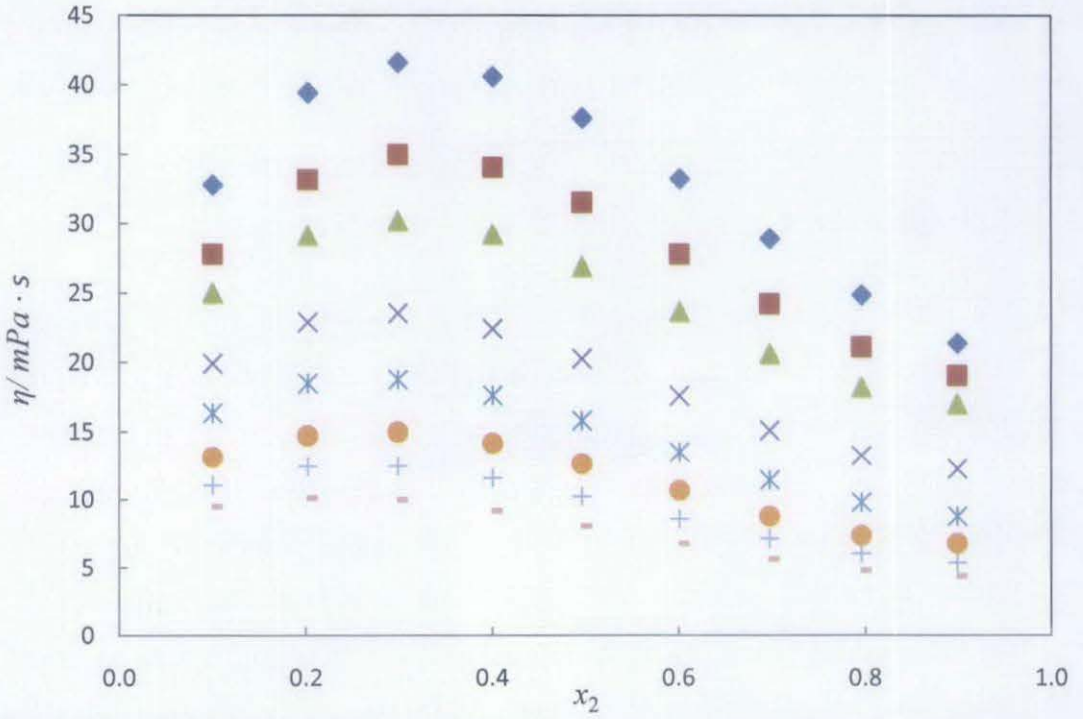

Figure 4.14. Plot of experimental values of viscosity, η, of the ternary mixtures for [bmim][BF_4] (x_1) + MEA (x_2) water (x_3) against mole fraction of MEA at constant: a) $z = 0.08$; b) $z = 0.32$; c) z = 5.03 at temperatures: ◆, 293.15 K; ■, 298.15 K; ▲, 303.15 K; X, 313.15 K; ✳, 323.15 K; ●, 333.15 K; +, 343.15 K; ▬, 353.15 K.

Correlation of viscosity data for ternary systems.

The results for viscosity measurements of the ternary mixtures ([bheaa] + MEA + water and [bmim][BF_4] + MEA + water) also show a variation with mole fractions of MEA (x_2). Therefore, similar to density, the viscosity data were also being correlated as a function of mole fractions of MEA (x_2) using the following equations:

$$\eta = A_0 + A_1 x_2 + A_2 x_2^{\,2} + A_3 x_2^{\,3} + A_n x_2^{\,4} \qquad (4.9)$$

where η is the viscosity, A_0, A_1, A_2, A_3 and A_n are the correlation coefficients and x_2 is the mole fraction of MEA. A fourth order polynomial was found to fit well with the viscosity data for [bheaa] + MEA + water systems for all 'z's while a third (z = 0.08) and fourth order (z = 0.32 and 5.03) polynomial was found to fit well for [bmim][BF_4] + MEA + water systems. All estimated coefficients are estimated using least square method, and the values are presented in Table B-7 and Table B-8 of Appendix B together with the standard deviation (σ) for [bheaa] + MEA + water and [bmim][BF_4] + MEA + water system respectively.

4.3 Refractive index

Refractive index is an optical property which is used to identify a particular component in a solution by means of its concentration. It can also be used to confirm the purity and to measure the concentration of a substance in a solution. The refractive indices of all the binary mixtures including the pure MEA, [bheaa] and [bmim][BF_4] were measured using the digital refractometer (model ATAGO RX-5000) with a measuring accuracy of $\pm 4.10^{-5}$. The apparatus was calibrated by measuring the refractive index of milipore quality water and again validated using several established data of pure organic liquids. All the measurements were made in triplicate and the average values are considered for further analysis. The complete description of the apparatus used have been discussed in section 3.3.3.

The comparison of refractive indices between the experimental data and published literature data for pure solvents namely MEA, [bheaa] and [bmim][BF_4] is shown in Figure 4.15. The calculated error were found to be ≤ 3.3% for [bheaa], ≤ 3.3% for MEA, and ≤ 0.25% for [bmim][BF_4].

The measured refractive index data for pure components involved ([bheaa], [bmim][BF_4] and MEA) are presented in Table 4.3. It can be seen that the value of refractive index for pure [bheaa] (MW: 165.20 $g.mol^{-1}$) is higher than the value of refractive index of pure [bmim][BF_4] (MW: 226.02 $g.mol^{-1}$) and pure MEA(MW: 61.08 $g.mol^{-1}$).

Table 4.3. Refractive index values of pure ILs and MEA at temperature from (303.15 to 353.15) K

T/ K	n_D		
	[bheaa]	[bmim][BF_4]	MEA
303.15	1.48008	1.42369	1.45273
313.15	1.47793	1.42128	1.44913
323.15	1.47575	1.41900	1.44561
333.15	1.47313	1.41656	1.44213
343.15	1.47086	1.41388	1.43851
353.15	1.46849	1.41135	1.43472

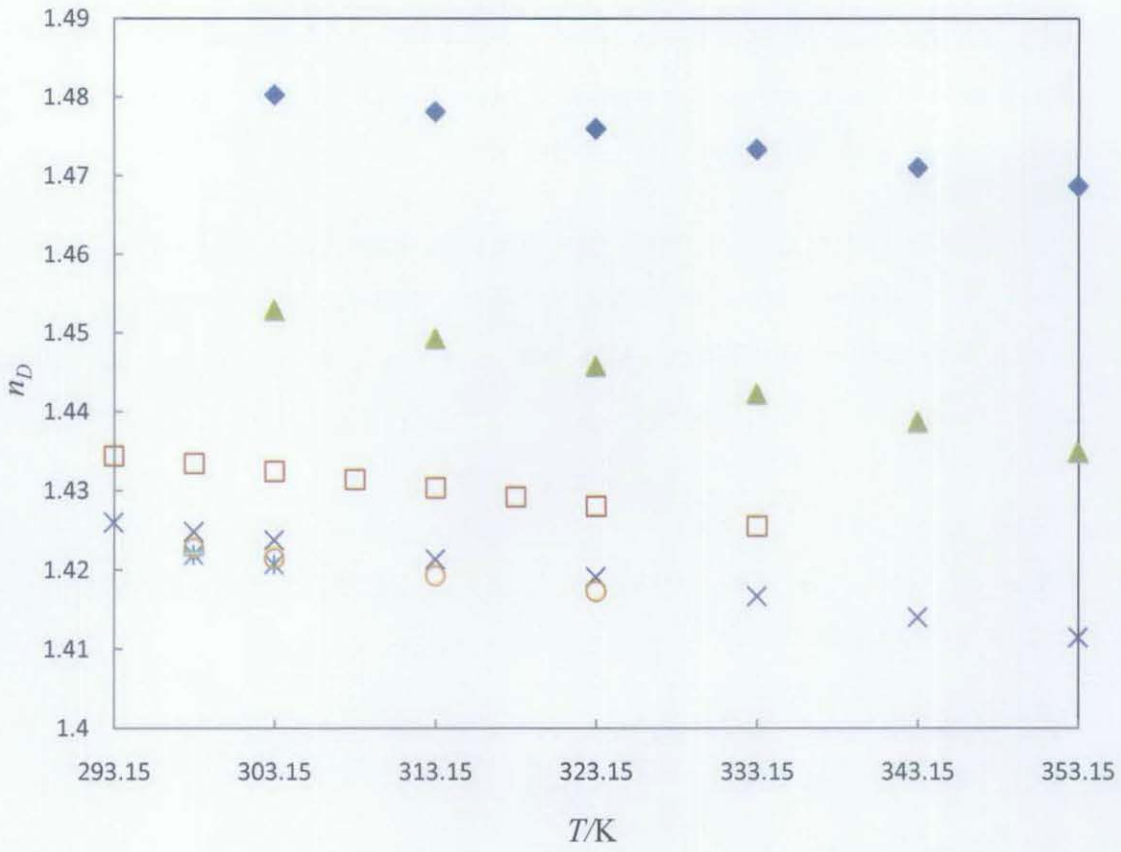

Figure 4.15. Comparison of experimental refractive index data with literature: ◆, [bheaa] this work; □, kurnia *et al.* (2009); ▲ , MEA this work; X , [bmim][BF_4] this work; ✳ , Soriano *et al.* (2009); ○, Kim *et al.* (2004); ▬, Malham *et al.* (2008).

4.3.1 Binary mixtures

[bheaa] system

Refractive indeices of both [bheaa] – water system and [bheaa]– MEA system are presented in Table C-1 of Appendix C. As can be seen from the table, the refractive index of both systems show a similar trend whereby it decreased with increasing temperature and increase with increasing mole fraction of [bheaa]. Figures 4.16 and 4.17 show the plot of refractive index against composition of [bheaa] at different temperatures for [bheaa] - water and [bheaa] - MEA system, respectively.

[bmim][BF_4] system

The refractive indices of [bmim][BF_4] - water and [bmim][BF_4] – MEA systems are presented in Table C-2 of Appendix C. The refractive index values for [bmim][BF_4] – water mixtures increase with increasing composition of [bmim][BF_4] and decrease with temperature, which are in good agreement with the observations of Malham et al (2008). While on the other hand, the refractive index for [bmim][BF_4] – MEA mixtures decrease with increasing composition of [bmim][BF_4] and temperature due to the fact that the refractive index for pure MEA is higher for the pure [bmim][BF_4]. The effect of temperature on the refractive index values are shown in Figures 4.18 and 4.19 for bmim][BF_4] - water and [bmim][BF_4] – MEA system respectively. Both systems show decreasing values of refractive index with increaseing temperature.

Correlation of refractive index data for binary systems.

A similar behaviour as density and viscosity on the dependency of the data with composition were also observed for the refractive index data. Therefore, the results on the refractive indices of all systems involving both ILs ([bheaa] and [bmim][BF_4]) were correlated as a function of composition using the following form of polynomial equation

$$n_D = A_0 + A_1 x + A_2 x^2 + A_3 x^3 + A_n x^4 \qquad (4.10)$$

where n_D is the refractive index, A_0, A_1, A_2, A_3 and A_n are the correlation coefficients and x is the mole fraction of ILs. The correlation coefficients for both systems are presented in Table C-3 of Appendix C together with the standard deviations (σ). Similar to the behaviour of density and viscosity with respect to temperature, the refractive index values were also found to decrease with temperature. Hence, the correlation coefficients of equation (4.10) were further correlated as a function of temperature using the following equation

$$A_n = B_0 + B_1 T + B_2 T^2 + B_3 T^3 + B_k T^k \qquad (4.11)$$

where A_n is the correlation coefficients obtained using equation (4.10), B_0, B_1, B_2, B_3 and B_k are the correlation coefficients (for equation (4.11)) as the function of temperature and T is the experimental temperature (K). The correlation coefficients of equation (4.11) are presented in Table C-4 of Appendix C together with the standard deviations (σ). Both the correlation coefficients were estimated by using least square method.

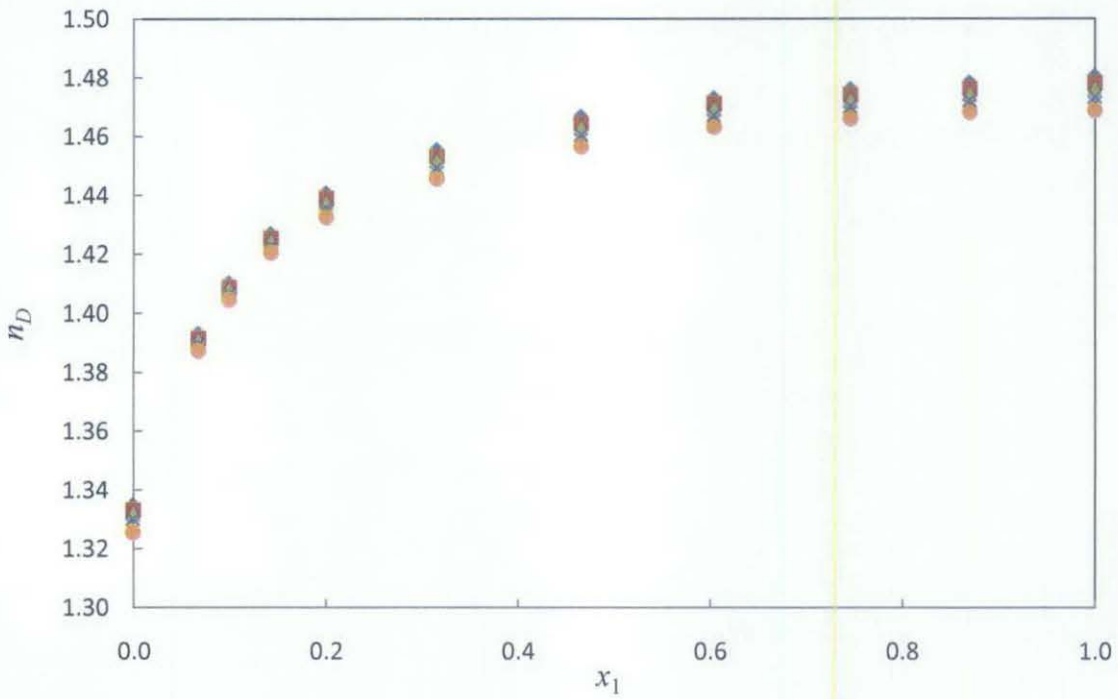

Figure 4.16. Plot of experimental values of refractive index n_D against x_1 for [bheaa] (1) + water (2) binary mixture: ◆, 303.15 K; ■, 313.15 K; ▲, 323.15 K; X, 333.15 K; ✳, 343.15 K; ●, 353.15 K.

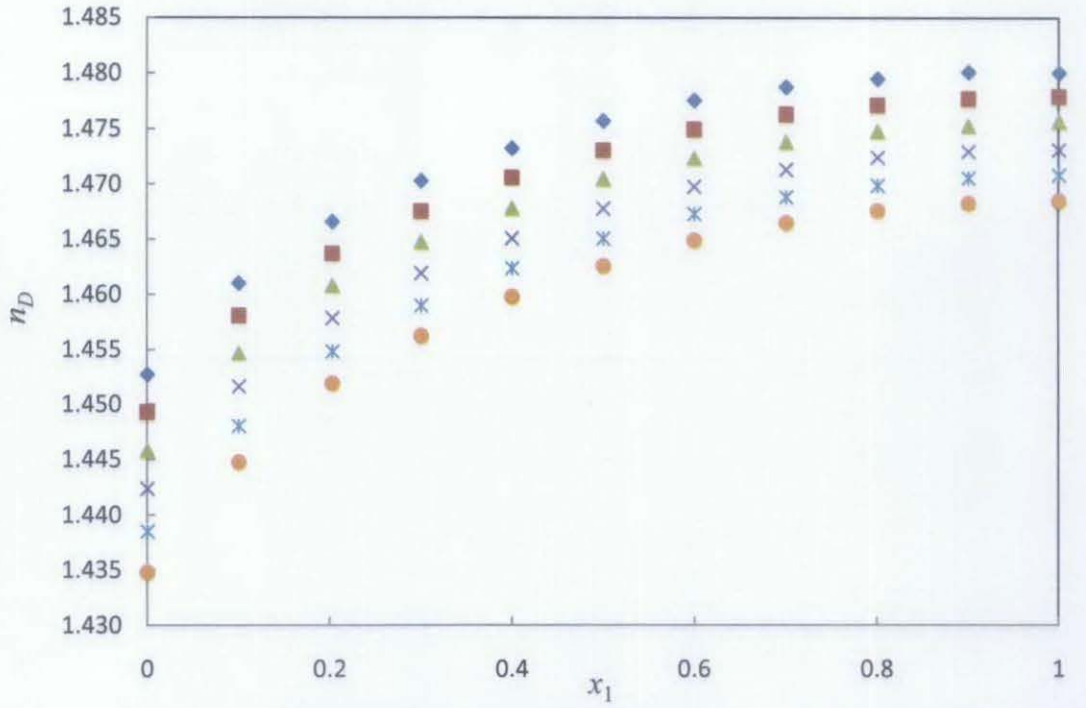

Figure 4.17. Plot of experimental values of refractive index, n_D against x_1 for [bheaa] (1) + MEA (2) binary mixture: ◆, 303.15 K; ■, 313.15 K; ▲, 323.15 K; X, 333.15 K; ✳, 343.15 K; ●, 353.15 K.

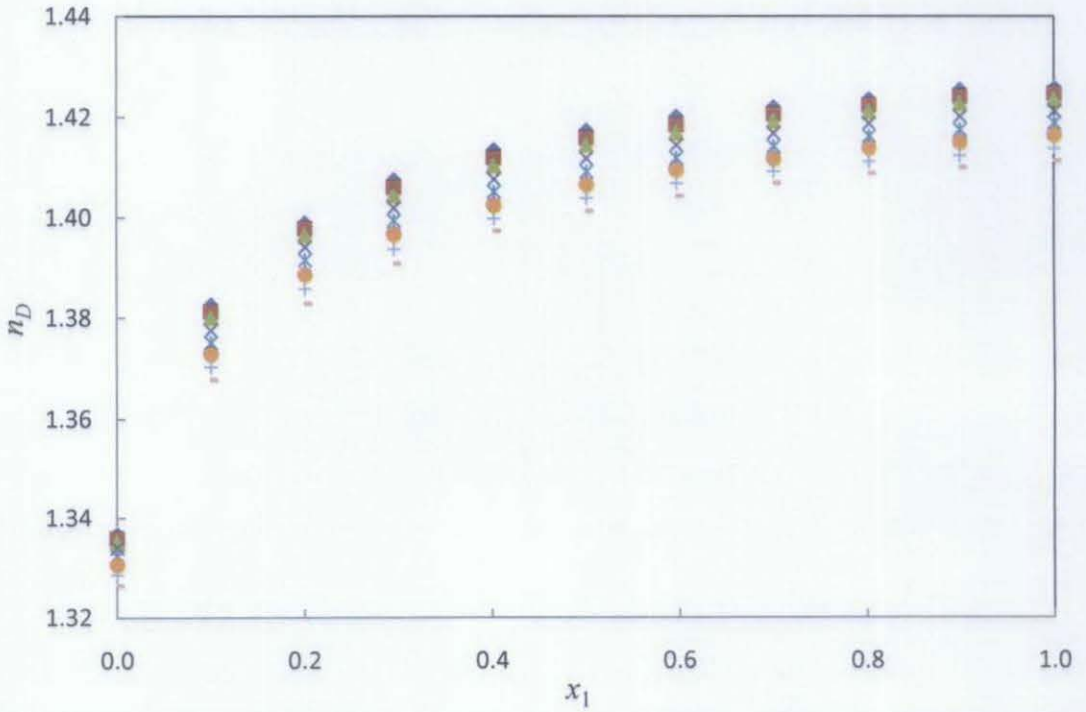

Figure 4.18. Plot of experimental values of refractive index n_D against x_1 for [bmim][BF_4] (1) + water (2) binary mixture: ◆, 293.15 K; ■, 298.15 K; ▲, 303.15 K; X, 313.15 K; ✳, 323.15 K; ●, 333.15 K; +, 343.15 K; , —, 353.15 K

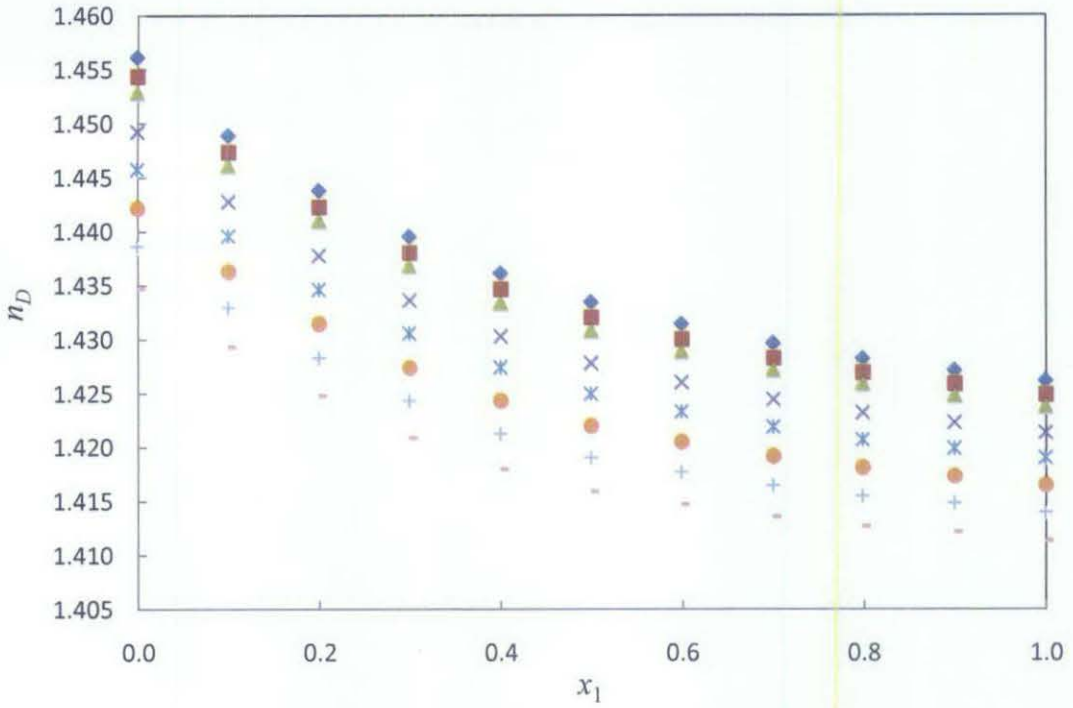

Figure 4.19. Plot of experimental values of refractive index n_D against x_1 for [bmim][BF_4] (1) + MEA (2) binary mixture: ◆ , 293.15 K; ■ , 298.15 K; ▲, 303.15 K; X, 313.15 K; ✳ , 323.15 K; ● , 333.15 K; + , 343.15 K; , —, 353.15 K

4.3.2 Ternary Mixtures

The experimental values of reafractive index for the ternary system of [bheaa] + MEA + water at temperature ranging from 303.15 to 353.15 K are presented in Table C-5 of Appendix C and the effect of refractive index on temperature are demonstrated in Figure 4.20. It can be seen that the refractive index values for all ratios 'z' decrease with increasing temperatures. For z = 0.11, the refractive index was found to increase with increasing mole fraction of MEA while for z = 0.62 and z = 4.03, the refractive index are found to decrease with increasing mole fraction of MEA.

For the ternary system involving [bmim][BF_4] + MEA + water, the refractive index values at temperature ranging from 293.15 to 353.15 K are presented in Table C-6 of Appendix C. The variation of refractive index for all ratios 'z' at different temperatures studied are shown in Figure 4.21. In contrast with the ternary mixtures of [bheaa] system, the refractive indices of [bmim][BF_4] + MEA + water system was

observed to increase with increasing mole fraction of MEA at all 'z's and decreased with increasing temperatures. It can also be seen that the refractive index values increase with the ratio, z (mole of ILs/ mole of water).

a)

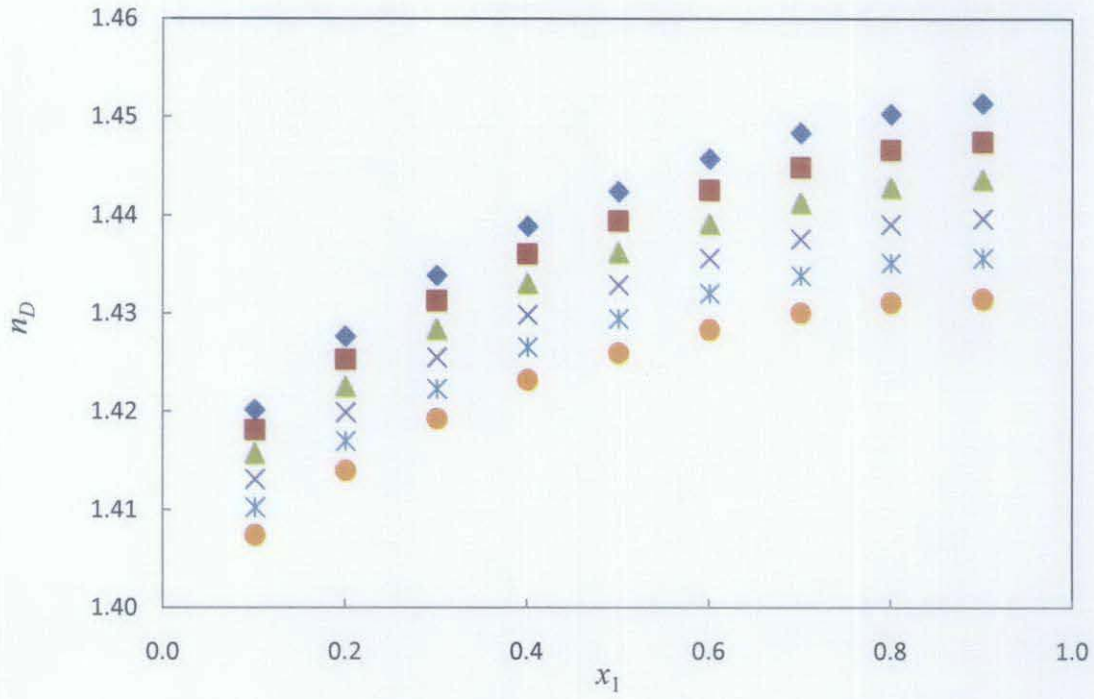

b)

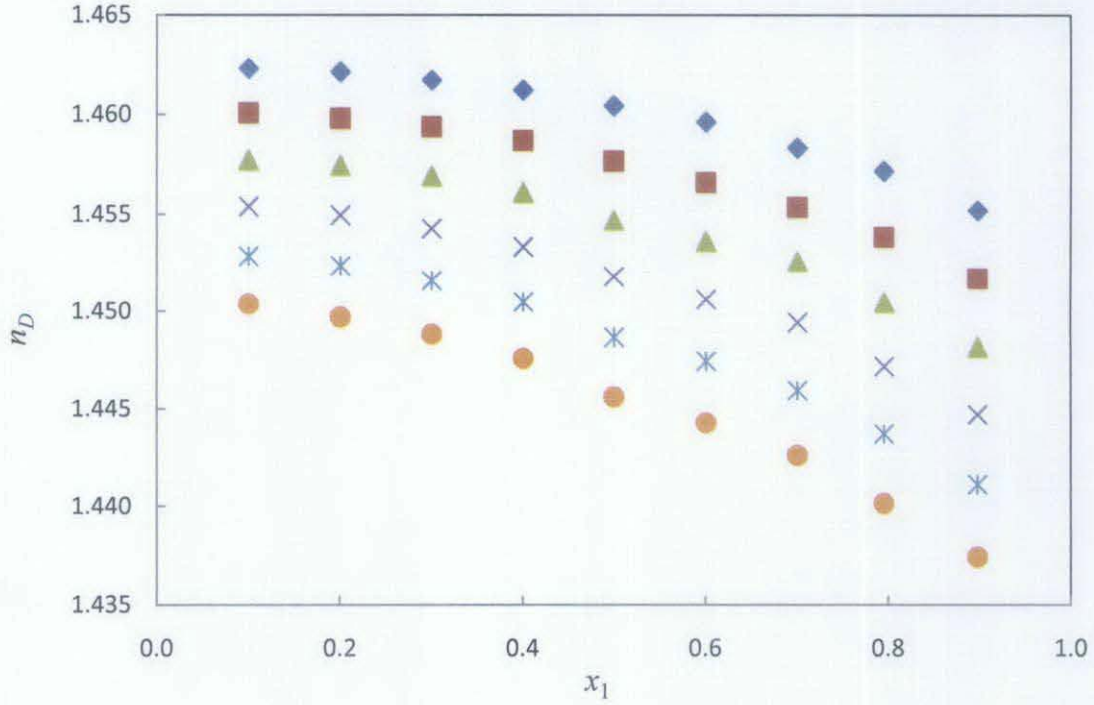

c)

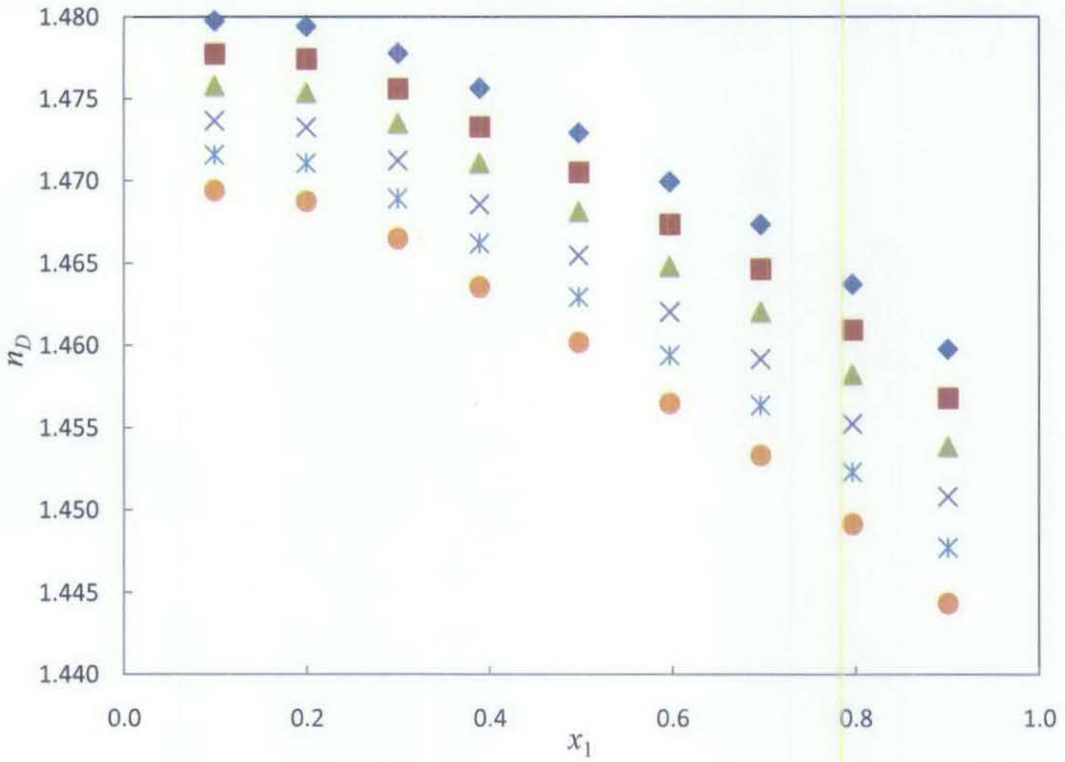

Figure 4.20. Plot of experimental values of refractive index, n_D, of the ternary mixtures for [bheaa] (x_1) + MEA (x_2) water (x_3) against mole fraction of MEA at constant: a) z = 0.11; b) z = 0.62; c) z = 4.03 at temperatures: ◆ , 303.15 K; ■ , 313.15 K; ▲, 323.15 K; X, 333.15 K; ✳ , 343.15 K; ● , 353.15 K.

both ternary mixtures are presented in Table C-7 and Table C-8 of Appendix C together with the standard deviation (σ) for [bheaa] + MEA + water and [bmim][BF_4] + MEA + water system respectively.

4.4 Excess Properties

The excess properties of the mixed liquid solvents, namely the excess molar volume, viscosity deviation and refractive index deviation can be deduced from the measured physical properties (density, viscosity and refractive index). The knowledge of these excess properties is valuable in understanding the differences and changes that might happen in terms of the molecular size, structure and forces undergone by the pure solvents when mixed with other compounds. The excess properties can also help in understanding the interaction between the solvents namely hydrogen bonding, dipole-dipole etc. Excess molar volume can indicate that the intermolecular forces between the different molecules of the mixtures can cause an expansion or a contraction after mixing. The addition of another component can results in dramatic change on the viscosity as well as on the refractive index of the pure solvents. Hence, by calculating the deviation of both properties, it can be seen that whether the mixed solvents deviate positively or negatively depending on the interactions of the components.

4.4.1 Excess Molar Volume

The volume of mixtures of two liquids will not be equal to the total volume of its pure constituents due to the intermolecular forces. The intermolecular forces between the different molecules of the mixtures can be less or more stronger than they are in the pure liquids and can cause an expansion or contraction of the volume after mixing. This phenomenon are called the excess molar volume. When two components, (1) and (2) respectively, are being brought together but not allowed to mix, the total volume V of (1) and (2) can be expressed as

$$V^0 = n_1 V_1^0 + n_2 V_2^0 \tag{4.13}$$

where n_1 and n_2 are the number of moles of each components. When mixing occurs, the volume of the mixture changes from initial volume (V^0) to the final volume (V). The changes from V^0 to V can be defined as the excess volume (V^E) with the following expression

$$V^E = V - V^0 \tag{4.14}$$

Combining equation (4.13) and (4.14) produce

$$V^E = V - \left(n_1 V_1^0 + n_2 V_2^0\right) \tag{4.15}$$

Equation (4.15) can be described as excess molar volume 'V_m^E',

$$V_m^E = \frac{V^E}{n_1 + n_2} \tag{4.16}$$

Therefore, equation (4.16) gives

$$V_m^E = \frac{V - \left(n_1 V_1^0 + n_2 V_2^0\right)}{n_1 + n_2} \tag{4.17}$$

$$V = V_1 + V_2 \tag{4.18}$$

By incorporating density and combining equation (4.17) and (4.18) to yield

$$V_m^E = \frac{\sum_{i=1}^{c} x_i M_i}{\rho} - \sum_{i=1}^{c} \frac{x_i M_i}{\rho_i} \quad . \tag{4.19}$$

where ρ is the density of mixture; ρ_i is the density of pure components i, x_i is the mole fraction of pure component i and M_i are the molecular weight of pure component i.

4.4.1.1 Binary Mixtures

[bheaa] system

The calculated excess molar volumes (V^E) for both binary systems involving [bheaa] are presented in Table D-1 of Appendix D. The excess molar volume of [bheaa] - water and [bheaa] – MEA systems are found to decrease with increasing temperature. The effect of temperature as well as mole fraction of [bheaa] (x_1) on V^E is demonstrated in Figure 4.22 and 4.23, respectively.

Excess molar volume of mixtures are commonly related with the differences and the changes of structure undergone by the pure component. From the results it can be seen that the excess molar volume is negative for [bheaa] -water system with the maximum negative value is at x_{bheaa}= 0.3159. The negative values for the [bheaa] - water system could be attributed to the fact that a possible efficient packing of water molecules with [bheaa] and/ or a possible attractive interaction during the mixing of [bheaa] with water especially at higher temperature since the negativity is increasing with temperatures. These interactions however are greatly depend on the composition as well as the temperature. In contrast with the [bheaa] -water system, for [bheaa] – MEA, it exhibits mostly positive excess molar volume except at higher temperatures, where V^E is slightly negative for dilute ionic liquid solutions and positive for concentrated ionic liquid solutions. The change in excess molar volume may be attributed to the strong interaction with amine solutions at low ionic liquid concentrations especially at higher temperature that it cause a contraction on

the volume of the solutionss, and the interaction becomes weak with increasing ionic liquid concentrations.

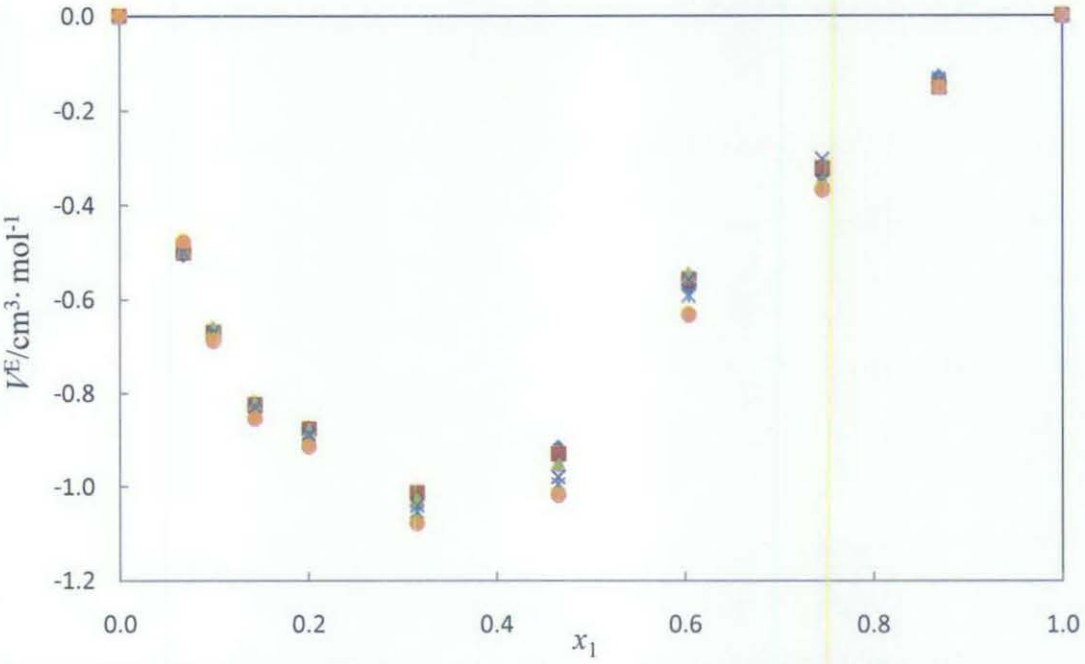

Figure 4.22. Plot of experimental values of excess molar volumes V^E against x_1 for [bheaa] (1) + water (2) binary mixture: ◆, 303.15 K; ■, 313.15 K; ▲, 323.15 K; X, 333.15 K; ✳, 343.15 K; ●, 353.15 K.

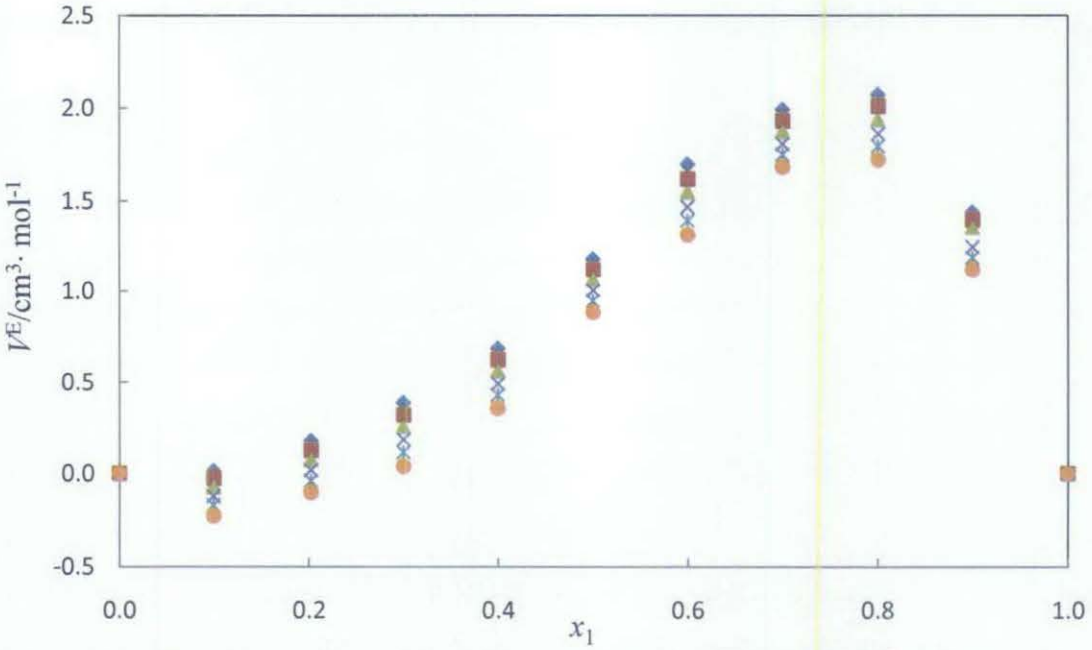

Figure 4.23. Plot of experimental values of excess molar volumes V^E against x_1 for [bheaa] (1) + MEA (2) binary mixture: ◆, 303.15 K; ■, 313.15 K; ▲, 323.15 K; X, 333.15 K; ✳, 343.15 K; ●, 353.15 K.

[bmim][BF$_4$] system

The calculated excess molar volumes for [bmim][BF_4] – Water and [bmim][BF_4] – MEA systems are presented in Table D-2 of Appendix D and the plot of V^E against mole fraction of [bmim][BF_4] (x_1) are shown in Figure 4.24 and 4.25, respectively.

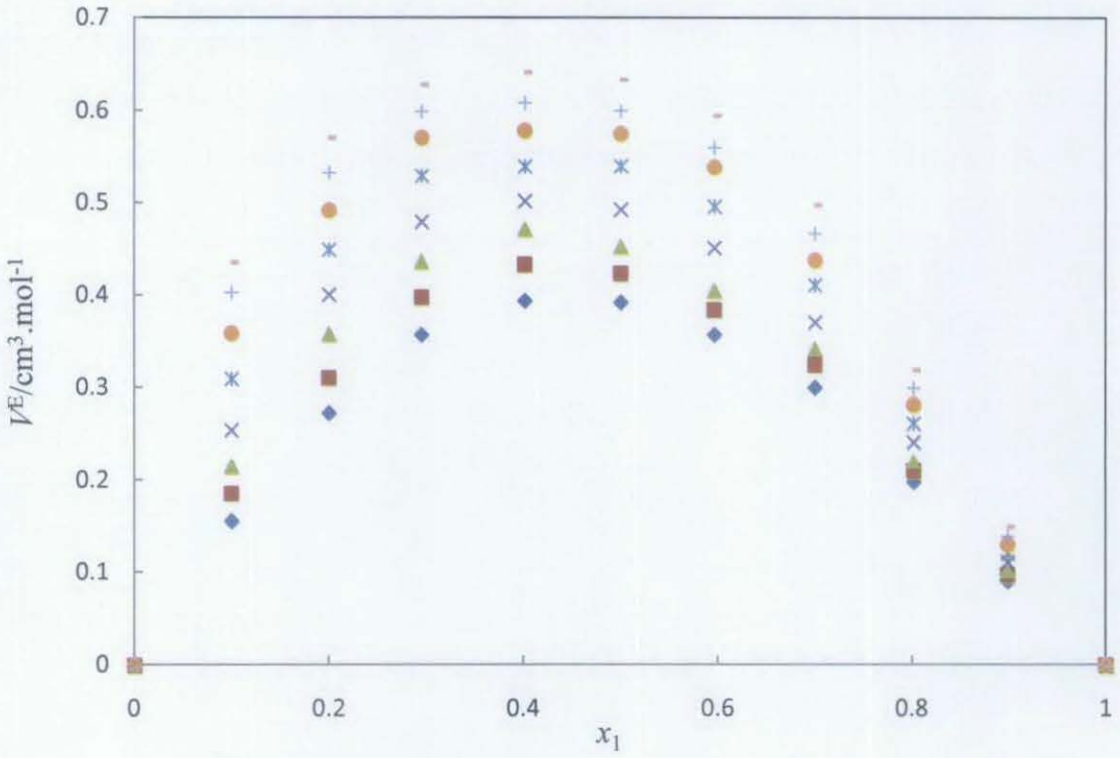

Figure 4.24. Plot of experimental values of excess molar volumes V^E against x_1 for [bmim][BF_4] (1) + water (2) binary mixture: ◆, 293.15 K; ■, 298.15 K; ▲, 303.15 K; X, 313.15 K; ✳, 323.15 K; ●, 333.15 K; +, 343.15 K; , —, 353.15 K.

The results show that the binary mixtures of [bmim][BF_4] with water and MEA exibit positive deviation from ideality, with the highest value at $x_{[bmim][BF4]} = 0.4016$ for [bmim][BF_4] – water system and $x_{[bmim][BF4]} = 0.2994$ for [bmim][BF_4] – MEA system. The magnitude of the excess volume increases with increasing temperatures. The increase in the magnitude of the positive V^E values with temperature were attributed to the decreasing importance of hydrogen bonding effect with increasing

temperature. The positive value indicate that there is a volume expansion on the mixing and that the interaction between unlike molecules are weaker and insufficient to cause volume contraction. The dependence of V^E on temperature and composition for the mixtures can also be explained by the variation in inter molecular forces between the compounds or the variation in the molecular packing, which are due to the differences in size and shape of the molecules forming a binary mixture with other compound. Form the results of V^E for all binary mixtures, it can be said that the intermolecular interaction between unlike molecules in the binary mixtures of [bheaa] + water and [bheaa] + MEA are stronger than the pure components while the molecular interaction in both binary systems involving [bmim][BF_4] are weaker than the pure components and has cause an expansion on the volume of the solutions.

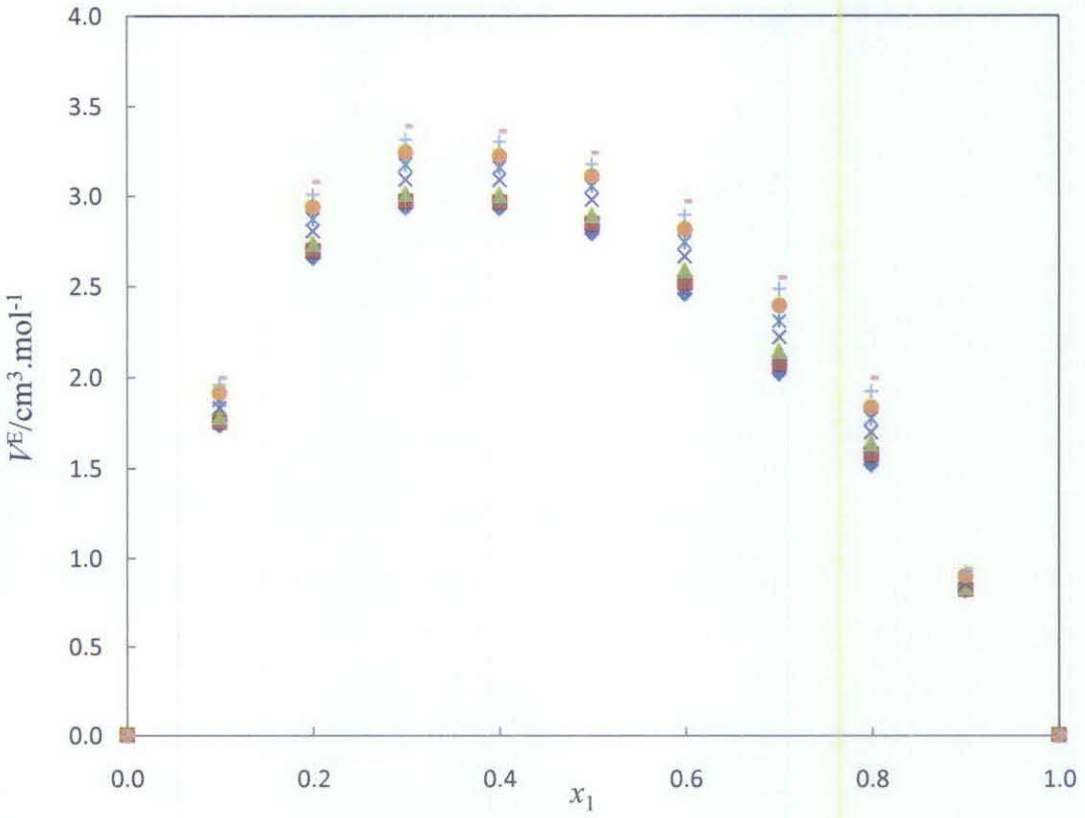

Figure 4.25. Plot of experimental values of excess molar volumes V^E against x_1 of [bmim][BF_4] for [bmim][BF_4] (1) + MEA (2) binary mixture: ◆, 293.15 K; ■, 298.15 K; ▲, 303.15 K; X, 313.15 K; ✳, 323.15 K; ●, 333.15 K; +, 343.15 K; , —, 353.15 K.

Correlation of excess molar volumes for the binary mixtures

The estimated excess molar volume for all the binary systems involving ([bheaa] + water, [bheaa] + MEA, [bmim][BF_4] + water, [bmim][BF_4] + MEA) are correlated using the following Redlich-Kister type polynomial equation:

$$V^E = x_i x_j \sum_{i=0}^{n} A_k \left(x_i - x_j\right)^k \tag{4.20}$$

where V^E and x are the excess properties and the mole fraction respectively. The estimated parameters of the Redlich-Kister equation for representing excess molar volumes for [bheaa] + water and [bheaa] + MEA are presented in Table D-3 of Appendix D while the parameters of the Redlich Kister equation for [bmim][BF_4] + water and [bmim][BF_4] + MEA are presented in and Table D-4 of Appendix D. It was found that the correlation fits well with sixth and fifth order polynomial equation for both binary systems involving [bheaa] and [bmim][BF_4] respectively.

Analysis on the correlation coefficients for all binary mixtures show the variation of the coefficients with temperature. Hence, an attempt has been made to correlate the correlation coefficients as a function of temperature using the following equation:

$$A_k = B_0 + B_1 T + B_2 T^2 + B_3 T^3 + B_n T^n \tag{4.21}$$

where A_k is the parameter with the function of x. The order (k) and the coefficients (A_k and B_n) of the Redlich Kister polynomial equation were obtained using the method of least squares. The estimated parameters together with the standard

deviations (equation 4.3) are presented in Table D-5 of Appendix D for [bheaa] systems and in Table D-6 of Appendix D for [bmim][BF_4] systems.

4.4.1.2 Ternary Mixtures

The calculated excess molar volumes for the ternary system of [bheaa] + MEA + water are presented in Table D-7 of Appendix D. The effect of temperature on the excess molar volume of the ternary system are presented in Figure 4.26.

a)

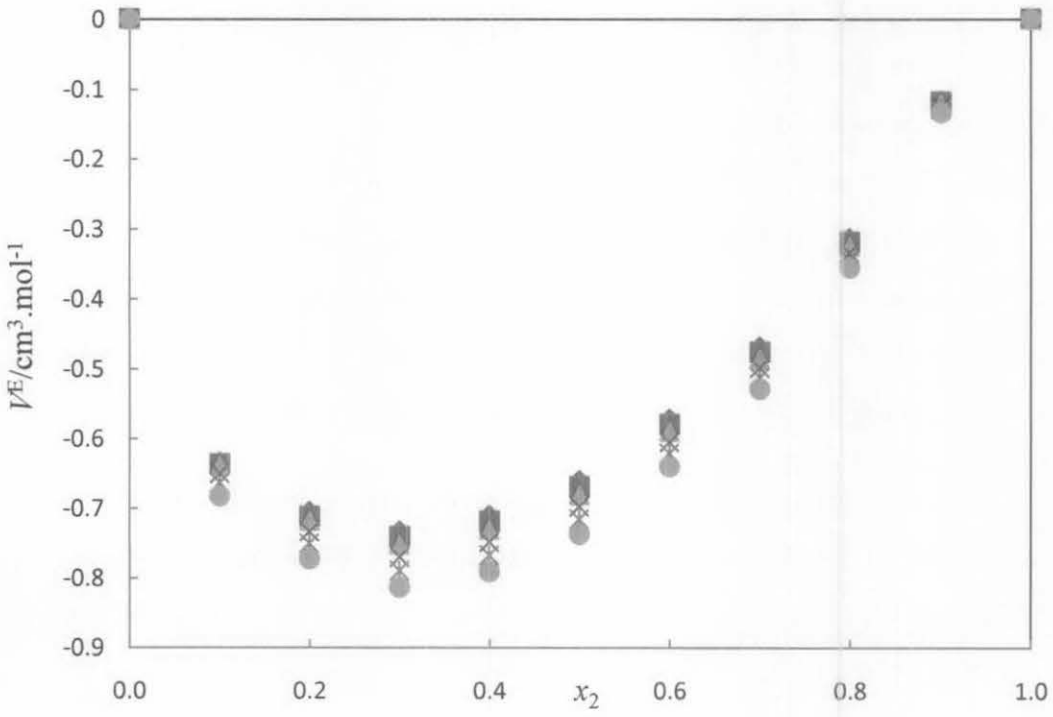

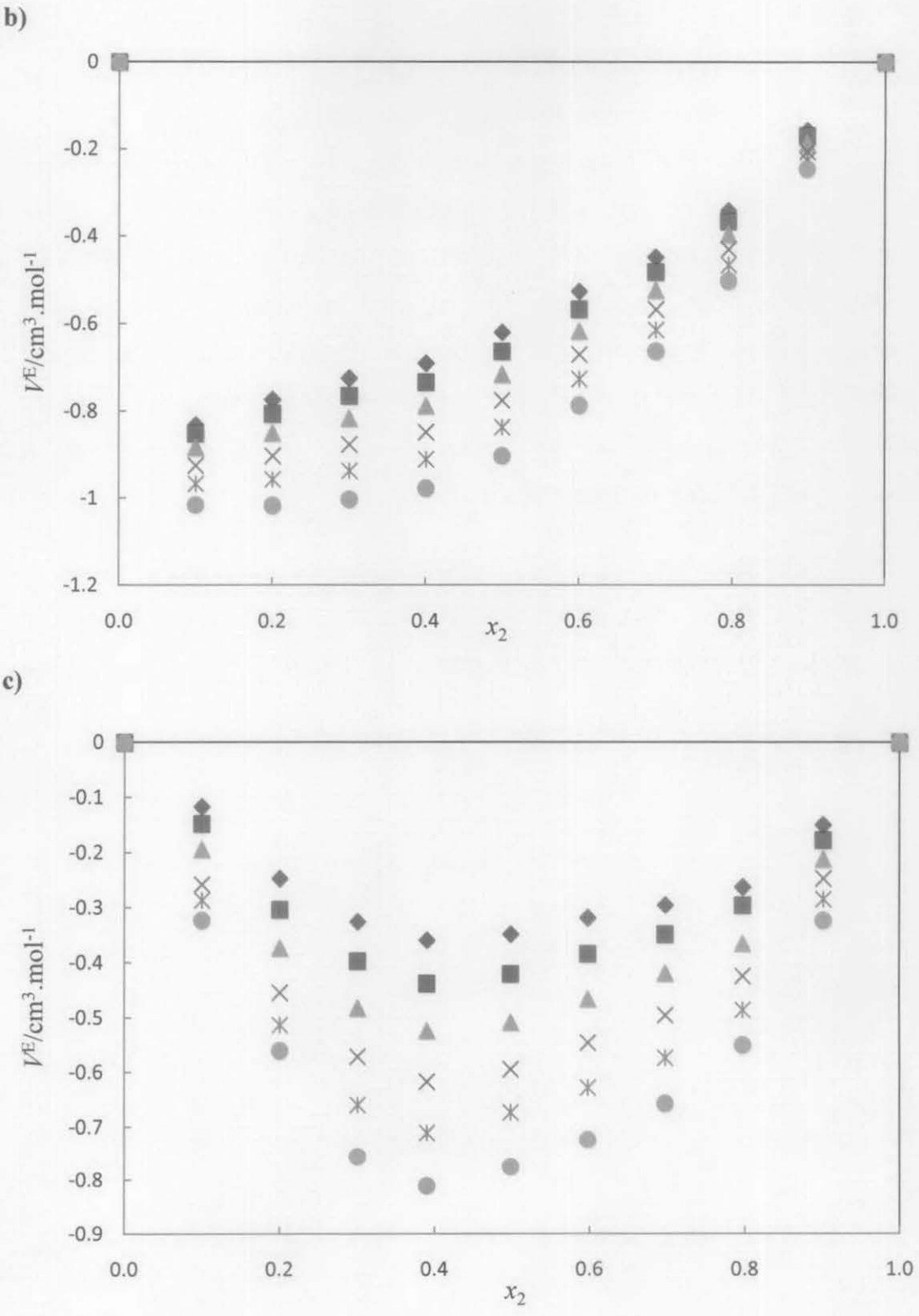

Figure 4.26. Plot of experimental values of excess molar volume, V^E, of the ternary mixtures for [bheaa] (x_1) + MEA (x_2) water (x_3) against mole fraction of MEA at constant: a) z = 0.11; b) z = 0.62; c) z = 4.03 at temperatures: ◆ , 303.15 K; ■ , 313.15 K; ▲, 323.15 K; ╳, 333.15 K; ✳ , 343.15 K; ● , 353.15 K.

From the analysis of the results obtained, it can be seen that the excess molar volume for all 'z' values exhibit mostly negative. For z = 0.11, the excess molar volume shows totally negative with the maximum negative value occurs at x_{MEA} = 0.3002. For z = 0.62, the excess molar volume also shows negative value for the whole composition range and the highest negative value at x_{MEA} = 0.0998 whereas for z = 4.03, the maximum negative value was at x_{MEA} = 0.3895. Based on the observation, it can be seen that the negativity is higher at lower 'z' value whereby the concentration of [bheaa] are less and therefore, it can be said that the decreasing amount of ILs in the solutions has increase the interaction of the molecules. It can also be seen that the excess molar volume decrease with an increase in temperature for all ratios studied.

Meanwhile, the estimated excess molar volume for the ternary system of [bmim][BF_4] + MEA + water are presented in Table D-8 of Appendix D. Figure 4.27 show the effect of temperature and mole fraction of [bmim][BF_4] on excess molar volumes.

a)

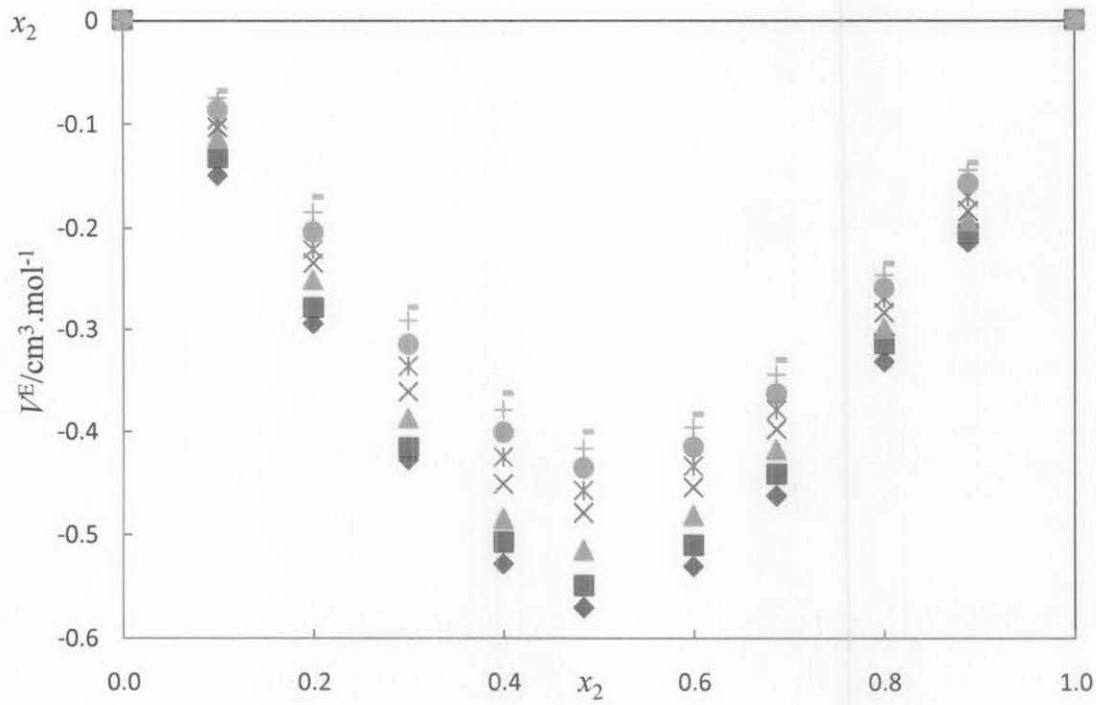

b)

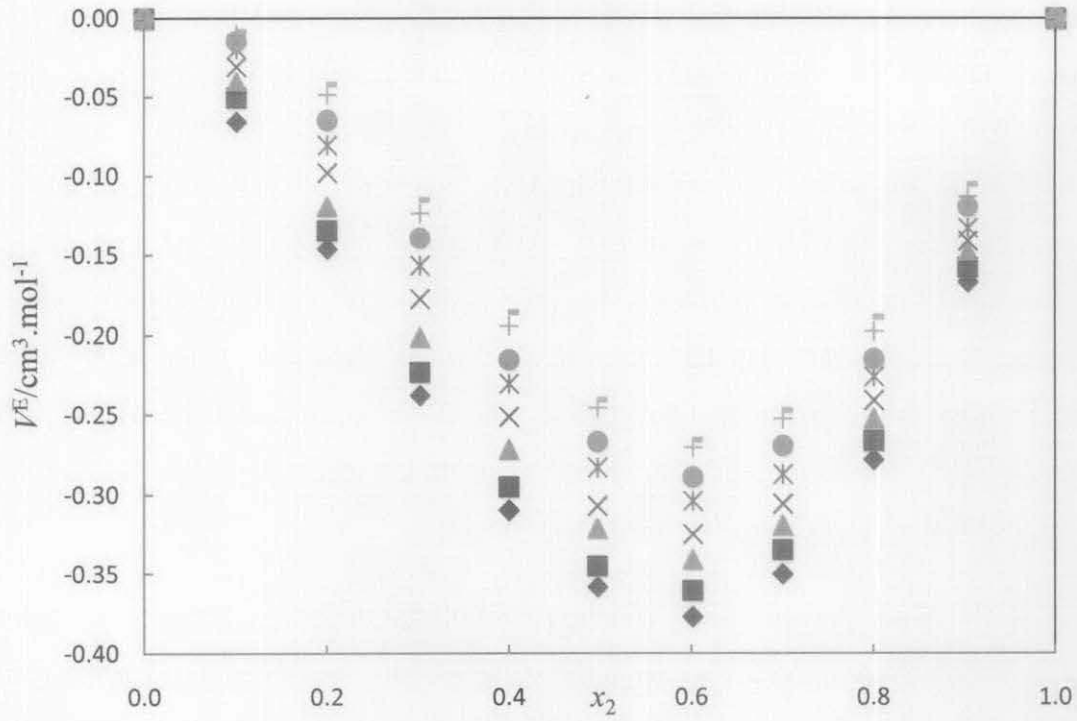

c)

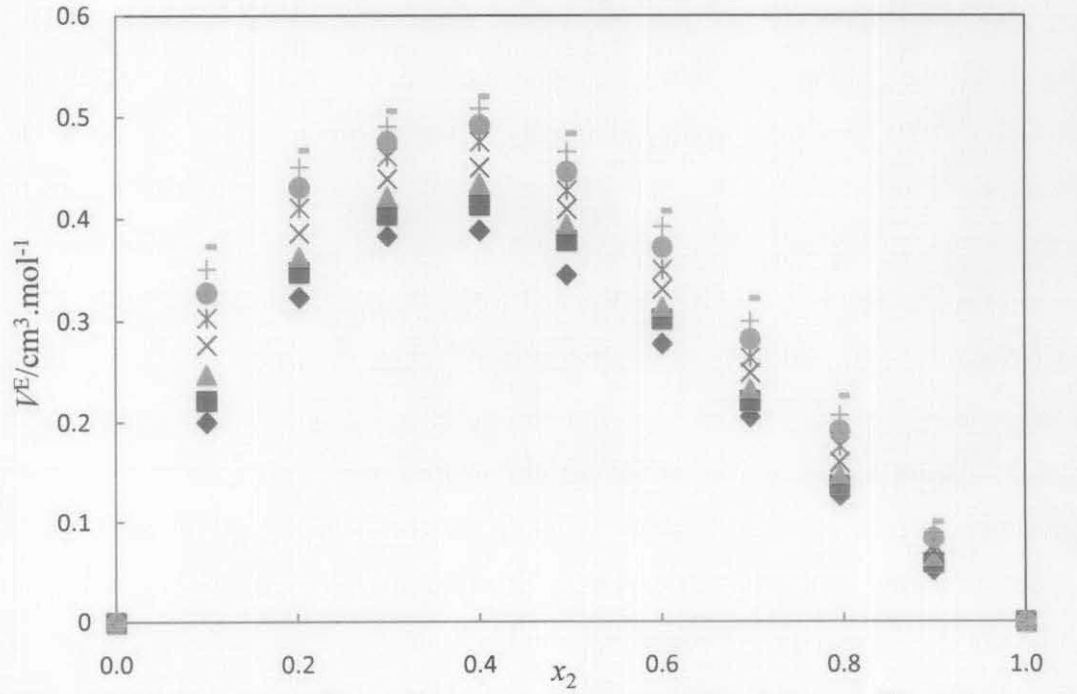

Figure 4.27. Plot of experimental values of excess molar volume, V^E, of the ternary mixtures for [bmim][BF_4] (x_1) + MEA (x_2) water (x_3) against mole fraction of MEA at all constant: a) $z = 0.08$; b) $z = 0.32$; c) z = 5.03 at temperatures: ◆, 293.15 K; ■, 298.15 K; ▲, 303.15 K; ✕, 313.15 K; ✳, 323.15 K; ●, 333.15 K; +, 343.15 K; ▬, 353.15 K.

The estimated excess molar volumes for [bmim][BF_4] + MEA + water system are found to increase with an increase in temperature. For z = 0.08 and z = 0.32, the excess molar volumes are negative with the maximum negative values were at x_{MEA} = 0.4841 and x_{MEA} = 0.6011, respectively, while for z= 5.03, the excess molar volume shows a positive sign with the highest value at x_{MEA} = 0.3997. The negativity was observed to be of higher value at z = 0.08 than z = 0.32 and it was found out that the composition of water is more in the former solutions than in the latter solutions. Hence, it can be said that the interaction of water molecules in the solution are dominating over the whole interactions. The lower composition of water at the solution of z = 5.03 is believe to cause the volume expansion on the solution and thus encourage the value of V^E to a postive values.

The results of execss molar volume represent the difference between the molar volume of the real solution and the molar volume of an ideal solution (Deenadayalu et.al., 2010). The magnitude and sign of the excess molar volume indicates two possibilities: (i) a positive sign (the breakdown of self-associated molecules (ii) a negative sign (due to the packing effect and/ or (ion-dipole) and/or strong intermolecular interactions between the associated molecules (Deenadayalu and Bhjrajh, 2008). Therefore, the negative value of excess molar volume for the ternary systems of [bheaa] + MEA + water indicate that ion-dipole interactions and packing effect between [bheaa], MEA, and water are dominating over dissociation of the intermolecular hydrogen bond in MEA and water (Deenadayalu and Bhjrajh, 2008). Meanwhile for [bmim][BF_4] + MEA + water system, the calculated excess molar volume show variation in the sign. For the lower value of z, the estimated excess molar volume are negative, which might due to the packing effect of water molecules into [bmim][BF_4] matrices, while for the higher value of z, a positive value is obtained indicating an expansion in volume with a possible breakdown of self-associated molecules (Deenadayalu and Bhjrajh, 2008). However, in these two systems, the excess molar volume of [bheaa] + MEA + water ternary system is more negative than [bmim][BF_4] + MEA + water system and therefore it can be said that the interaction of MEA and water molecules with [bheaa] is more than the interaction of MEA and water with [bmim][BF_4].

Correlation of excess molar volumes for the ternary mixtures

The estimated excess molar volume for [bheaa] + MEA + water and [bmim][BF_4] + MEA + water system are correlated using the following form of Cibulka equation:

$$V^E = \sum_{i,j=1,2;1,3;2,3;} V_{i,j}^E\left(x_i, x_j\right) - x_1 x_2 x_3 \left(b_0 - b_1 x_1 - b_2 x_2\right) \tag{4.22}$$

where x_1, x_2, and x_3 are the mole fractions of the IL, MEA and water, respectively, and V^E is the excess molar volume. The former equation contains three parameters (b_0, b_1, and b_2) which is the correction over the three binary contributions for each ternary systems. For solving Cibulka equation, the required binary data of MEA + water were collected from Lee and Lin (1995) and Tseng *et al.* (1963) and used for the further calculations. The estimated parameters for [bheaa] + MEA + water system and and [bmim][BF_4] + MEA + water system together with the the standard deviations are presented in Table D-9 and Table D-10 of Appendix D.

4.4.2 Viscosity Deviation

The measured viscosity data for all binary and ternary systems are used for calculating the viscosity deviation by using the following equation:

$$\Delta\eta = \eta - \sum_{i}^{N} x_i \eta_i \tag{4.23}$$

where x_i represent the mole fraction, η and η_i are the dynamic viscosity of the binary system and the pure component respectively.

4.4.2.1 Binary Mixtures

[bheaa] system

The estimated viscosity deviations for [bheaa] + water and [bheaa] + MEA system are presented in Table E-1 of Appendix E. From the results obtained, it can be seen that the viscosity deviations for [bheaa] - water system are negative over the entire range of compositions with a maximum negative value $x_{[bheaa]}$ 0.3159 and 0.4659 at all temperatures except for temperature 333.15 K. On the other hand, [bheaa] – MEA system shows an asyymmetric curve with negative values occur for $x_{[bheaa]} \leq 0.5998$ and becoming positive for all other concentration. The variation of the viscosity deviations with temperature are demonstrated in Figures 4.28 and 4.29 for [bheaa]-water and [bheaa] – MEA system respectively. It can be seen that the viscosiy deviation also increase with an increase in temperature.

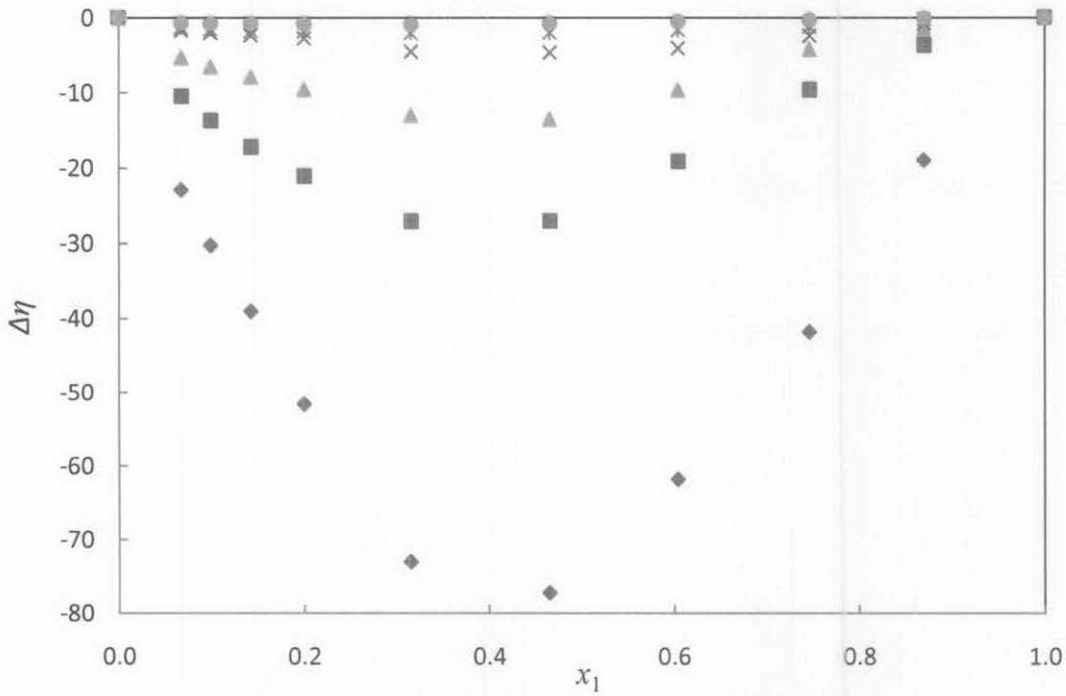

Figure 4.28. Plot of experimental values of viscosity deviation $\Delta\eta$ against x_1 for [bheaa] (1) + water (2) binary mixture: ◆ , 303.15 K; ■ , 313.15 K; ▲, 323.15 K; X, 333.15 K; ✳ , 343.15 K; ● , 353.15 K.

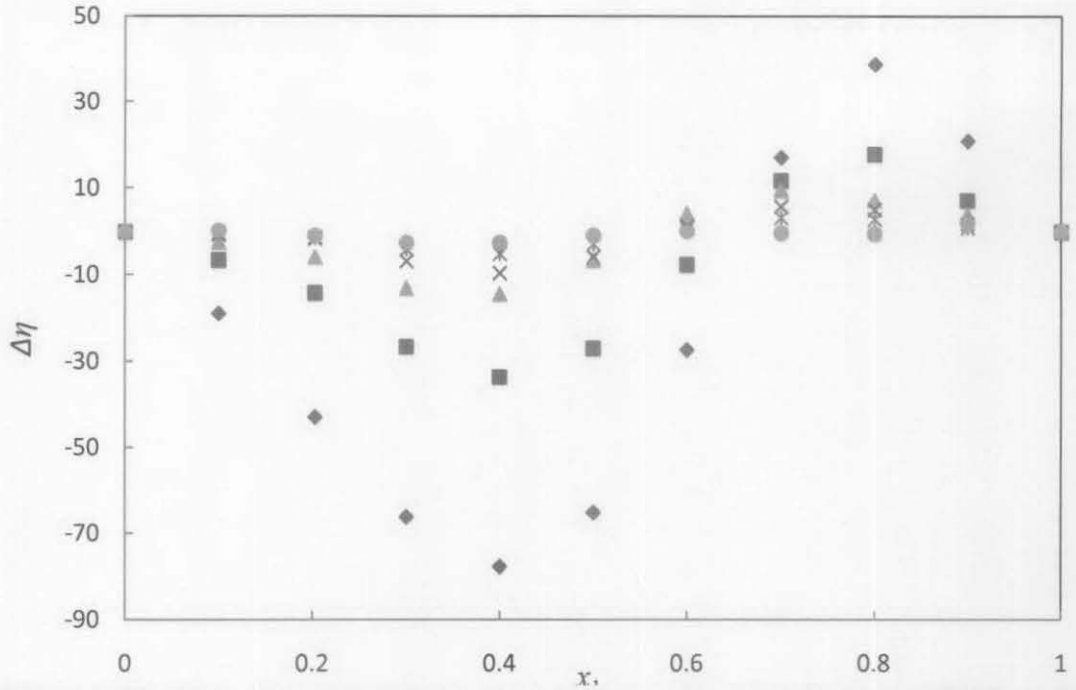

Figure 4.29. Plot of experimental values of viscosity deviation $\Delta\eta$ against x_1 for [bheaa] (1) + MEA (2) binary mixture: ◆, 303.15 K; ■, 313.15 K; ▲, 323.15 K; ╳, 333.15 K; ✳, 343.15 K; ●, 353.15 K.

[bmim][BF4] system

The estimated viscosity deviations for both systems involving [bmim][BF_4] are presented in Table E-2 of Appendix E and the variation of viscosity deviation with temperature are shown plotted in Figures 4.30 and 4.31 for [bmim][BF_4] – Water and [bmim][BF_4] – MEA systems respectively.

Negative deviations are observed over the entire range of composition and temperature for both the systems. The maximum deviation occured at higher concentration of [bmim][BF_4] due to the significant difference between the viscosity of pure [bmim][BF_4] and pure MEA and water.

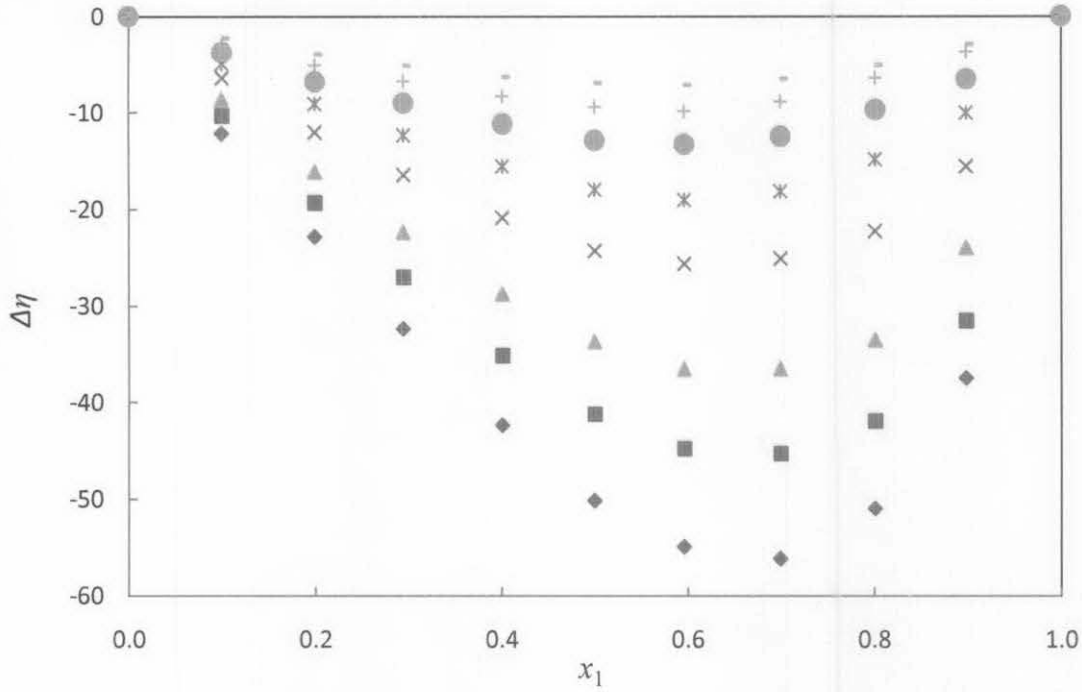

Figure 4.30. Plot of experimental values of viscosity deviation $\Delta\eta$ against x_1 for [bmim][BF_4] (1) + water (2) binary mixture: ◆ , 293.15 K; ■ , 298.15 K; ▲, 303.15 K; X, 313.15 K; ✳ , 323.15 K; ● , 333.15 K; + , 343.15 K; , —, 353.15 K

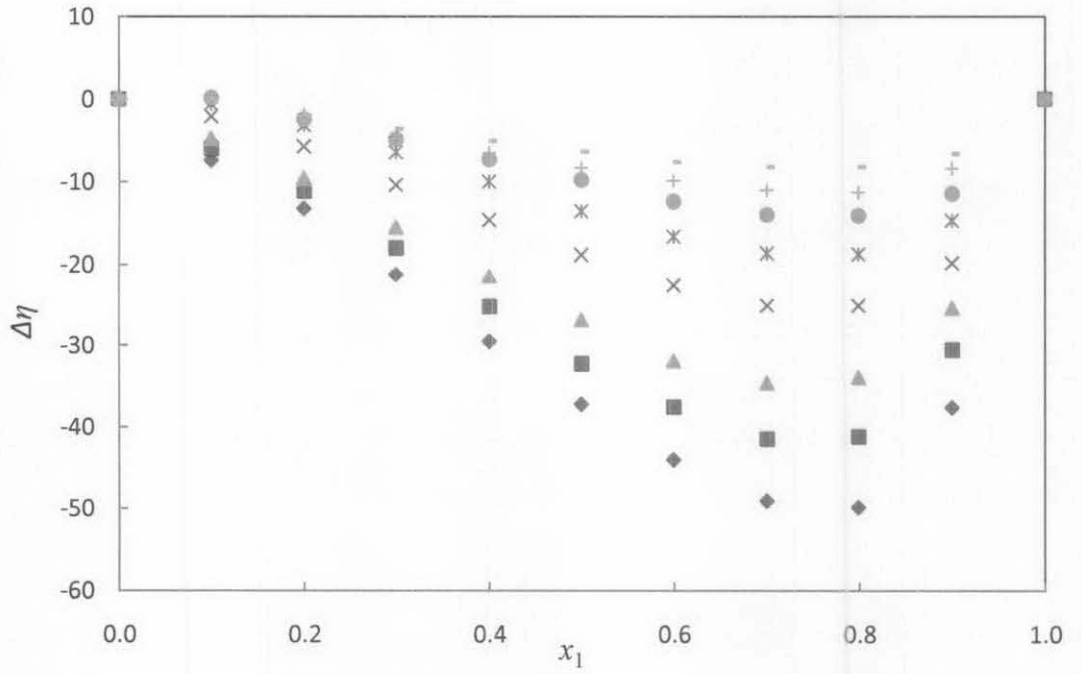

Figure 4.31. Plot of experimental values of viscosity deviation $\Delta\eta$ against x_1 for [bmim][BF_4] (1) + MEA (2) binary mixture: ◆ , 293.15 K; ■ , 298.15 K; ▲, 303.15 K; X, 313.15 K; ✳ , 323.15 K; ● , 333.15 K; + , 343.15 K; , —, 353.15 K

Correlation of viscosity deviation for binary systems

The values of the viscosity deviation for all binary systems involved were correlated using the following Redlich-Kister polynomial equation:

$$\Delta\eta = x_i x_j \sum_{i-0}^{n} A_k \left(x_i - x_j\right)^k \tag{4.24}$$

where $\Delta\eta$ and x are the viscosity deviation and the mole fraction respectively. The estimated parameters for the correlation of viscosity deviation together with the standard deviations calculated by using equation (4.3) are presented in Table E-3 and Table E-4 of Appendix E for [bheaa] and [bmim][BF_4] based binary systems respectively.

Similar to excess molar volumes, the estimated parameters of the Redlich-Kister equation for viscosity deviation also show dependency on the temperature. Therefore, the correlation coefficients are further correlated as a function of temperature using equation 4.21.

The estimated parameters for the correlation are presented in Table E-5 and Table E-6 of Appendix E for [bheaa] and [bmim][BF_4] binary systems respectively. It was found that the correlation of Redlich-Kister equation fits well with fifth order polynomial equation while for the correlation coefficients as a function of temperature, it fits well with fourth order polynomial equation for all binary systems involved ([bheaa] + water, [bheaa] + MEA, [bmim][BF_4] + water, [bmim][BF_4] + MEA).

4.4.2.2 Ternary Mixtures

The estimated viscosity deviations for [bheaa] + MEA + water system are shown in Table E-7 of Appendix E. From the results, it can be seen that the values of viscosity deviation increase with a decrease in mole fraction of [bheaa] for a fixed value of z and that the magnitude is observed to increase with an increase in the value of z. The viscosity deviation for $z = 0.62$ and $z = 4.03$, the values exhibit totally positive while for $z = 0.11$, an asymmetric curve is observed with the negative value

at $x_{MEA} \leq 0.3002$. The highest positive values for viscosity deviation were observed for the solution of $z = 4.03$ due to the higher concentration of [bheaa] in the solution. The variation of viscosity deviation with temperatures are shown in Figure 4.32 and it was found that viscosity deviation for all values of 'z' decrease with an increase in temperature.

a)

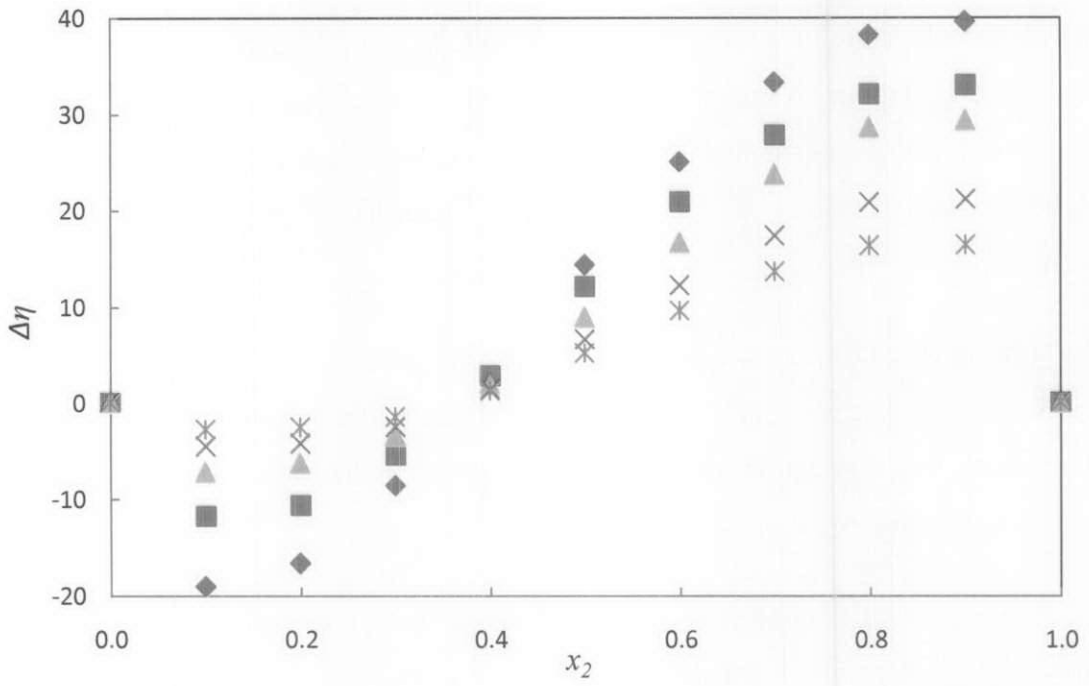

b)

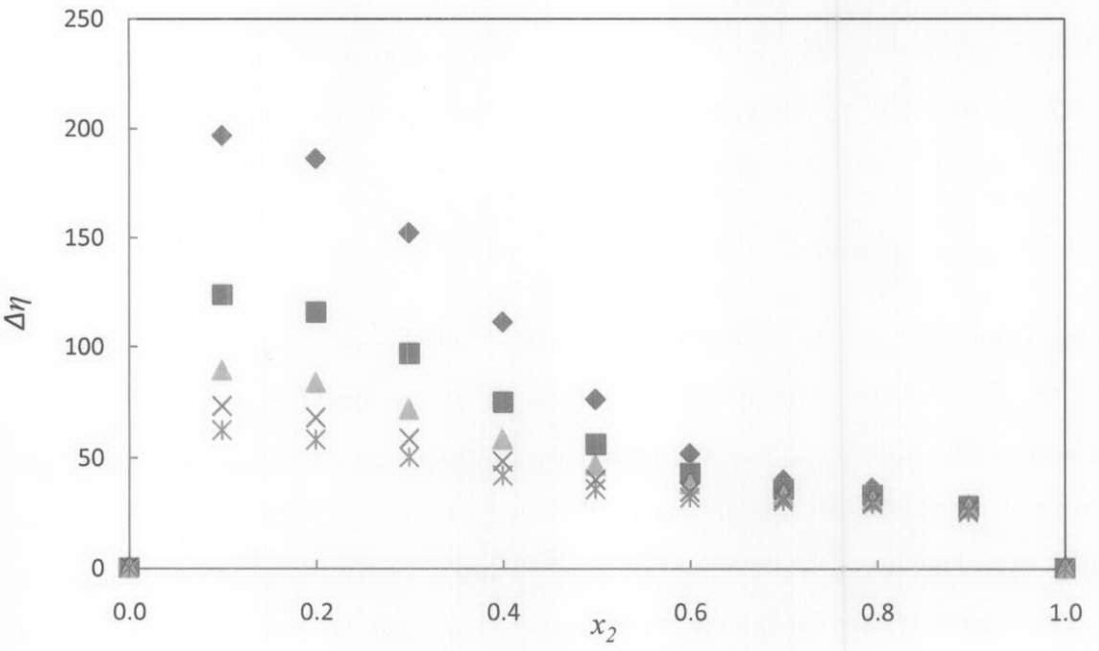

c)

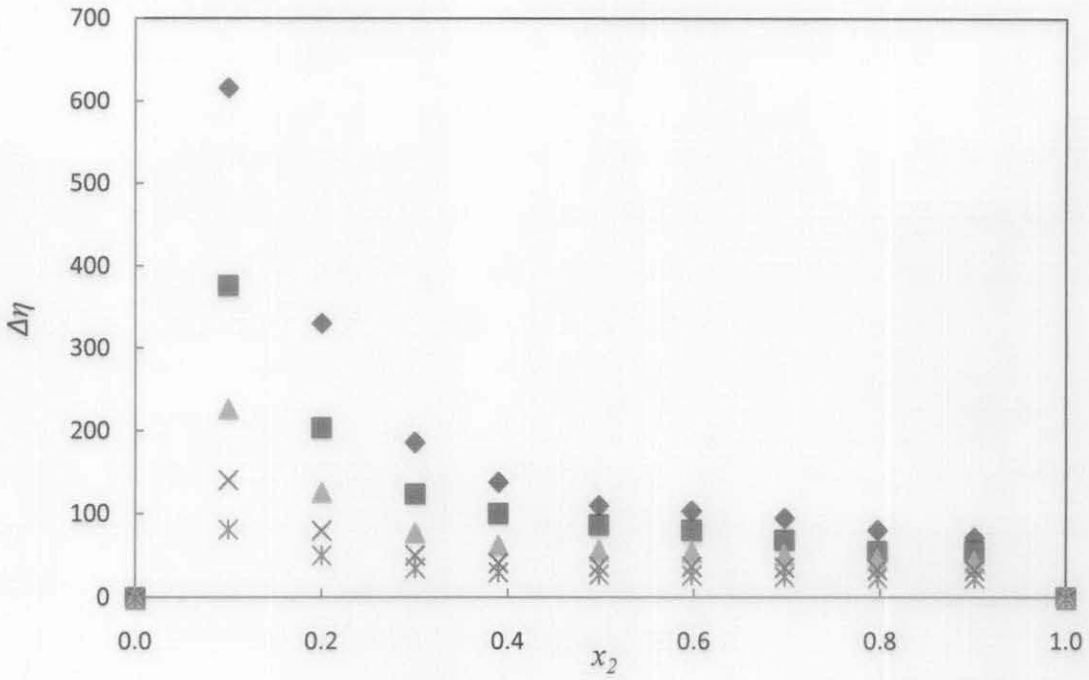

Figure 4.32. Plot of experimental values of viscosity deviation, $\Delta\eta$, of the ternary mixtures for [bheaa] (x_1) + MEA (x_2) water (x_3) against mole fraction of MEA at all constant: a) z = 0.11; b) z = 0.62; c) z = 4.03 at temperatures: ◆ , 303.15 K; ■ , 313.15 K; ▲, 323.15 K; X, 333.15 K; ✳ , 343.15 K..

The results for the viscosity deviation of [bmim][BF_4] + MEA + water system are presented in Table E-8 of Appendix E and the plot of viscosity deviation at different temperatures studied are shown in Figure 4.33. It can be seen that the viscosity deviations decrease with increasing temperature.

From the results obtained, it can also be seen that the magnitude of viscosity deviation decrease with increasing z values. Meanwhile, the value of viscosity deviation also increase with increasing mole fraction of MEA for a fixed value of z. The viscosity deviation for z = 0.08 and z = 0.32 show an asymmetric curve while for z = 5.03, the viscosity deviation show totally negative values with increasing magnitude towards the increasing mole fraction of MEA. The negative values of the asymmetric curve were observed to occur at low MEA concentrations while the positive values were observed at higher concentration of MEA.

a)

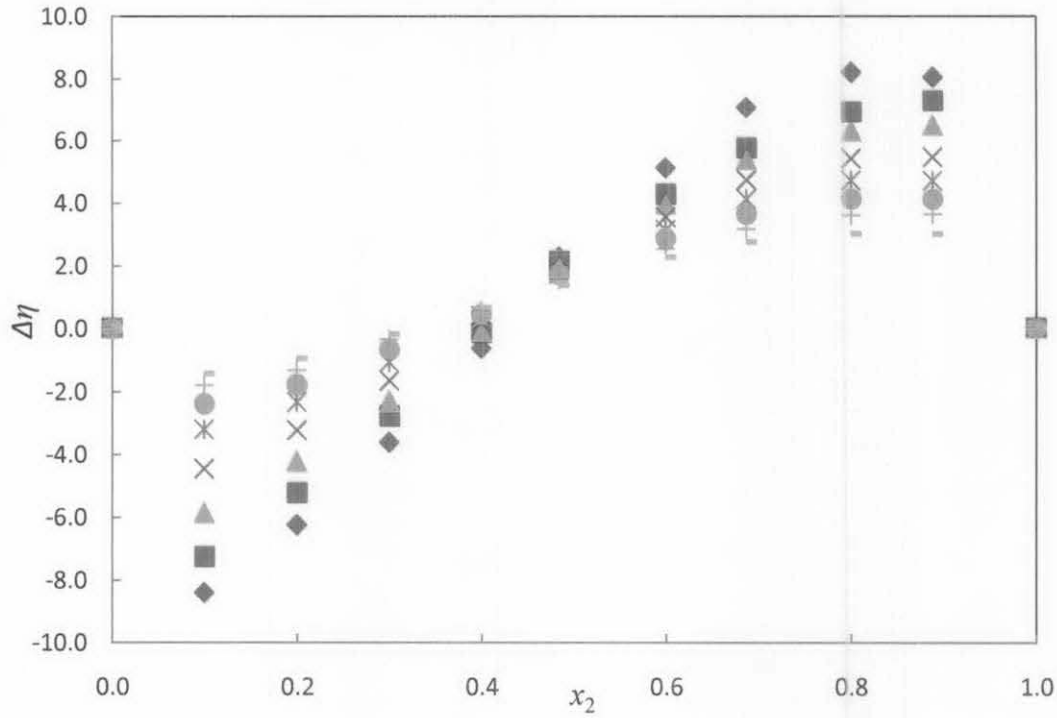
10.0
8.0
6.0
4.0
2.0
0.0
-2.0
-4.0
-6.0
-8.0
-10.0
Δη
0.0
0.2
0.4
0.6
0.8
1.0
x2

b)

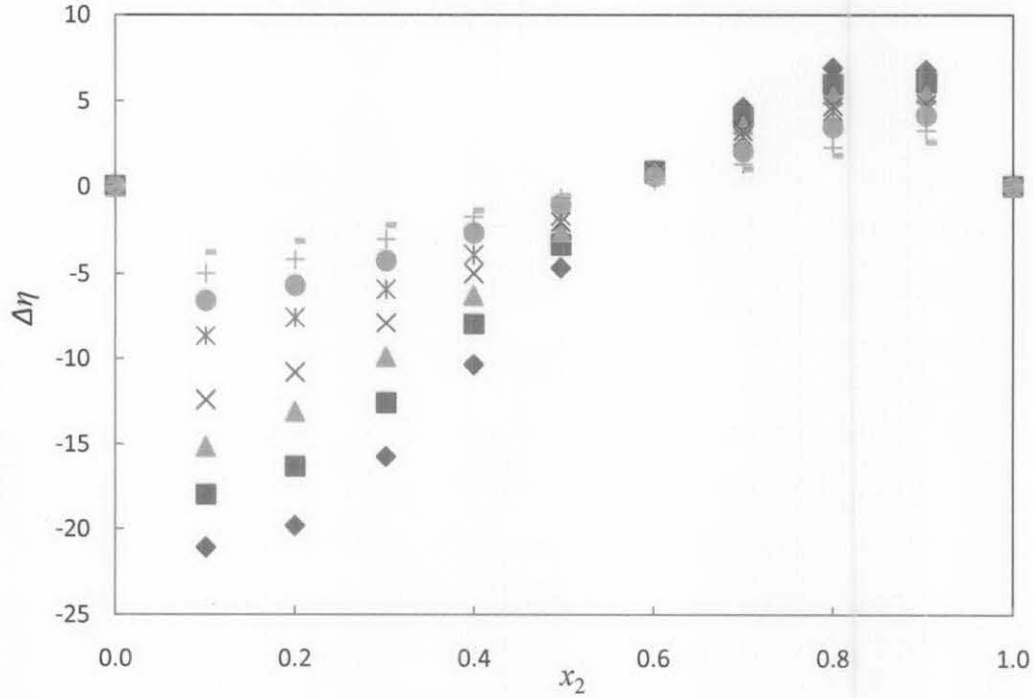
10
5
0
-5
-10
-15
-20
-25
Δη
0.0
0.2
0.4
0.6
0.8
1.0
x2

c)

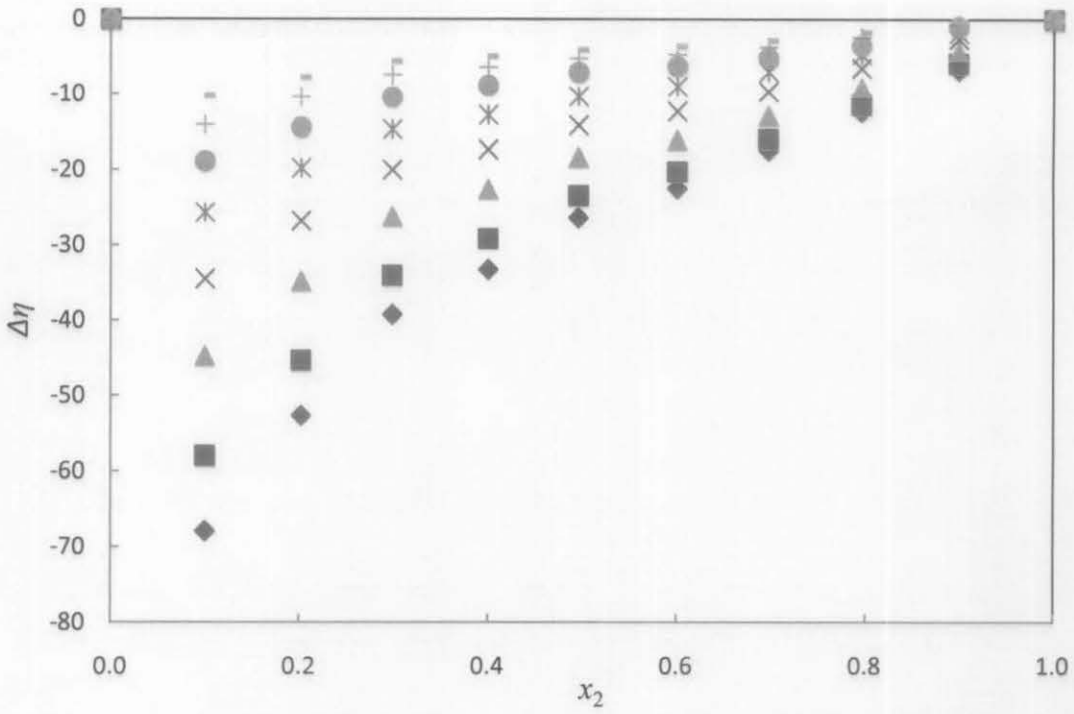

Figure 4.33. Plot of experimental values of viscosity deviation, $\Delta\eta$, of the ternary mixtures for [bmim][BF_4] (x_1) + MEA (x_2) water (x_3) against mole fraction of MEA at all constant: a) $z = 0.08$; b) $z = 0.32$; c) z = 5.03 at temperatures: ◆ , 293.15 K; ■ , 298.15 K; ▲, 303.15 K; X, 313.15 K; ✳ , 323.15 K; ● , 333.15 K; +, 343.15 K; ▬, 353.15 K.

Correlation of viscosity deviation for the ternary mixtures.

The estimated viscosity deviations for [bheaa] + MEA + water and [bmim][BF_4] + MEA + water system are correlated using the following Cibulka equation:

$$\Delta\eta = \sum_{i,j=1,2;1,3;2,3;} \Delta\eta_{i,j}\left(x_i, x_j\right) - x_1 x_2 x_3 \left(b_0 - b_1 x_1 - b_2 x_2\right) \qquad (4.25)$$

where x_1, x_2, and x_3 are the mole fractions of ILs, MEA and water, respectively, and $\Delta\eta$ is the viscosity deviation. The former equation contains three parameters (b_0, b_1, and b_2) which is the correction over the three binary contributions for each ternary

systems. Table E-9 and Table E-10 of Appendix E show the estimated parameters together with the standard deviation calculated using equation (4.3).

4.4.3 Refractive Index Deviation

The refractive index deviation Δn_D for all the binary and ternary mixtures involved were calculated from the experimental refractive index values using the following equation

$$\Delta n_D = n_D - \Sigma x_i n_{Di} \tag{4.26}$$

where n_D are refractive index of the binary mixture, n_{Di} refer refractive index of the pure component *i*.

4.4.3.1 Binary Mixtures

[bheaa] system

The estimated refractive index deviations for both systems are presented in Table F-1 of Appendix F. Figures 4.34 and 4.35 show the calculated refractive index deviations with the maximum value at $x_{[bheaa]} \approx 0.2005$ and $x_{[bheaa]} \approx 0.4000$, for [bheaa] + water and [bheaa] + MEA system respectively. It can be seen from both figures that the refractive index deviation exhibit positive values for all temperatures and the magnitude increased with increasing temperature.

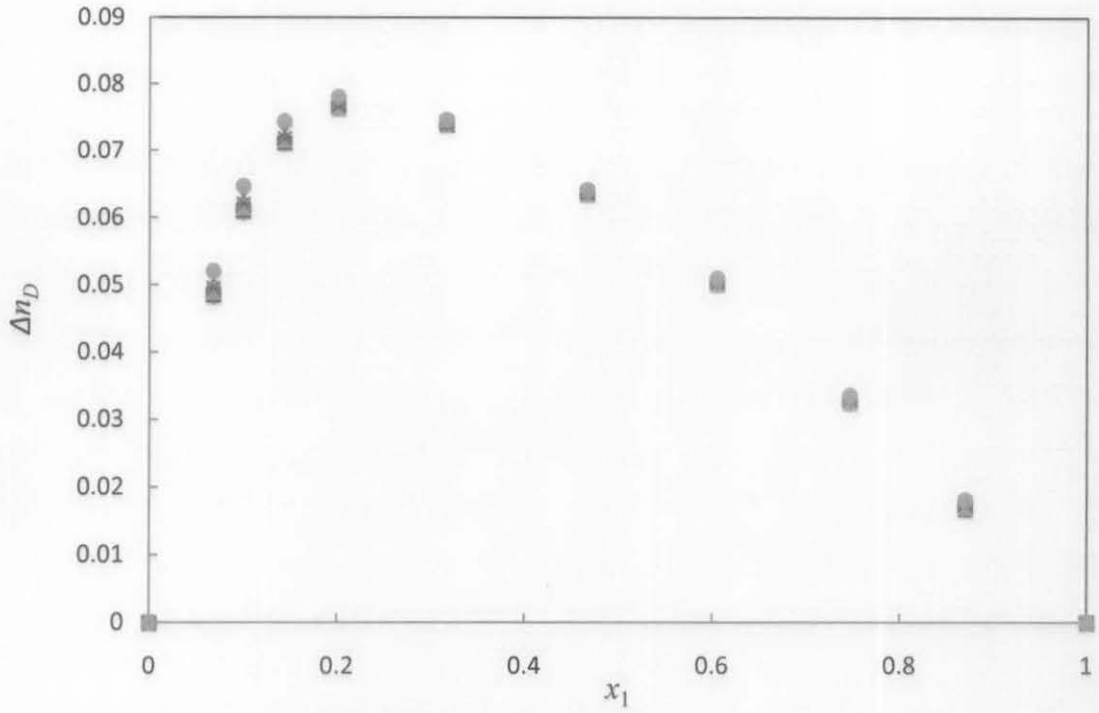

Figure 4.34. Plot of experimental values of refractive index deviation Δn_D against x_1 for [bheaa] (1) + water (2) binary mixture: ◆, 303.15 K; ■, 313.15 K; ▲, 323.15 K; X, 333.15 K; ✳, 343.15 K; ●, 353.15 K.

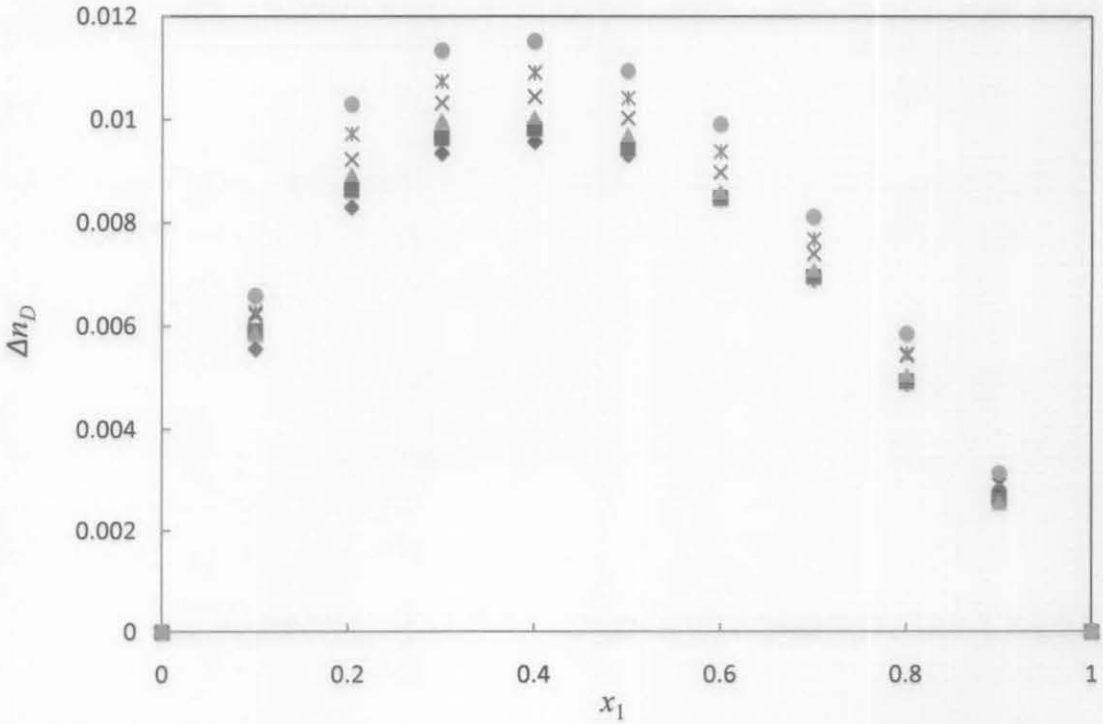

Figure 4.35. Plot of experimental values of refractive index deviation Δn_D against x_1 for [bheaa] (1) + MEA (2) binary mixture: ◆, 303.15 K; ■, 313.15 K; ▲, 323.15 K; X, 333.15 K; ✳, 343.15 K; ●, 353.15 K.

[bmim][BF4] system

The estimated refractive index deviation for [bmim][BF_4] – water and [bmim][BF_4] – MEA systems are presented in Table F-2 of Appendix F. It can be observed that the refractive index deviations for [bmim][BF_4] – water exhibit positive value with maximum at $x_{[bmim][BF_4]}$ = 0.2000 while the refractive index deviations for [bmim][BF_4] – MEA exhibit negative value with maximum at $x_{[bmim][BF_4]}$ = 0.4004. Even though both systems showed a different behaviour, the value are still found to decrease with an increase in temperature. The variation of refractive index deviation with temperature are shown in Figures 4.36 and 4.37 for [bmim][BF_4] – water and [bmim][BF_4] – MEA systems respectively.

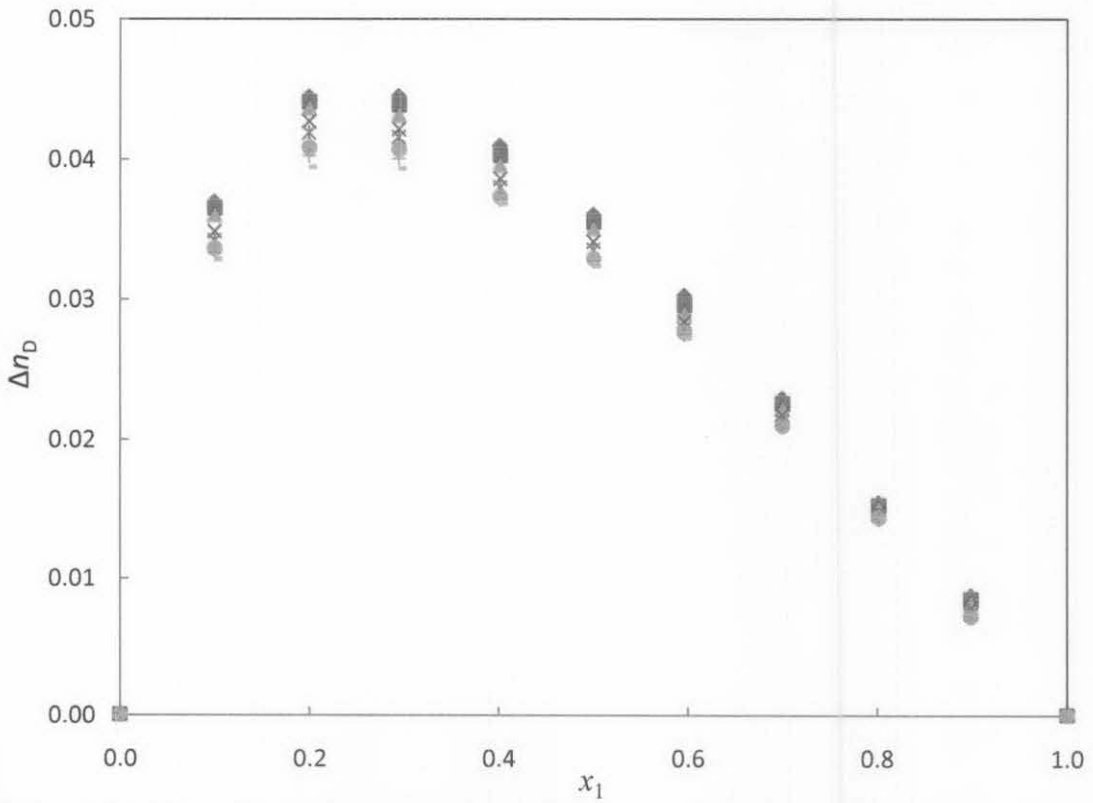

Figure 4.36. Plot of experimental values of refractive index deviation Δn_D against x_1 for [bmim][BF_4] (1) + water (2) binary mixture: ◆ , 293.15 K; ■ , 298.15 K; ▲, 303.15 K; X, 313.15 K; ✳ , 323.15 K; ● , 333.15 K; + , 343.15 K; , —, 353.15 K.

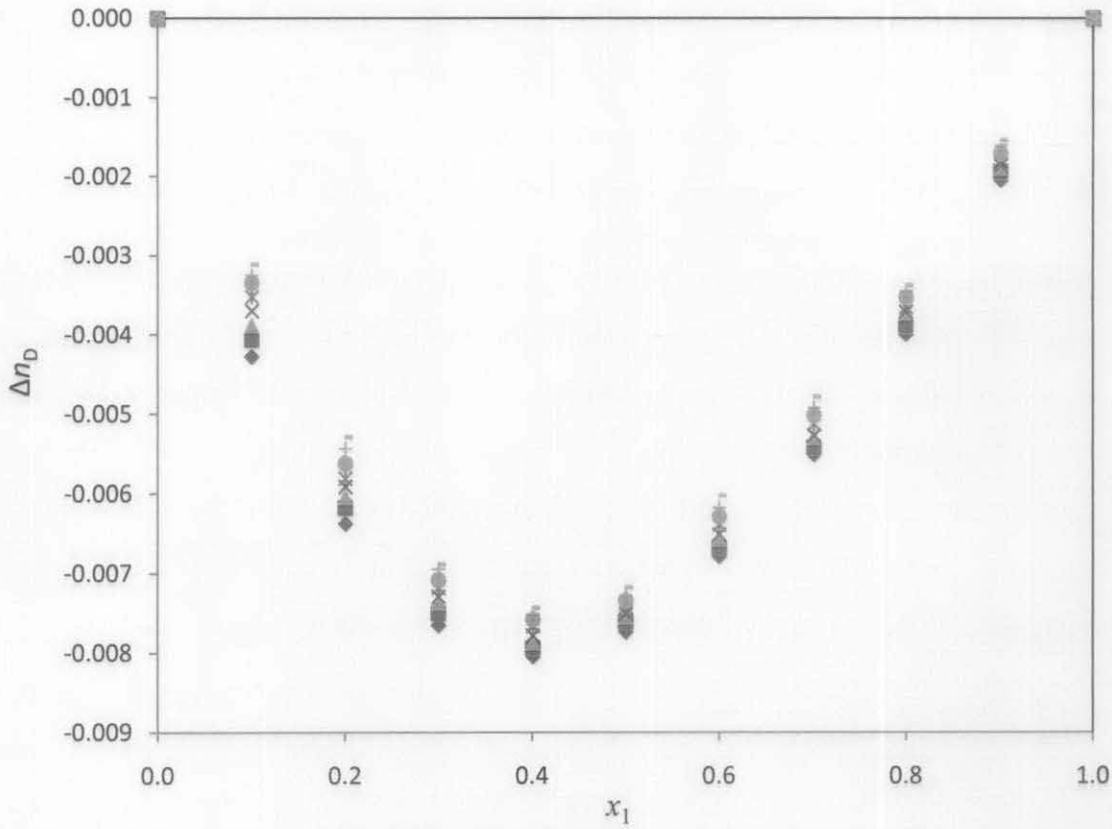

Figure 4.37. Plot of experimental values of refractive index deviation Δn_D against x_1 for [bmim][BF_4] (1) + MEA (2) binary mixture: ◆ , 293.15 K; ■ , 298.15 K; ▲, 303.15 K; X, 313.15 K; ✳ , 323.15 K; ● , 333.15 K; + , 343.15 K; , —, 353.15 K

Correlation of refractive index deviation for binary systems.

The estimated values of the refractive index deviations for all binary systems involved ([bheaa] + water, [bheaa] + MEA, [bmim][BF_4] + water, [bmim][BF_4] + MEA) have been correlated using the following Redlich Kister polynomial equation:

$$\Delta n_D = x_i x_j \sum_{i-0}^{n} A_k \left(x_i - x_j\right)^k \tag{4.27}$$

where Δn_D and x are the refractive index deviation and the mole fraction respectively. A fifth order polynomial was found to fit well with the Redich-Kister

polynomial equation for [bheaa] systems and the estimated parameters are presented in Table F-3 of Appendix F. Meanwhile, a fourth order polynomial was found to fit well with the Redlich-Kister polynomial equation for [bmim][BF_4] systems and the estimated parameters are presented in Table F-4 of Appendix F.

All the estimated correlation coefficients of equation 4.27 are again found to be a function of temperature. Hence, equation 4.21 was used to correlate the parameters as a function of temperature. A second order polynomial equation for [bheaa] systems was used to represent the data while a third and second order polynomial equation was used for [bmim][BF_4] – water and [bmim][BF_4] – MEA systems respectively. The estimated parameters are presented in Table F-5 and Table F-6 of Appendix F for [bheaa] and [bmim][BF_4] binary systems respectively.

4.4.3.2 Ternary Mixtures

The refractive index deviations of [bheaa] + MEA + water are presented in Table F-7 of Appendix F, and the variation of the deviation with temperatures are shown in Figure 4.38. The refractive index deviation for all ratios (z) are also observed to decrease with increasing temperature.

The results show that the value of refractive index deviation exhibit positive for all ' z's and the magnitude are found to decrease with decreasing mole fraction of [bheaa] (x_1) for any fixed value of z. From Figures a, b and c, it can be observed that the highest value for refractive index deviation occur at the lower value of 'z' and that for all figures, the highest value of refractive index deviation was at $x_{MEA} \approx 0.1000$.

For the case of [bmim][BF_4] + MEA + water system, the results for refractive index deviations are presented in Table F-8 of Appendix F. From the estimated refractive index data, it can be seen from Figure 4.39 that the refractive index deviation for $z = 0.08$ and $z = 0.32$ show a positive value with the highest value at $x_{MEA} \approx 0.1000$. On the other hand, the refractive index deviation for $z = 5.03$ were found to have an asymmetric curve with negative value occur at higher concentration of MEA. The highest positive value was observed at $x_{MEA} = 0.0998$ while the highest negative value was observed at $x_{MEA} = 0.6969$.

a)

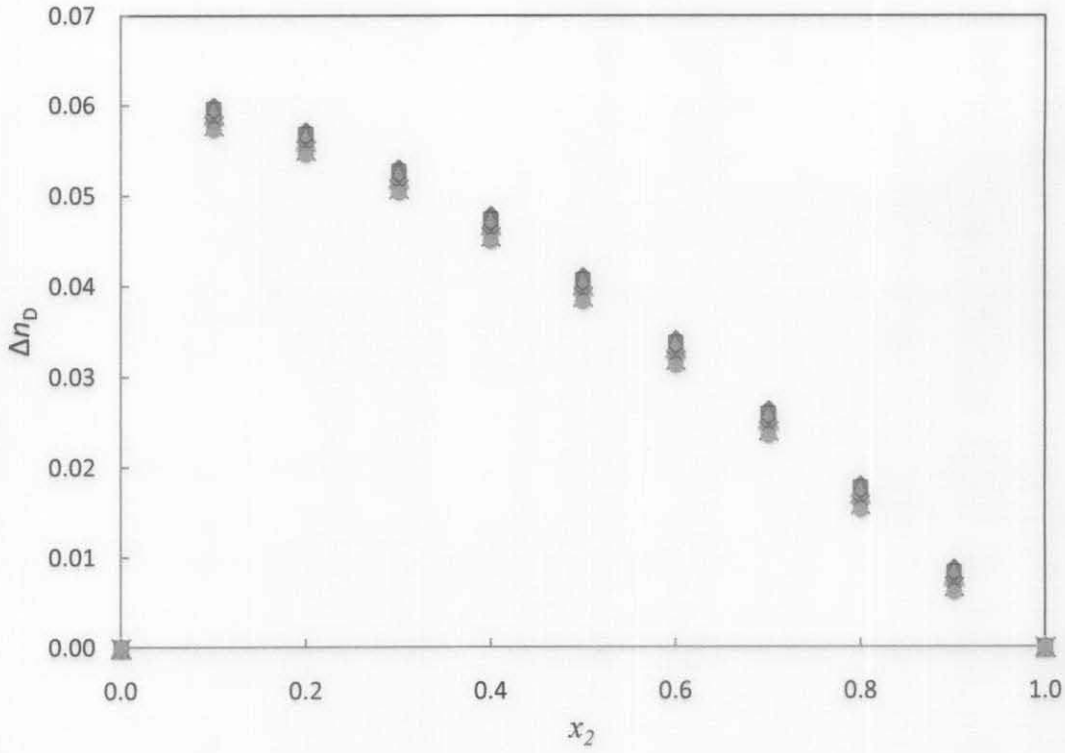
0.07
0.06
0.05
0.04
0.03
0.02
0.01
0.00
Δn_D
0.0
0.2
0.4
0.6
0.8
1.0
x_2

b)

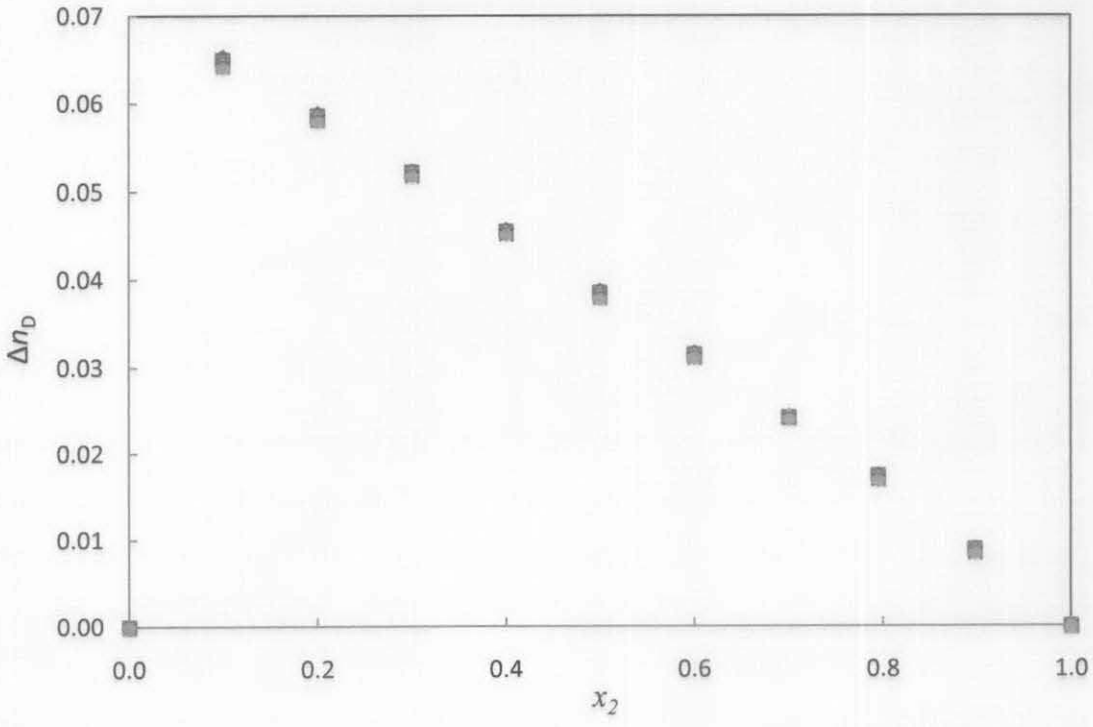
0.07
0.06
0.05
0.04
0.03
0.02
0.01
0.00
Δn_D
0.0
0.2
0.4
0.6
0.8
1.0
x_2

c)

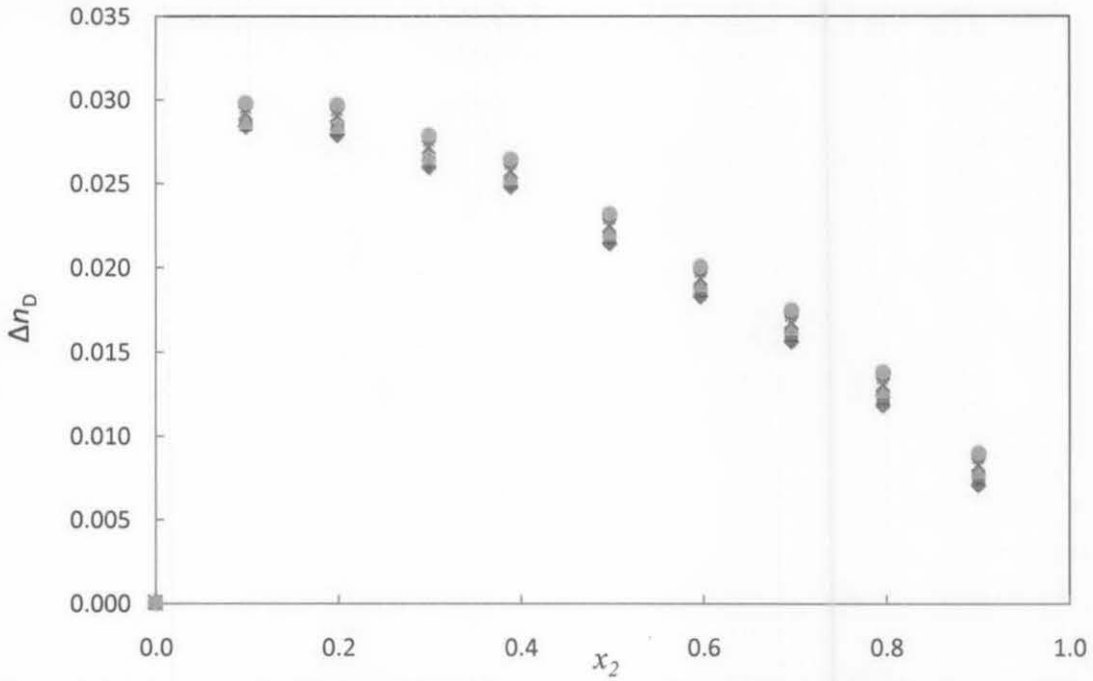

Figure 4.38. Plot of experimental values of refractive index deviation, Δn_D, of the ternary mixtures for [bheaa] (x_1) + MEA (x_2) water (x_3) against mole fraction of MEA at all constant: a) z = 0.11; b) z = 0.62; c) z = 4.03 at temperatures: ◆, 303.15 K; ■, 313.15 K; ▲, 323.15 K; X, 333.15 K; ✳, 343.15 K; ●, 353.15 K

Correlation of refractive index deviation for ternary systems.

The refractive index deviation for both ternary systems have been correlated using the following Cibulka equation:

$$\Delta n_D = \sum_{i,j=1,2;1,3;2,3;} \Delta n_{D_{i,j}}(x_i, x_j) - x_1 x_2 x_3 (b_0 - b_1 x_1 - b_2 x_2) \qquad (4.28)$$

where x_1, x_2, and x_3 are the mole fractions of the IL, MEA and water, respectively, and Δn_D is the refractive index deviation. The former equation contains three parameters (b_0, b_1, and b_2) represents the correction over the three binary contributions for each ternary systems. The estimated parameters of the correlation are presented in Table F-9 and Table F-10 of Appendix F for [bheaa] + MEA + water and [bmim][BF_4] + MEA + water system respectively, together with the standard deviation calculated using equation (4.3).

a)

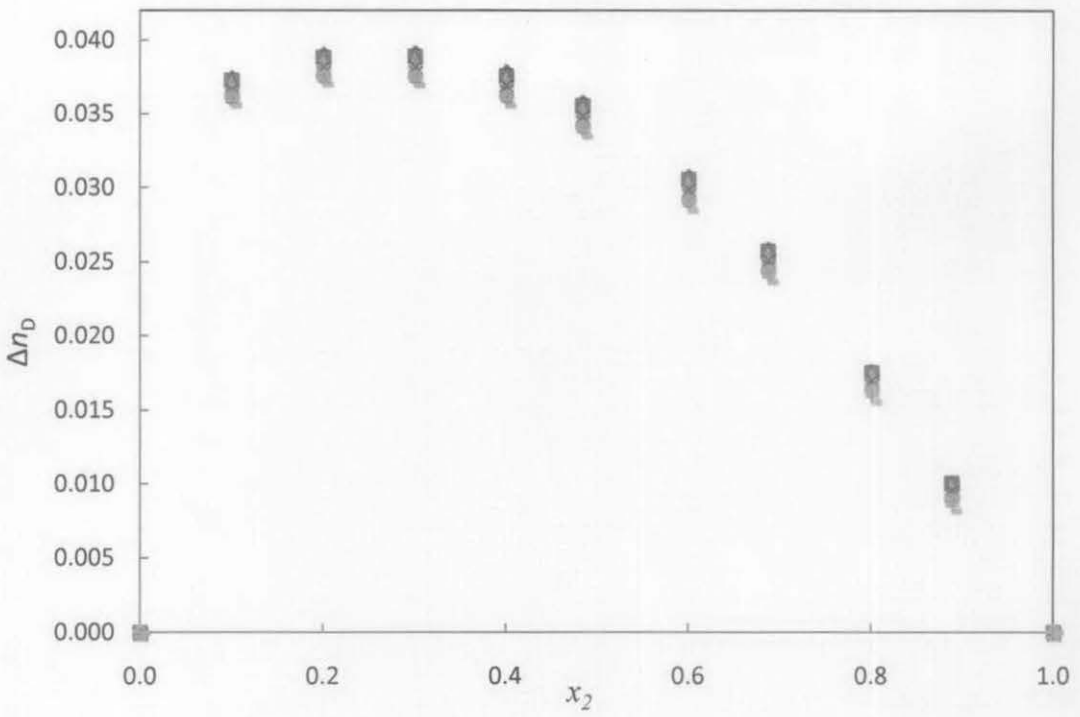
0.040
0.035
0.030
0.025
0.020
0.015
0.010
0.005
0.000
Δn_D
0.0
0.2
0.4
0.6
0.8
1.0
x_2

b)

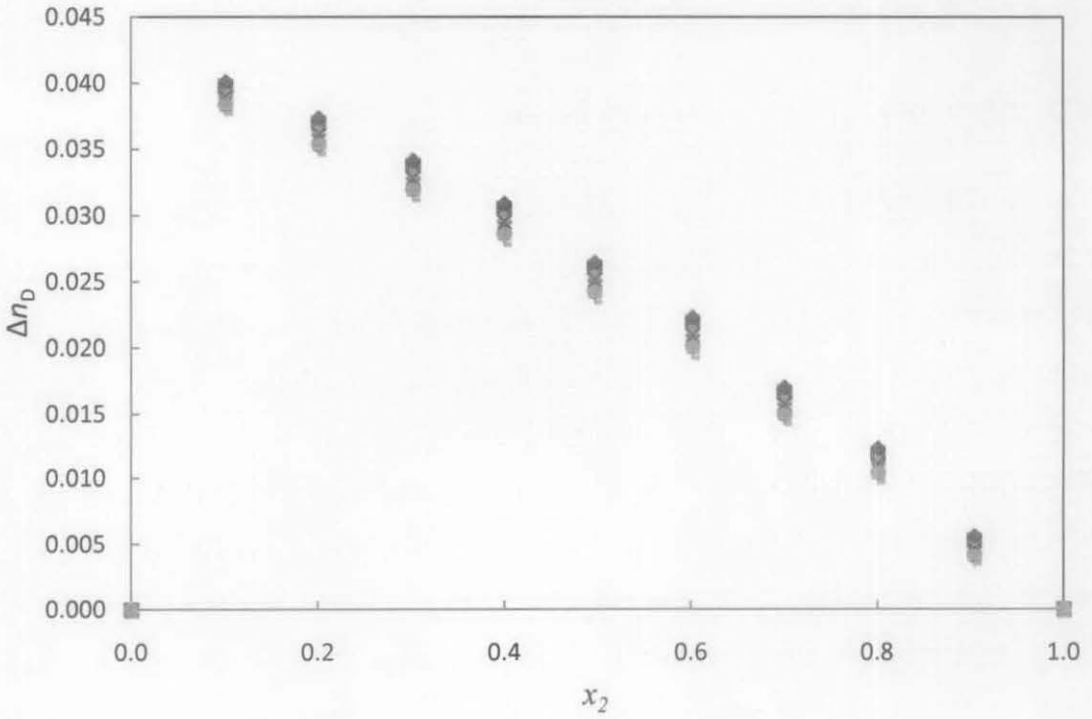
0.045
0.040
0.035
0.030
0.025
0.020
0.015
0.010
0.005
0.000
Δn_D
0.0
0.2
0.4
0.6
0.8
1.0
x_2

c)

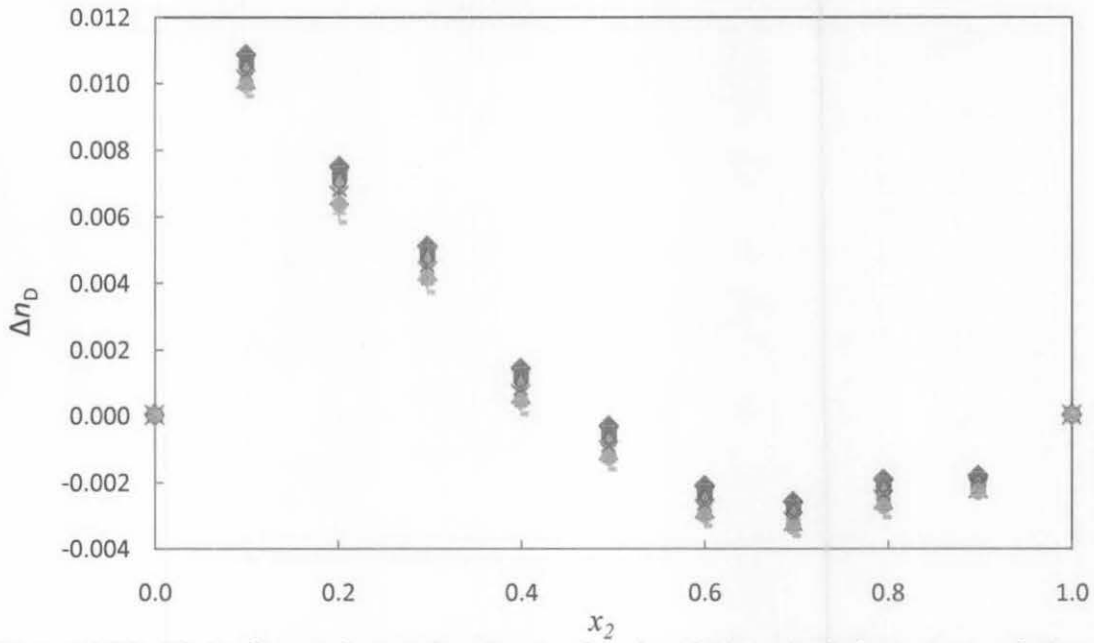

Figure 4.39. Plot of experimental values refractive index deviation, Δn_D, of the ternary mixtures for [bmim][BF_4] (x_1) + MEA (x_2) water (x_3) against mole fraction of MEA at all constant: a) $z = 0.08$; b) $z = 0.32$; c) z = 5.03 at temperatures: ◆ , 293.15 K; ■ , 298.15 K; ▲, 303.15 K; X, 313.15 K; ✳ , 323.15 K; ● , 333.15 K; +, 343.15 K; ▬, 353.15 K.

4.5 Solubility of CO_2 in various solvents

The crucial part of CO_2 absorption, especially in natural gas is the development of more efficient solvents for reducing the cost of carbon dioxide absorption process. In the present work, the solubility of CO_2 in two different solvents involving two types of ILs namely bis(2-hydroxyethyl)ammonium acetate [bheaa] from hydroxyl ammonium type ILs and 1-butyl-3-methylimidazolium tetrafluoroborate [bmim][BF_4] from imidazolium type ILs with Monoethanolamie (MEA) and water was experimentally measured at five different pressures between (100 to 1600) kPa at 298.15 K. The solubility of CO_2 was measured using a high pressure gas solubility cell with a pressure drop method. The complete description of the apparatus and methods used have been discussed in section 3.4. The absorption capabilities have been compared between the two ILs ([bheaa] and [bmim][BF_4]) in their aqueous solutions as well as their mixture with MEA. The effect of ILs concentration as well as the MEA concentration in the solvent, on the solubility of CO_2 were also

evaluated. The effect of operating conditions including temperature and pressure on the solubility of CO_2 for both ILs are also discussed. For this purpose, three different temperatures of 298.15 K, 308.15 K and 313.15 K and five different pressures between (100 to 1600) kPa were used. Finally, the effects of anion and cation are also discussed and compared between the two ionic liquids ([bheaa] and [bmim][BF_4]) used in the present study. The details of CO_2 solubility results obtained by using different mixtures solvent are presented in Table 4.4.

4.5.1 Binary and Ternary System

The solubility of CO_2 in the binary as well as the ternary mixture of solvents has been studied by researchers including the mixtures of few types of alkanolamines, mixtures of alkanolamine with water as well as mixtures of ILs with water. For the case of solubility of CO_2 in pure ILs, the results show that pure [bmim][BF_4] has the higher capacity for CO_2 capture when compared with pure [bheaa]. Similarly, an aqueous solution of [bmim][BF_4] was also found to have high CO_2 loading than the aqueous solution of [bheaa]. The reason could be attributed to the fact that the viscosity of pure [bheaa] are much more higher than the pure [bmim][BF_4]. For comparison with pure ILs, it can be seen that, with the addition of water, the solubility of CO_2 increased significantly. For instance, the solubility of CO_2 in 20wt% aqueous solution of both ILs showed almost six times higher than the solubility of CO_2 by using the pure ILs due to the high viscosity of the pure ILs. Meanwhile, when MEA was added to the aqueous ionic solution, the CO_2 solubility behaviour changes. The CO_2 solubility of [bheaa] + MEA aqueous solution was found to be better than the aqueous solution of [bheaa]. On the other hand, the CO_2 solubility of [bmim][BF_4] + MEA aqueous solution was suprisingly found to be less than the aqueous solution of [bmim][BF_4] but better than the CO_2 solubility in 20wt% MEA. This can be explained by the fact that the presence of the soluble carbamate in the former solutions has reduce the surface for the absorption activity, thus reducing the solubility of CO_2. The presence of the soluble carbamate was caused by the chemical absorption of the solvents and it is believe to have affected the CO_2 olubility. The comparison of the results on the solubility of CO_2 between the pure ILs and their binary and ternary mixtures are shown in Table 4.5.

Table 4.4. Absorption of CO_2 in various solutions of [bheaa] and [bmim][BF_4] at $T = 298$ K.

Bis(2-hydroxyethyl)ammonium acetate [bheaa] system										
Aqueous IL	p/ kPa	n_{CO2} / n_{IL}	p/ kPa	n_{CO2} / n_{IL}	p/ kPa	n_{CO2} / n_{IL}	p/ kPa	n_{CO2} / n_{IL}	p/ kPa	n_{CO2} / n_{IL}
20%	1489	0.3981	1173	0.2994	857	0.1980	568	0.1748	370	0.1112
40%	1499	0.2383	1166	0.1806	859	0.1408	572	0.0968	370	0.0806
60%	1501	0.1571	1151	0.1162	850	0.0972	582	0.0707	384	0.0551
80%	1502	0.0995	1162	0.0812	839	0.0655	583	0.0440	392	0.0336
100%	1497	0.0567	1182	0.0501	853	0.0443	587	0.0305	385	0.0293
MEA aqueous in 20% IL	p/ kPa	n_{CO2} / n_{IL}	p/ kPa	n_{CO2} / n_{IL}	p/ kPa	n_{CO2} / n_{IL}	p/ kPa	n_{CO2} / n_{IL}	p/ kPa	n_{CO2} / n_{IL}
5%	1505	0.6712	1190	0.5484	866	0.4657	586	0.3957	396	0.3306
10%	1506	0.8777	1194	0.7968	883	0.7379	587	0.6914	403	0.5132
15%	1499	1.1687	1193	0.9921	875	0.8873	587	0.8182	412	0.6590
20%	1509	1.2168	1189	1.0332	871	0.9606	584	0.8701	392	0.6809
1-butyl-3-methylimidazolium tetraflouroborate [bmim][BF_4] system										
Aqueous IL	p/ kPa	n_{CO2} / n_{IL}	p/ kPa	n_{CO2} / n_{IL}	p/ kPa	n_{CO2} / n_{IL}	p/ kPa	n_{CO2} / n_{IL}	p/ kPa	n_{CO2} / n_{IL}
20%	1508	3.7910	1246	2.9337	949	1.1944	640	0.8343	362	0.1201
40%	1483	2.1936	1231	1.7987	918	1.2364	646	0.7766	353	0.3184
60%	1476	1.1768	1189	0.7865	908	0.5249	635	0.2576	351	0.0382
80%	1511	0.8667	1204	0.6261	911	0.4089	627	0.1953	344	0.0346
100%	1502	0.5113	1198	0.3453	923	0.1954	634	0.0843	353	0.0013
MEA aqueous in 20% IL	p/ kPa	n_{CO2} / n_{IL}	p/ kPa	n_{CO2} / n_{IL}	p/ kPa	n_{CO2} / n_{IL}	p/ kPa	n_{CO2} / n_{IL}	p/ kPa	n_{CO2} / n_{IL}
5%	1479	0.3371	1217	0.4002	923	0.4090	631	0.3735	352	0.3035
10%	1488	0.6423	1204	0.7338	957	0.7026	654	0.6119	360	0.4813
15%	1498	0.6632	1214	0.9018	934	0.8263	617	0.8262	361	0.6184
20%	1509	0.9198	1215	1.016	918	1.2445	621	0.8786	362	0.6685

Table 4.5. Comparison data on the solubility of CO_2 between the pure ILs, ILs + water and ILs + water + MEA at temperature 298.15 K.

P (kPa)	n_{CO2} / n_{IL}	P (kPa)	n_{CO2} / n_{IL}
Pure			
[bmim][BF_4]		[bheaa]	
1502.43	0.5113	1497.23	0.0567
1197.89	0.3453	1182.13	0.0501
923.16	0.1954	852.67	0.0443
634.23	0.0843	587.39	0.0305
353.24	0.0013	384.88	0.0293
Binary Mixtures			
20wt% aqueous [bmim][BF_4]		20wt% aqueous [bheaa]	
1508.00	3.7910	1489.26	0.3981
1246.00	2.9337	1173.14	0.2994
949.00	1.1944	857.00	0.1980
640.00	0.8343	568.20	0.1748
362.00	0.1201	369.97	0.1112
Ternary Mixtures			
20wt% [bmim][BF_4] + 20wt% MEA		20wt% [bheaa] + 20wt% MEA	
1509.02	0.9198	1508.63	1.2168
1215.26	1.0160	1188.70	1.0332
918.36	1.2445	870.52	0.9606
621.39	0.8786	583.75	0.8701
362.00	0.6685	391.69	0.6809

4.5.1.1 CO_2 absorption studies

Aqueous and pure ILs

The measured solubility of CO_2 in pure and aqueous solution of [bheaa] and [bmim][BF_4] as well as in ILs + MEA aqueous solution at 5 different pressures (100 to 1600 kPa) and T = 298.15 K are presented in Table 4.4. Figure 4.40 and 4.41 show the plots of CO_2 loading against pressure for [bheaa] and [bmim][BF_4] aqueous solutions, respectively.

The results showed that the trends are nearly similar, with the maximum value occured for 20wt% aqueous IL solutions for both the systems. The absorption capabilities also showed a decreasing trend with increasing concentrations of ionic liquid. It can also be observed that the 20wt% aqueous IL solution for [bheaa] and [bmim][BF_4] systems show at least 3.50 and 6.50 times, respectively, greater absorption capabilities than the pure ILs which has the minimum absorption capabilities. It is believed that this might be attributed to the high viscosity of the pure [bheaa] and [bmim][BF_4].

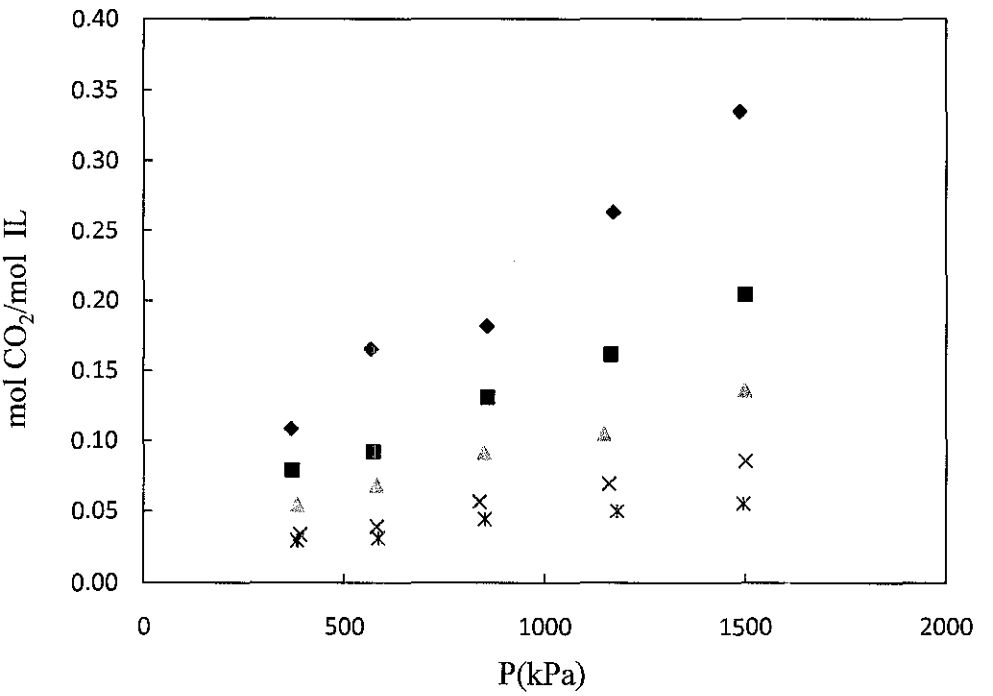

Figure 4.40. Plot of experimental value of CO_2 loading versus pressure for aqueous [bheaa] solutions: ◆ , 20wt%; ■ , 40wt%; ▲, 60wt%; X, 80wt%; ✳ , 100wt%.

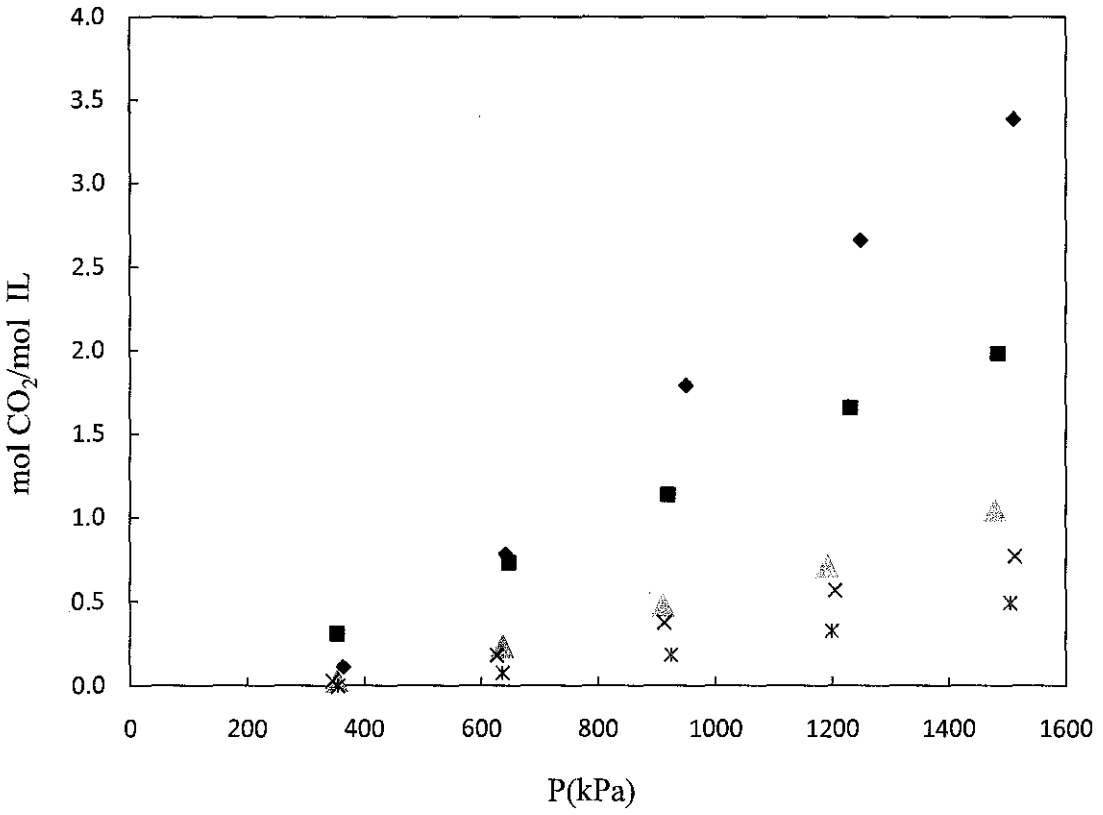

Figure 4.41. Plot of experimental value of CO_2 loading versus pressure for aqueous [bmim][BF_4] solutions: ◆, 20wt%; ■, 40wt%; ▲, 60wt%; X, 80wt%; ✳, 100wt%.

Aqueous solutions of ILs + MEA

Since 20wt% aqueous IL has the highest CO_2 loading, the amine concentrations were also retained below 20wt% and the amount of CO_2 absorption were measured at 5 different pressures (100 to 1600 kPa). An increase in the concentration of MEA in the solution leads to an increase in CO_2 loading as can be seen in Figures 4.42 and 4.43 for [bheaa] and [bmim][BF_4] systems, respectively.

Before further discussions, some justification on the role of monoethanolamine (MEA) in both of the ILs system involved must be made. MEA act as the supporting solvent for CO_2 absorption in [bheaa] system while in [bmim][BF_4] system, instead of MEA, [bmim][BF_4] acts as the supporting solvent. The reason for this behavior could be explained as follows: based on the experimental results, at its 20wt% aqueous solution, CO_2 loading for MEA is lower when compared with 20wt%

aqueous solution of[bmim][BF_4] and higher when compare with aqueous solution of [bheaa]. Therefore, the way to analyze the data for this system is opposite to each other. But the objective of the study to investigate CO_2 loading in two different type of mixed solutions namely MEA in [bmim][BF_4] and [bheaa] is not affected. Eventhough the difference in analysing the data is opposite, the observed trend is almost similar for both systems.

From the results obtained, it can also be seen that the highest loading of CO_2 was recorded for 20wt% MEA in 20wt% ILs solutions followed by 15wt%, 10wt%, and 5wt% of MEA concentration, respectively for both [bheaa] and [bmim][BF_4] systems at all pressures studied. In other words, it can be said that the CO_2 loading was found to increase with concentrations of MEA in both ILs. The reason of the observed behaviour was because the CO_2 in the gas phase dissolves into a solution of water and amine compounds, thus, encourage the amines to react with CO_2 in solution to form protonated amine (AH^+), bicarbonate $(HCO3)^-$, and carbamate. As these reaction occurs, more CO_2 was driven from the gas phase into the solution due to the lower chemical potential of the liquid phase compounds at this condition (GCEP energy Assessment Analysis, 2005). Therefore, with the increase amount of MEA in the solution, has increase the amount of the absorbed CO_2. The CO_2 loading in the soutions with 20wt% MEA in 20wt% [bheaa] was found to be three times higher with respect to the 20wt% of the pure [bheaa] and the increment was higher (as high as six times) especially at higher pressure conditions. On the other hand, the CO_2 loading in the solution of 20wt% MEA in 20wt% [bmim][BF_4] was found to have almost 4 times higher than the solution of 20wt% of pure MEA. The measured solubility of CO_2 in aqueous solution of [bheaa] + MEA and [bmim][BF_4] + MEA at 5 different pressures and T= 298.15 K are presented in Table 4.4.

For explaining the CO_2 absorption in aqueous solution of [bmim][BF_4] + MEA the following established mechanism can be used (Mathonat *et al.*, 1998; Palmer *et al.*, 2008; Astarita *et al.*, 1983):

$$2EtONH_2 + 2CO_2 \longleftrightarrow 2EtONH_2^+COO^- \quad (4.29)$$

$$EtONH_2^+COO^- + B \longleftrightarrow EtONHCOO^- + BH^+ \quad (4.30)$$

$$EtONH_2^+COO^- + EtONH_2 \rightarrow EtONH_3^+ + EtONHCOO^- \quad (4.31)$$

$$EtONH_2^+COO^- + H_2O \longleftrightarrow EtONHCOO^- + H_3O^+ \quad (4.32)$$

During the reaction of CO_2 with primary amines such as MEA, a zwitterion intermediate ($EtONH_2^+COO^-$) is formed, which is further followed by deprotonation by B, where B can abstract a proton from the zwitterion intermediate such as RNH_2, H_2O OH^-, and MEA. The zwitterion intermediate thus formed will react with B to form soluble carbamate [Kamps *et al.*, 2003]. The product formed during the CO_2 capture involving the aqueous solution of [bmim][BF_4] + MEA showed the presence of soluble carbamate which was confirmed by the turbidness of the product solution. The presence of the soluble carbamate decreases the surface available for further absorption/reaction to take place and thus, reduceing the amount of CO_2 loading. But further analysis have shown that the CO_2 loading in the aqueous solution of [bmim][BF_4] + MEA is better than the 20wt% aqueous MEA solution. For comparison purposes, the experimental results on the 20wt% aqueous MEA solution is shown in Table 4.6.

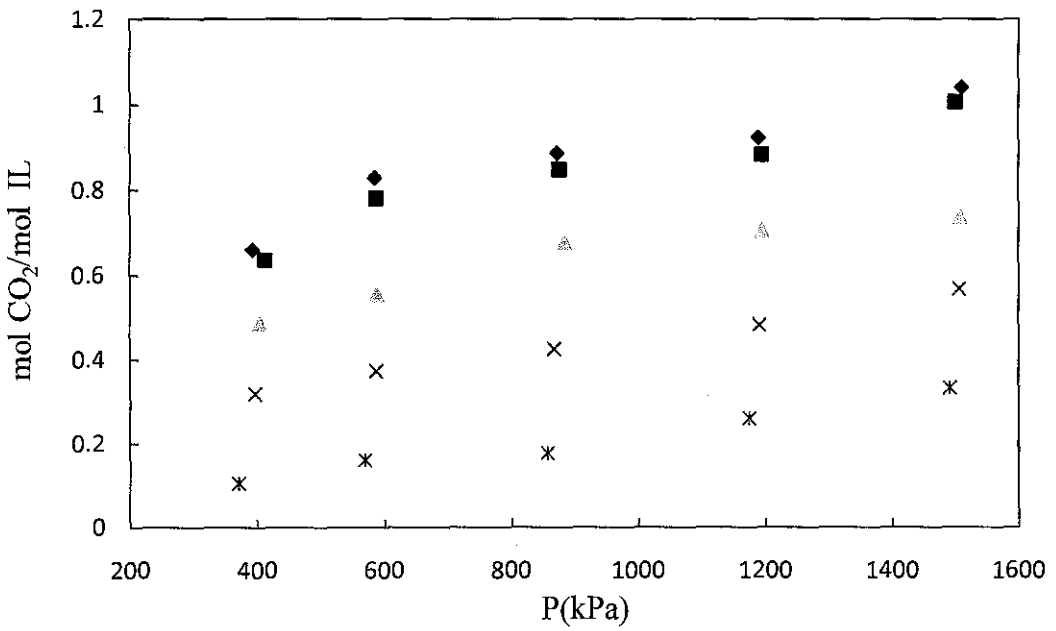

Figure 4.42. Plot of experimental value of CO_2 in aqueous solutions of MEA in 20% [bheaa] solution versus pressure: ◆, 20wt%IL + 20wt%MEA; ■, 20wt%IL + 15wt%MEA; ▲, 20wt%IL + 10wt%MEA; X, 20wt%IL + 5wt%MEA; ✳, 20wt%IL.

In contrast to the analysis of the aqueous solution of [bmim][BF_4] + MEA, the aqueous solution of [bheaa] + MEA shows that the addition of MEA increases the CO_2 loading by several times when compared to 20wt% aqueous IL solution or 20wt% aqueous MEA solution.

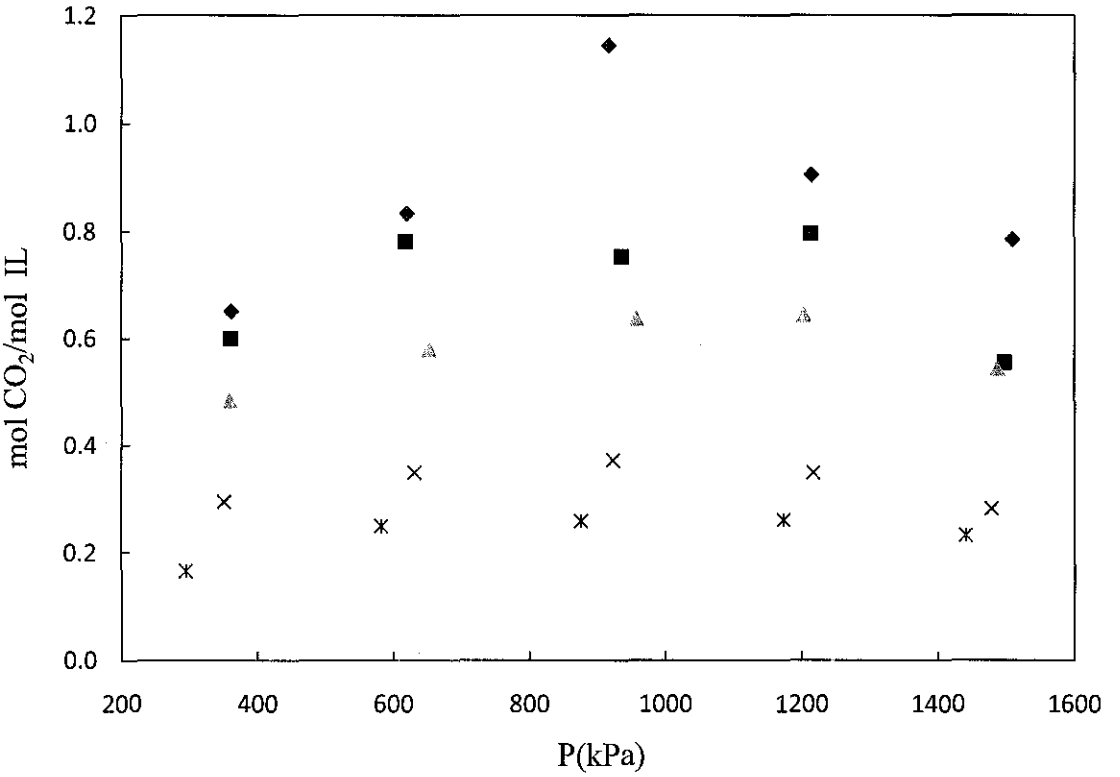

Figure 4.43. Plot of experimental value of CO_2 in aqueous solutions of MEA in 20wt% [bmim][BF_4] solution versus pressure: ◆ , 20wt%IL + 20wt%MEA; ■ , 20wt%IL + 15wt%MEA; ▲, 20wt%IL + 10wt%MEA; X, 20wt%IL + 5wt%MEA; ✳ , 20wt%MEA.

The observation of the final product has shown a clear solution without any trace of turbidity, thus indicating that the solubility of CO_2 by using this type of solvent is dominated by the physical process rather than the chemical reaction. The interaction of CO_2 and the absorbent in the physical absorption is weak relative to the chemical solvents, since it is not limited by the stoichiometry of the chemical system (GCEP energy Assessment Analysis, 2005). Noticeably, the CO_2 loading in 15wt% and 20wt% aqueous solutions of MEA in [bheaa] did not show any abvious difference at all 5 pressure conditions studied. At this particular compositions, the equilibrium

CO_2 loading approached to its maximum, which obviously seem to be independent of pressure and any further addition of MEA in between 15wt% and 20wt% or above this composition did not make any considerable changes in CO_2 loading.

Table 4.6 Amount of CO_2 absorbed in aqueous MEA (20%) solution at $T = 298$ K.

20% aqueous solution of MEA	
p/ kPa	n_{CO2} / n_{MEA}
294	0.1643
583	0.2478
876	0.2573
1173	0.2601
1441	0.2313

4.5.1.2 Rate of absorption

Aqueous and pure ILs

Figures 4.44 and 4.45 show the rate of absorption of CO_2 in [bheaa] and [bmim][BF_4] aqueous solutions at P = 1200 kPa and T = 298.15 K.

From both figures, it can be observed that the rate of obsorption was highest at lower concentration of ILs in the solution particularly at 20wt% and 40wt% of IL solutions. For comparison purposes, the rate of absorption of the 20wt% and 40wt% of the [bheaa] solutions was higher than the rate of absorption of 20wt% and 40wt% of [bmim][BF_4] solutions. It took less than 50 minutes for the former solutions (20wt% and 40wt% of the [bheaa] solutions) to achieve equilibrium while the latter

solutions (20wt% and 40wt% of [bmim][BF_4] solutions) achieve equilibrium in more than 100 minutes especially for 20wt% of [bmim][BF_4] solutions. From the figures, it can be said that an increase in water content in the solutions, increases the rate of absorption and reduce the time to achieve equilibrium. Apart from CO_2 loading, the addition of water also affects the rate of CO_2 absorption. The trend clearly shows that the water content play a major role in accelerating the absorption activity. The rate of absorption was found to have higher value at lower concentration of ILs in the solutions. The time to achieve equilibrium was also longer at higher concentration of ILs. This can be explained by the fact that the viscosity of the solution decreases with an increase in water content (Dallos *et al.*, 2001). The addition of more water in the solutions has accelerate the absorption activity. This can be explained by the fact that the addition of water has increase the free volume or free space within the solutions that were formerly 'packed' with the long chain of ILs molecules. Therefore, with more free space available, it is more easy for the molecules of CO_2 to dissolve and thus, reducing the time to achieve equilibrium. In addition to that, based on the report for the *Clean Air Task Force* (2009), water is soluble in CO_2 and that the absorption in coal-fired power plants favor the use of aqueous solutions of chemicals that react reversibly with dissolved CO_2. Therefore, besides the diffusivity of CO_2, it can also be said that viscous solvents has also affected the rate of absorption and thus limiting the CO_2 uptake. The same trends were also observed for all other pressures studied.

Aqueous solutions of ILs + MEA

The results on the CO_2 solubility in aqueous solution of ILs + MEA at T = 298 K for both ILs are presented in Table 4.4. Figures 4.46 and 4.47 show the rate of absorption of aqueous solutions of [bheaa] with MEA and [bmim][BF_4] with MEA respectively (at P = 1200 kPa and T = 298.15 K). The results on the CO_2 loading by aqueous solution of [bheaa] + MEA are compared with those obtained for 20wt% [bheaa] while the results on CO_2 loading by aqueous solution of [bmim][BF_4] + MEA are compared with those of 20wt% MEA aqueous solution and the details are discussed in the earlier section (4.5.1.1).

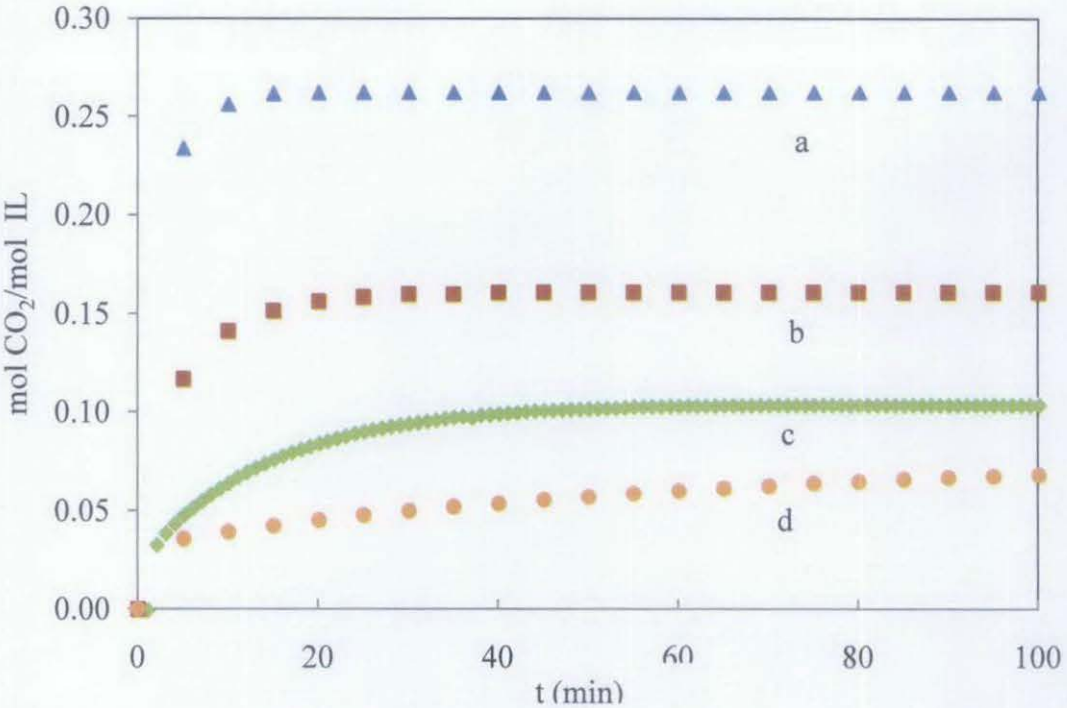

Figure 4.44. Rate of absorption of CO_2 in aqueous solutions of [bheaa] at P = 1200 kPa and T = 298.15K: a, 20wt%; b, 40wt%; c, 60wt%; d, 80wt%.

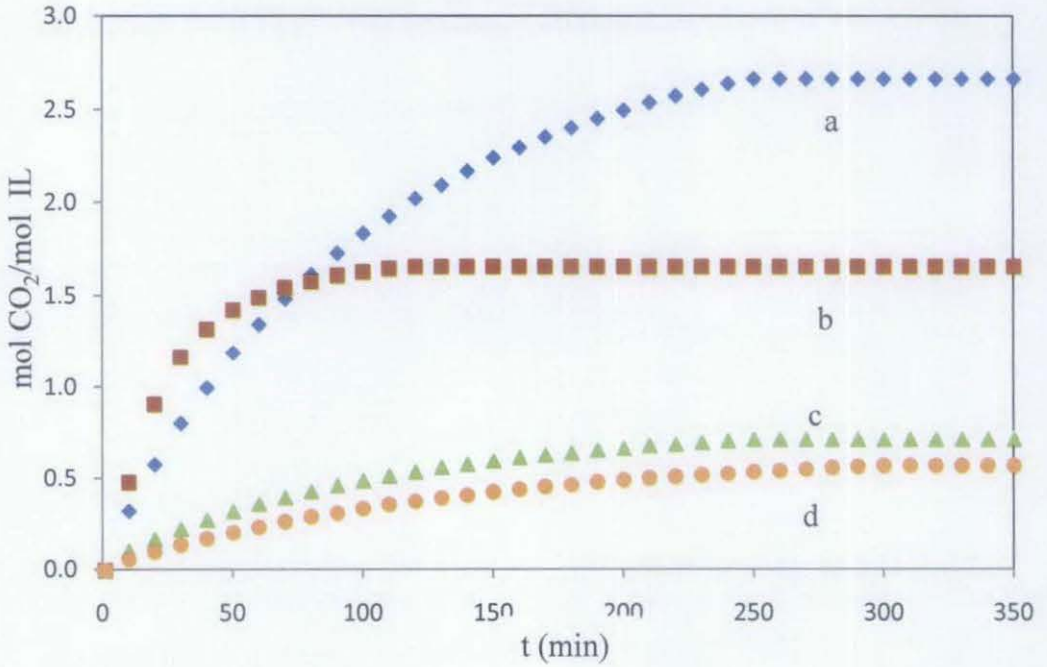

Figure 4.45. Rate of absorption of CO_2 in aqueous solutions of [bmim][BF_4] at P = 1200 kPa and T = 298.15 K: a, 20wt%; b, 40wt%; c, 60wt%; d, 80wt%.

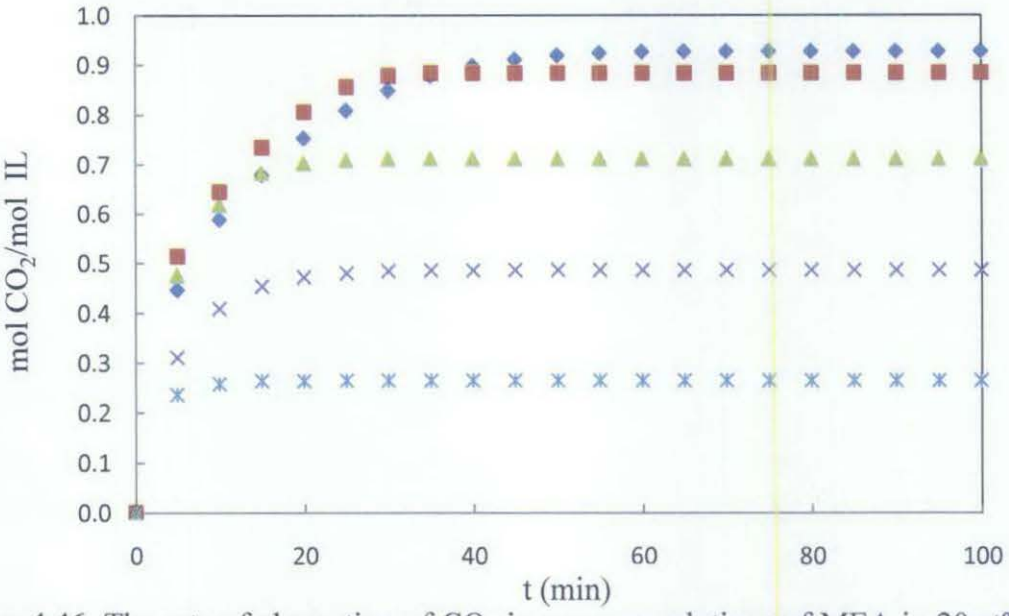

Figure 4.46. The rate of absorption of CO_2 in aqueous solutions of MEA in 20wt% [bheaa] at P = 1200 kPa and T = 298.15 K: ◆ , 20wt%IL + 20wt %MEA; ■, 20wt%IL + 15wt%MEA; ▲, 20wt%IL + 10wt%MEA; X, 20wt%IL + 5wt%MEA; ✳, 20wt%IL.

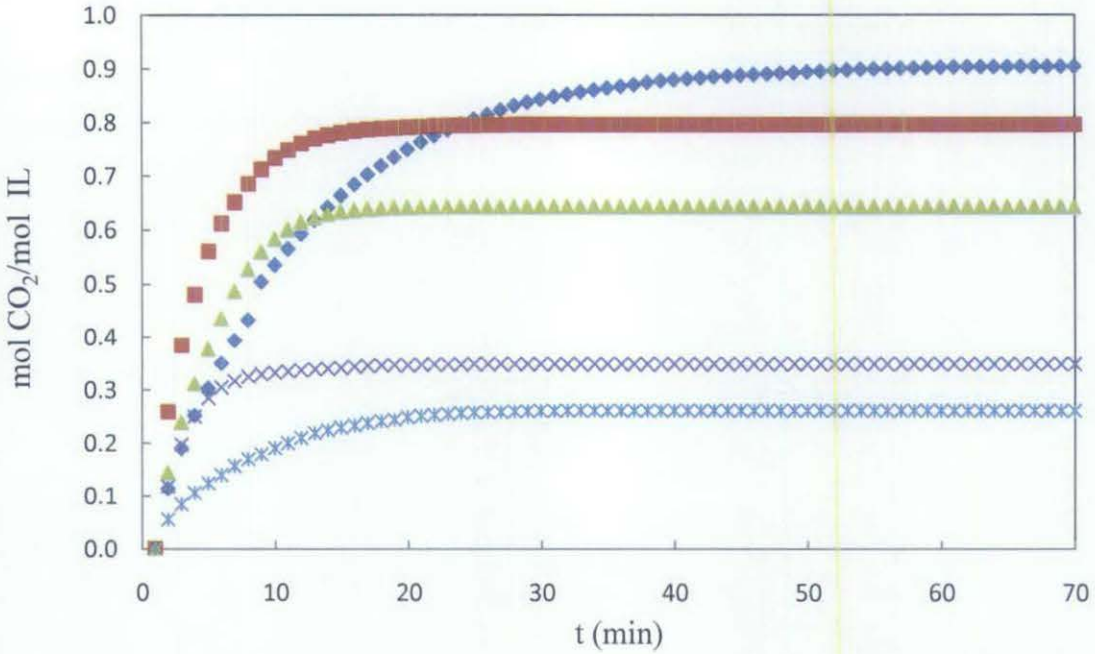

Figure 4.47. The rate of absorption of CO_2 in aqueous solutions of MEA in 20wt% [bmim][BF_4] at P = 1200 kPa and T = 298.15 K: ◆ , 20wt%IL + 20wt%MEA; ■ , 20wt%IL + 15wt%MEA; ▲, 20wt%IL + 10wt%MEA; X, 20wt%IL + 5wt%MEA; ✳ , 20wt%MEA.

For [bheaa] + MEA aqueous solutions, the amount of MEA did not show any obvious difference on the rate of absorption. The only difference observed is that the 20wt% [bheaa] + 20wt% MEA aqueous solution have a slower rate than any other solutions since the equilibrium was achieved ≈ 80 minutes, while the other solutions achieved their equilibrium in ≤ 30 minutes. This might be due to the reaction at higher concentration of MEA in the solutions which encourage the absorption activity to a longer time.

For [bmim][BF_4] + MEA aqueous solutions, an almost similar trends with [bheaa] + MEA aqueous solutions were obtained. The 20wt% [bmim][BF_4] + 20wt% MEA aqueous solution shows a slower rate than any other solutions and the equilibrium was achieved in ≈ 70 minutes, while the other solutions, it took ≈ 30 minutes. The rate of absorption of these types of aqueous solutions can be explained by the fact that the formation of soluble carbamate in the solution reduces the rate of the CO_2 absorption and hence it takes longer time for attaining equilibrium. In addition to that, more time are needed to break the chemical bonds between the solvents and the absorbed CO_2. This statement can be supported by the present results where the absorption of CO_2 in MEA (20wt%) in [bmim][BF_4] took longer time, compared to the aqueous solution of 5wt% MEA in [bmim][BF_4].

4.5.2 Effect of Pressure and Temperature on Absorption

The solubility of CO_2 in aqueous MEA solution exhibits chemical reaction while solubility of CO_2 in ILs usually exhibit physical solubility (Kamps *et al.*, 2003). The criteria for the types of solubility that exhibits by the solution used for the absorption depends on relation between the absorption and the pressures. The solubility of CO_2 in [bheaa], either in their aqueous solutions or their mixture with MEA, increases with increasing pressure of the gas above the surface of the solvent. Therefore, with observed trends for aqueous [bheaa] solutions and aqueous [bheaa] + MEA solutions, show that the physical solubility predominates the process and therefore increases the solubility linearly with increasing pressure.

On the other hand, the solubility of CO_2 in the aqueous solution of [bmim][BF_4] shows practically linear relation with the gas pressure and as expected that the

solvent involving ILs usually exhibit only physical solubility. In contrast with that, the aqueous solution of [bmim][BF_4] + MEA did not show direct proportion between the pressure and the solubility, indicating that the process might involve chemical reaction (which normally occurs when using MEA as solvent). Therefore, it can be said that chemical reaction dominates the process that occured in the aqueous solution of [bmim][BF_4] + MEA. The behaviour for the solubility of CO_2 against pressures are shown in Figures 4.40 and 4.41 for the aqueous solution of [bheaa] and [bmim][BF_4] while Figure 4.42 and 4.43 show the solubility of CO_2 against pressures for the aqueous solution of [bheaa] + MEA and [bmim][BF_4] + MEA respectively.

In order to study and compare the effect of temperature, CO_2 absorptions were measured at 3 different temperatures (298.15, 308.15, 313.15) K. For this purpose 20% MEA solution in 20% [bheaa] at 1509 kPa and 20% MEA solution in 20% [bmim][BF_4] at 918.36 kPa were used, since this particular compositions gave the highest CO_2 absorption. A complete results on the CO_2 absorptions at different temperature for both systems are presented in Table 4.7.

Table 4.7. Amount absorbed in aqueous 20% MEA + 20% IL at T = (298.15 to 313.15) K at pressure with higher CO_2 loading.

20% MEA solution in 20% [bheaa]					
T= 298.15 K		T= 308.15 K		T= 313.15 K	
p/ kPa	n_{CO2} / n_{IL}	p/ kPa	n_{CO2} / n_{IL}	p/ kPa	n_{CO2} / n_{IL}
1491	1.2168	1505	1.2543	1509	1.2312
20% MEA solution in 20% [bmim][BF_4]					
T= 298.15 K		T= 308.15 K		T= 313.15 K	
p/ kPa	n_{CO2} / n_{IL}	p/ kPa	n_{CO2} / n_{IL}	p/ kPa	n_{CO2} / n_{IL}
918	1.2445	900	0.8442	895	0.5578

Figure 4.48 shows the effect of temperature on the aqueous solution of [bheaa] + MEA. The results show that there is no appreciable change in the CO_2 loading due to an increase in temperature for the range studied in the present work, which also agrees with the reported similar trends of Feng *et. al*, 2010 and Portugal *et al.*, 2007. It was also found that an increase in temperature led to higher/faster rate of absorption, particularly for temperatures 308.15 K and 313.15 K and the equilibrium was achiecved within first 10 minutes whereas for 298.15K it took 40 minutes to attain equilibrium which might be attributed to the reduction in viscosity, density as well as increasing diffusivity at higher temperatures.

Figure 4.49 shows the effect of temperature on the aqueous solution of MEA in [bmim][BF_4]. For this system, it is observed that with an increase in temperature, the CO_2 solubility decreases. This might be explained by the increase in vapour pressure due to an increase in temperature, therefore affected the absorption process. The results obtained are supported by similar trends reported by Anthony *et. al* (2002), Husson-Borg *et. al* (2003) and Sairi *et. al* (2011). It can also be seen that the rate of absorption at T = 298.15 K is slower than the rate of absorption at higher temperatures.

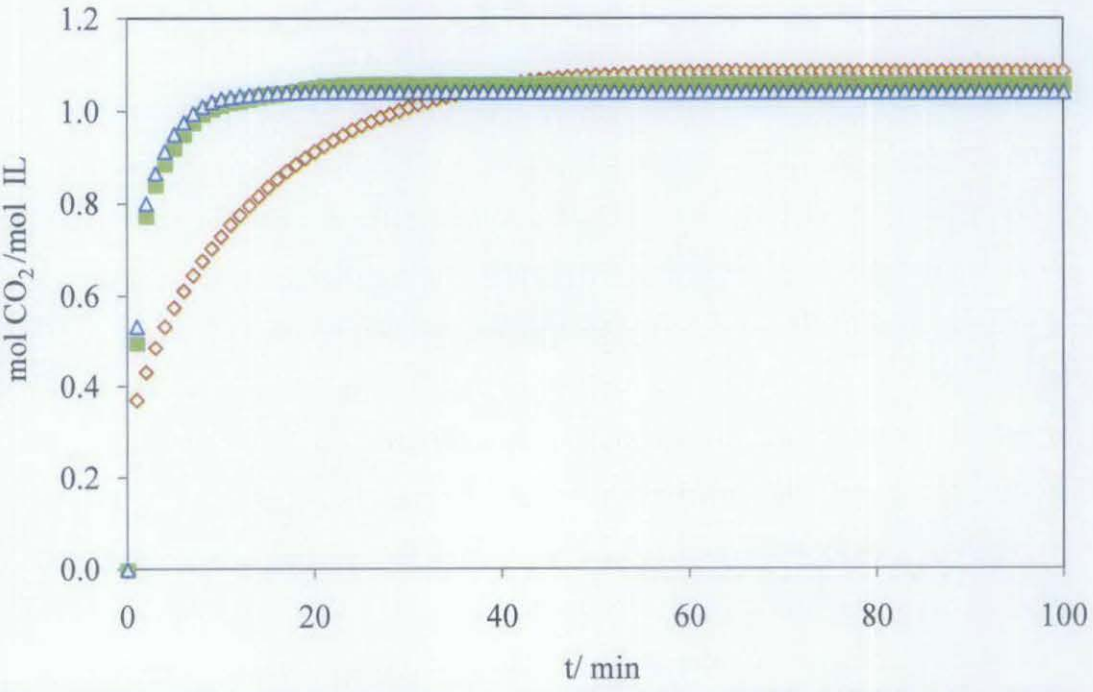

Figure 4.48. Effect of temperature on the absorption of CO_2 in [bheaa] – MEA aqueous solutions: ◇ ,T=298.15K; ■ , T=308.15K; △ , T=313.15K

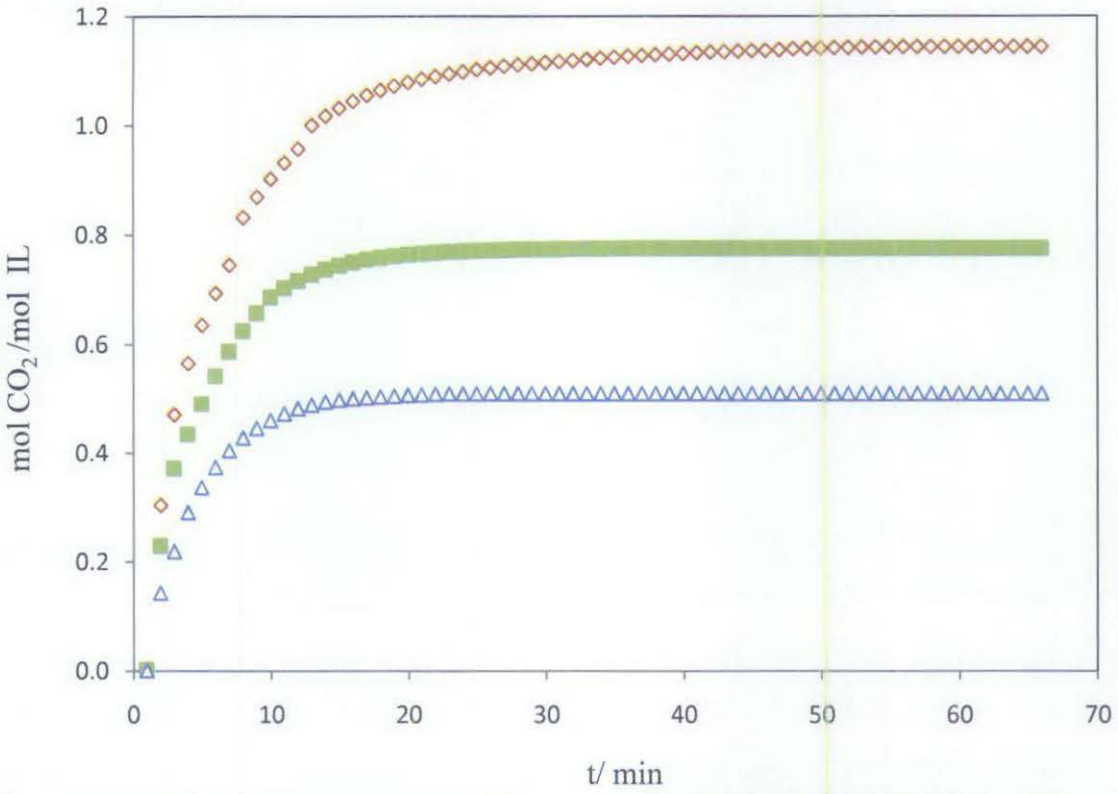

Figure 4.49. Effect of temperature on the absorption of CO_2 in [bmim][BF_4] – MEA aqueous solutions: ◇ ,T=298.15K; ■ , T=308.15K; △ , T=313.15K

4.5.3 Effect of anion and cation

As discussed in the earlier section (section 4.5.1), [bmim][BF_4] at its pure as well as in aqueous state has higher CO_2 loading than [bheaa], which might be due to the higher viscosity of [bheaa] when compared to [bmim][BF_4]. As discussed in the earlier section, the diffusivity of CO_2 is determined by the viscosity of the solvent and hence [bmim][BF_4] has higher CO_2 loading. In addition to that, the higher CO_2 loading for [bmim][BF_4] were also contributed by the presence of acidic hydrogen attached to the C2 carbon in the imidazolium ring of [bmim][BF_4], which particularly acts as a potential additional mechanism for CO_2 solvation (Cadena *et al.* 2004). This theory is supported by the results obtained by Welton *et al.* (2003) who used a series of solvatochromic dyes to determine the Kamlet – Taft parameters of various ILs. In their work, they demonstrated the ability of imidazolium- based ILs to donate a hydrogen to solutes is significantly greater for ILs that possess a hydrogen rather than a methyl group attached to the C2 carbon. Therefore, it explained the higher CO_2 loading in [bmim][BF_4] at its pure state.

For the case of the mixture of aqueous ILs and MEA solutions, the CO_2 loading in the mixture of [bheaa] with MEA aqueous solutions are higher when compared to the mixture of [bmim][BF_4] with MEA aqueous solutions particularly at higher pressures. This can be attributed to the fact that the structure of [bheaa] contain the amine group that can react readily with CO_2 to form zwitterions intermediate. The zwitterions intermediate will then transfer proton to MEA (base) and thus will increase the CO_2 loading. This mechanism is almost similar to the mechanism explained for MEA due to the presence of amine group. The higher loading of CO_2 in these mixtures might be due to their specific interactions between the gas and the acetate anion.

Many researchers have discussed the possible factors that can contribute to the high solubility of CO_2 in mixed solvents involving ionic liquids. Based on his own experiments and analysis, Kazarian *et al.* (2000) concluded that there are evidence for chemical interactions between the anion and CO_2, although those interactions were probably not large enough to be considered as sole factor. They also observed Lewis acid- base interactions where the anions act as the Lewis base. However, with many unclear factors, note should be taken that the solubility of CO_2 in the mixtures of ILs and MEA aqueous solution is higher than that in pure ILs or the conventional MEA solutions, particularly with the imidazolium and hydroxyl type ILs. These two types of ILs used in the present study are not the task- spesific ILs (TSIL) which has high viscosity and expensive. Feng *et al.* (2010) studied the mixtures of four types of TSIL with N-methyldiethanolamine (MDEA) namely., tetramethylammonium glycinate ([N_{1111}][Gly]) + MDEA, tetraethylammonium glycinate ([N_{2222}][Gly]) + MDEA, tetramethylammonium lysinate ([N_{1111}][Lys]) + MDEA and tetraethylammonium lysinate ([N_{2222}][Lys]) + MDEA. The comparison of the results obtained by Feng *et al.* with the present work are shown in Table 4.8. Even with the usage of TSIL, the CO_2 loading for the system studied in this work is higher when compared with the result obtained by Feng *et al.* particularly with the aqueous mixtures of 20wt% ILs with higher MEA content.

Table 4.8. Comparison with literature data with aqueous mixtures of present ILs + MEA at pressure with highest CO_2 loading.

Aqueous Mixtures of ILs + alkanolamine	CO_2 loading
20%[bheaa] + 5% MEA	0.671
20%[bheaa] + 10% MEA	0.877
20%[bheaa] + 15% MEA	1.169
20%[bheaa] + 20% MEA	1.217
20%[bmim][BF_4] + 5% MEA	0.409
20%[bmim][BF_4] + 10% MEA	0.703
20%[bmim][BF_4] + 15% MEA	0.826
20%[bmim][BF_4] + 20% MEA	1.245
15%[N_{1111}][Gly] + 15% MDEA[26]	0.562
15%[N_{2222}][Gly] + 15% MDEA[26]	0.643
15%[N_{1111}][Lys] + 15% MDEA[26]	0.694
15%[N_{2222}][Lys] + 15% MDEA[26]	0.740

4.5.4 Summary

The physical properties namely, density, viscosity and refractive index for pure ([bheaa] and [bmim][BF_4]), binary mixtures ([bheaa] + water, [bheaa] + MEA, [bmim][BF_4] + water, [bmim][BF_4] + MEA) and ternary mixtures ([bheaa] + MEA +

water and [bmim][BF_4] + MEA + water) have been measured at a temperature range of (293.15 to 353.15)K over the whole range of composition. The excess properties namely excess molar volume, viscosity and refractive index deviations have been deduced from the experimental measurements and correlated using Redlich Kister (binary mixtures) and Cibulka equation (ternary mixtures). Satisfactory correlations for the composition and temperature dependence of the measured and the excess properties were obtained.

Present results showed that the pure [bmim][BF_4] has higher CO_2 solubility than the pure [bheaa]. Studies on the solubility of CO_2 in aqueous solution of both ILs also show that the aqueous solution of [bmim][BF_4] has higher CO_2 solubility than the aqueous solution of [bheaa]. In contrast with the results on the solubility of CO_2 in pure and aqueous solution, the solubility of CO_2 for the aqueous solution of [bheaa] + MEA were found to be higher than the solubility of CO_2 for the aqueous solution of [bmim][BF_4] + MEA at almost all investigated pressures. The solubility of CO_2 for the aqueous solution of [bheaa] + MEA were also found to be higher than the aqueous solution of [bheaa] especially with higher concentrations of MEA while the solubility of CO_2 for the aqueous solution of [bmim][BF_4] + MEA were found to be higher than the aqueous solution of [bmim][BF_4] only at lower pressures. As have been discussed in chapter 2, the highly concentrated MEA cannot be used since it can cause corrosion through the reaction of MEA with the material of the equipments used. Hence, in this present work, the concentration of MEA used was retained under 20wt% in order to reduce the risk of corrosion to the equipments despite maintaining its efficiency in the absorption of CO_2. Since, the amount of MEA used in the present work for the absorption of CO_2 is lower than the amount of MEA used in industry, therefore, the corrosion problem caused by the amine solution can be reduce, thus reducing the limitation of the usage of the present solvent.

In the absorption process, two steps are involved: 1) the absorption process using suitable solvents; 2) the regenaration process of captured gases from the solvents. Despite the absorption process, the regenaration process also plays an important role since it requires high energy consumption. Although the regenaration process has not

been discussed, all solvents used in this work are ensure to behave in such a way that it can be applied in industries and has low limitation with respect to regenaration process. The real coal-fired power plants favor the use of aqueous solutions of chemicals that react reversibly with dissolved CO_2 (combine with CO_2 in the scrubber and release it at high temperatures in the stripper). Hence in this work, the usage of the aqueous solution of ILs with water content as high as 60wt%, are believe can reduce the limitation of using the solvents in industries in regards to the regenaration process. But the study on the effect of the solvents to the regeneration process must be further investigate and the mechanism during the process must be further be discussed in future work.

The present results on the solubility of CO_2 indicated that an industrially attractive hybrid solvent for effective CO_2 capture, could be developed by incorporating the desirable properties of both ionic liquids as well as amines through mixing of the targeted ILs with selective amines. Therefore, based on the present results, it can be concluded that both hybrid solvents ([bheaa] + MEA and [bmim][BF_4] + MEA aqueous solution) used in this work has high potential for commercial application particularly in CO_2 solubility

CHAPTER 5

CONCLUSIONS AND RECOMMENDATIONS

5.1 Conclusions

The present work reports the study on the development of hybrid solvents for the effective solubility of CO_2 by mixing two ionic liquids (ILs) namely, bis(2-hydroxyethyl)ammonium acetate [bheaa] from hydroxyl ammonium type ILs and 1-butyl-3-methylimidazolium tetrafluoroborate [bmim][BF_4] from imidazolium type ILs with monoethanolamine (MEA) and water.

The physical properties namely, density, viscosity and refractive index for pure ([bheaa] and [bmim][BF_4]), binary mixtures ([bheaa] + water, [bheaa] + MEA, [bmim][BF_4] + water, [bmim][BF_4] + MEA) and ternary mixtures ([bheaa] + MEA + water and [bmim][BF_4] + MEA + water) have been measured at various compositions and temperatures from (293.15 to 353.15) K. The measured physical properties of the binary and ternary mixtures has been used to deduced the excess properties including the excess molar volumes, viscosity deviation and refractive index deviations as well as the thermal expansion coefficients. The densities, viscosities and refractive indices was found to increase with decreasing temperature for all binary and ternary mixtures.

The solubility of CO_2 in the binary and ternary mixtures of [bheaa] and [bmim][BF_4] with MEA and water were measured at five different pressures $\leq$ 1600

kPa and at T = 298.15K using the pressure drop method. The analysis of the experimental results showed that the pure and aqueous solution of [bmim][BF_4] has higher CO_2 solubility than the pure and aqueous solution of [bheaa]. Meanwhile, for the mixtures of MEA in ILs, it was found that the solubility of CO_2 for the aqueous solution of [bheaa] + MEA was higher than the solubility of CO_2 for the aqueous solution of [bmim][BF_4] +MEA solutions. The maximum CO_2 loading for 20wt% [bheaa] + 20wt% MEA aqueous solutions has occured at P = 1509 kPa while the maximum CO_2 loading for 20wt% [bmim][BF_4] + 20wt% MEA aqueous solutions has occured at P = 918.36 kPa. The effects of temperature on the aqueous solution of [bheaa] + MEA at fixed pressure shows that the solubility did not show any significant difference on the amount of absorbed CO_2 but the rate of absorption is lower at lower temperature while the CO_2 loading was decreasing with the increase in temperature for the aqueous solution of [bmim][BF_4] + MEA at particular pressure but no significant difference were observed on the rate of absorption.

The present results on the solubility of CO_2 indicated that both hybrid solvents ([bheaa] + MEA and [bmim][BF_4] + MEA aqueous solution) used in this work has high potential for commercial application particularly due to their efficiency towards CO_2 capture. The present results also indicated that the aqueous solutions of [bheaa] + MEA were found to have better CO_2 loading than the aqueous solution of [bmim][BF_4] + MEA. Based on the results it was also found that the CO_2 loading are higher for ternary mixtures, namely the aqueous solution of 20wt% MEA in the aqueous solution of 20% of involved ILs.

5.2 Recommendations

Based on the present research, the following are the suggestions/ recommendations for the future work to be carried out:

1. To carry out the CO_2 solubility studies at high pressure and relatively high temperature conditions.

2. To use ILs of different families in combination with targetted alkanolamines for the efficient capture of CO_2.

3. To study the regeneration possibilities of the hybrid solvents.

4. To study the thermal properties, transport properties, thermal conductivity as well as kinematic mechanism of the mixtures.

REFERENCES

A. Aboudheir, P. Tontiwachwuthikul, A. Chakma, R. Idem, "Kinetics of the reactive absorption of carbon dioxide in high CO_2- loaded, concentrated aqueous monoethanolamine solutions." *Chem. Eng. Sc.*, vol. 58, pp. 5195- 5200, 2003.

A. Aboudheir, P. Tontiwachwuthikul, A. Chakma, R. Idem, "Kinetics of the reactive absorption of carbon dioxide in high CO_2- loaded concentrated aqueous monoethanolamine solutions," *Chemical Engineering Science* vol. 58, pp. 5195-5210, 2003.

A. Arce, A. Arce Jr., A. Soto, "Physical and excess properties of binary and ternary mixtures of 1,1-di methylethoxy-butane, methanol, ethanol and water

A. Arce, A. Soto, J. Ortega, G. Sabater, "Mixing properties of tris(2-hydroxyethyl)methylammonium methylsulfate, water, and methanol at 298.15 K, Data treatment using several correlation equations." *J. Chem. Thermodyn.*, vol. 40, pp. , 2008.

A. Arce, A. Soto, J. Ortega, G. Sabater, "Mixing properties of tris(2-hydroxyl) methylmonium methylsulfate, water, and methanol at 298.15 K. Data treatment using several correlation equations," J. *Chem. Thermodyn*, vol. 41, pp. 235 – 242, 2009.

A. Dallos, T. Altsach, L. Kotsis, "Enthalpies of absorption and solubility of carbon dioxide in aqueous polyamine solutions," *J. Therm Anal. Cal.* vol. 65, pp. 419- 423, 2001.

A.F. Portugal, P.W.J. Derks, G.E. Versteeg, "Characterization of potassium glycinate for carbon dioxide absorption purposes." *Chem. Eng. Sci.* vol. 62, pp. 6534- 6547, 2007.

A. Finotello, E.B. Jason, C. Dean, D.N. Richard, "Room temperature ionic liquid: temperature dependence of gas solubility selectivities." *Ind. Eng. Chem. Res.* vol. 47, pp. 453-459, 2008.

A. Finotello, E.B. Jason, S. Narayan, C. Dean, D.N. Richard, "Ideal gas solubilities and solubility selectivities in a binary mixtures of room temperature ionic liquid." *J. Phys. Chem. B* vol. 112, pp. 2335-2339, 2008.

A. Finotello, J. E. Bara, D. Camper, R. D. Noble, "Room-temperature ionic liquids: temperature dependence of gas solubility selectivity." *Ind. Eng. Chem. Res.* vol. 37, pp.3453- 3459, 2008.

A. Gaur, J. W. Park, S. Maken, H. J. Song, J. J. Park, " Landfill gas (LFG) processing via adsorption and alkanolamine absorption" *Fuel Proccess. Tech.* vol. 91, pp.635-640 , 2010.

A. J. Kidnay and W. R Parrish, *Fundamentals of Natural Gas Processing;* Taylor & Francis; Boca Raton, pp. 1-23, 2006.

A. Muhammad, M. I. Abdul Mutlib, T. Murugesan, M. Shafeeq, Densities and excess properties of N-methyldiethanolamine solutions from (298.15 to 338.15) K," *J. Chem. Eng. Data*, vol. 53, pp. 2217- 2221, 2008.

A. N. Soriano, B. T. Doma Jr, M. H. Li, "Measurement of density and refractive index for 1-n-butyl-3-methylimidazolium-based Ionic Liquids." *J. Chem thermodyn.* vol. 41, pp. 301- 307, 2009.

A.P.S. Kamps, D. Tuma, J. Xia, G. Maurer, "Solubility of CO_2 in the ionic liquid [bmim][PF_6]," *J. Chem. Eng. Data* vol. 48, pp. 746- 749, 2003.

A.P.S. Kamps, D. Tuma, J. Xia, G. Maurer., "Solubility of CO_2 in the ionic liquid [bmim][PF6]," *J. Chem. Eng. Data*, vol. 48, pp. 746-749, 2003.

A. Pineiro, P. Brocos, A. Amigo, M. Pintos, R. Bravo, "Physical properties of ionic liquids based on 1-alkyl-3-methylimidazolium cation and hexaflourophosphate as

anion and temperature dependence" *J. Chem. Thermodyn.*, vol. 31, pp. 931- 942, 1999.

Aronu, U. E.; Svendsen, H. F.; Hoff, K. A.;Juliussen, O. Solvent selection for carbon dioxide absorption. Energy Procedia, pp. 1051- 1057, 2009.

A. Samanta and S. S. Bandyopadhyay, "Absorption of carbon dioxide into aqueous solutions of piperazine activated 2-amino-2-metyl-1-propanol" *Chem. Eng. Sc.* vol. 64, pp. 1185- 1194, 2009.

A. Valtz, C. Coquelet, C. Nikitine, D. Richon, "Volumetirc properties of the water + ethylenediamine mixture at atmospheric pressure from 288.15 to 353.15 K." *Thermochim. Acta*, vol. 443, pp. 251- 255, 2006.

B. C. Lee, S. L. Outcalt, "Solubilities of gases in the ionic liquid 1-butyl-3-methlimidazolium bis(trifluoromethylsulphonyl) imide," *J. Chem Eng. Data*, vol. 51, pp. 892-897, 2006.

B. Lemoine, Y- G. Li, R. Cadours, C. Bouallou, D. Richon, "Partial vapor pressure of CO_2 and H_2S over aqueous methyldiethanolamine solutions." *Fluid Phase Equilib,* , vol. 172, pp. 261- 277, 2000.

B. Mokhtarani, A. Sharifi, H. R. Mortaheb, M. Mirzaei, M. Mafi, F. Sadeghian, Density and viscosity of 1-butyl-3-methylimidazolium nitrate with ethanol, 1-propanol, or 1-butanol at several temperature." *J. Chem Thermodyn.* vol. 41, pp. 1432- 1438, 2009.

C. Cadena, J.L. Anthony, J.K. Shah, T.I. Morrow, J.F. Brennecke, E.J. Maginn, "Why is CO_2 is so soluble in imidazolium- based ionic liquids," *J. Am. Chem. Soc.* vol. 126, pp. 5300- 5308, 2004

C. Chan, Y. Maham, A. E. Mather, C. Mathonat, "Densities and volumetric properties of the aqueous solutions of 2-amino-2-methyl-1-propanol, *n*-butyldiethanolamine and *n*-propylethanolamine at temperatures from 298.15 to 353.15 K." *Fluid Phase Equilib.*, vol. 198, pp. 239- 250, 2002.

C. Coquelat, A. Valtz, D. Richon, "Volumetric properties of water + monoethanolamine + methanol mixtures at atmospheric pressure from 283.15 to 353.15 K." *J. Chem. Eng. Data*, vol. 50, pp. 412- 418, 2005.

C. Dean, E.B. Jason, L.G. Douglas, D.N. Richard, "RTIL-Amine solution: tunable solvents for efficient and reversible capture of CO_2." *Ind. Eng. Chem*, vol. 47 pp. 8496-8498, 2008.

C. Mathonat,V. Majer, A.E. Mather, J.P.E. Grolier, "Use of flow calorimetry for determining enthalpies of absorption and the solubility of CO_2 in aqueous monoethanolamine solutions." *I&EC Res.* vol. 37, pp. 4136- 4141, 1998.

C. S. Tan and J. E. Chan, "Absorption of carbon dioxide with piperazine and its mixtures ina rotating packed bed." *Sep. Pur. Tech.*, vol. 49, pp. 174- 180, 2006.

D. Camper, C. Becker, C. Koval. R. Noble, "Diffusion and solubility measurements in room temperature ionic liquids" *Ind. Eng. Chem. Res.* Vol. 45, pp. 445- 450, 2006.

D. Champer, J. E. Bara, L. G. Douglas, R. D. Noble, "RTIL-Amine solution: Tunable solvents for efficient and reversible capture of CO_2," *Ind. Eng. Chem.*, vol. 47 (21), pp. 8496-8498, 2008.

D. Silkenbaumer, B. Rumpf, R. N. Lichtenthaler, "Solubility of carbon dioxide in aqueous solutions of 2-amino-2methyl-1-propanol and *N*-Methyldiethanolamine and their mixtures in the temperature range from 313 to 353 K and pressures up to 2.7 MPa." *Ind. Eng. Chem. Res.* Vol. 37, pp. 3133- 3141, 1998.

E. D. Bates, R. D. Mayton, I. Ntai, "CO_2 capture by a task- spesific ionic liquid, *J. Chem. Eng. Data*, vol. 124, pp. 926- 927, 2002.

E. J. Gonzalez, B. Gonzalez, N.Calvar, A. Dominguez, "Physicl properties of binary mixtures of the ionic liquid 1-ethyl-3-methylimidazolium ethyl sulfate wit several alcohols at T = (298.15, 313.15 and 328.15) K and atmospheric pressure." J. *Chem. Eng. Data*, vol. 52, pp. 1641- 1648, 2007.

E. K. Shin, B. C. Lee, J. S. Lim, " High-presure solubilities of carbon dioxide in ionic liquids: 1-alkyl-3-methylimidazolium bis(triflouromethylsulfonyl) imide," *J. of Supercrit. Fluids.* vol. 45, pp. 282- 292, 2008

E. V. Ivanov and A. V. Kustov, "Volumetric properties of (water + hexamethylphosphoric triamide) from (288.15 to 308.15) K," *J. Chem. Thermodyn.*, vol. 42, pp. 1087- 1093, 2010.

F. Murrieta-Guevara, M. E. Rebolledo-Libreros, A. Romero-Martinez, A. Trejo, "Solubility of CO_2 in aqueous mixtures of diethanolamine with methyldiethanolamine and 2-amino-2-methyk-1-propanol" *Fluid Phase Equilib.* vol. 150, pp. 721- 729, 1998.

A. Gaur, J. W. Park, S. Maken, H. J. Song, J. J. Park, " Landfill gas (LFG) processing via adsorption and alkanolamine absorption" *Fuel Proccess. Tech.* vol. 91, pp.635-640 , 2010.

F. Y. Jou, J. J. Carrol, A. E. Mather, F. D. Otto, "Solubility of carbon dioxide and hydrogen sulfide in a 35wt% aqueous solutions of methyldiethanolamine." *Can. J. Chem. Eng.*, vol. 71, pp. 264- 268, 1993.

F.-Y. Jou, S. E. Mather, F. D. Otto, "The solubility of CO_2 in a 30 mass percent monoethanolamine solution," *Can, J. Chem. Eng.*, vol. 73, pp. 140- 147, 1995.

F. –Y. Jou, J. J. Carroll, A. E. Mather, F. D. Otto, "The solubility of carbon dioxide and hydrogen sulfide in a 35 wt% aqueous solution of methyldiethanolamine," *Can. J. Chem. Eng.*, vol. 71, pp. 264- 268. 1993

F. Y. Jou and A. E. Mather, "Solubility of carbon dioxide in an aqueous mixture of metyldiethanolamine and *N*-methylpyrrolidone at elevated pressures." *Flud Phase Equilib.*, vol. 228-229, pp. 465- 469, 2005.

G. A. Trine, E. O. Lars, A. E. Dag, "Density and viscosity of MEA + water + CO_2 from (25 to 80) ^{0}C," *J. Chem. Eng. Data*, vol. 54, pp. 3090-3100, 2009.

G. Astarita, D. W. Savage, A. Bisio, *Gas Treating with Chemical Solvents;* John Wiley & Sons: New York, 1983.

G. H. Li, S.J. Zhang, Z.X. Li, M.Y. Li, X.P. Zhang, "Effect of ionic liquid on the oxidative esterification from methacrolein to methyl methacrylate" *J. Chem. Eng. Chin. Univ.* vol. 6, pp. 1137-1138, 2004.

G. Koch, "Corrosion cost preventive strategies in the United States." CC Technologies & NACE International, 2001.

G. Q. Wang, X. G. Yuan, K. T. Yu, "Review on mass transfer correlations for packed columns," *Ind. Eng. Chem. Res.*, vol. 44, pp. 8715- 8729, 2005.

G. S. Fonseca, G. Machado, S. R. Teixeira, G. H. Fecher, J. Morais, M. C. M. Alves. J. Dupont, "Synthesis and characterization of catalytic iridium nanoparticles in imidazolium ionic liquids." *J. Coll. Interf. Sc.* vol. 301, pp. 193- 204, 2006.

G. W. Xu, C- F. Zhang, S- J. Qin, W- H. Gao, H- B. Liu, "Gas- Liquid equilibrium in a CO_2- MDEA- H_2O system and the effect of piperazine on it." *Ind. Eng. Chem. Res,* , vol. 37, pp. 1473- 1477, 1998.

H. Arcis, L. Rodier, K. Ballerat- Busserolles, J. Coxam, "Modelling of (vapor+ liquid) equilibrium and enthalphy of solution of carbon dioxide (CO_2) in aqueous methyldiethanolamine (MDEA) solutions." *J. Chem. Thermodyn.*, vol. 41, pp. 783-789, 2009.

H. Gao, F. Qi, H. Wang, "Densities and volumetric properties of binary mixtures of the ionic liquids 1-butyl-3-methylimidazolium tetraflouroborate with benzaldehyde at T= (298.15 to 313.15) K," *J. Chem. Thermodyn*, vol. 41, pp. 888-892, 2009.

H Rodriguez, and J. Brennecke, "Temperature and composition dependence of the density and viscosity of binary mixtures of water and ionic liquids." *J. Chem. Eng. Data*, vol. 51, pp. 2145-2155, 2006.

I. B. Malham, M. Turmine, "Viscosities and refractive indices of binary mixtures of 1-butyl-3-methylimidazolium tetrafluoroborate and 1-butyl-2,3-dimethylimidazolium

tetrafluoroborate with water at 298 K." *J. Chem. Thermodyn.* vol. *40*, pp. 718- 723, 2008.

I. Prigogine, *The molecular Theory of Solutions*; North Holland Pub. Co.: New York, 1957.

J. Armstrong. "" *Oil Gas J.* vol. 104, pp. 12- , 2006.

J. Aguila- Hernandez, A. Trejo, B. E. Garcia Flores, "Surface tension and form behavior of aqueous solutions of blends of three alkanolamine, as a function of temperature, *Colloids Surf. A.: Physicochem. Eng. Aspects*, vol. 308, pp. 33- 46, 2007.

J. Aguila- Hernandez, A. Trejo, B. E. Garcia-flores, R. Molnar, "Viscometric and volumetric behavior of binary mixtures of sulfolane and N- methylpyrrolidone with monoethanolamine and diethanolamine in the range 303- 373 K." *Fluid Phase Equilib.*, vol. 267, pp. 172- 180, 2008

J. Davison, P. Freund, A. Smith, "Putting carbon back into the ground." *IEA Greenhouse Gas R&D Programme*, 2001.

J. F. Brennecke and E. J, Maginn, "Ionic liquids: Innovative fluids for chemical processing." *AIChe*, vol. 47, pp. 2384- 2389, 2001.

J. F. Wang, S.J. Zhang, H.P. Chen, X. Li, M.L. Zhang, "Properties of ionic liquids and its application in catalytic reactions." *Chin. J. Pro. Eng.* vol. 3, pp. 177-185, 2003.

J. G. Huddleston, A. E. Visser, W. M. Reichert, H. D. Willauer, G. A. Broker, R. D. Roger, "Characterization and comparison of hydrophilic and hydrophobic room temperature ionic liquids incorporating the imidazolium cation." *Green chem.* vol. 3, pp. 156- 164, 2001.

J. H. Song, S. B. Park, J. H. Yoon, H. Lee, "Solubility of carbon dioxide in monoethanolamine + ethylene glycol + water and monoethanolamine + poly(ethylene glycol) + water at 333.2 K." *J. Chem. Eng. Data*, vol. 42, pp 143- 144, 1997.

J. H. Song, S. B. Park, J. H. Yoon, H. Lee, "Densities and viscosities of monoethanolamine + ethylene glycol + water," *J. Chem. Eng. Data*, vol. 41, pp. 1152-1154, 1996.

J. Kagimoto, K. Fukumoto, H. Ohno, "Effect of tetrabutylphosphonium cation on the physico- chemical propertties of amino acid ionic liquids." *Chem. Commun.*, vol. , pp. 2254- 2256, 2006.

J. Kumelan, A.P. Kamps, I. Urukova, D. Tuma, G. Maurer, "Solubility of CO_2 in the ionic liquid [bmim][Tf_2N]." *J. Chem. Thermodyn.*, vol 38, pp. 1396- 1401, 2006.

J. Kumelan, A. P. Kamps, D. Tuma, G. Maurer, "Solubility of CO_2 in the ionic liquids [bmim][CH_3SO_4] and [bmim][PF_6]." *J. Chem. Eng. Data*, vol. 51, pp. 1802- 1807, 2006.

J.L. Anthony, E.J. Maginn, J.F. Brennecke, "Solubilities and thermodynamics properties of gases in the ionic liquid 1-n-butyl-3-methylimidazolium hexaflourophosphate," *J. Phys. Chem. B* vol. 106, pp. 7315-7320, 2002.

J. L. Anthony, E. J. Maginn, J. F. Brennecke, "Solubilities and thermodynamics properties of gases in the ionic liquid 1-*n*-butyl-3-methyimidazolium hexaflourophosphate" *J. Phys. Chem. B*, vol. 106, pp. 7315- 7320, 2002.

J. L. Anthony, E.J. Maginn, J.F. Brennecke, "Solubilities and thermodynamics properties of gases in the ionic liquid 1-n-butyl-3-methylimidazolium hexaflourophosphate." *J. Phys. Chem. B*, vol. 106, pp. 7315-7320, 2002.

J. L. Anthony, E.J. Maginn, J.F. Brennecke, "Solutions thermodynamics of imidazolium- based ionic liquid and water."*J. Phys. Chem. B*, vol. 105, pp. 10942-10949, 2001.

J. M. Zhang, S. J. Zhang, K. Dong, "Supported absortpion of CO_2 by tetrabutylphosphonium amino acid ionic liquids." *Chem. Eur. J.* vol. 12, pp. 4021-4026, 2006.

J. S. Eckert, "Selecting the proper distillation column packing," *Chem Eng. Prog.*, 66 vol. 3, pp. 39- 44, 1970.

J. S. Rowlinson, *Liquids and Liquids Mixtures*; Butterwoth: London, 1969J. S. Wilkes, "A short history of ionic liquids from molten salts to neoteric solvents," *Green Chem.* vol. 4, pp. 73- 80, 2002.

K. A. Kurnia, C. D. Wilfred, M. I. Mutalib, T. Murugesan, "Thermophysical properties of hydroxyl ammonium ionic liquid," *J. Chem. Thermodyn.* Vol. 41, pp. 517- 521, 2009.

K. Fukumoto, M. Yoshizawa, H. Ohno, "Room temperature ionic liquids from 20 naturak amino acids." *J. Chem. Eng. Data*, vol. 127, pp. 2398- 2399, 2005.

L. Crowhurst, P.R. Mawdsley, J.M. Perez- Arlandis, P.A. Salter, T. Welton, "Solvent-solute interactions in ionic liquids," *Phys. Chem. Chem. Phys.* vol. 5, pp. 2790- 2794, 2003

M. A. Iglesias-Otero, J. Troncoso, E. Carballo, L. Romani, "Density and refractive index in mixtures of ionic liquids and orgainic solvent: Correlations and predictions." *J. Chem. Thermodyn.* vol. 40, pp. 949- 956, 2008.

M. Almasi and H. Iloukhani, "Densities, viscosities, refractive indices of binary mixtures of methyl ethyl ketone + pentanol isomers at different temperatures." *J. Chem. Eng. Data*, vol. 55, pp 3918- 3922, 2010.

M. Anouti, M. Caillon- Caravanier, Y. Dridi, J. Jacquemin, C. Hardacre, "Liquid densities, heat capacities, refractive index, and excess quantities for {protic ionic liquids + water} binary system." *J. Chem. Thermodyn.*, vol. 41, pp. 799- 808, 2009.

M. Anouti, A. Vigeant, J. Jacquemin, C. Brigouleix, D. Lemordant, "Volumetric properties, viscosities and refarctive index of the protic ionic liquid, pyrrolidinium octanoate, in molecular solvents." *J. Chem. Thermodyn*, vol. 42, pp. 834- 845, 2010.

M. B. Shiflett and A. Yokozeki "Solubilities and diffusivities of carbon dioxide in ionic liquids: [bmim][PF_6] and [bmim][BF_4]." *Ind. Eng. Chem. Res.* vol. 44, pp. 4453-4464, 2005.

M. B. Shiflett and A.Yokozeki, "Solubility of CO_2 in room temperature ionic liquid [C_6mim][Tf_2N]," *J. Phys. Chem. B.* vol. 111, pp. 2070- 2074, 2007.

M. Gupta, I. Coyle, K. Thambimuthu, "CO_2 capture technologies and opportunities in Canada." *Canadian CC&S Tech. Roadmap Workshop*, 2003.

M. J. Lee and T. K. Lin, "Density and viscosity for monoethanolamine + water, ethanol, and 2-propanol." *J. Chem. Eng. Data*, vol. 40, pp. 336- 339, 1995.

M. K. Park, O. C. Sndall, "Solubility of carbon dioxide and nitrous oxide in 50 mass methyldiethanolamine." *J. Chem. Eng. Data*, vol. 46, pp. 166- 168, 2001.

M. Kundu and S.S. Bandyopadhyay, " Solubility of CO_2 in water + diethanolamine + *N* – methydiethanolamine" *Fluid Phase Equilib.* vol. 248, pp. 158- 167, 2006.

M. Tariq, P. A. S. Forte, M. F. Costa Gomez, J. N. Canongia Lopes, L. P. N. Rebelo, "Densities and refractive indices of imidazolium- and phosphonium - based ionic liquids: Effect of temperature, alkyl chain length, and anion," *J. Chem. Thermodyn.*, vol. 41, pp. 790- 798, 2009.

N. A. Sairi, R. Yusoff, Y. Alias, M. K. Aroua, "Solubilities of CO_2 in aqueous *N*-Methyldiethanolamine and guanidinium trifluoromethanesulfonate ionic lquids systems at elevated pressures." *Flud Phase Equilib.*, vol. 300, pp. 89- 94, 2011.

N. Deenadayalu, I. Bahadur, T. Hofman, "Ternary excess molar volume of {methyltrioctylammonium bis(triflouromethylsulfonyl)imide ethanol + methyl acetate, or ethyl acetate} systems at T= (298.15, 303.15, and 313.15) K." *J. Chem. Thermodyn*, vol. 42, pp. 726- 733, 2010.

N. Hafeidh, A. Toumi, M. Bouanz, "Dynamic viscosity study of binary mixtures triethylamine + water at temperatures ranging from (283.15 to 291.35) K." *J. Chem. Eng. Data*, vol. 54, pp. 2195-2199, 2009.

N. Mohd Yunus, M. Ibrahim Mutalib, M. Azmi Bustam, Zakaria Man Thanabalan Murugesan, Thermophysical properties of 1-alkylpyridinum bis(trifluoromethylsulfonyl) imide ionic liquids." *J. Chem. Thermodyn.* vol. 42, pp. 491- 495,2010.

N. Palmer, S. Cavallaro, J.C.J. Bart, "Carbon dioxide absorption by MEA: A preliminary evaluation of a bubbling column reactor." *J. Therm Anal. Cal.* vol. 91 pp. 87- 91, 2008.

N. Palmer, S. Cavallaro, J. C. J. Bart, "Carbon dioxide absorption by MEA: A preliminary evaluation of a bubbling column reactor." *Journal of Thermal Analysis & Calorimetry*, vol. 91 pp. 87- 91, 2008.

P.A. Hunt, "Why does a reduction in hydrogen bonding lead to an increase in viscosity for the 1-butyl-2,3-dimethylimidazolium-based ionic liquids?" *J. Phys. Chem. B*, vol. 111, pp. 4844 - 4853, 2007 .

P. Husson- Borg, V. Majer, M.F.C. Gomez, "Solubilities of oxygen and carbon dioxide in butyl methyl imidazolium tetraflouroborate as a function of temperature and at pressure close to atmospheric pressure," *J. Chem. Eng. Data* vol. 48, pp. 480-485, 2003.

P. Husson- Borg, V. Majer, M. F. J.C. Gomes, "Solubilities of oxygen and carbon dioxide in butyl methyl imidazolium tetraflouroborate as a function of temperature and at pressure close to atmospheric pressure," *J. Chem. Eng. Data*, vol. 48, pp. 480 – 485, 2003.

P. K. Alvaro, T. Dirk, X. Jianzhong, M. Gerd, "Solubility of CO_2 in the ionic liquid [bmim][PF6]." *J. Chem. Eng. Data* vol. 48 pp. 746-749, 2003.

P. Wasserscheid, T. Welton, "Ionic liquids in synthesis." *Wiley- VCH, Weinheim*, 2003.

P. Wang, J. Gong, B. Wang, M. Zhang, J. Wang, "Solubility of deflazacort in binary solvent mixtures." *J. Chem. Eng. Data*, vol. 54, pp. 162- 164, 2009.

Q. Xia, F. B. Zhang, G. L. Zhang, J. C. Ma, L. Zhao, "Solubility of sebacic acid in binary water + ethanol solvent mixtures." *J. Chem. Eng. Data*, vol. 53, pp. 838- 840, 2004.

R. Battino, "Volumes change on mixing for binary mixtures of liquids." *Chem Rev.*, vol. 71, pp. 5- 45, 1971.

R. Francesconi, C. Castellari, F. Comelli, S. Ottani, "Thermodynamic study of binary mixtures containing glycols or polyethylene glycols + benzyl alcohol at 308.15 K." *J. Chem. Eng. Data*, vol. 49, pp. 363- 367, 2004.

R. R. Mira, C. Kroeze, "Greenhouse gas emissions from willow-based electricity: a scenario analysis for Portugal and The Netherlands" *Energy Policy* vol. 34, pp. 1367-1377, 2006.

S.G. Kazarian, B.J. Briscoe, T. Welton, "Combining ionic liquids and supercritical fluids: in situ ATR- IR study of CO_2 dissolved in two ionic liquids at high pressures,: *Chem. Commun.*, pp. 2047- 2048, 2000

S. J. Zhang, X. Li, H.P. Chen, J.F. Wang, J.M. Zhang, M.L.J. Zhang, "Determination of physical properties for the binary system 1-ethyl-3-methylimidazolium tetraflouroborate + H_2O." *J. Chem. Eng. Data,* vol. 49, pp. 760- 764, 2004.

S. W Rho, K. P. Yoo, J. S. Lee, S. C. Nam, J. E. Son, B. M. Min, "Solubility of CO_2 in aqueous methyldiethanolamine. *J. Chem. Eng. Data*, vol. 42, pp. 1161- 1164, 1997.

S. Zhang, X. Yuan, Y. Chen, X. Zhang, "Solubilities of CO_2 in 1-butyl-3-methylimidazloium hexaflourophosphate and 1,1,3,3-tetramethylguanidum Lactate at elavated pressures." *J. Chem. Eng. Data*, vol. 50, pp. 1582- 1585, 2005.

Thitakamol, B.; Veawab, A.; Aroonwilas, A. Environmental Impacts of Absorption – based CO_2 capture unit for post- combustion treatment of flue gas from coal- fired power plant. *Intern. Journal of Greenhouse Gas Control* 2007, 318- 342.

T. Singh and A. Kumar "Physical and excess properties of a room temperature ionic liquid (1-methyl-3-octylimidazolium tetrafluoroborate) with alkoxyethanols (C_1E_m, *m*

= 1 to 3) at T = (298. 15 to 318.15) K." *J. Chem. Thermodyn.*, vol. 40, pp. 417- 423, 2009.

U. R Kapadi, D. G. Hundiwale, N. B. Patil, M. K. Lande, "Viscosities, excess molar volume of binary mixtures of ethanolamine with water at 303.15, 308.15, 313.15 and 318.15 K," *Fluid Phase Equilib.*, vol. 201, pp. 335-341. 2002

V. Ermatchkov, P.-S Kamps, G. Maurer, "Solubility of carbon dioxide in queous N-methyldiethanolamine in the low gas loading region." *Ind. Eng. Chem. Res*, vol. 45, pp. 6081- 6091,2006.

V. Kamavaram, R. G. Reddy, "Theermal stabilities of di-alkylimidazolium chloride ionic liquids." *Int. J. Therm. Sc.* vol. pp. , 2007.

X. L. Yuan, S.Z. Zhang, J. Liu, X. Lu, "Solubilities of CO_2 in hydroxyl ammonium ionic liquid at elevated pressure." *Fluid Phase Equilib.* vol. 257, pp. 195- 200, 2007.

X. X. Li, G. Zhou, D. S. Liu, W. W. Cao, "Excess molar volume and viscosity deviation for the binary mixture of diethylene glycol monobutyl ether + water from (293.15 to 333.15) K at atmospheric pressure." *J. Chem. Eng. Data*, vol. 54, pp. 890-892, 2009.

Y.-G. Li and A. E Mather, "Correlation and prediction of the solubility of carbon dioxide in a mixed alkanolamine solution," *Ind. Eng. Chem. Res.*, vol. 33, pp. 2006 – 2015, 1994.

Y. Geng, S. Chen, T. Wang, D. Yu, C. Peng, H. Liu, Y. Hu, "Density, viscosity and electrical conductivity of 1-butyl-3-methylimidazolium hexafluorophosphate + monoethanolamine + *N,N*-dimethylethanolamine," *J. Mol. liq.*, vol. 143, pp. 100-108. 2008.

Y. Liu, L. Zhang, S. Watanisiri, "Repsenting vapor - liquid equilibrium for an aqueous MEA- CO_2 system using the electrolyte nonrandom- two- liquid model," *Ind. Eng. Chem. Res.* vol. 38, pp. 2080- 2090, 1999.

Y. Maham, T. T. Teng, L. G. Hepler, A. E. Mather, "Volumeric properties of aqueous solutions of monoethanolamine, mono- and dimethylethanolamines at temperatures from 5 to 80 ^{0}C." *Thermochim. Acta*, vol. 386, pp. 111- 118, 2002.

Y. Maham, C. –N. Liew, A. E. Mather, "Viscosities and excess properties of aqueous solution of ethanolamine from 25^{0}C to 80^{0}C. " *J. Sol. Chem.* vol. 31 (9), pp. 743- 756, 2002.

Y. M. Tseng, A. R. Thompson, "Densities and refractive index of aqueous monoethanolamine, diethanolamine and triethanolamine." *J. Chem. Eng. Data,* vol. 2, pp. 264- 265, 1963.

Y. Tian, X. Wang, J. Wang, "Densities and viscosities of 1-butyl-3-methyl imidazolium tetraflouroborate + molecular solvents binary mixtures," *J. Chem. Eng Data*, vol. 53, pp. 2056 – 2059, 2008.

Z. Atik and K. Lourdani, "Volumetric properties of binary and ternary mixtures of diisopropyl ether, α, α, α- trifluorotoluene, 2, 2, 2-trifluoroethanol, and ethanol at a temperature 298.15 K and pressure 101 kPa." *J. Chem. Thermodyn.*, vol. 39, pp. 576-582, 2007.

Z. Feng, F. Cheng- Gang, W. You-Ting, W. Yuan-Tao, "Absorption of CO_2 in the aqueous solutions of functionalized ionic liquids and MDEA," *J. Chem. Eng. Data* vol. 160, pp. 691-697, 2010.

PUBLICATIONS

1. **Malyanah M. Taib** and Thanapalan Murugesan, "Densities and Excess Molar Volumes of Binary Mixtures of Bis(2-hydroxyethyl)ammonium Acetate + Water and Monoethanolamine + Bis(2-hydroxyethyl)ammonium Acetate at Temperatures from (303.15 to 353.15) K." *J. Chem. Eng Data*, 55, 5910- 5913, 2010.

2. **Malyanah M. Taib** and Thanapalan Murugesan, "Solubilities of CO2 in Aqueous Solutions of Ionic Liquids (ILs) and Monoethanolamine (MEA) at Pressures from (100 to 1600 kPa)." *Chemical Engineering Journal* (2010), doi: 10.1016/j.cej.2011.09.048

3. **Malyanah M. Taib** and Thanapalan Murugesan, "Density, Refractive Index, and Excess Properties of 1-Butyl-3-methylimidazolium Tetraflouroborate with Water and Monoethanolamine." *J. Chem. Eng Data* (2011), Articles ASAP (As Soon As Publishable), doi: 10.1021/je2007204.

4. **Malyanah M. Taib** and Thanapalan Murugesan, " Physical and Excess Properties of Ternary Mixtures of 1-Butyl-3-Methylimidazolium Tetrafluoroborate + Monoethanolamine + Water at Temperature from (303.15 to 353.15)K" *J. Chem. Eng Data* (2012), Under Revision. (**Impact factor: 2.087**)

5. **Malyanah M. Taib** and Thanapalan Murugesan, "Densities, Refractive Index and Excess Properties of of Bis(2-hydroxyethyl)ammonium acetate ([bheaa]) + Monoethanolamine + Water System at Temperature from (303.15 to 353.15)K" J. Molecular Liquids (2012), Under Revision. (**Impact factor – 1.649**)

APPENDIX A

Table A-1: Experimental densities (ρ) of systems involving [bheaa] at temperatures from (303.15 to 353.15) K.

[bheaa] + Water System				[bheaa] + MEA System			
x_1	ρ (g·cm^{-3})	x_1	ρ (g·cm^{-3})	x_1	ρ (g·cm^{-3})	x_1	ρ (g·cm^{-3})
T=303.15K		T=333.15K		T=303.15K		T=333.15K	
0.0000	0.99570	0.0000	0.98320	0.0000	1.01067	0.0000	0.98675
0.0678	1.07890	0.0678	1.06330	0.1000	1.04310	0.1000	1.02190
0.0995	1.10040	0.0995	1.08390	0.2028	1.06717	0.2028	1.04692
0.1432	1.11980	0.1432	1.10260	0.3000	1.08483	0.3000	1.06558
0.2005	1.13360	0.2005	1.11610	0.4000	1.09884	0.4000	1.07989
0.3159	1.15160	0.3159	1.13370	0.5000	1.10844	0.5000	1.08975
0.4659	1.16060	0.4659	1.14270	0.5998	1.11624	0.5998	1.09853
0.6045	1.16254	0.6045	1.14328	0.7001	1.12506	0.7001	1.10723
0.7465	1.16500	0.7465	1.14550	0.8004	1.13464	0.8004	1.11723
0.8700	1.16660	0.8700	1.14740	0.9000	1.14910	0.9000	1.13150
1.0000	1.16862	1.0000	1.14928	1.0000	1.16862	1.0000	1.14928
T=313.15K		T=343.15K		T=313.15K		T=343.15K	
0.0000	0.9922	0.0000	0.97780	0.0000	1.00277	0.0000	0.97862
0.0678	1.0741	0.0678	1.05720	0.1000	1.03600	0.1000	1.01473
0.0995	1.0952	0.0995	1.07800	0.2028	1.06048	0.2028	1.04005
0.1432	1.1142	0.1432	1.09660	0.3000	1.07848	0.3000	1.05904
0.2005	1.1279	0.2005	1.10990	0.4000	1.09258	0.4000	1.07344
0.3159	1.1457	0.3159	1.12750	0.5000	1.10228	0.5000	1.08338
0.4659	1.1547	0.4659	1.13640	0.5998	1.11045	0.5998	1.09248
0.6045	1.1561	0.6045	1.13720	0.7001	1.11921	0.7001	1.10114
0.7465	1.1586	0.7465	1.13950	0.8004	1.12886	0.8004	1.11129
0.8700	1.1605	0.8700	1.14100	0.9000	1.14313	0.9000	1.12550
1.0000	1.1623	1.0000	1.14276	1.0000	1.16229	1.0000	1.14276

T=323.15K		T=353.15K		T=323.15K		T=353.15K	
0.0000	0.9881	0.0000	0.97180	0.0000	0.99480	0.0000	0.97040
0.0678	1.0688	0.0678	1.05000	0.1000	1.02900	0.1000	1.00750
0.0995	1.0896	0.0995	1.07180	0.2028	1.05373	0.2028	1.03309
0.1432	1.1085	0.1432	1.09040	0.3000	1.07206	0.3000	1.05241
0.2005	1.1221	0.2005	1.10370	0.4000	1.08627	0.4000	1.06693
0.3159	1.1399	0.3159	1.12120	0.5000	1.09605	0.5000	1.07694
0.4659	1.1488	0.4659	1.13000	0.5998	1.10452	0.5998	1.08635
0.6045	1.1497	0.6045	1.13026	0.7001	1.11325	0.7001	1.09496
0.7465	1.1525	0.7465	1.13300	0.8004	1.12309	0.8004	1.10524
0.8700	1.1540	0.8700	1.13440	0.9000	1.13711	0.9000	1.11940
1.0000	1.1558	1.0000	1.13612	1.0000	1.15584	1.0000	1.13612

Table A-2: Experimental densities (ρ) of systems involving [bmim][BF_4] at temperatures from (293.15 to 353.15) K.

[bmim][BF_4] + Water System				[bmim][BF_4] + MEA System			
x_1	ρ (g·cm^{-3})	x_1	ρ (g·cm^{-3})	x_1	ρ (g·cm^{-3})	x_1	ρ (g·cm^{-3})
T=293.15K		T=323.15K		T=293.15K		T=323.15K	
0.0000	0.99822	0.0000	0.98810	0.0000	1.01623	0.0000	0.99480
0.1000	1.10369	0.1000	1.08338	0.0999	1.06467	0.0999	1.04111
0.2000	1.14095	0.2000	1.11948	0.2001	1.09643	0.2001	1.07278
0.2950	1.15958	0.2950	1.13793	0.2994	1.12225	0.2994	1.09887
0.4016	1.17298	0.4016	1.15147	0.4004	1.14193	0.4004	1.11905
0.5002	1.18160	0.5002	1.15987	0.4999	1.15655	0.4999	1.13347
0.5963	1.18801	0.5963	1.16622	0.5994	1.16902	0.5994	1.14585
0.6997	1.19337	0.6997	1.17168	0.7005	1.17949	0.7005	1.15634
0.8014	1.19782	0.8014	1.17635	0.7992	1.18810	0.7992	1.16525
0.8988	1.20132	0.8988	1.17992	0.9002	1.19652	0.9002	1.17492
1.0000	1.20416	1.0000	1.18281	1.0000	1.20416	1.0000	1.18281
T=298.15K		T=333.15K		T=298.15K		T=333.15K	
0.0000	0.99705	0.0000	0.98320	0.0000	1.01251	0.0000	0.98675
0.1000	1.10040	0.1000	1.07605	0.0999	1.06078	0.0999	1.03318
0.2000	1.13732	0.2000	1.11233	0.2001	1.09238	0.2001	1.06489
0.2950	1.15586	0.2950	1.13080	0.2994	1.11837	0.2994	1.09118
0.4016	1.16924	0.4016	1.14435	0.4004	1.13810	0.4004	1.11156
0.5002	1.17793	0.5002	1.15277	0.4999	1.15255	0.4999	1.12618
0.5963	1.18435	0.5963	1.15903	0.5994	1.16495	0.5994	1.13840
0.6997	1.18970	0.6997	1.16461	0.7005	1.17554	0.7005	1.14882
0.8014	1.19422	0.8014	1.16929	0.7992	1.18412	0.7992	1.15795
0.8988	1.19772	0.8988	1.17291	0.9002	1.19289	0.9002	1.16785
1.0000	1.20057	1.0000	1.17583	1.0000	1.20057	1.0000	1.17583
T=303.15K		T=343.15K		T=303.15K		T=343.15K	
0.0000	0.99570	0.0000	0.97780	0.0000	1.01067	0.0000	0.97862
0.1000	1.09703	0.1000	1.06866	0.0999	1.05687	0.0999	1.02521
0.2000	1.13342	0.2000	1.10512	0.2001	1.08849	0.2001	1.05698
0.2950	1.15211	0.2950	1.12382	0.2994	1.11447	0.2994	1.08358

0.4016	1.16547	0.4016	1.13732	0.4004	1.13429	0.4004	1.10401
0.5002	1.17425	0.5002	1.14579	0.4999	1.14867	0.4999	1.11883
0.5963	1.18072	0.5963	1.15206	0.5994	1.16091	0.5994	1.13100
0.6997	1.18607	0.6997	1.15755	0.7005	1.17148	0.7005	1.14137
0.8014	1.19061	0.8014	1.16229	0.7992	1.18017	0.7992	1.15051
0.8988	1.19412	0.8988	1.16595	0.9002	1.18925	0.9002	1.16085
1.0000	1.19698	1.0000	1.16890	1.0000	1.19698	1.0000	1.16890
T=313.15K		*T*=353.15K		*T*=313.15K		*T*=353.15K	
0.0000	0.99220	0.0000	0.97180	0.0000	1.00277	0.0000	0.97040
0.1000	1.09058	0.1000	1.06140	0.0999	1.04901	0.0999	1.01717
0.2000	1.12658	0.2000	1.09786	0.2001	1.08064	0.2001	1.04906
0.2950	1.14511	0.2950	1.11677	0.2994	1.10667	0.2994	1.07591
0.4016	1.15853	0.4016	1.13024	0.4004	1.12656	0.4004	1.09667
0.5002	1.16710	0.5002	1.13872	0.4999	1.14100	0.4999	1.11153
0.5963	1.17345	0.5963	1.14499	0.5994	1.15335	0.5994	1.12365
0.6997	1.17890	0.6997	1.15052	0.7005	1.16393	0.7005	1.13416
0.8014	1.18345	0.8014	1.15534	0.7992	1.17272	0.7992	1.14322
0.8988	1.18699	0.8988	1.15904	0.9002	1.18205	0.9002	1.15390
1.0000	1.18986	1.0000	1.16204	1.0000	1.18986	1.0000	1.16204

Table A-3: Fitting Parameters of ρ vs x_1 and Errors for the Correlation of Density (eq. 4.1) for [bheaa] – water, [bheaa] – MEA, [bmim][BF_4] – water and [bmim][BF_4] – MEA Binary Mixtures.

T/K	A_0	A_1	A_2	A_3	A_4	σ
			[bheaa] - Water			
303.15	1.00274	1.21485	-3.35430	3.87495	-1.57178	0.00555
313.15	0.99909	1.19569	-3.30007	3.80991	-1.54438	0.00542
323.15	0.99482	1.17991	-3.24968	3.74425	-1.51547	0.00528
333.15	0.98990	1.16914	-3.21424	3.69345	-1.49091	0.00526
343.15	0.98442	1.16240	-3.19493	3.67304	-1.48413	0.00522
353.15	0.97806	1.16252	-3.19523	3.67103	-1.48218	0.00502
			[bheaa] – MEA			
303.15	1.01046	0.37184	-0.49313	0.27916	-	0.00044
313.15	1.00267	0.37780	-0.49796	0.27958	-	0.00037
323.15	0.99489	0.38355	-0.50261	0.27994	-	0.00032
333.15	0.98705	0.38888	-0.50609	0.27967	-	0.00038
343.15	0.97909	0.39488	-0.51138	0.28056	-	0.00047
353.15	0.97106	0.40097	-0.51685	0.28150	-	0.00060
			[bmim][BF_4] – Water			
293.15	1.01226	0.83850	-1.29809	0.65926	-	0.00992
298.15	1.01076	0.82313	-1.26809	0.64196	-	0.00969
303.15	1.00902	0.80939	-1.24237	0.62809	-	0.00941
313.15	1.00499	0.79028	-1.20817	0.60954	-	0.00905
323.15	1.00023	0.77371	-1.17736	0.59277	-	0.00861
333.15	0.99480	0.76139	-1.15375	0.57975	-	0.00826
343.15	0.98891	0.75239	-1.13585	0.56963	-	0.00793
353.15	0.98262	0.74609	-1.12333	0.56274	-	0.00774
			[bmim][BF_4] – MEA			
293.15	1.01701	0.53192	-0.76759	0.62594	-0.20335	0.00067
298.15	1.01353	0.52723	-0.75228	0.60526	-0.19333	0.00065

303.15	1.01015	0.52195	-0.73449	0.58036	-0.18107	0.00059
313.15	1.00286	0.51545	-0.71190	0.55208	-0.16866	0.00055
323.15	0.99517	0.51250	-0.69679	0.52906	-0.15709	0.00056
333.15	0.98712	0.51278	-0.69002	0.51536	-0.14933	0.00060
343.15	0.97899	0.51370	-0.68445	0.50209	-0.14127	0.00064
353.15	0.97077	0.51462	-0.67722	0.48675	-0.13268	0.00069

Table A-4: Fitting Parameters of A_n (Table A-3) vs T and Errors for the Correlation of Density (eq. 4.2) for [bheaa] – water, [bheaa] – MEA, [bmim][BF_4] – water and [bmim][BF_4] – MEA Binary Mixtures.

	B_0	B_1	B_2	B_3	B_4	σ
				[bheaa] - Water		
A_0	1.13374	-0.00139	6.0498E-06	-9.4830E-09	-	3.0227E-05
A_1	-0.62435	0.02647	-1.0781E-04	1.3357E-07	-	2.0707E-04
A_2	14.8709	-0.19607	6.7954E-04	-7.6228E-07	-	7.3099E-04
A_3	-690.390	8.41782	-3.8110E-02	7.6370E-05	-5.7182E-08	7.7638E-04
A_4	469.236	-5.71570	2.5939E-02	-5.2164E-05	3.9233E-08	9.5795E-04
				[bheaa] - MEA		
A_0	1.21233	-0.00056	-3.4363E-07	-	-	2.0259E-05
A_1	0.22881	0.00038	2.9868E-07	-	-	1.8132E-04
A_2	-0.46263	0.00021	-1.0258E-06	-	-	4.3609E-04
A_3	0.35739	-0.00051	8.4529E-07	-	-	2.5264E-04
				[bmim][BF_4] – Water		
A_0	0.84039	0.00149	-3.0713E-06	-	-	1.0227E-04
A_1	9.53853	-0.07199	1.9801E-04	-1.8307E-07	-	6.2821E-04
A_2	-191.191	2.29021	-1.0390E-02	2.1006E-05	-1.5955E-08	9.5394E-04
A_3	129.443	-1.56025	7.1042E-03	-1.4405E-05	1.0965E-08	5.4202E-04
				[bmim][BF_4] – MEA		
A_0	1.09720	0.00014	-1.4168E-06	-	-	1.0806E-04
A_1	7.56498	-0.06136	1.7757E-04	-1.7094E-07	-	4.0326E-04
A_2	78.5167	-1.05967	5.2396E-03	-1.1385E-05	9.1950E-09	7.6579E-04
A_3	-20.1464	0.35123	-2.0226E-03	4.8955E-06	-4.2923E-09	1.3378E-03
A_4	-30.8581	0.33829	-1.3953E-03	2.5477E-06	-1.7314E-09	7.9220E-04

Table A-5: Fitting Parameters of ρ vs T and Errors for the Correlation of Density (eq. 4.5) for [bheaa] (1) – water and [bheaa] (1) – MEA Binary Mixtures.

x_1	A_0	A_1	A_2	σ
		[bheaa] - Water		
0.0000	0.80251	0.00160	-3.1607E-06	4.0178E-05
0.0678	0.96206	0.00121	-2.7143E-06	1.5639E-04
0.0995	1.15538	0.00015	-1.1071E-06	3.6253E-05
0.1432	1.21767	-0.00010	-7.5000E-07	1.3093E-05
0.2005	1.23668	-0.00012	-7.3214E-07	3.0472E-05
0.3159	1.26708	-0.00019	-6.4286E-07	5.2372E-05
0.4659	1.26755	-0.00013	-7.3214E-07	-3.0472E-05
0.6045	1.33502	-0.00051	-2.0482E-07	1.6291E-04
0.7465	1.35740	-0.00063	-1.7857E-08	1.9335E-04
0.8700	1.32236	-0.00040	-3.7500E-07	8.8882E-05
1.0000	1.33103	-0.00044	-3.2446E-07	2.5248E-05
		[bheaa] - MEA		
0.0000	1.21215	-0.00054	-3.9804E-07	4.1927E-06
0.1000	1.23324	-0.00056	-2.3750E-07	3.0409E-05
0.2028	1.23926	-0.00047	-3.2214E-07	5.0766E-06
0.3000	1.24539	-0.00043	-3.3607E-07	3.1287E-06
0.4000	1.25769	-0.00043	-3.2321E-07	3.0472E-06
0.5000	1.26233	-0.00040	-3.4643E-07	1.7728E-06
0.5998	1.25522	-0.00034	-3.9518E-07	1.1666E-05
0.7001	1.26610	-0.00035	-3.8750E-07	6.5137E-06
0.8004	1.27447	-0.00035	-3.5696E-07	2.0184E-05
0.9000	1.31744	-0.00052	-1.0179E-07	1.1132E-04
1.0000	1.33103	-0.00044	-3.2446E-07	2.5248E-05

Table A-6: Fitting Parameters of ρ vs T and Errors for the Correlation of Density for (eq. 4.5) [bmim][BF_4] (1) – water and [bmim][BF_4] (1) – MEA Binary Mixtures.

x_1	A_0	A_1	A_2	σ
		[bmim][BF_4] - Water		
0.0000	0.77723	0.00175	-3.3905E-06	8.0345E-05
0.1000	1.21206	-0.00009	-9.5638E-07	1.3721E-04
0.2000	1.34450	-0.00068	-5.7862E-08	1.2513E-04
0.2950	1.39630	-0.00089	2.7196E-07	6.7415E-05
0.4016	1.39957	-0.00083	1.8097E-07	9.3966E-05
0.5002	1.42165	-0.00091	2.9770E-07	3.3099E-05
0.5963	1.43087	-0.00092	3.1505E-07	3.2502E-05
0.6997	1.41837	-0.00081	1.5748E-07	4.4184E-05
0.8014	1.43225	-0.00088	2.5926E-07	3.3066E-06
0.8988	1.43756	-0.00089	2.8684E-07	3.3551E-06
1.0000	1.44333	-0.00091	3.2219E-07	4.7679E-06
		[bmim][BF_4] - MEA		
0.0000	1.08420	0.00022	-1.5300E-06	1.2374E-04
0.0999	1.27453	-0.00065	-2.1454E-07	5.2557E-06
0.2001	1.32292	-0.00076	-4.3960E-08	3.5809E-05
0.2994	1.37127	-0.00091	2.1730E-07	2.9416E-05
0.4004	1.39379	-0.00095	2.9495E-07	3.8506E-05
0.4999	1.43629	-0.00113	5.8412E-07	6.0414E-05
0.5994	1.44719	-0.00111	5.5593E-07	9.2108E-05
0.7005	1.45800	-0.00111	5.5298E-07	6.1330E-05
0.7992	1.45034	-0.00102	4.2377E-07	8.5818E-05
0.9002	1.43861	-0.00092	3.2734E-07	4.6569E-06
1.0000	1.44333	-0.00091	3.2219E-07	4.7679E-06

Table A-7: Thermal Expansion Coefficients (α) of [bheaa](1) – water and [bheaa] (1) – MEA Binary Mixtures.

T/K	303.15	313.15	323.15	333.15	343.15	353.15
x_1	α/ K^{-1}					
			[bheaa] - Water			
	303.15	313.15	323.15	333.15	343.15	353.15
0.0000	0.00032	0.00039	0.00045	0.00052	0.00059	0.00066
0.0678	0.00041	0.00046	0.00051	0.00056	0.00062	0.00068
0.0995	0.00047	0.00049	0.00052	0.00054	0.00056	0.00059
0.1432	0.00049	0.00051	0.00052	0.00054	0.00056	0.00057
0.2005	0.00050	0.00051	0.00053	0.00054	0.00056	0.00058
0.3159	0.00050	0.00051	0.00053	0.00054	0.00056	0.00057
0.4659	0.00050	0.00051	0.00053	0.00054	0.00056	0.00057
0.6045	0.00054	0.00055	0.00056	0.00056	0.00057	0.00058
0.7465	0.00055	0.00055	0.00056	0.00056	0.00056	0.00057
0.8700	0.00054	0.00055	0.00056	0.00057	0.00058	0.00059
1.0000	0.00054	0.00055	0.00056	0.00057	0.00058	0.00059
			[bheaa] - MEA			
0.0000	0.000777	0.000791	0.000805	0.000820	0.000835	0.000850
0.1000	0.000670	0.000680	0.000689	0.000698	0.000708	0.000718
0.2028	0.000623	0.000633	0.000644	0.000654	0.000664	0.000675
0.3000	0.000582	0.000592	0.000602	0.000612	0.000622	0.000632
0.4000	0.000566	0.000575	0.000584	0.000594	0.000604	0.000613
0.5000	0.000553	0.000562	0.000572	0.000581	0.000591	0.000601
0.5998	0.000518	0.000528	0.000538	0.000548	0.000558	0.000569
0.7001	0.000518	0.000528	0.000537	0.000547	0.000557	0.000568
0.8004	0.000502	0.000511	0.000520	0.000529	0.000538	0.000548
0.9000	0.000510	0.000515	0.000519	0.000524	0.000528	0.000533
1.0000	0.000543	0.000551	0.000560	0.000569	0.000578	0.000587

Table A-8: Thermal Expansion Coefficients (α) of [bmim][BF_4](1) – water and [bmim][BF_4] (1) – MEA Binary Mixtures.

T/K	293.15	298.15	303.15	313.15	323.15	333.15	343.15	353.15
x_1	α/ K^{-1}							
				[bmim][BF4] - Water				
0.0000	0.000240	0.000274	0.000309	0.000378	0.000449	0.000520	0.000592	0.000665
0.1000	0.000589	0.000599	0.000610	0.000631	0.000653	0.000675	0.000698	0.000721
0.2000	0.000624	0.000626	0.000629	0.000634	0.000639	0.000644	0.000649	0.000655
0.2950	0.000628	0.000628	0.000627	0.000626	0.000625	0.000625	0.000624	0.000623
0.4016	0.000614	0.000615	0.000615	0.000616	0.000616	0.000617	0.000617	0.000618
0.5002	0.000619	0.000619	0.000618	0.000617	0.000615	0.000614	0.000613	0.000611
0.5963	0.000620	0.000619	0.000618	0.000617	0.000615	0.000613	0.000612	0.000610
0.6997	0.000605	0.000605	0.000606	0.000607	0.000608	0.000609	0.000610	0.000611
0.8014	0.000604	0.000604	0.000603	0.000603	0.000602	0.000601	0.000600	0.000599
0.8988	0.000601	0.000600	0.000600	0.000598	0.000597	0.000596	0.000594	0.000593
1.0000	0.000599	0.000598	0.000597	0.000595	0.000594	0.000592	0.000590	0.000588
				[bmim][BF4] - MEA				
0.0000	0.000668	0.000685	0.000703	0.000738	0.000775	0.000812	0.000850	0.000889
0.0999	0.000731	0.000736	0.000741	0.000751	0.000760	0.000770	0.000781	0.000791
0.2001	0.000717	0.000720	0.000723	0.000729	0.000735	0.000741	0.000748	0.000754
0.2994	0.000700	0.000701	0.000701	0.000702	0.000703	0.000704	0.000705	0.000706
0.4004	0.000677	0.000676	0.000676	0.000675	0.000675	0.000674	0.000673	0.000672
0.4999	0.000677	0.000675	0.000672	0.000666	0.000660	0.000654	0.000648	0.000642
0.5994	0.000673	0.000670	0.000668	0.000663	0.000657	0.000652	0.000646	0.000640
0.7005	0.000668	0.000666	0.000663	0.000658	0.000653	0.000648	0.000642	0.000636
0.7992	0.000649	0.000647	0.000646	0.000643	0.000640	0.000636	0.000633	0.000630
0.9002	0.000610	0.000609	0.000608	0.000606	0.000604	0.000603	0.000601	0.000598
1.0000	0.000599	0.000598	0.000597	0.000595	0.000594	0.000592	0.000590	0.000588

Table A-9: Experimental densities (ρ) of [bheaa] + MEA + Water System at temperatures from (293.15 to 353.15) K.

x_1	x_2	T = 293.15	T = 303.15	T = 313.15	T = 323.15	T = 333.15	T = 343.15	T = 353.15
					$z\ (x_1/x_3) = 0.11$			
0.0892	0.1003	1.09047	1.08505	1.07953	1.07369	1.06773	1.06156	1.05519
0.0790	0.1999	1.08111	1.07531	1.06942	1.06323	1.05695	1.05048	1.04382
0.0694	0.3002	1.07215	1.06600	1.05970	1.05327	1.04669	1.03995	1.03303
0.0594	0.3999	1.06314	1.05663	1.05001	1.04327	1.03640	1.02938	1.02221
0.0495	0.4997	1.05475	1.04795	1.04104	1.03403	1.02691	1.01965	1.01225
0.0396	0.5997	1.04656	1.03950	1.03234	1.02510	1.01775	1.01029	1.00268
0.0299	0.7000	1.03911	1.03183	1.02445	1.01700	1.00946	1.00182	0.99405
0.0199	0.7994	1.03149	1.02398	1.01640	1.00876	1.00104	0.99322	0.98528
0.0099	0.9007	1.02395	1.01625	1.00849	1.00066	0.99277	0.98478	0.97669
					$z\ (x_1/x_3) = 0.62$			
0.3439	0.0998	1.14774	1.14201	1.13618	1.13031	1.12440	1.11841	1.11231
0.3064	0.2001	1.13469	1.12898	1.12315	1.11728	1.11136	1.10536	1.09926
0.2680	0.3000	1.12161	1.11580	1.10990	1.10396	1.09795	1.09187	1.08569
0.2297	0.4001	1.10866	1.10267	1.09660	1.09049	1.08431	1.07806	1.07171
0.1915	0.4993	1.09490	1.08872	1.08246	1.07615	1.06978	1.06333	1.05679
0.1531	0.5999	1.08048	1.07405	1.06754	1.06099	1.05437	1.04767	1.04088
0.1149	0.6998	1.06625	1.05948	1.05265	1.04578	1.03883	1.03181	1.02470
0.0760	0.7948	1.05118	1.04409	1.03694	1.02973	1.02247	1.01512	1.00769
0.0381	0.8974	1.03470	1.02725	1.01973	1.01217	1.00453	0.99682	0.98902
					$z\ (x_1/x_3) = 4.03$			
0.7208	0.0995	1.15867	1.15642	1.15039	1.14434	1.13835	1.13201	1.12562
0.6405	0.1999	1.15280	1.14878	1.14291	1.13700	1.13108	1.12492	1.11850
0.5610	0.3001	1.14561	1.13972	1.13390	1.12806	1.12213	1.11616	1.11014
0.4681	0.3895	1.13428	1.12840	1.12260	1.11671	1.11077	1.10478	1.09873
0.3989	0.4977	1.12167	1.11617	1.11014	1.10415	1.09800	1.09172	1.08557
0.3191	0.5972	1.10723	1.10143	1.09519	1.08902	1.08270	1.07634	1.07001
0.2392	0.6966	1.09082	1.08454	1.07801	1.07156	1.06508	1.05855	1.05195
0.1594	0.7968	1.07154	1.06479	1.05781	1.05121	1.04436	1.03746	1.03048
0.0803	0.9011	1.04765	1.04043	1.03318	1.02589	1.01855	1.01115	1.00368

Table A-10: Experimental densities (ρ) of [bmim][BF_4] + MEA + Water System at temperatures from (293.15 to 353.15) K.

T/ K		293.15	298.15	303.15	313.15	323.15	333.15	343.15	353.15
x_1	x_2								
					$z\,(x_1/x_3) = 0.08$				
0.0664	0.0998	1.08307	1.07984	1.07703	1.07110	1.06497	1.05838	1.05153	1.04451
0.0592	0.2000	1.07566	1.07228	1.06933	1.06272	1.05598	1.04880	1.04141	1.03387
0.0523	0.3002	1.06925	1.06581	1.06293	1.05570	1.04831	1.04073	1.03297	1.02523
0.0444	0.3999	1.06221	1.05842	1.05580	1.04809	1.04041	1.03254	1.02459	1.01658
0.0359	0.4841	1.05476	1.05089	1.04806	1.04012	1.03237	1.02440	1.01639	1.00822
0.0296	0.5997	1.04693	1.04300	1.04040	1.03246	1.02453	1.01648	1.00831	1.00011
0.0218	0.6871	1.03910	1.03511	1.03267	1.02475	1.01675	1.00865	1.00041	0.99211
0.0148	0.8004	1.03110	1.02712	1.02492	1.01696	1.00892	1.00084	0.99262	0.98431
0.0079	0.8885	1.02442	1.02057	1.01847	1.01051	1.00240	0.99421	0.98593	0.97765
					$z\,(x_1/x_3) = 0.32$				
0.2155	0.1011	1.14320	1.13952	1.13644	1.12985	1.12312	1.11637	1.10953	1.10263
0.1943	0.2003	1.13129	1.12762	1.12455	1.11753	1.11048	1.10333	1.09608	1.08891
0.1701	0.3018	1.11873	1.11495	1.11188	1.10460	1.09729	1.08992	1.08249	1.07509
0.1453	0.3996	1.10582	1.10200	1.09902	1.09162	1.08412	1.07661	1.06890	1.06132
0.1206	0.4967	1.09249	1.08866	1.08579	1.07833	1.07059	1.06290	1.05502	1.04733
0.0972	0.6011	1.07882	1.07489	1.07222	1.06455	1.05670	1.04886	1.04087	1.03303
0.0729	0.6998	1.06426	1.06033	1.05785	1.05007	1.04212	1.03410	1.02601	1.01802
0.0486	0.7999	1.04893	1.04503	1.04271	1.03483	1.02682	1.01879	1.01057	1.00241
0.0245	0.9036	1.03311	1.02924	1.02711	1.01918	1.01117	1.00300	0.99484	0.98660
					$z\,(x_1/x_3) = 5.03$				
0.7478	0.0998	1.19166	1.18749	1.18382	1.17653	1.16932	1.16216	1.15505	1.14800
0.6677	0.2015	1.18210	1.17791	1.17442	1.16712	1.15985	1.15266	1.14551	1.13841
0.5679	0.2980	1.17058	1.16643	1.16302	1.15571	1.14840	1.14119	1.13399	1.12682
0.5009	0.3997	1.16001	1.15582	1.15247	1.14510	1.13767	1.13035	1.12305	1.11580
0.4122	0.4957	1.14625	1.14199	1.13880	1.13136	1.12390	1.11645	1.10899	1.10157
0.3346	0.6004	1.13111	1.12694	1.12394	1.11635	1.10877	1.10115	1.09354	1.08598
0.2496	0.6969	1.11189	1.10782	1.10499	1.09730	1.08962	1.08190	1.07415	1.06634
0.1660	0.7954	1.08803	1.08403	1.08143	1.07365	1.06581	1.05796	1.05005	1.04207
0.0829	0.8983	1.05730	1.05341	1.05113	1.04328	1.03540	1.02745	1.01946	1.01134

Table A-11: Fitting Parameters of ρ vs x_1 and Errors for the Correlation of Density for (eq. 4.6) [bheaa] + MEA + water system at temperatures from (293.15 to 353.15) K.

T/K	A_0	A_1	A_2	σ
		$z\ (x_1/\ x_3) = 0.11$		
293.15	1.10020	-0.09860	0.01565	0.00014
303.15	1.09519	-0.10290	0.01712	0.00015
313.15	1.09012	-0.10742	0.01884	0.00016
323.15	1.08461	-0.11092	0.01987	0.00017
333.15	1.07900	-0.11453	0.02107	0.00017
343.15	1.07316	-0.11789	0.02217	0.00018
353.15	1.06709	-0.12108	0.02322	0.00019
		$z\ (x_1/\ x_3) = 0.62$		
293.15	1.15926	-0.11686	-0.02408	0.00032
303.15	1.15356	-0.11654	-0.02665	0.00032
313.15	1.14774	-0.11613	-0.02925	0.00027
323.15	1.14188	-0.11572	-0.03186	0.00026
333.15	1.13599	-0.11542	-0.03439	0.00024
343.15	1.13001	-0.11506	-0.03696	0.00022
353.15	1.12393	-0.11475	-0.03948	0.00021
		$z\ (x_1/\ x_3) = 4.03$		
293.15	1.16224	-0.02462	-0.11302	0.00068
303.15	1.16042	-0.03656	-0.10586	0.00090
313.15	1.15424	-0.03424	-0.10986	0.00085
323.15	1.14797	-0.03163	-0.11391	0.00088
333.15	1.14182	-0.02981	-0.11734	0.00089
343.15	1.13525	-0.02680	-0.12168	0.00088
353.15	1.12844	-0.02293	-0.12680	0.00088

Table A-12: Fitting Parameters of ρ vs x_1 and Errors for the Correlation of Density for (eq. 4.6) [bmim][BF_4] + MEA + Water System at temperatures from (293.15 to 353.15) K.

T/K	A_0	A_1	A_2	A_3	σ
			$z\,(x_1/x_3) = 0.08$		
293.15	1.09008	-0.06905	-0.00582	-	0.00048
298.15	1.08720	-0.07206	-0.00373	-	0.00051
303.15	1.08437	-0.07255	-0.00220	-	0.00055
313.15	1.07917	-0.08096	0.00393	-	0.00055
323.15	1.07359	-0.08778	0.00854	-	0.00055
333.15	1.06742	-0.09342	0.01246	-	0.00055
343.15	1.06092	-0.09824	0.01574	-	0.00055
353.15	1.05426	-0.10282	0.01887	-	0.00055
			$z\,(x_1/x_3) = 0.32$		
293.15	1.15474	-0.11214	-0.02487	-	0.00025
298.15	1.15120	-0.11311	-0.02422	-	0.00023
303.15	1.14810	-0.11332	-0.02275	-	0.00025
313.15	1.14173	-0.11655	-0.02106	-	0.00024
323.15	1.13536	-0.12030	-0.01892	-	0.00025
333.15	1.12885	-0.12345	-0.01743	-	0.00025
343.15	1.12235	-0.12732	-0.01519	-	0.00027
353.15	1.11566	-0.12981	-0.01434	-	0.00029
			$z\,(x_1/x_3) = 5.03$		
293.15	1.20372	-0.12608	0.104261	-0.1617	0.000548
298.15	1.199572	-0.12619	0.103767	-0.16063	0.000557
303.15	1.195782	-0.12464	0.102103	-0.15861	0.000563
313.15	1.188392	-0.1234	0.098274	-0.15652	0.000553
323.15	1.181175	-0.1233	0.096526	-0.15565	0.000543
333.15	1.173939	-0.12219	0.092215	-0.15321	0.000536
343.15	1.166778	-0.12135	0.088204	-0.15094	0.000533
353.15	1.159649	-0.12033	0.083918	-0.14881	0.000541

Table A-13: Fitting Parameters of ρ vs T and Errors for the Correlation of Density (eq. 4.5) for [bheaa] + MEA + water system

x_2	A_0	A_1	A_2	σ
		$z\,(x_1/x_3) = 0.11$		
0.1003	1.16098	4.7781E-05	-9.8362E-07	2.1984E-05
0.1999	1.17234	-5.3646E-05	-8.7859E-07	2.1235E-05
0.3002	1.18460	-1.6114E-04	-7.5893E-07	1.0805E-05
0.3999	1.19431	-2.5304E-04	-6.6333E-07	1.1554E-05
0.4997	1.20065	-3.2325E-04	-5.9524E-07	1.0738E-05
0.5997	1.20577	-3.8733E-04	-5.3155E-07	1.1747E-05
0.7000	1.21067	-4.4801E-04	-4.6821E-07	1.0192E-05
0.7994	1.21407	-5.0099E-04	-4.1571E-07	1.2196E-05
0.9007	1.21495	-5.3897E-04	-3.8417E-07	9.9063E-06
		$z\,(x_1/x_3) = 0.62$		
0.0998	1.28714	-3.8031E-04	-3.2476E-07	1.2821E-05
0.2001	1.27269	-3.7142E-04	-3.3881E-07	1.1207E-05
0.3000	1.26104	-3.7375E-04	-3.4762E-07	1.1198E-05
0.4001	1.25380	-3.9516E-04	-3.4104E-07	1.0560E-05
0.4993	1.24568	-4.1419E-04	-3.4164E-07	1.0289E-05
0.5999	1.23860	-4.3944E-04	-3.4100E-07	1.0075E-05
0.6998	1.23486	-4.7808E-04	-3.3131E-07	1.1056E-05
0.7948	1.22932	-5.1073E-04	-3.3083E-07	1.0330E-05
0.8974	1.22270	-5.4189E-04	-3.3917E-07	7.6246E-06
		$z\,(x_1/x_3) = 4.03$		
0.0995	1.05375	1.1346E-03	-2.6398E-06	7.0638E-04
0.1999	1.15749	4.5469E-04	-1.6012E-06	3.1801E-04
0.3001	1.29915	-4.6870E-04	-1.8821E-07	2.8673E-05
0.3895	1.28512	-4.5054E-04	-2.1869E-07	2.2264E-05
0.4977	1.23927	-2.3157E-04	-5.7738E-07	9.5803E-05
0.5972	1.24598	-3.4888E-04	-4.2351E-07	7.3340E-05
0.6966	1.26038	-5.2019E-04	-1.9821E-07	3.7262E-05
0.7968	1.25621	-5.8602E-04	-1.5024E-07	9.5803E-05
0.9011	1.23586	-5.6709E-04	-2.5583E-07	1.1109E-05

Table A-14: Fitting Parameters of ρ vs T and Errors for the Correlation of Density (eq. 4.5) for [bmim][BF_4] + MEA + water system.

x_2	A_0	A_1	A_2	σ
		$z\,(x_1/x_3) = 0.08$		
0.0998	1.13734	1.9042E-04	-1.2834E-06	1.1895E-04
0.2000	1.14042	1.7228E-04	-1.3424E-06	8.6516E-05
0.3002	1.15496	7.7618E-05	-1.2611E-06	1.7359E-04
0.3999	1.15743	4.0121E-05	-1.2441E-06	2.7400E-04
0.4841	1.17330	-9.3786E-05	-1.0588E-06	2.3624E-04
0.5997	1.14469	4.1039E-05	-1.2767E-06	3.0506E-04
0.6871	1.11813	1.6006E-04	-1.4651E-06	3.4366E-04
0.8004	1.09666	2.4234E-04	-1.5886E-06	4.0313E-04
0.8885	1.07403	3.4442E-04	-1.7502E-06	4.4791E-04
		$z\,(x_1/x_3) = 0.32$		
0.1011	1.30937	-4.7981E-04	-2.9894E-07	1.0769E-04
0.2003	1.28908	-3.9918E-04	-4.7507E-07	1.0617E-04
0.3018	1.28041	-4.0542E-04	-4.9883E-07	1.3038E-04
0.3996	1.24819	-2.7213E-04	-7.2856E-07	1.7036E-04
0.4967	1.21948	-1.6525E-04	-9.1369E-07	2.2794E-04
0.6011	1.19659	-9.8487E-05	-1.0340E-06	2.8457E-04
0.6998	1.16006	4.6293E-05	-1.2718E-06	3.4638E-04
0.7999	1.12237	1.9029E-04	-1.5025E-06	3.7768E-04
0.9036	1.09021	2.9322E-04	-1.6630E-06	4.3108E-04
		$z\,(x_1/x_3) = 5.03$		
0.0998	1.45942	-1.0727E-03	5.4099E-07	1.2557E-04
0.2015	1.43436	-9.7515E-04	3.8854E-07	1.2761E-04
0.2980	1.40893	-8.8666E-04	2.4888E-07	1.2398E-04
0.3997	1.39145	-8.3675E-04	1.5917E-07	1.3538E-04
0.4957	1.35335	-6.7857E-04	-9.7458E-08	1.7238E-04
0.6004	1.31443	-5.2139E-04	-3.5590E-07	1.9911E-04
0.6969	1.26212	-3.0770E-04	-6.9912E-07	2.2863E-04
0.7954	1.20728	-1.0637E-04	-1.0246E-06	2.9389E-04
0.8983	1.13841	1.3389E-04	-1.3994E-06	3.7545E-04

Table A-15: Thermal Expansion Coefficients (α) of [bheaa] (1) + MEA (2) + water (3) system

T/K	293.15	303.15	313.15	323.15	333.15	343.15	353.15
x_2	α/ K^{-1}						
				$z\ (x_1/\ x_3) = 0.11$			
0.1003	0.000485	0.000506	0.000526	0.000548	0.000569	0.000591	0.000613
0.1999	0.000526	0.000545	0.000565	0.000585	0.000605	0.000625	0.000646
0.3002	0.000565	0.000583	0.000601	0.000619	0.000637	0.000656	0.000675
0.3999	0.000604	0.000620	0.000637	0.000653	0.000671	0.000688	0.000706
0.4997	0.000637	0.000653	0.000669	0.000685	0.000701	0.000718	0.000735
0.5997	0.000668	0.000683	0.000698	0.000713	0.000729	0.000744	0.000761
0.7000	0.000695	0.000709	0.000724	0.000738	0.000753	0.000768	0.000783
0.7994	0.000722	0.000735	0.000749	0.000763	0.000777	0.000792	0.000806
0.9007	0.000746	0.000760	0.000773	0.000787	0.000801	0.000815	0.000830
				$z\ (x_1/\ x_3) = 0.62$			
0.0998	0.000497	0.000505	0.000514	0.000522	0.000531	0.000539	0.000548
0.2001	0.000502	0.000511	0.000520	0.000528	0.000537	0.000546	0.000556
0.3000	0.000515	0.000524	0.000533	0.000542	0.000551	0.000561	0.000570
0.4001	0.000537	0.000546	0.000555	0.000564	0.000574	0.000584	0.000593
0.4993	0.000561	0.000571	0.000580	0.000590	0.000600	0.000610	0.000620
0.5999	0.000592	0.000602	0.000612	0.000622	0.000632	0.000643	0.000654
0.6998	0.000631	0.000641	0.000651	0.000662	0.000673	0.000684	0.000695
0.7948	0.000670	0.000681	0.000692	0.000704	0.000715	0.000727	0.000739
0.8974	0.000716	0.000728	0.000740	0.000752	0.000764	0.000777	0.000790
				$z\ (x_1/\ x_3) = 4.03$			
0.0995	0.000356	0.000403	0.000451	0.000499	0.000548	0.000598	0.000649
0.1999	0.000420	0.000450	0.000480	0.000510	0.000541	0.000573	0.000605
0.3001	0.000505	0.000511	0.000517	0.000523	0.000529	0.000536	0.000542
0.3895	0.000510	0.000517	0.000523	0.000530	0.000537	0.000544	0.000551
0.4977	0.000508	0.000521	0.000534	0.000548	0.000561	0.000575	0.000589
0.5972	0.000539	0.000550	0.000561	0.000572	0.000583	0.000594	0.000606
0.6966	0.000583	0.000590	0.000598	0.000605	0.000612	0.000620	0.000628
0.7968	0.000629	0.000636	0.000643	0.000650	0.000657	0.000664	0.000672
0.9011	0.000684	0.000694	0.000704	0.000714	0.000724	0.000734	0.000745

Table A-16: Thermal Expansion Coefficients (α) of [bmim][BF_4] (1) + MEA (2) + water (3) system.

T/K	293.15	298.15	303.15	313.15	323.15	333.15	343.15	353.15
x_2	α/ K^{-1}							
				z (x_1/ x_3) = 0.08				
0.0998	0.000519	0.000532	0.000546	0.000573	0.000600	0.000628	0.000657	0.000686
0.2000	0.000572	0.000586	0.000600	0.000629	0.000658	0.000689	0.000719	0.000750
0.3002	0.000619	0.000633	0.000647	0.000675	0.000703	0.000733	0.000763	0.000793
0.3999	0.000649	0.000663	0.000677	0.000705	0.000734	0.000764	0.000794	0.000825
0.4841	0.000677	0.000690	0.000702	0.000728	0.000754	0.000780	0.000807	0.000835
0.5997	0.000676	0.000690	0.000705	0.000735	0.000765	0.000796	0.000828	0.000861
0.6871	0.000690	0.000689	0.000700	0.000739	0.000774	0.000809	0.000845	0.000882
0.8004	0.000690	0.000686	0.000704	0.000740	0.000777	0.000815	0.000854	0.000894
0.8885	0.000690	0.000700	0.000704	0.000744	0.000785	0.000826	0.000869	0.000912
				z (x_1/ x_3) = 0.32				
0.1011	0.000573	0.000577	0.000582	0.000590	0.000599	0.000608	0.000617	0.000627
0.2003	0.000599	0.000605	0.000611	0.000623	0.000636	0.000649	0.000662	0.000675
0.3018	0.000624	0.000630	0.000637	0.000650	0.000663	0.000677	0.000691	0.000705
0.3996	0.000632	0.000641	0.000650	0.000667	0.000685	0.000704	0.000722	0.000741
0.4967	0.000642	0.000652	0.000663	0.000684	0.000706	0.000728	0.000751	0.000774
0.6011	0.000653	0.000665	0.000677	0.000701	0.000726	0.000751	0.000776	0.000802
0.6998	0.000657	0.000671	0.000686	0.000715	0.000744	0.000775	0.000805	0.000837
0.7999	0.000658	0.000675	0.000692	0.000726	0.000760	0.000796	0.000832	0.000869
0.9036	0.000660	0.000678	0.000697	0.000734	0.000773	0.000812	0.000852	0.000894
				z (x_1/ x_3) = 5.03				
0.0998	0.000634	0.000632	0.000629	0.000624	0.000618	0.000613	0.000607	0.000602
0.2015	0.000632	0.000631	0.000630	0.000627	0.000624	0.000621	0.000619	0.000616
0.2980	0.000633	0.000633	0.000633	0.000632	0.000632	0.000632	0.000631	0.000631
0.3997	0.000641	0.000642	0.000642	0.000644	0.000645	0.000646	0.000648	0.000649
0.4957	0.000642	0.000645	0.000648	0.000654	0.000660	0.000666	0.000672	0.000678
0.6004	0.000645	0.000651	0.000656	0.000667	0.000678	0.000689	0.000700	0.000712
0.6969	0.000645	0.000654	0.000662	0.000680	0.000697	0.000715	0.000733	0.000752
0.7954	0.000650	0.000661	0.000673	0.000697	0.000721	0.000746	0.000771	0.000797
0.8983	0.000649	0.000665	0.000680	0.000712	0.000744	0.000777	0.000811	0.000845

APPENDIX B

Table B-1: Experimental viscosity (η) of systems involving [bheaa] at temperatures from (303.15 to 343.15) K.

[bheaa] + Water System				[bheaa] + MEA System			
x_1	η/ mPa·s	x_1	η/ mPa·s	x_1	η/ mPa·s	x_1	η/ mPa·s
T=303.15K		T=333.15K		T=303.15K		T=333.15K	
0.0000	2.03	0.0000	1.40	0.0000	15.40	0.0000	4.79
0.0678	2.60	0.0678	2.61	0.0678	33.16	0.0678	9.45
0.0995	6.88	0.0995	4.06	0.0995	46.80	0.0995	14.05
0.1432	14.08	0.1432	6.27	0.1432	59.12	0.1432	14.01
0.2005	22.45	0.2005	9.20	0.2005	84.08	0.2005	16.62
0.3159	43.32	0.3159	14.01	0.3159	133.17	0.3159	25.70
0.4659	94.06	0.4659	22.53	0.4659	207.47	0.4659	38.08
0.6045	160.20	0.6045	31.07	0.6045	288.49	0.6045	47.95
0.7465	232.15	0.7465	40.91	0.7465	346.91	0.7465	52.48
0.8700	300.25	0.8700	49.70	0.8700	365.38	0.8700	54.55
1.0000	366.90	1.0000	58.03	1.0000	380.90	1.0000	58.03
T=313.15K		T=343.15K		T=313.15K		T=343.15K	
0.0000	1.80	0.0000	1.27	0.0000	9.96	0.0000	3.63
0.0678	2.46	0.0678	1.48	0.0678	20.11	0.0678	6.88
0.0995	4.93	0.0995	2.42	0.0995	29.76	0.0995	9.26
0.1432	9.29	0.1432	3.81	0.1432	33.60	0.1432	9.85
0.2005	15.80	0.2005	5.84	0.2005	43.35	0.2005	12.21
0.3159	30.66	0.3159	9.97	0.3159	66.69	0.3159	17.78
0.4659	57.82	0.4659	15.57	0.4659	102.71	0.4659	24.88
0.6045	90.73	0.6045	21.04	0.6045	138.89	0.6045	30.71
0.7465	125.91	0.7465	26.74	0.7465	161.76	0.7465	33.71
0.8700	154.16	0.8700	32.35	0.8700	167.80	0.8700	35.01

1.0000	181.36	1.0000	37.50	1.0000	177.36	1.0000	37.50
T=323.15K		T=353.15K		T=323.15K		T=353.15K	
0.0000	1.62	0.0000	1.14	0.0000	6.65	0.0000	2.82
0.0678	1.84	0.0678	1.27	0.0678	13.49	0.0678	5.38
0.0995	3.76	0.0995	1.98	0.0995	19.38	0.0995	6.54
0.1432	6.70	0.1432	3.03	0.1432	21.05	0.1432	6.98
0.2005	10.73	0.2005	4.45	0.2005	28.76	0.2005	9.26
0.3159	18.70	0.3159	7.24	0.3159	45.68	0.3159	13.19
0.4659	33.07	0.4659	11.09	0.4659	65.54	0.4659	16.52
0.6045	50.67	0.6045	14.83	0.6045	79.98	0.6045	18.20
0.7465	70.15	0.7465	18.54	0.7465	86.84	0.7465	20.23
0.8700	85.09	0.8700	21.83	0.8700	92.43	0.8700	25.08
1.0000	99.57	1.0000	25.27	1.0000	97.57	1.0000	25.27

Table B-2: Experimental viscosity (η) of systems involving [bmim][BF_4] at temperatures from (293.15 to 353.15) K.

[bmim][BF_4] + Water System				[bmim][BF_4] + MEA System			
x_1	η/ mPa·s	x_1	η/ mPa·s	x_1	η/ mPa·s	x_1	η/ mPa·s
T=293.15K		T=323.15K		T=293.15K		T=323.15K	
0.0000	2.32	0.0000	1.62	0.0000	19.15	0.0000	6.65
0.1000	3.00	0.1000	1.89	0.0999	22.95	0.0999	10.82
0.2000	5.26	0.2000	3.07	0.2001	28.35	0.2001	13.12
0.2950	8.03	0.2950	4.88	0.2994	31.48	0.2994	14.63
0.4016	11.76	0.4016	7.37	0.4004	34.54	0.4004	15.89
0.5002	16.72	0.5002	10.19	0.4999	38.01	0.4999	17.14
0.5963	24.37	0.5963	14.25	0.5994	42.43	0.5994	18.85
0.6997	36.50	0.6997	20.64	0.7005	48.74	0.7005	21.74
0.8014	54.83	0.8014	29.39	0.7992	59.05	0.7992	26.38
0.8988	80.95	0.8988	39.38	0.9002	82.65	0.9002	35.30
1.0000	131.59	1.0000	54.91	1.0000	131.59	1.0000	54.91
T=298.15K		T=333.15K		T=298.15K		T=333.15K	
0.0000	2.15	0.0000	1.40	0.0000	17.44	0.0000	4.79
0.1000	2.78	0.1000	1.65	0.0999	20.91	0.0999	8.57
0.2000	4.76	0.2000	2.68	0.2001	25.21	0.2001	9.78
0.2950	7.49	0.2950	4.31	0.2994	27.69	0.2994	11.01
0.4016	11.07	0.4016	6.46	0.4004	30.02	0.4004	12.33
0.5002	15.85	0.5002	8.76	0.4999	32.37	0.4999	13.51
0.5963	22.82	0.5963	12.26	0.5994	36.52	0.5994	14.58
0.6997	33.65	0.6997	17.24	0.7005	42.10	0.7005	16.75
0.8014	48.19	0.8014	24.12	0.7992	51.71	0.7992	20.29
0.8988	69.26	0.8988	31.26	0.9002	71.91	0.9002	26.70
1.0000	111.92	1.0000	41.90	1.0000	111.92	1.0000	41.90

T=303.15K		T=343.15K		T=303.15K		T=343.15K	
0.0000	2.03	0.0000	1.27	0.0000	15.40	0.0000	3.63
0.1000	2.56	0.1000	1.45	0.0999	18.55	0.0999	6.79
0.2000	4.33	0.2000	2.39	0.2001	21.65	0.2001	7.53
0.2950	6.90	0.2950	3.69	0.2994	23.58	0.2994	7.68
0.4016	10.40	0.4016	5.49	0.4004	25.57	0.4004	8.70
0.5002	14.60	0.5002	7.49	0.4999	28.10	0.4999	9.78
0.5963	20.65	0.5963	10.07	0.5994	30.94	0.5994	11.13
0.6997	30.28	0.6997	14.33	0.7005	36.25	0.7005	12.96
0.8014	42.70	0.8014	19.98	0.7992	44.78	0.7992	15.54
0.8988	61.28	0.8988	25.78	0.9002	61.28	0.9002	21.37
1.0000	94.70	1.0000	32.77	1.0000	94.70	1.0000	32.77
T=313.15K		T=353.15K		T=313.15K		T=353.15K	
0.0000	1.80	0.0000	1.14	0.0000	9.96	0.0000	2.82
0.1000	2.24	0.1000	1.30	0.0999	13.96	0.0999	4.95
0.2000	3.51	0.2000	2.08	0.2001	16.40	0.2001	5.43
0.2950	5.70	0.2950	3.23	0.2994	17.82	0.2994	6.06
0.4016	8.64	0.4016	4.70	0.4004	19.67	0.4004	6.95
0.5002	12.06	0.5002	6.46	0.4999	21.53	0.4999	7.92
0.5963	17.33	0.5963	8.64	0.5994	23.83	0.5994	8.90
0.6997	25.04	0.6997	11.82	0.7005	27.56	0.7005	10.64
0.8014	34.92	0.8014	15.77	0.7992	33.53	0.7992	12.87
0.8988	48.35	0.8988	20.30	0.9002	44.97	0.9002	16.79
1.0000	71.00	1.0000	25.72	1.0000	71.00	1.0000	25.72

Table B-3: Fitting Parameters of η vs x_1 (eq. 4.7) and Errors for the Correlation of Viscosity for [bheaa] – water, [bheaa] – MEA, [bmim][BF_4] – water and [bmim][BF_4] – MEA Binary Mixtures.

T/K	A_0	A_1	A_2	A_3	A_4	A_5	A_6	σ
				[bheaa] - Water				
303.15	1.09982	-6.52845	220.488	-704.766	1158.42	-929.266	288.824	0.08623
313.15	1.68757	-38.0953	957.511	-3187.46	6189.69	-5642.68	1894.72	0.15028
323.15	1.50424	-19.0992	698.785	-2568.61	5037.11	-4561.35	1523.24	0.22725
333.15	1.29588	-1.76077	342.115	-1292.98	2366.18	-2007.56	637.819	0.23953
343.15	1.21195	-3.62706	243.241	-646.610	868.014	-552.065	130.351	0.11135
353.15	1.09982	-8.52845	229.488	-761.766	1262.42	-1026.27	321.824	0.08623
				[bheaa] - MEA				
303.15	15.5920	44.3630	2460.29	-16092.6	41557.6	-43124.5	15520.0	0.82019
313.15	9.88707	38.3316	1400.05	-9476.67	24308.7	-25296.5	9193.61	0.35033
323.15	6.36067	137.339	-640.416	958.717	1683.08	-3985.52	1938.30	1.27892
333.15	4.61149	60.8396	94.5116	-1962.96	6345.90	-7305.37	2820.68	0.77778
343.15	3.56299	46.8711	-74.4175	-525.315	2449.58	-3134.00	1271.29	0.30256
353.15	2.70482	83.9966	-784.444	3175.32	-5776.25	4912.58	-1588.51	0.52149
				[bmim][BF4] - Water				
293.15	2.35952	-28.2692	511.840	-2187.85	4576.35	-4387.33	1647.42	0.23510
298.15	2.20075	-25.2649	451.387	-1920.87	4084.15	-3984.39	1501.67	0.20351
303.15	2.05435	-20.6690	355.550	-1471.06	3121.76	-3039.11	1151.16	0.14925
313.15	1.82644	-13.4012	224.502	-839.203	1663.07	-1530.83	554.020	0.12789
323.15	1.64991	-13.7634	214.870	-782.314	1448.38	-1250.91	417.966	0.16363
333.15	1.42721	-12.7328	215.384	-771.931	1400.28	-1172.08	375.514	0.15298
343.15	1.28246	-8.67536	120.101	-352.465	523.926	-316.248	62.8222	0.10085
353.15	1.14822	-4.67589	76.7858	-206.443	298.754	-187.691	42.8435	0.01996
				[bmim][BF4] - MEA				
293.15	19.1020	22.0315	319.748	-1627.09	3518.27	-3564.63	1458.21	0.23157
298.15	17.4044	22.2351	241.535	-1267.76	2715.79	-2711.20	1089.95	0.17224
303.15	15.3975	27.9666	127.135	-867.674	2023.93	-2131.37	881.599	0.11415
313.15	9.97439	44.0361	-28.2286	-368.180	1258.33	-1552.89	701.603	0.13902
323.15	6.66575	48.1410	-78.9210	-141.835	793.368	-1085.19	512.665	0.09521
333.15	4.82582	51.8769	-185.371	345.503	-206.512	-130.776	160.309	0.19702
343.15	3.62722	58.1463	-359.086	1072.55	-1500.32	947.114	-189.483	0.06798
353.15	2.84623	31.2618	-142.852	326.065	-279.102	5.6971	86.7814	0.11919

Table B-4: Fitting Parameters of A_n (Table B-3) vs T (eq. 4.8) and Errors for the Correlation of Viscosity for [bheaa] – water, [bheaa] – MEA, [bmim][BF_4] – water and [bmim][BF_4] – MEA Binary Mixtures.

	B_0	B_1	B_2	B_3	B_4	B_5	σ
				[bheaa] - Water			
A_0	-1412.24	12.7910	-0.03850	3.85E-05	-	-	0.07640
A_1	1.7E+6	-21038.3	94.8905	-0.18999	0.00014	-	0.02697
A_2	-27.9E+6	333.9E+3	-1498.94	2.98725	-0.00223	-	0.38448
A_3	63.3E+6	-749.4E+3	3322.79	-6.53830	0.00482	-	0.14081
A_4	-110.9E+6	1.3E+6	-5751.51	11.2385	-0.00822	-	0.08734
A_5	99.3E+6	-1.2E+6	5120.34	-9.97520	0.00727	-	0.34470
A_6	-32.8E+6	384.2E+3	-1683.87	3.27277	-0.00238	-	0.01734
				[bheaa] - MEA			
A_0	-388.3E+3	5959.13	-36.4925	0.11149	-0.00017	1.03E-07	1.90E-10
A_1	248.0E+6	-3.8E+6	22923.8	-69.6024	0.10558	-6.4E-05	1.56E-07
A_2	-3.7E+9	56.2E+6	-341.7E+3	1038.31	-1.57629	0.00096	1.62E-06
A_3	17.6E+9	-267.4E+6	1.6E+6	-4946.18	7.51127	-0.00456	9.59E-06
A_4	-34.8E+9	530.3E+6	-3.2E+6	9813.89	-14.9067	0.00905	2.50E-05
A_5	30.8E+9	-468.5E+6	2.9E+6	-8671.89	13.1735	-0.00800	1.56E-05
A_6	-10.0E+9	152.9E+6	-930771	2830.44	-4.29985	0.00261	6.81E-06
				[bmim][BF4] - Water			
A_0	9737.35	-147.433	0.89256	-0.00270	4.08E-06	-2.5E-09	0.00991
A_1	3.0E+6	-47356.1	294.553	-0.91469	0.00142	-8.8E-07	0.32802
A_2	-65.9E+6	1.0E+6	-6403.08	19.9107	-0.03091	1.92E-05	0.44956
A_3	310.6E+6	-4.8E+6	30151.5	-93.7358	0.14550	-9E-05	0.72921
A_4	-692.1E+6	10.8E+6	-67039.4	208.214	-0.32291	0.00020	0.22948
A_5	709.9E+6	-11.0E+6	68672.6	-213.159	0.33040	-0.00020	0.98985
A_6	-265.8E+6	4.1E+6	-25686.4	79.6928	-0.12347	7.64E-05	1.66882
				[bmim][BF4] - MEA			
A_0	-563.4E+3	8614.83	-52.5998	0.16034	-0.00024	1.48E-07	0.12261
A_1	9.4E+6	-146.1E+3	911.445	-2.84078	0.00442	-2.8E-06	0.49413
A_2	-95.9E+6	1.5E+6	-9478.50	29.7471	-0.04663	2.92E-05	0.77720
A_3	300.0E+6	-4.7E+6	29895.8	-94.2083	0.14826	-9.3E-05	0.44990
A_4	-387.2E+6	6.2E+6	-39180.7	124.362	-0.19708	0.00012	1.41147
A_5	194.5E+6	-3.2E+6	20393.4	-65.7972	0.10590	-6.8E-05	0.06866
A_6	-15.1E+6	281.8E+3	-2039.74	7.22819	-0.01260	8.67E-06	0.85134

Table B-5: Experimental Viscosity (η) of [bheaa] + MEA + Water System at temperatures from (303.15 to 343.15) K.

x_1	x_2	$T = 303.15$	$T = 313.15$	$T = 323.15$	$T = 333.15$	$T = 343.15$
				$z\,(x_1/x_3) = 0.11$		
0.0892	0.1003	16.80	6.87	3.56	2.24	1.91
0.0790	0.1999	16.82	7.00	4.01	2.30	2.00
0.0694	0.3002	22.70	11.31	6.42	3.80	2.95
0.0594	0.3999	31.55	18.52	11.27	7.49	5.52
0.0495	0.4997	41.09	26.90	17.79	12.45	9.34
0.0396	0.5997	49.50	34.70	25.10	17.88	13.66
0.0299	0.7000	55.50	40.69	31.70	22.80	17.61
0.0199	0.7994	58.10	43.97	36.14	26.01	20.17
0.0099	0.9007	57.20	43.94	36.43	26.14	20.14
				$z\,(x_1/x_3) = 0.62$		
0.3439	0.0998	325.40	188.20	124.73	94.05	75.90
0.3064	0.2001	302.40	174.30	115.90	87.10	70.50
0.2680	0.3000	255.60	149.20	100.60	75.80	61.53
0.2297	0.4001	202.25	121.11	84.01	63.87	52.20
0.1915	0.4993	154.40	96.19	69.20	53.80	44.97
0.1531	0.5999	117.40	77.10	57.55	46.58	40.01
0.1149	0.6998	92.86	64.05	49.40	41.90	37.12
0.0760	0.7948	76.60	55.18	43.60	38.43	34.77
0.0381	0.8974	56.40	44.12	37.00	32.90	29.83
				$z\,(x_1/x_3) = 4.03$		
0.7208	0.0995	884.00	509.00	301.30	184.60	110.50
0.6405	0.1999	570.50	323.02	192.83	119.53	76.70
0.5610	0.3001	398.46	229.50	137.40	85.80	58.86
0.4681	0.3895	317.63	189.75	113.80	71.60	50.80
0.3989	0.4977	265.53	164.79	100.90	63.90	45.80
0.3191	0.5972	231.50	144.80	92.00	59.43	42.30
0.2392	0.6966	194.74	119.54	80.90	54.01	38.15
0.1594	0.7968	152.50	92.44	67.70	47.40	33.70
0.0803	0.9011	115.90	78.90	58.01	42.50	30.76

Table B-6: Experimental Viscosity (η) of [bmim][BF_4] + MEA + Water System at temperatures from (293.15 to 353.15) K.

T/K		293.15	298.15	303.15	313.15	323.15	333.15	343.15	353.15
x_1	x_2								
					$z\ (x_1/x_3) = 0.08$				
0.0664	0.0998	4.15	3.71	3.36	2.73	2.44	2.03	1.78	1.51
0.0592	0.2000	7.07	6.48	5.70	4.28	3.42	2.68	2.26	1.98
0.0523	0.3002	10.49	9.71	8.35	6.20	4.82	3.85	3.24	2.74
0.0444	0.3999	14.13	13.00	11.22	8.29	6.35	4.97	4.13	3.55
0.0359	0.4841	17.35	15.63	13.59	10.06	7.67	6.20	5.06	4.20
0.0296	0.5997	21.34	18.85	16.62	12.28	9.33	7.49	6.13	5.15
0.0218	0.6871	23.75	20.81	18.52	13.63	10.33	8.25	6.72	5.59
0.0148	0.8004	25.88	22.94	20.33	14.76	11.12	8.83	7.21	5.87
0.0079	0.8885	26.31	23.88	21.07	15.04	11.18	8.84	7.23	5.83
					$z\ (x_1/x_3) = 0.32$				
0.2155	0.1011	10.70	9.33	7.24	5.07	4.89	3.86	3.25	2.81
0.1943	0.2003	10.91	10.20	8.77	6.02	5.36	4.23	3.61	3.09
0.1701	0.3018	13.58	12.83	11.18	8.11	6.22	5.01	4.26	3.59
0.1453	0.3996	17.41	16.24	13.94	10.08	7.40	5.94	4.98	3.99
0.1206	0.4967	21.55	19.62	16.75	12.12	8.82	6.91	5.53	4.38
0.0972	0.6011	25.55	22.89	19.50	14.18	10.49	7.93	6.07	4.77
0.0729	0.6998	28.09	24.92	21.42	15.74	11.88	8.73	6.46	5.11
0.0486	0.7999	28.95	25.66	22.36	16.35	12.59	9.50	6.90	5.45
0.0245	0.9036	27.46	24.71	21.66	15.64	11.92	9.56	7.38	5.82
					$z\ (x_1/x_3) = 5.03$				
0.7478	0.0998	32.88	27.85	25.09	19.99	16.43	13.22	11.16	9.54
0.6677	0.2015	39.52	33.25	29.26	22.98	18.57	14.80	12.54	10.19
0.5679	0.2980	41.69	35.05	30.31	23.63	18.84	15.06	12.55	10.06
0.5009	0.3997	40.67	34.12	29.35	22.50	17.71	14.25	11.69	9.24
0.4122	0.4957	37.71	31.59	27.01	20.35	15.90	12.73	10.32	8.11
0.3346	0.6004	33.33	27.85	23.77	17.67	13.61	10.75	8.66	6.82
0.2496	0.6969	29.00	24.28	20.74	15.19	11.55	8.83	7.21	5.67
0.1660	0.7954	24.94	21.17	18.32	13.33	9.90	7.40	6.12	4.84
0.0829	0.8983	21.46	19.12	17.11	12.36	8.87	6.83	5.43	4.41

Table B-7: Fitting Parameters of η vs x_1 (eq. 4.9) and Errors for the Correlation of Viscosity for [bheaa] + MEA + water system at temperatures from (303.15 to 343.15) K.

T/K	A_0	A_1	A_2	A_3	A_4	σ
			$z\ (x_1/\ x_3) = 0.11$			
303.15	26.0160	-150.545	651.573	-686.085	211.961	0.01486
313.15	13.7991	-110.418	458.077	-418.142	96.4531	0.08791
323.15	5.42671	-27.0527	76.2966	133.951	-158.672	0.07004
333.15	4.42885	-30.3737	84.6072	69.7973	-107.267	0.09247
343.15	3.07167	-14.1491	19.0127	129.405	-121.863	0.08877
			$z\ (x_1/\ x_3) = 0.62$			
303.15	301.818	558.244	-3718.78	5169.92	-2294.12	0.01993
313.15	179.466	244.714	-1820.02	2569.77	-1150.91	0.04536
323.15	121.424	119.148	-991.540	1399.82	-623.716	0.06642
333.15	91.5978	91.8144	-785.140	1178.22	-555.557	0.02318
343.15	73.4139	82.8100	-678.169	1053.77	-513.960	0.05197
			$z\ (x_1/\ x_3) = 4.03$			
303.15	1403.95	-6538.59	14635.35	-15074.11	5687.11	0.03446
313.15	836.638	-4212.03	10338.81	-11558.07	4701.18	0.03848
323.15	488.632	-2389.17	5667.00	-6061.74	2360.04	0.07274
333.15	295.877	-1413.54	3295.86	-3456.41	1324.35	0.01896
343.15	168.192	-733.001	1715.73	-1840.99	723.389	0.02550

Table B-8: Fitting Parameters of η vs x_1 (eq. 4.9) and Errors for the Correlation of Viscosity for [bmim][BF_4] + MEA + Water System at temperatures from (293.15 to 353.15)K.

T/K	A_0	A_1	A_2	A_3	A_4	σ
			$z\,(x_1/x_3) = 0.08$			
293.1500	2.30332	13.0879	62.9011	-53.1135	-	0.04024
298.1500	1.09133	23.1663	27.1182	-27.4202	-	0.07121
303.1500	1.58730	14.3870	37.0470	-32.1589	-	0.01389
313.1500	1.71212	6.85118	36.1494	-30.3775	-	0.00903
323.1500	1.92052	2.00241	33.4557	-26.9897	-	0.01052
333.1500	1.75649	-0.38515	31.4241	-24.8125	-	0.05016
343.1500	1.53885	-0.16648	24.6140	-19.4007	-	0.04267
353.1500	1.29713	0.17431	20.1776	-16.4907	-	0.02956
			$z\,(x_1/x_3) = 0.32$			
293.1500	14.1268	-56.5345	246.782	-232.915	52.1442	0.00899
298.1500	11.1339	-34.9545	187.790	-191.458	49.6267	0.02080
303.1500	6.78361	-2.21397	71.0732	-49.1331	-7.34310	0.01386
313.1500	4.65456	-1.12940	50.1163	-29.8926	-10.2623	0.08687
323.1500	4.47520	4.52228	-11.2333	67.6626	-56.0802	0.01551
333.1500	3.77351	-1.37578	21.4199	-9.56758	-5.06101	0.04849
343.1500	3.33687	-4.39115	39.6264	-57.3657	26.9864	0.02322
353.1500	2.64603	0.21728	14.8586	-21.6439	10.2295	0.02012
			$z\,(x_1/x_3) = 5.03$			
293.1500	20.3942	159.520	-372.689	277.168	-65.1067	0.02674
298.1500	17.8116	127.322	-287.154	187.357	-26.3391	0.02611
303.1500	17.2716	99.8978	-229.152	141.472	-11.5718	0.01751
313.1500	13.7810	80.7183	-200.482	141.355	-22.4344	0.03205
323.1500	11.7026	62.5567	-165.011	125.862	-26.2649	0.01477
333.1500	10.1011	39.5531	-86.1617	25.0977	19.2523	0.01771
343.1500	7.93155	43.3548	-120.047	96.3415	-22.1202	0.01579
353.1500	7.69332	25.2243	-73.2532	52.3388	-7.31736	0.01873

APPENDIX C

Table C-1: Experimental refractive index (n_D) of systems involving [Bheaa] at temperatures from (303.15 to 353.15) K.

[bheaa] + Water System				[bheaa] + MEA System			
x_1	n_D	x_1	n_D	x_1	n_D	x_1	n_D
T=303.15K		T=333.15K		T=303.15K		T=333.15K	
0.0000	1.33549	0.0000	1.33085	0.0000	1.45273	0.0000	1.44213
0.0678	1.39268	0.0678	1.38915	0.1000	1.46110	0.1000	1.45173
0.0995	1.40982	0.0995	1.40621	0.2028	1.46665	0.2028	1.45790
0.1432	1.42642	0.1432	1.42239	0.3000	1.47035	0.3000	1.46198
0.2005	1.44024	0.2005	1.43543	0.4000	1.47330	0.4000	1.46517
0.3159	1.45504	0.3159	1.44913	0.5000	1.47577	0.5000	1.46783
0.4659	1.46635	0.4659	1.46025	0.5998	1.47763	0.5998	1.46984
0.6045	1.47266	0.6045	1.46694	0.7001	1.47881	0.7001	1.47134
0.7465	1.47570	0.7465	1.46994	0.8004	1.47954	0.8004	1.47245
0.8700	1.47796	0.8700	1.47212	0.9000	1.48015	0.9000	1.47298
1.0000	1.48008	1.0000	1.47313	1.0000	1.48008	1.0000	1.47313
T=313.15K		T=343.15K		T=313.15K		T=343.15K	
0.0000	1.33422	0.0000	1.32881	0.0000	1.44913	0.0000	1.43851
0.0678	1.39150	0.0678	1.38854	0.1000	1.45810	0.1000	1.44812
0.0995	1.40860	0.0995	1.40560	0.2028	1.46377	0.2028	1.45489
0.1432	1.42508	0.1432	1.42149	0.3000	1.46755	0.3000	1.45905
0.2005	1.43871	0.2005	1.43387	0.4000	1.47060	0.4000	1.46244
0.3159	1.45315	0.3159	1.44725	0.5000	1.47306	0.5000	1.46517
0.4659	1.46424	0.4659	1.45849	0.5998	1.47497	0.5998	1.46735
0.6045	1.47093	0.6045	1.46494	0.7001	1.47631	0.7001	1.46888
0.7465	1.47393	0.7465	1.46778	0.8004	1.47715	0.8004	1.46991
0.8700	1.47596	0.8700	1.47014	0.9000	1.47771	0.9000	1.47060

1.0000	1.47793	1.0000	1.47086	1.0000	1.47793	1.0000	1.47086
T=323.15K		T=353.15K		T=323.15K		T=353.15K	
0.0000	1.33264	0.0000	1.32665	0.0000	1.44561	0.0000	1.43472
0.0678	1.39023	0.0678	1.38714	0.1000	1.45476	0.1000	1.44482
0.0995	1.40735	0.0995	1.40440	0.2028	1.46089	0.2028	1.45199
0.1432	1.42378	0.1432	1.42032	0.3000	1.46485	0.3000	1.45630
0.2005	1.43695	0.2005	1.43225	0.4000	1.46788	0.4000	1.45984
0.3159	1.45115	0.3159	1.44527	0.5000	1.47053	0.5000	1.46263
0.4659	1.46234	0.4659	1.45627	0.5998	1.47240	0.5998	1.46495
0.6045	1.46899	0.6045	1.46292	0.7001	1.47388	0.7001	1.46653
0.7465	1.47186	0.7465	1.46579	0.8004	1.47485	0.8004	1.46764
0.8700	1.47398	0.8700	1.46797	0.9000	1.47534	0.9000	1.46829
1.0000	1.47575	1.0000	1.46849	1.0000	1.47575	1.0000	1.46849

Table C-2: Experimental refractive index (n_D) of systems involving [bmim][BF_4] at temperatures from (293.15 to 353.15) K.

[bmim][BF_4] + Water System				[bmim][BF_4] + MEA System			
x_1	n_D	x_1	n_D	x_1	n_D	x_1	n_D
T=293.15K		T=323.15K		T=293.15K		T=323.15K	
0.0000	1.33693	0.0000	1.33264	0.0000	1.45601	0.0000	1.44561
0.1000	1.38292	0.1000	1.37539	0.0999	1.44991	0.0999	1.43978
0.2000	1.39951	0.2000	1.39191	0.2001	1.44389	0.2001	1.43437
0.2950	1.40771	0.2950	1.39997	0.2994	1.43940	0.2994	1.43020
0.4016	1.41388	0.4016	1.40524	0.4004	1.43589	0.4004	1.42717
0.5002	1.41784	0.5002	1.40933	0.4999	1.43332	0.4999	1.42445
0.5963	1.42062	0.5963	1.41195	0.5994	1.43129	0.5994	1.42292
0.6997	1.42252	0.6997	1.41433	0.7005	1.42954	0.7005	1.42148
0.8014	1.42410	0.8014	1.41642	0.7992	1.42820	0.7992	1.42032
0.8988	1.42608	0.8988	1.41783	0.9002	1.42712	0.9002	1.41932
1.0000	1.42631	1.0000	1.41900	1.0000	1.42631	1.0000	1.41900
T=298.15K		T=333.15K		T=298.15K		T=333.15K	
0.0000	1.33607	0.0000	1.33085	0.0000	1.45432	0.0000	1.44213
0.1000	1.38136	0.1000	1.37300	0.0999	1.44855	0.0999	1.43631
0.2000	1.39778	0.2000	1.38950	0.2001	1.44225	0.2001	1.43077
0.2950	1.40599	0.2950	1.39759	0.2994	1.43802	0.2994	1.42750
0.4016	1.41195	0.4016	1.40285	0.4004	1.43458	0.4004	1.42422
0.5002	1.41581	0.5002	1.40691	0.4999	1.43184	0.4999	1.42184
0.5963	1.41855	0.5963	1.40958	0.5994	1.42990	0.5994	1.42014
0.6997	1.42030	0.6997	1.41200	0.7005	1.42799	0.7005	1.41880
0.8014	1.42199	0.8014	1.41396	0.7992	1.42688	0.7992	1.41775
0.8988	1.42387	0.8988	1.41529	0.9002	1.42585	0.9002	1.41707
1.0000	1.42425	1.0000	1.41656	1.0000	1.42425	1.0000	1.41656
T=303.15K		T=343.15K		T=303.15K		T=343.15K	
0.0000	1.33549	0.0000	1.32891	0.0000	1.45273	0.0000	1.43862

0.1000	1.38017	0.1000	1.37058	0.0999	1.44655	0.0999	1.43291
0.2000	1.39621	0.2000	1.38550	0.2001	1.44075	0.2001	1.42766
0.2950	1.40456	0.2950	1.39336	0.2994	1.43648	0.2994	1.42410
0.4016	1.41044	0.4016	1.39999	0.4004	1.43322	0.4004	1.42130
0.5002	1.41420	0.5002	1.40400	0.4999	1.43027	0.4999	1.41904
0.5963	1.41703	0.5963	1.40693	0.5994	1.42855	0.5994	1.41739
0.6997	1.41934	0.6997	1.40930	0.7005	1.42689	0.7005	1.41605
0.8014	1.42120	0.8014	1.41123	0.7992	1.42559	0.7992	1.41530
0.8988	1.42271	0.8988	1.41244	0.9002	1.42429	0.9002	1.41397
1.0000	1.42369	1.0000	1.41368	1.0000	1.42369	1.0000	1.41368
T=313.15K		T=353.15K		T=313.15K		T=353.15K	
0.0000	1.33422	0.0000	1.32661	0.0000	1.44913	0.0000	1.43472
0.1000	1.37772	0.1000	1.36786	0.0999	1.44309	0.0999	1.42970
0.2000	1.39417	0.2000	1.38301	0.2001	1.43765	0.2001	1.42456
0.2950	1.40199	0.2950	1.39099	0.2994	1.43333	0.2994	1.42104
0.4016	1.40774	0.4016	1.39736	0.4004	1.43025	0.4004	1.41839
0.5002	1.41165	0.5002	1.40138	0.4999	1.42753	0.4999	1.41617
0.5963	1.41448	0.5963	1.40435	0.5994	1.42573	0.5994	1.41490
0.6997	1.41686	0.6997	1.40688	0.7005	1.42416	0.7005	1.41357
0.8014	1.41879	0.8014	1.40884	0.7992	1.42296	0.7992	1.41267
0.8988	1.42017	0.8988	1.41003	0.9002	1.42206	0.9002	1.41202
1.0000	1.42128	1.0000	1.41135	1.0000	1.42128	1.0000	1.41135

Table C-3: Fitting Parameters of n_D vs x_1 (eq. 4.10) and Errors for the Correlation of Refractive Index for [bheaa] – water, [bheaa] – MEA, [bmim][BF_4] – water and [bmim][BF_4] – MEA Binary Mixtures.

T/K	A_0	A_1	A_2	A_3	A_4	A_5	σ
			[bheaa] – Water				
303.15	1.34816	0.63300	-1.02009	0.52402	-	-	0.00737
313.15	1.34711	0.62932	-1.01435	0.52089	-	-	0.00750
323.15	1.34581	0.62753	-1.01311	0.52064	-	-	0.00764
333.15	1.34453	0.62539	-1.01032	0.51887	-	-	0.00792
343.15	1.34325	0.62701	-1.01842	0.52455	-	-	0.00829
353.15	1.34159	0.62845	-1.02421	0.52834	-	-	0.00858
			[bheaa] – MEA				
303.15	1.45438	0.06187	-0.03703	-	-	-	0.00088
313.15	1.45103	0.06370	-0.03780	-	-	-	0.00100
323.15	1.44617	0.08827	-0.09713	0.03873	-	-	0.00042
333.15	1.44279	0.09038	-0.09820	0.03854	-	-	0.00049
343.15	1.43906	0.09413	-0.10220	0.04022	-	-	0.00044
353.15	1.43532	0.09890	-0.10761	0.04228	-	-	0.00048
			[bmim][BF4] - Water				
293.15	1.33743	0.61486	-2.14469	3.86016	-3.34857	1.10711	0.00100
298.15	1.33654	0.61219	-2.14469	3.87003	-3.75965	1.11068	0.00093
303.15	1.33593	0.60620	-2.13056	3.57669	-2.85820	1.11297	0.00090
313.15	1.33459	0.59156	-2.07120	3.74717	-3.66139	1.08083	0.00076
323.15	1.33299	0.58099	-2.02747	3.46699	-2.89540	1.06113	0.00071
333.15	1.33122	0.57218	-2.00781	3.66546	-3.42224	1.07799	0.00074
343.15	1.32921	0.56495	-1.98725	3.64921	-3.22750	1.08552	0.00078
353.15	1.32708	0.55632	-1.95300	3.59251	-3.18248	1.07118	0.00085
			[bmim][BF4] - MEA				
293.15	1.45485	-0.05849	0.03051	-	-	-	0.00066
298.15	1.45325	-0.05776	0.03018	-	-	-	0.00063
303.15	1.45173	-0.05708	0.02989	-	-	-	0.00063

313.15	1.44822	-0.05583	0.02973	-	-	-	0.00060
323.15	1.44475	-0.05433	0.02932	-	-	-	0.00060
333.15	1.44135	-0.05312	0.02906	-	-	-	0.00059
343.15	1.43778	-0.05172	0.02872	-	-	-	0.00059
353.15	1.43403	-0.05012	0.02836	-	-	-	0.00060

Table C-4: Fitting Parameters of A_n (Table B-3) vs T(eq. 4.11) and Errors for the Correlation of Refractive Index for [bheaa] – water, [bheaa] – MEA, [bmim][BF_4] – water and [bmim][BF_4] – MEA Binary Mixtures.

	B_0	B_1	B_2	B_3	σ
			[bheaa] - Water		
A_0	1.33195	2.1153E-04	-5.2137E-07	-	6.0284E-05
A_1	1.41056	-4.6882E-03	7.0047E-06	-	4.3625E-04
A_2	-2.81094	1.1051E-02	-1.6969E-05	-	1.3883E-03
A_3	1.61258	-6.7479E-03	1.0416E-05	-	9.9006E-04
			[bheaa] – MEA		
A_0	1.33195	2.1153E-04	-5.2137E-07	-	6.0284E-05
A_1	1.41056	-4.6882E-03	7.0047E-06	-	4.3625E-04
A_2	-2.81094	1.1051E-02	-1.6969E-05	-	1.3883E-03
A_3	1.61258	-6.7479E-03	1.0416E-05	-	9.9006E-04
			[bmim][BF4] – Water		
A_0	1.29856	3.8269E-04	-8.5483E-07	-	8.4104E-05
A_1	1.46228	-4.4417E-03	5.3153E-06	-	1.4312E-03
A_2	11.1776	-0.13627	4.5219E-04	-4.8603E-07	9.8578E-03
A_3	235.108	-2.09855	6.3341E-03	-6.3657E-06	9.4172E-02
A_4	-177.352	1.59004	-4.8391E-03	4.9077E-06	1.6825E-02
A_5	7.48951	-0.05149	1.3617E-04	-1.1831E-07	9.5626E-03
			[bmim][BF4] – MEA		
A_0	1.55664	-3.4654E-04	-	-	1.5302E-04
A_1	-0.09871	1.3719E-04	-	-	8.6544E-05
A_2	0.04020	-3.3538E-05	-	-	8.1015E-05

Table C-5: Experimental Refractive Index (n_D) of [bheaa] + MEA + Water System at temperatures from (293.15 to 343.15) K

T/ K		293.15	303.15	313.15	323.15	333.15	343.15	353.15
x_1	x_2							
		z (x_1/ x_3) = 0.11						
0.0892	0.1003	1.42250	1.42031	1.41817	1.41581	1.41320	1.41036	1.40753
0.0790	0.1999	1.43017	1.42776	1.42538	1.42271	1.42001	1.41711	1.41407
0.0694	0.3002	1.43642	1.43398	1.43135	1.42849	1.42562	1.42245	1.41935
0.0594	0.3999	1.44165	1.43903	1.43615	1.43319	1.42996	1.42670	1.42334
0.0495	0.4997	1.44552	1.44254	1.43950	1.43635	1.43297	1.42956	1.42605
0.0396	0.5997	1.44892	1.44586	1.44261	1.43930	1.43574	1.43214	1.42842
0.0299	0.7000	1.45142	1.44847	1.44492	1.44140	1.43771	1.43396	1.43012
0.0199	0.7994	1.45372	1.45038	1.44671	1.44295	1.43918	1.43526	1.43118
0.0099	0.9007	1.45472	1.45152	1.44752	1.44381	1.43979	1.43579	1.43155
		z (x_1/ x_3) = 0.62						
0.3439	0.0998	1.46455	1.46239	1.46011	1.45778	1.45543	1.45341	1.45096
0.3064	0.2001	1.46447	1.46221	1.45983	1.45752	1.45499	1.45242	1.44974
0.2680	0.3000	1.46409	1.46179	1.45941	1.45698	1.45431	1.45164	1.44887
0.2297	0.4001	1.46372	1.46129	1.45872	1.45616	1.45337	1.45054	1.44763
0.1915	0.4993	1.46323	1.46049	1.45768	1.45477	1.45183	1.44873	1.44565
0.1531	0.5999	1.46247	1.45968	1.45662	1.45368	1.45065	1.44854	1.44531
0.1149	0.6998	1.46146	1.45837	1.45537	1.45265	1.44946	1.44655	1.44331
0.0760	0.7948	1.46012	1.45722	1.45386	1.45052	1.44722	1.44375	1.44017
0.0381	0.8974	1.45860	1.45524	1.45171	1.44822	1.44473	1.44116	1.43746
		z (x_1/ x_3) = 4.03						
0.7208	0.0995	1.47949	1.47940	1.47751	1.47572	1.47352	1.47152	1.46938
0.6405	0.1999	1.47842	1.47935	1.47743	1.47554	1.47322	1.47110	1.46872
0.5610	0.3001	1.47717	1.47770	1.47559	1.47354	1.47118	1.46886	1.46636
0.4681	0.3895	1.47594	1.47338	1.47117	1.46900	1.46651	1.46414	1.46154
0.3989	0.4977	1.47436	1.47287	1.47049	1.46805	1.46543	1.46289	1.46014
0.3191	0.5972	1.47248	1.46988	1.46734	1.46475	1.46201	1.45932	1.45643
0.2392	0.6966	1.47014	1.46730	1.46463	1.46199	1.45912	1.45629	1.45328
0.1594	0.7968	1.46713	1.46369	1.46092	1.45816	1.45519	1.45222	1.44909
0.0803	0.9011	1.46311	1.45972	1.45677	1.45379	1.45075	1.44765	1.44430

Table C-6: Experimental Refractive Index (n_D) of [bmim][BF_4] + MEA + Water System at temperatures from (303.15 to 343.15) K.

T/K		293.15	298.15	303.15	313.15	323.15	333.15	343.15	353.15
x_1	x_2								
					$z\,(x_1/x_3) = 0.08$				
0.0664	0.0998	1.39162	1.39036	1.38932	1.38734	1.38517	1.38288	1.38030	1.37770
0.0592	0.2000	1.40548	1.40427	1.40315	1.40105	1.39875	1.39635	1.39366	1.39088
0.0523	0.3002	1.41684	1.41548	1.41432	1.41200	1.40954	1.40694	1.40406	1.40115
0.0444	0.3999	1.42685	1.42538	1.42415	1.42160	1.41888	1.41603	1.41300	1.40988
0.0359	0.4841	1.43375	1.43211	1.43071	1.42786	1.42495	1.42198	1.41881	1.41545
0.0296	0.5997	1.44134	1.43959	1.43813	1.43501	1.43179	1.42857	1.42516	1.42165
0.0218	0.6871	1.44583	1.44425	1.44263	1.43935	1.43600	1.43264	1.42911	1.42547
0.0148	0.8004	1.45103	1.44958	1.44791	1.44454	1.44108	1.43759	1.43390	1.42999
0.0079	0.8885	1.45401	1.45237	1.45063	1.44715	1.44365	1.44000	1.43617	1.43214
					$z\,(x_1/x_3) = 0.32$				
0.2155	0.1011	1.40748	1.40608	1.40494	1.40284	1.40055	1.39818	1.39553	1.39285
0.1943	0.2003	1.41645	1.41486	1.41362	1.41120	1.40865	1.40598	1.40317	1.40020
0.1701	0.3018	1.42275	1.42116	1.41974	1.41714	1.41441	1.41161	1.40851	1.40537
0.1453	0.3996	1.42816	1.42657	1.42494	1.42213	1.41921	1.41626	1.41304	1.40976
0.1206	0.4967	1.43354	1.43183	1.43022	1.42724	1.42417	1.42113	1.41781	1.41441
0.0972	0.6011	1.43892	1.43710	1.43541	1.43223	1.42893	1.42562	1.42214	1.41855
0.0729	0.6998	1.44380	1.44181	1.44008	1.43666	1.43327	1.42987	1.42628	1.42261
0.0486	0.7999	1.44850	1.44650	1.44477	1.44114	1.43762	1.43411	1.43037	1.42656
0.0245	0.9036	1.45289	1.45095	1.44907	1.44535	1.44180	1.43817	1.43433	1.43045
					$z\,(x_1/x_3) = 5.03$				
0.7478	0.0998	1.42532	1.42397	1.42277	1.42027	1.41783	1.41527	1.41248	1.40976
0.6677	0.2015	1.42790	1.42645	1.42510	1.42240	1.41978	1.41698	1.41400	1.41105
0.5679	0.2980	1.42832	1.42678	1.42535	1.42245	1.41970	1.41682	1.41371	1.41062
0.5009	0.3997	1.43038	1.42881	1.42738	1.42440	1.42150	1.41850	1.41533	1.41214
0.4122	0.4957	1.43180	1.43024	1.42878	1.42575	1.42277	1.41970	1.41647	1.41318
0.3346	0.6004	1.43588	1.43426	1.43276	1.42958	1.42645	1.42326	1.41995	1.41653
0.2496	0.6969	1.43951	1.43785	1.43627	1.43295	1.42973	1.42646	1.42305	1.41953
0.1660	0.7954	1.44425	1.44254	1.44090	1.43750	1.43411	1.43072	1.42723	1.42360
0.0829	0.8983	1.45001	1.44825	1.44660	1.44305	1.43957	1.43611	1.43250	1.42878

Table C-7: Fitting Parameters of n_D vs x_1 (eq. 4.12) and Errors for the Correlation of Refractive Index for [bheaa] + MEA + water system at temperatures from (293.15 to 353.15) K.

T/K	A_0	A_1	A_2	σ
		$z\ (x_1/\ x_3) = 0.11$		
293.15	1.41502	0.08324	-0.04376	0.00033
303.15	1.41307	0.08098	-0.04288	0.00036
313.15	1.41115	0.07870	-0.04285	0.00034
323.15	1.40898	0.07635	-0.04223	0.00033
333.15	1.40666	0.07405	-0.04173	0.00036
343.15	1.40401	0.07241	-0.04162	0.00037
353.15	1.40134	0.07082	-0.04180	0.00037
		$z\ (x_1/\ x_3) = 0.62$		
293.15	1.46426	0.00303	-0.01032	0.00010
303.15	1.46223	0.00205	-0.01079	0.00010
313.15	1.46006	0.00130	-0.01166	0.00009
323.15	1.45781	0.00090	-0.01272	0.00020
333.15	1.45558	-0.00048	-0.01270	0.00021
343.15	1.45333	-0.00105	-0.01358	0.00046
353.15	1.45097	-0.00233	-0.01380	0.00049
		$z\ (x_1/\ x_3) = 4.03$		
293.15	1.47944	-0.00091	-0.01861	0.00030
303.15	1.48094	-0.00875	-0.01626	0.00077
313.15	1.47921	-0.00998	-0.01640	0.00077
323.15	1.47762	-0.01165	-0.01623	0.00077
333.15	1.47554	-0.01272	-0.01626	0.00077
343.15	1.47368	-0.01410	-0.01626	0.00076
353.15	1.47164	-0.01555	-0.01621	0.00075

Table C-8: Fitting Parameters of n_D vs x_1 (eq. 4.12) and Errors for the Correlation of Refractive Index for [bmim][BF_4] + MEA + water system at temperatures from (293.15 to 353.15) K.

T/K	A_0	A_1	A_2	σ
		$z\ (x_1/x_3) = 0.08$		
293.15	1.37787	0.15104	-0.07427	0.00049
298.15	1.37686	0.14929	-0.07300	0.00052
303.15	1.37592	0.14849	-0.07314	0.00054
313.15	1.37430	0.14563	-0.07234	0.00061
323.15	1.37247	0.14302	-0.07160	0.00067
333.15	1.37043	0.14091	-0.07128	0.00069
343.15	1.36804	0.13926	-0.07126	0.00071
353.15	1.36564	0.13742	-0.07127	0.00072
		$z\ (x_1/x_3) = 0.32$		
293.15	1.40083	0.07746	-0.02234	0.00058
298.15	1.39950	0.07647	-0.02209	0.00057
303.15	1.39854	0.07469	-0.02116	0.00057
313.15	1.39665	0.07217	-0.02067	0.00055
323.15	1.39463	0.06944	-0.01955	0.00055
333.15	1.39243	0.06730	-0.01892	0.00053
343.15	1.38998	0.06513	-0.01822	0.00053
353.15	1.38750	0.06278	-0.01732	0.00051
		$z\ (x_1/x_3) = 5.03$		
293.15	1.42627	-0.00398	0.03349	0.00059
298.15	1.42496	-0.00464	0.03369	0.00057
303.15	1.42379	-0.00541	0.03395	0.00055
313.15	1.42140	-0.00697	0.03428	0.00053
323.15	1.41909	-0.00848	0.03451	0.00052
333.15	1.41663	-0.00997	0.03495	0.00049
343.15	1.41390	-0.01117	0.03522	0.00047
353.15	1.41131	-0.01288	0.03573	0.00045

APPENDIX D

Table D-1 Calculated excess molar volume (V^E) of systems involving [bheaa] at temperatures from (303.15 to 353.15) K.

[bheaa] + Water System				[bheaa] + MEA System			
x_1	V^E/ cm^3·mol^{-1}	x_1	V^E/ cm^3·mol^{-1}	x_1	V^E/ cm^3·mol^{-1}	x_1	V^E/ cm^3·mol^{-1}
T=303.15K		T=333.15K		T=303.15K		T=333.15K	
0.0000	0.00000	0.0000	0.00000	0.0000	0.00000	0.0000	0.00000
0.0678	-0.50506	0.0678	-0.49922	0.0678	0.00997	0.0678	-0.12442
0.0995	-0.67867	0.0995	-0.66984	0.0995	0.17499	0.0995	0.01464
0.1432	-0.83665	0.1432	-0.82897	0.1432	0.38334	0.1432	0.18167
0.2005	-0.88474	0.2005	-0.88745	0.2005	0.68054	0.2005	0.49071
0.3159	-1.01643	0.3159	-1.04006	0.3159	1.17128	0.3159	1.00015
0.4659	-0.91859	0.4659	-0.98041	0.4659	1.69175	0.4659	1.46211
0.6045	-0.58064	0.6045	-0.55894	0.6045	1.98884	0.6045	1.80195
0.7465	-0.33936	0.7465	-0.30426	0.7465	2.06919	0.7465	1.85691
0.8700	-0.13215	0.8700	-0.13608	0.8700	1.43303	0.8700	1.24117
1.0000	0.00000	1.0000	0.00000	1.0000	0.00000	1.0000	0.00000
T=313.15K		T=343.15K		T=313.15K		T=343.15K	
0.0000	0.00000	0.0000	0.00000	0.0000	0.00000	0.0000	0.00000
0.0678	-0.49957	0.0678	-0.49721	0.0678	-0.02588	0.0678	-0.17487
0.0995	-0.67063	0.0995	-0.67760	0.0995	0.12527	0.0995	-0.04261
0.1432	-0.82496	0.1432	-0.83906	0.1432	0.32036	0.1432	0.11115
0.2005	-0.87714	0.2005	-0.89482	0.2005	0.62267	0.2005	0.42590
0.3159	-1.01380	0.3159	-1.05530	0.3159	1.11886	0.3159	0.94365
0.4659	-0.92925	0.4659	-0.99623	0.4659	1.61671	0.4659	1.38766
0.6045	-0.55832	0.6045	-0.59393	0.6045	1.92979	0.6045	1.74317
0.7465	-0.32318	0.7465	-0.35389	0.7465	2.01033	0.7465	1.78929
0.8700	-0.15153	0.8700	-0.14825	0.8700	1.39644	0.8700	1.18136
1.0000	0.00000	1.0000	0.00000	1.0000	0.00000	1.0000	0.00000
T=323.15K		T=353.15K		T=323.15K		T=353.15K	
0.0000	0.00000	0.0000	0.00000	0.0000	0.00000	0.0000	0.00000
0.0678	-0.49333	0.0678	-0.47896	0.0678	-0.07493	0.0678	-0.22952
0.0995	-0.66317	0.0995	-0.68883	0.0995	0.07209	0.0995	-0.10328
0.1432	-0.82178	0.1432	-0.85479	0.1432	0.25302	0.1432	0.03650
0.2005	-0.87779	0.2005	-0.91460	0.2005	0.55865	0.2005	0.35474
0.3159	-1.02875	0.3159	-1.07848	0.3159	1.06201	0.3159	0.88145
0.4659	-0.95348	0.4659	-1.01901	0.4659	1.54224	0.4659	1.30757
0.6045	-0.54946	0.6045	-0.63384	0.6045	1.86878	0.6045	1.67988
0.7465	-0.35013	0.7465	-0.36946	0.7465	1.93506	0.7465	1.71852
0.8700	-0.14260	0.8700	-0.15317	0.8700	1.35034	0.8700	1.11767
1.0000	0.00000	1.0000	0.00000	1.0000	0.00000	1.0000	0.00000

Table D-2: Calculated excess molar volume (V^E) of systems involving [bmim][BF_4] at temperatures from (293.15 to 353.15) K.

[bmim][BF_4] + Water System				[bmim][BF_4] + MEA System			
x_1	V^E/ $cm^3 \cdot mol^{-1}$	x_1	V^E/ $cm^3 \cdot mol^{-1}$	x_1	V^E/ $cm^3 \cdot mol^{-1}$	x_1	V^E/ $cm^3 \cdot mol^{-1}$
T=293.15K		T=323.15K		T=293.15K		T=323.15K	
0.0000	0.00000	0.0000	0.00000	0.0000	0.00000	0.0000	0.00000
0.1000	0.15621	0.1000	0.31035	0.0999	1.73305	0.0999	1.87202
0.2000	0.27311	0.2000	0.44993	0.2001	2.65560	0.2001	2.86868
0.2950	0.35765	0.2950	0.53014	0.2994	2.93138	0.2994	3.16921
0.4016	0.39435	0.4016	0.53999	0.4004	2.92730	0.4004	3.15372
0.5002	0.39267	0.5002	0.54036	0.4999	2.78837	0.4999	3.04964
0.5963	0.35761	0.5963	0.49652	0.5994	2.45519	0.5994	2.73833
0.6997	0.30080	0.6997	0.41150	0.7005	2.01679	0.7005	2.30605
0.8014	0.19899	0.8014	0.26214	0.7992	1.51373	0.7992	1.76932
0.8988	0.09094	0.8988	0.12107	0.9002	0.81344	0.9002	0.87890
1.0000	0.00000	1.0000	0.00000	1.0000	0.00000	1.0000	0.00000
T=298.15K		T=333.15K		T=298.15K		T=333.15K	
0.0000	0.00000	0.0000	0.00000	0.0000	0.00000	0.0000	0.00000
0.1000	0.18594	0.1000	0.35905	0.0999	1.75658	0.0999	1.91174
0.2000	0.31081	0.2000	0.49240	0.2001	2.69720	0.2001	2.93535
0.2950	0.39758	0.2950	0.57126	0.2994	2.96938	0.2994	3.24106
0.4016	0.43289	0.4016	0.57843	0.4004	2.96516	0.4004	3.22017
0.5002	0.42324	0.5002	0.57554	0.4999	2.84381	0.4999	3.10567
0.5963	0.38422	0.5963	0.53916	0.5994	2.52068	0.5994	2.81403
0.6997	0.32442	0.6997	0.43819	0.7005	2.07198	0.7005	2.39355
0.8014	0.21024	0.8014	0.28163	0.7992	1.57360	0.7992	1.83024
0.8988	0.09690	0.8988	0.13027	0.9002	0.82453	0.9002	0.89917
1.0000	0.00000	1.0000	0.00000	1.0000	0.00000	1.0000	0.00000
T=303.15K		T=343.15K		T=303.15K		T=343.15K	
0.0000	0.00000	0.0000	0.00000	0.0000	0.00000	0.0000	0.00000
0.1000	0.21579	0.1000	0.40362	0.0999	1.78308	0.0999	1.95356
0.2000	0.35839	0.2000	0.53326	0.2001	2.73249	0.2001	3.00493
0.2950	0.43685	0.2950	0.59995	0.2994	3.01041	0.2994	3.30954
0.4016	0.47201	0.4016	0.60921	0.4004	3.00266	0.4004	3.29706
0.5002	0.45300	0.5002	0.60056	0.4999	2.88958	0.4999	3.17159
0.5963	0.40550	0.5963	0.56062	0.5994	2.58481	0.5994	2.89024
0.6997	0.34242	0.6997	0.46729	0.7005	2.14031	0.7005	2.48161
0.8014	0.22044	0.8014	0.30041	0.7992	1.63174	0.7992	1.91822
0.8988	0.10115	0.8988	0.13981	0.9002	0.83509	0.9002	0.91919
1.0000	0.00000	1.0000	0.00000	1.0000	0.00000	1.0000	0.00000

T=313.15K		T=353.15K		T=313.15K		T=353.15K	
0.0000	0.00000	0.0000	0.00000	0.0000	0.00000	0.0000	0.00000
0.1000	0.25479	0.1000	0.43539	0.0999	1.82944	0.0999	1.99797
0.2000	0.40077	0.2000	0.57075	0.2001	2.80170	0.2001	3.07785
0.2950	0.47991	0.2950	0.62836	0.2994	3.09035	0.2994	3.38672
0.4016	0.50220	0.4016	0.64156	0.4004	3.08653	0.4004	3.36001
0.5002	0.49289	0.5002	0.63345	0.4999	2.97436	0.4999	3.23900
0.5963	0.45120	0.5963	0.59478	0.5994	2.66195	0.5994	2.96836
0.6997	0.37144	0.6997	0.49745	0.7005	2.21763	0.7005	2.54613
0.8014	0.24150	0.8014	0.31919	0.7992	1.69427	0.7992	1.99450
0.8988	0.11105	0.8988	0.14920	0.9002	0.85771	0.9002	0.93970
1.0000	0.00000	1.0000	0.00000	1.0000	0.00000	1.0000	0.00000

Table D-3: Estimated Parameter and Standard Deviation of the Redlich Kister Equation for Excess Molar Volume V^E of systems involving [bheaa] for Temperature 303.15 to 353.15 K.

T/K	A_0	A_1	A_2	A_3	A_4	A_5	A_6	σ/cm^3.mol^{-1}
[bheaa] (1) - Water (2) System								
303.15	-3.466	4.786	4.785	-9.972	-25.35	15.33	26.65	0.083
313.15	-3.476	5.167	5.661	-11.63	-28.20	16.52	28.73	0.072
323.15	-3.530	5.686	6.023	-15.57	-31.61	22.08	34.45	0.067
333.15	-3.638	5.703	7.115	-13.59	-32.16	18.69	32.43	0.063
343.15	-3.730	5.548	7.032	-14.25	-33.67	20.36	35.46	0.075
353.15	-3.879	5.346	8.057	-13.11	-38.20	19.18	40.63	0.103
[bheaa] (1) - MEA (2) Systems								
303.15	4.717	9.972	4.727	-0.917	9.389	1.243	-13.61	0.086
313.15	4.481	9.923	4.147	-0.886	10.66	1.296	-14.83	0.066
323.15	4.228	10.00	3.764	-1.878	10.63	2.687	-14.90	0.046
333.15	3.960	9.957	3.091	-1.439	12.79	1.106	-18.98	0.039
343.15	3.710	10.00	2.538	-1.726	13.93	1.281	-20.78	0.038
353.15	3.435	10.04	1.998	-2.023	15.14	1.473	-22.82	0.050

Table D-4: Estimated Parameter and Standard Deviation of the Redlich-Kister Equation for Excess Molar Volume V^E of systems involving [bmim][BF_4] for Temperature 293.15 to 353.15 K.

T/K	A_0	A_1	A_2	A_3	A_4	A_5	σ/cm^3.mol^{-1}
[bmim][BF4](1) - Water(2) Mixtures							
293.15	1.57133	-0.28115	0.23511	0.01286	-0.96193	-0.50393	0.00803
298.15	1.69983	-0.49622	0.09174	0.22626	-0.53251	-0.69022	0.00404
303.15	1.81682	-0.63011	0.27390	0.05356	-0.62385	-0.54485	0.00425
313.15	1.97446	-0.54473	0.37660	-0.88128	-0.52058	0.24987	0.00391
323.15	2.15720	-0.44466	0.32864	-1.63882	-0.02182	0.41812	0.00575
333.15	2.31577	-0.48368	0.37588	-1.89462	0.26600	0.27077	0.00897
343.15	2.41733	-0.47149	0.44232	-1.92028	0.66121	-0.35125	0.00613
353.15	2.55078	-0.40256	0.48158	-2.44576	0.83984	-0.08930	0.00540
[bmim][BF4](1) - MEA (2) Mixtures							
293.15	11.0423	-4.80288	5.21858	-4.29059	-0.28791	2.84596	0.01779
298.15	11.2435	-4.58148	5.63973	-4.67397	-0.89104	2.71976	0.02313
303.15	11.4295	-4.34441	6.26084	-4.84885	-1.81078	2.16076	0.02351
313.15	11.7575	-4.41747	6.63021	-4.39739	-2.23943	1.22822	0.02441
323.15	12.0389	-4.35674	7.50900	-4.17056	-3.42910	0.37319	0.02573
333.15	12.2879	-4.20667	8.45769	-4.67417	-4.74603	0.45488	0.02208
343.15	12.5551	-4.22465	9.50725	-3.63204	-6.14923	-1.50523	0.02426
353.15	12.8138	-4.20301	10.33493	-3.60540	-7.12879	-1.96186	0.02967

Table D-5: Fitting Parameter of A_n (Table D-3) vs T (eq. 4.21) and Errors for the Correlation of Excess Molar Volume V^E of systems involving [bheaa] for Temperature 303.15 to 353.15 K.

	V^E/ cm^3·mol^{-1}					
	B_0	B_1	B_2	B_3	B_4	σ
	[bheaa] + Water system					
A_0	-1576.66	19.0169	-0.08618	0.00017	-1.3125E-07	0.00628
A_1	18236.9	-223.694	1.02704	-0.00209	1.5937E-06	0.03310
A_2	24127.8	-297.651	1.37504	-0.00282	2.1646E-06	0.20670
A_3	-88064.2	1085.315	-5.00557	0.01024	-7.8375E-06	0.83845
A_4	-123782	1537.495	-7.15206	0.01477	-1.1417E-05	0.25355
A_5	127404	-1567.04	7.21543	-0.01474	1.1271E-05	1.38746
A_6	193311	-2394.38	11.1084	-0.02288	1.7646E-05	1.12321
	[bheaa] + MEA system					
A_0	-1090.44	13.3812	-0.06108	0.00012	-9.3750E-08	0.00301
A_1	3793.02	-46.2009	0.21141	-0.00043	3.2708E-07	0.02104
A_2	9033.14	-110.617	0.50804	-0.00104	7.9167E-07	0.03983
A_3	-41234.8	505.811	-2.32392	0.00474	-3.6208E-06	0.21084
A_4	-56674.9	696.103	-3.20235	0.00654	-5.0021E-06	0.30992
A_5	59171.2	-731.566	3.38718	-0.00696	5.3562E-06	0.43680
A_6	59326.7	-738.246	3.43917	-0.00711	5.5000E-06	0.57076

Table D-6: Fitting Parameter of A_n (Table D-4) vs T (eq. 4.21) and Errors for the Correlation of Excess Molar Volume V^E of systems involving [bmim][BF_4] for Temperature 293.15 to 353.15 K

	V^E/ $cm^3 \cdot mol^{-1}$					
	B_0	B_1	B_2	B_3	B_4	σ
	[bmim][BF_4] + Water system					
A_0	-290.434	3.40995	-0.01507	2.9845E-05	-2.2260E-08	0.35403
A_1	7960.11	-97.9047	0.45096	-9.2204E-04	7.0610E-07	0.09977
A_2	2074.93	-25.9611	0.12156	-2.5249E-04	1.9630E-07	0.11054
A_3	-28410.9	352.095	-1.63310	3.3602E-03	-2.5882E-06	1.05342
A_4	-7933.50	99.2480	-0.46508	9.6721E-04	-7.5300E-07	0.64596
A_5	30671.8	-382.484	1.78506	-3.6953E-03	2.8631E-06	0.42367
	[bmim][BF_4] + MEA system					
A_0	-246.425	2.71525	-0.01071	1.8688E-05	-1.1989E-08	0.00388
A_1	-6823.79	83.8868	-0.38661	7.9115E-04	-6.0649E-07	0.05103
A_2	-12262.8	152.466	-0.70986	1.4669E-03	-1.1346E-06	0.07881
A_3	8394.45	-103.362	0.47660	-9.7602E-04	7.4917E-07	0.26107
A_4	20268.6	-252.057	1.17426	-2.4282E-03	1.8797E-06	0.12403
A_5	3232.38	-39.1885	0.17838	-3.6050E-04	2.7237E-07	0.32391

Table D-7: Calculated excess molar volume (V^E) of [bheaa] + MEA + Water System at temperatures from (303.15 to 353.15) K.

T/ K		303.15	313.15	323.15	333.15	343.15	T = 353.15
x_1	x_2						
				$z\ (x_1/\ x_3) = 0.11$			
0.0892	0.1003	-0.63506	-0.63614	-0.63809	-0.6502	-0.66388	-0.68245
0.0790	0.1999	-0.70506	-0.71111	-0.71732	-0.73325	-0.75073	-0.77257
0.0694	0.3002	-0.73287	-0.73991	-0.75164	-0.76997	-0.78987	-0.81347
0.0594	0.3999	-0.71024	-0.71796	-0.73016	-0.74828	-0.76786	-0.79076
0.0495	0.4997	-0.66055	-0.66857	-0.68047	-0.69757	-0.71597	-0.73714
0.0396	0.5997	-0.57156	-0.57899	-0.58985	-0.6052	-0.6217	-0.64011
0.0299	0.7000	-0.469	-0.4756	-0.48529	-0.49837	-0.51277	-0.52874
0.0199	0.7994	-0.31397	-0.31831	-0.3246	-0.33411	-0.34401	-0.35504
0.0099	0.9007	-0.11731	-0.11812	-0.12028	-0.12423	-0.12848	-0.13318
				$z\ (x_1/\ x_3) = 0.62$			
0.3439	0.0998	-0.83038	-0.85072	-0.88135	-0.92351	-0.9654	-1.01498
0.3064	0.2001	-0.77302	-0.80592	-0.8485	-0.90146	-0.95533	-1.01629
0.2680	0.3000	-0.72412	-0.76531	-0.81549	-0.87494	-0.93549	-1.00232
0.2297	0.4001	-0.69037	-0.73439	-0.78656	-0.84696	-0.90886	-0.97656
0.1915	0.4993	-0.61848	-0.66327	-0.71533	-0.77453	-0.83547	-0.90152
0.1531	0.5999	-0.52505	-0.5671	-0.61538	-0.66968	-0.72579	-0.78627
0.1149	0.6998	-0.44734	-0.48213	-0.52185	-0.56637	-0.61251	-0.66245
0.0760	0.7948	-0.34082	-0.3666	-0.39594	-0.42962	-0.46448	-0.50201
0.0381	0.8974	-0.15653	-0.17033	-0.18637	-0.20469	-0.22409	-0.24515
				$z\ (x_1/\ x_3) = 4.03$			
0.7208	0.0995	-0.11556	-0.14759	-0.19216	-0.25628	-0.2848	-0.32271
0.6405	0.1999	-0.24559	-0.30326	-0.37178	-0.45315	-0.51179	-0.56003
0.5610	0.3001	-0.32458	-0.39672	-0.48084	-0.57048	-0.65804	-0.7548
0.4681	0.3895	-0.35802	-0.43754	-0.52276	-0.61608	-0.70896	-0.80998
0.3989	0.4977	-0.34728	-0.4202	-0.50701	-0.59349	-0.67182	-0.77426
0.3191	0.5972	-0.31783	-0.38357	-0.46454	-0.54529	-0.62664	-0.72261
0.2392	0.6966	-0.2941	-0.3483	-0.41776	-0.4946	-0.57255	-0.65634
0.1594	0.7968	-0.26111	-0.29579	-0.3637	-0.42346	-0.48466	-0.55019
0.0803	0.9011	-0.14871	-0.17732	-0.2096	-0.24558	-0.28288	-0.32301

Table D-8: Calculated excess molar volume (V^E) of [bmim][BF_4] + MEA + Water System at temperatures from (293.15 to 353.15) K.

T/ K		293.15	298.15	303.15	313.15	323.15	333.15	343.15	353.15
x_1	x_2								
					$z\ (x_1/x_3) = 0.08$				
0.0664	0.0998	-0.14991	-0.13233	-0.11388	-0.10376	-0.09639	-0.08622	-0.07512	-0.06797
0.0592	0.2000	-0.29523	-0.27875	-0.25213	-0.23529	-0.22178	-0.20396	-0.1856	-0.17046
0.0523	0.3002	-0.42857	-0.41597	-0.38775	-0.36184	-0.3371	-0.31507	-0.29248	-0.27881
0.0444	0.3999	-0.52873	-0.5072	-0.48588	-0.45218	-0.42615	-0.40124	-0.37972	-0.36313
0.0359	0.4841	-0.57112	-0.54915	-0.51549	-0.48003	-0.45867	-0.43606	-0.41792	-0.40032
0.0296	0.5997	-0.53131	-0.51037	-0.48253	-0.45559	-0.4349	-0.41577	-0.39706	-0.3832
0.0218	0.6871	-0.46387	-0.442	-0.41839	-0.39859	-0.37992	-0.36348	-0.34541	-0.33049
0.0148	0.8004	-0.33277	-0.31433	-0.29922	-0.28438	-0.27038	-0.2602	-0.24768	-0.23605
0.0079	0.8885	-0.21522	-0.20587	-0.19315	-0.18426	-0.17042	-0.15777	-0.14504	-0.13784
					$z\ (x_1/x_3) = 0.32$				
0.2155	0.1011	-0.06526	-0.05023	-0.03992	-0.03024	-0.01891	-0.01412	-0.00955	-0.00816
0.1943	0.2003	-0.14549	-0.13424	-0.11861	-0.09743	-0.07975	-0.06423	-0.04792	-0.04175
0.1701	0.3018	-0.23738	-0.22306	-0.20055	-0.17695	-0.15583	-0.13893	-0.12304	-0.11473
0.1453	0.3996	-0.30925	-0.29472	-0.27107	-0.25087	-0.22985	-0.21503	-0.19346	-0.18533
0.1206	0.4967	-0.3577	-0.34483	-0.32073	-0.30659	-0.28231	-0.26639	-0.24511	-0.24021
0.0972	0.6011	-0.3765	-0.36051	-0.34032	-0.32445	-0.30329	-0.28856	-0.26982	-0.2654
0.0729	0.6998	-0.34964	-0.33466	-0.31886	-0.30532	-0.28651	-0.26911	-0.252	-0.24683
0.0486	0.7999	-0.27764	-0.2662	-0.25195	-0.24052	-0.22557	-0.2146	-0.19717	-0.1884
0.0245	0.9036	-0.16662	-0.15758	-0.14746	-0.14071	-0.13242	-0.11922	-0.11231	-0.10491
					$z\ (x_1/x_3) = 5.03$				
0.7478	0.0998	0.201011	0.222029	0.248579	0.277541	0.30411	0.328659	0.351867	0.373608
0.6677	0.2015	0.324109	0.348198	0.363404	0.386687	0.411865	0.431592	0.451857	0.468106
0.5679	0.2980	0.383699	0.404634	0.422192	0.440297	0.46227	0.476665	0.491745	0.506311
0.5009	0.3997	0.389052	0.414	0.435991	0.45123	0.476889	0.492766	0.509349	0.520567
0.4122	0.4957	0.346112	0.378912	0.395117	0.410244	0.428921	0.446927	0.467136	0.484272
0.3346	0.6004	0.278346	0.302222	0.314044	0.331932	0.35085	0.372681	0.3935	0.408042
0.2496	0.6969	0.205898	0.221132	0.233168	0.24963	0.264852	0.28256	0.300897	0.322493
0.1660	0.7954	0.127061	0.138381	0.148821	0.161506	0.177437	0.192102	0.207465	0.226252
0.0829	0.8983	0.052078	0.0588	0.064612	0.071279	0.077057	0.084279	0.090442	0.100431

Table D-9: Estimated Parameters and Standard Deviation of Cibulka Equation for Excess Molar Volume V^E of [bheaa] + MEA + water system for Temperature from (303.15 to 353.15) K

T/ K	303.15	313.15	323.15	333.15	343.15	353.15
	[bheaa] + MEA + water system					
B_0	7.14509	8.33416	9.64876	11.0848	12.4957	14.0505
B_1	7.64875	6.40699	4.96559	2.97320	2.09953	1.25385
B_2	-14.5198	-14.5785	-14.4856	-13.9386	-14.4718	-15.1580
σ	0.19712	0.18378	0.16943	0.15769	0.15061	0.14623

Table D-10: Estimated Parameters and Standard Deviation of Cibulka Equation for Excess Molar Volume V^E of [bmim][BF_4] + MEA + water system for Temperature from (293.15 to 353.15) K.

T/ K	293.15	298.15	303.15	313.15	323.15	333.15	343.15	353.15
	[bmim][BF_4] + MEA + water system							
B_0	-8.85804	-9.03322	-9.17069	-9.32995	-9.64881	-9.73960	-9.93120	-9.85720
B_1	48.1280	48.6023	48.4701	48.6828	48.9008	48.9603	48.8468	49.2473
B_2	-39.2789	-39.5773	-39.3080	-39.3603	-39.2585	-39.2262	-38.9212	-39.3950
σ	0.22485	0.22525	0.22093	0.21697	0.21550	0.21495	0.21465	0.21636

APPENDIX E

Table E-1: Calculated viscosity deviation ($\Delta\eta$) of systems involving [bheaa] at temperatures from (303.15 to 353.15) K.

[bheaa] + Water System				[bheaa] + MEA System			
x_1	$\Delta\eta$	x_1	$\Delta\eta$	x_1	$\Delta\eta$	x_1	$\Delta\eta$
T=303.15K		T=333.15K		T=303.15K		T=333.15K	
0.0000	0.00000	0.0000	0.00000	0.0000	0.00000	0.0000	0.00000
0.0678	-24.14713	0.0678	-2.63000	0.0678	-18.79333	0.0678	-0.66124
0.0995	-31.46726	0.0995	-2.97579	0.0995	-42.73526	0.0995	-1.53474
0.1432	-40.17979	0.1432	-3.23372	0.1432	-65.93130	0.1432	-6.75313
0.2005	-52.74037	0.2005	-3.55722	0.2005	-77.50831	0.2005	-9.46654
0.3159	-73.96432	0.3159	-5.27952	0.3159	-64.96006	0.3159	-5.70069
0.4659	-77.96613	0.4659	-5.25736	0.4659	-27.16975	0.4659	1.36116
0.6045	-62.38928	0.6045	-4.55954	0.6045	17.19283	0.6045	5.88586
0.7465	-42.23764	0.7465	-2.76525	0.7465	38.97398	0.7465	5.08178
0.8700	-19.21915	0.8700	-0.96662	0.8700	21.01400	0.8700	1.84025
1.0000	0.00000	1.0000	0.00000	1.0000	0.00000	1.0000	0.00000
T=313.15K		T=343.15K		T=313.15K		T=343.15K	
0.0000	0.00000	0.0000	0.00000	0.0000	0.00000	0.0000	0.00000
0.0678	-11.50666	0.0678	-2.24673	0.0678	-6.59271	0.0678	-0.13976
0.0995	-14.73792	0.0995	-2.45304	0.0995	-14.15889	0.0995	-1.24694
0.1432	-18.21105	0.1432	-2.64016	0.1432	-26.58203	0.1432	-3.94707
0.2005	-22.00400	0.2005	-2.69516	0.2005	-33.56334	0.2005	-4.96767
0.3159	-27.86162	0.3159	-2.74434	0.3159	-26.95634	0.3159	-2.79082
0.4659	-27.63816	0.4659	-2.58187	0.4659	-7.65895	0.4659	0.92729
0.6045	-19.61170	0.6045	-2.12892	0.6045	11.73099	0.6045	3.36671
0.7465	-9.92102	0.7465	-1.57152	0.7465	17.82690	0.7465	2.96722

0.8700	-3.85649	0.8700	-0.43972	0.8700	7.18036	0.8700	0.89241
1.0000	0.00000	1.0000	0.00000	1.0000	0.00000	1.0000	0.00000
T=323.15K		T=353.15K		T=323.15K		T=353.15K	
0.0000	0.00000	0.0000	0.00000	0.0000	0.00000	0.0000	0.00000
0.0678	-6.41553	0.0678	-1.51291	0.0678	-2.25281	0.0678	0.31066
0.0995	-7.60638	0.0995	-1.56679	0.0995	-5.70773	0.0995	-0.83444
0.1432	-8.94082	0.1432	-1.56704	0.1432	-12.87207	0.1432	-2.57125
0.2005	-10.53034	0.2005	-1.53471	0.2005	-14.24904	0.2005	-2.53729
0.3159	-13.85622	0.3159	-1.52275	0.3159	-6.42794	0.3159	-0.85172
0.4659	-14.18646	0.4659	-1.29359	0.4659	4.35563	0.4659	0.23507
0.6045	-10.15945	0.6045	-0.89086	0.6045	9.67921	0.6045	-0.33871
0.7465	-4.58207	0.7465	-0.60984	0.7465	7.42080	0.7465	-0.55290
0.8700	-1.74677	0.8700	-0.29966	0.8700	3.95406	0.8700	2.05985
1.0000	0.00000	1.0000	0.00000	1.0000	0.00000	1.0000	0.00000

Table E-2: Calculated viscosity deviation ($\Delta\eta$)of systems involving [bmim][BF_4] at temperatures from (293.15 to 353.15) K.

[bmim][BF_4] + Water System				[bmim][BF_4] + MEA System			
x_1	$\Delta\eta$	x_1	$\Delta\eta$	x_1	$\Delta\eta$	x_1	$\Delta\eta$
T=293.15K		T=323.15K		T=293.15K		T=323.15K	
0.0000	0.00000	0.0000	0.00000	0.0000	0.00000	0.0000	0.00000
0.1000	-12.24704	0.1000	-5.05850	0.0999	-7.42813	0.0999	-0.64201
0.2000	-22.90681	0.2000	-9.21093	0.2001	-13.30558	0.2001	-3.18025
0.2950	-32.41751	0.2950	-12.46154	0.2994	-21.33851	0.2994	-6.47115
0.4016	-42.46176	0.4016	-15.65230	0.4004	-29.62947	0.4004	-10.08183
0.5002	-50.25611	0.5002	-18.08641	0.4999	-37.34629	0.4999	-13.63525
0.5963	-55.02736	0.5963	-19.14980	0.5994	-44.11521	0.5994	-16.72451
0.6997	-56.26279	0.6997	-18.26522	0.7005	-49.17178	0.7005	-18.71640
0.8014	-51.09202	0.8014	-14.94243	0.7992	-49.96140	0.7992	-18.84121
0.8988	-37.55410	0.8988	-10.14184	0.9002	-37.72013	0.9002	-14.79644
1.0000	0.00000	1.0000	0.00000	1.0000	0.00000	1.0000	0.00000
T=298.15K		T=333.15K		T=298.15K		T=333.15K	
0.0000	0.00000	0.0000	0.00000	0.0000	0.00000	0.0000	0.00000
0.1000	-10.35206	0.1000	-3.79545	0.0999	-5.96044	0.0999	0.10796
0.2000	-19.34604	0.2000	-6.81551	0.2001	-11.13227	0.2001	-2.48048
0.2950	-27.04308	0.2950	-9.03764	0.2994	-18.04248	0.2994	-4.84666
0.4016	-35.15916	0.4016	-11.20117	0.4004	-25.24516	0.4004	-7.31287
0.5002	-41.21088	0.5002	-12.90239	0.4999	-32.29306	0.4999	-9.82404
0.5963	-44.79293	0.5963	-13.29237	0.5994	-37.55744	0.5994	-12.44888
0.6997	-45.30348	0.6997	-12.49374	0.7005	-41.52268	0.7005	-14.03267
0.8014	-41.93268	0.8014	-9.74148	0.7992	-41.23504	0.7992	-14.16246
0.8988	-31.54609	0.8988	-6.53902	0.9002	-30.59250	0.9002	-11.50244
1.0000	0.00000	1.0000	0.00000	1.0000	0.00000	1.0000	0.00000

T=303.15K		T=343.15K		T=303.15K		T=343.15K	
0.0000	0.00000	0.0000	0.00000	0.0000	0.00000	0.0000	0.00000
0.1000	-8.72883	0.1000	-2.97008	0.0999	-4.76671	0.0999	0.25094
0.2000	-16.22813	0.2000	-5.17690	0.2001	-9.61555	0.2001	-1.93414
0.2950	-22.45812	0.2950	-6.87062	0.2994	-15.57066	0.2994	-4.67676
0.4016	-28.83803	0.4016	-8.42913	0.4004	-21.58390	0.4004	-6.59407
0.5002	-33.77484	0.5002	-9.53777	0.4999	-26.94247	0.4999	-8.41379
0.5963	-36.63506	0.5963	-9.97770	0.5994	-31.99556	0.5994	-9.96401
0.6997	-36.58492	0.6997	-8.97738	0.7005	-34.70069	0.7005	-11.08319
0.8014	-33.59127	0.8014	-6.52926	0.7992	-33.99475	0.7992	-11.37659
0.8988	-24.03258	0.8988	-3.79548	0.9002	-25.50708	0.9002	-8.48645
1.0000	0.00000	1.0000	0.00000	1.0000	0.00000	1.0000	0.00000
T=313.15K		T=353.15K		T=313.15K		T=353.15K	
0.0000	0.00000	0.0000	0.00000	0.0000	0.00000	0.0000	0.00000
0.1000	-6.48224	0.1000	-2.30308	0.0999	-2.09877	0.0999	-0.15746
0.2000	-12.12644	0.2000	-3.97923	0.2001	-5.76991	0.2001	-1.97828
0.2950	-16.50956	0.2950	-5.16684	0.2994	-10.41519	0.2994	-3.61461
0.4016	-20.94673	0.4016	-6.31585	0.4004	-14.73221	0.4004	-5.03827
0.5002	-24.34876	0.5002	-6.97682	0.4999	-18.94228	0.4999	-6.35277
0.5963	-25.72980	0.5963	-7.16367	0.5994	-22.71178	0.5994	-7.65384
0.6997	-25.17775	0.6997	-6.51698	0.7005	-25.16089	0.7005	-8.22362
0.8014	-22.33627	0.8014	-5.07658	0.7992	-25.21039	0.7992	-8.25191
0.8988	-15.63820	0.8988	-2.93852	0.9002	-19.93442	0.9002	-6.64373
1.0000	0.00000	1.0000	0.00000	1.0000	0.00000	1.0000	0.00000

Table E-3: Estimated Parameter and Standard Deviation of the Redlich-Kister Equation for Viscosity Deviation $\Delta\eta$ of systems involving [bheaa] for Temperature from (303.15 to 353.15) K.

T/K	A_0	A_1	A_2	A_3	A_4	A_5	σ
[bheaa] (1) - Water (2) System							
303.15	-298.636	194.868	86.9412	-491.469	17.5568	597.119	0.15006
313.15	-105.425	97.7466	77.4607	-99.9997	-91.8592	107.616	0.04370
323.15	-46.3180	43.5007	55.4182	-48.6709	-67.5161	59.4539	0.08247
333.15	-25.3428	15.3406	20.4943	-48.5866	-14.4013	74.3180	0.15413
343.15	-5.12243	3.07541	-8.82595	-3.74699	9.08886	25.4210	0.01630
353.15	-3.16171	4.39054	-0.21128	-11.6518	-5.62663	20.9758	0.00300
[bheaa] (1) - MEA (2) System							
303.15	-258.681	532.700	1049.777	-188.440	-978.697	-331.757	0.14514
313.15	-103.987	291.736	509.386	-409.250	-534.183	166.268	0.09991
323.15	-33.6393	204.238	191.373	-551.320	-197.785	458.419	0.01359
333.15	-15.8763	136.860	98.3982	-421.159	-95.4909	368.769	0.02012
343.15	-15.2507	62.1359	104.946	-143.015	-119.162	93.5220	0.01843
353.15	-3.41879	36.2488	-43.9906	-175.332	107.830	218.759	0.00525

Table E-4: Estimated Parameter and Standard Deviation of the Redlich Kister Equation for Viscosity Deviation $\Delta\eta$ of systems involving [bmim][BF_4] for Temperature from (293.15 to 353.15) K.

T/K	A_0	A_1	A_2	A_3	A_4	A_5	σ
[bmim][BF_4] (1) - Water (2) System							
293.15	-201.044	-134.9	-50.5774	-5.86173	-102.694	-86.6255	0.10977
298.25	-164.836	-102.562	-37.8664	-12.3306	-100.108	-79.1954	0.01907
303.15	-134.796	-78.2344	-32.2294	-17.2349	-68.7023	-44.4584	0.12401
313.15	-96.7730	-51.4419	-17.0595	10.1327	-33.1176	-36.7618	0.09176
323.15	-72.4228	-38.2678	-0.67480	44.7086	-31.7810	-66.3257	0.05448
333.15	-51.4086	-24.9365	4.43818	46.9298	-18.7877	-53.5746	0.08133
343.15	-38.4191	-17.9628	5.94956	42.9262	-6.70908	-36.5456	0.05054
353.15	-27.9624	-9.40358	-0.11742	11.9711	-2.31112	-5.97732	0.01504
[bmim][BF_4] (1)- MEA (2) System							
293.15	-149.436	-143.047	-100.351	-162.068	-89.9799	87.4137	0.08882
298.25	-128.431	-123.598	-73.6235	-109.921	-69.2761	58.0957	0.10463
303.15	-108.689	-105.437	-57.2356	-58.0110	-53.3784	-9.17508	0.12507
313.15	-76.1690	-80.7097	-41.1516	-37.5865	-43.5496	-42.6220	0.10039
323.15	-54.6518	-68.2584	-31.7781	-25.0584	-33.6462	-37.6553	0.01847
333.15	-39.6697	-54.1323	-28.7048	11.6715	-8.05003	-81.5002	0.04396
343.15	-33.5546	-31.4822	-27.3812	-49.1676	11.2740	4.80891	0.07484
353.15	-25.6399	-26.6852	-15.5855	0.46040	-5.38168	-45.8226	0.03847

Table E-5: Fitting Parameter of A_n (Table E-3) vs T (eq. 4.21) and Errors for the Correlation of Viscosity Deviation $\Delta\eta$ of systems involving [bheaa] for Temperature from (303.15 to 353.15) K.

	$\Delta\eta$					
	B_0	B_1	B_2	B_3	B_4	σ
	[bheaa] + Water system					
A_0	-2.9723E+06	35510.5	-159.085	0.31672	-2.3641E-04	0.10468
A_1	4.1904E+05	-4858.77	21.1954	-0.04122	3.0157E-05	0.03599
A_2	6.8541E+05	-8673.88	41.1068	-0.08643	6.8022E-05	0.13970
A_3	-9.8787E+06	118819	-535.639	1.07260	-8.0499E-04	0.01698
A_4	2.6601E+06	-31444.5	139.148	-0.27322	2.0085E-04	0.09081
A_5	1.2499E+07	-150170	676.180	-1.35234	1.0136E-03	0.46553
	[bheaa] + MEA system					
A_0	-2.9282E+05	2868.28	-10.09605	0.01475	-7.1186E-06	0.30399
A_1	4.7717E+06	-57583.6	260.564	-0.52389	3.9485E-04	0.62643
A_2	-5.3784E+06	68467.4635	-325.228	0.68363	-5.3681E-04	0.03709
A_3	-1.4846E+07	1.8414E+05	-854.999	1.76130	-1.3582E-03	0.46359
A_4	1.1320E+07	-1.4090E+05	656.070	-1.35484	1.0471E-03	0.25107
A_5	1.7032E+07	-2.1238E+05	990.871	-2.05026	1.5875E-03	0.49985

Table E-6: Fitting Parameter of A_n (Table E-4) vs T (eq. 4.21) and Errors for the Correlation of Viscosity Deviation $\Delta\eta$ of systems involving [bmim][BF_4] for Temperature from (293.15 to 353.15) K.

	$\Delta\eta$							
	B_0	B_1	B_2	B_3	B_4	B_5	B_6	σ
	[bmim][BF_4] + Water system							
A_0	6.1376E+07	-1.1524E+06	9003.65	-37.4727	0.08762	-1.0915E-04	5.6589E-08	0.08009
A_1	6.8134E+07	-1.2806E+06	10016.2	-41.7293	0.09767	-1.2179E-04	6.3199E-08	0.11950
A_2	-1.0481E+08	1.9526E+06	-15142.4	62.5738	-0.14532	1.7983E-04	-9.2645E-08	0.03615
A_3	-2.8269E+08	5.2933E+06	-41255.4	171.306	-0.39970	4.9688E-04	-2.5711E-07	0.01960
A_4	3.4184E+08	-6.3401E+06	48950.8	-201.384	0.46561	-5.7362E-04	2.9419E-07	0.12382
A_5	5.9908E+08	-1.1159E+07	86528.4	-357.486	0.82998	-1.0268E-03	5.2875E-07	0.26772
	[bmim][BF_4] + MEA system							
A_0	3.4509E+07	-6.4633E+05	5039.91	-20.9444	0.04892	-6.0910E-05	3.1575E-08	0.18806
A_1	-1.8768E+06	5.3416E+04	-562.244	2.95401	-0.00837	1.2267E-05	-7.3287E-09	0.00688
A_2	-1.5498E+07	2.7665E+05	-2053.74	8.11337	-0.01799	2.1207E-05	-1.0387E-08	0.22078
A_3	8.9797E+08	-1.6909E+07	132550	-553.641	1.29957	-1.6254E-03	8.4630E-07	0.26117
A_4	1.0463E+08	-1.9577E+06	15240.9	-63.1871	0.14714	-1.8247E-04	9.4148E-08	0.19628
A_5	-1.5031E+09	2.8199E+07	-220238	916.592	-2.14393	2.6722E-03	-1.3866E-06	0.72111

Table E-7: Calculated Viscosity Deviation $\Delta\eta$ of [bheaa] + MEA + Water System at temperatures from (303.15 to 343.15) K.

x_1	x_2	T = 303.15	T = 313.15	T = 323.15	T = 333.15	T = 343.15
			$z\ (x_1/\ x_3) = 0.11$			
0.0892	0.1003	-19.0974	-11.7546	-7.29544	-4.54783	-2.82442
0.0790	0.1999	-16.7215	-10.6226	-6.35614	-4.25277	-2.60378
0.0694	0.3002	-8.65061	-5.39477	-3.50005	-2.54416	-1.54019
0.0594	0.3999	2.51939	2.80146	1.83051	1.37523	1.15681
0.0495	0.4997	14.3144	12.1335	8.80644	6.55438	5.09723
0.0396	0.5997	24.9865	20.8887	16.5829	12.2043	9.53811
0.0299	0.7000	33.2195	27.8192	23.6383	17.3395	13.6059
0.0199	0.7994	38.1252	32.0768	28.5544	20.7770	16.2917
0.0099	0.9007	39.5026	33.0076	29.3103	21.1277	16.3829
			$z\ (x_1/\ x_3) = 0.62$			
0.3439	0.0998	196.570	123.844	88.9275	72.8393	61.9366
0.3064	0.2001	185.906	115.856	83.2651	67.6725	57.6577
0.2680	0.3000	151.789	96.8393	71.2262	58.2099	49.8437
0.2297	0.4001	111.073	74.8084	57.8839	48.1095	41.6646
0.1915	0.4993	75.8131	55.9274	46.3112	39.8635	35.5820
0.1531	0.5999	51.4787	42.9113	37.9167	34.4774	31.7755
0.1149	0.6998	39.5646	35.9168	33.0126	31.6260	30.0358
0.0760	0.7948	36.2078	33.2466	30.5400	30.0342	28.8688
0.0381	0.8974	28.4699	28.1572	27.1380	26.3038	25.0600
			$z\ (x_1/\ x_3) = 4.03$			
0.7208	0.0995	617.638	376.964	228.577	142.044	82.8780
0.6405	0.1999	332.101	204.586	127.470	81.1824	51.7510
0.5610	0.3001	187.740	124.528	79.3261	51.6169	36.5559
0.4681	0.3895	139.594	100.721	64.3719	42.3725	31.6492
0.3989	0.4977	111.306	87.3085	57.7087	38.2264	28.9018
0.3191	0.5972	105.059	80.8335	56.1241	37.9380	28.0579
0.2392	0.6966	96.1230	69.1089	52.3506	36.7061	26.5680
0.1594	0.7968	81.6426	55.5114	46.4588	34.2733	24.7711
0.0803	0.9011	72.5330	55.3348	43.9987	33.5032	24.4531

Table E-8: Calculated Viscosity Deviation $\Delta\eta$ of [bmim][BF_4] + MEA + Water System at temperatures from (293.15 to 353.15) K.

T/K		293.15	298.15	303.15	313.15	323.15	333.15	343.15	353.15
x_1	x_2								
					$z\,(x_1/x_3) = 0.08$				
0.0664	0.0998	-8.43523	-7.26181	-5.89156	-4.47977	-3.22539	-2.39598	-1.81771	-1.43451
0.0592	0.2000	-6.26487	-5.22707	-4.24880	-3.24569	-2.35815	-1.79375	-1.34397	-0.95429
0.0523	0.3002	-3.64064	-2.77144	-2.32755	-1.66635	-1.09450	-0.68759	-0.38385	-0.19293
0.0444	0.3999	-0.65434	-0.13479	-0.09115	0.15870	0.35697	0.41971	0.52019	0.64485
0.0359	0.4841	2.24597	2.14087	1.90887	1.82927	1.70627	1.70851	1.51852	1.36235
0.0296	0.5997	5.09878	4.28143	3.94782	3.53895	3.11862	2.86045	2.51217	2.27226
0.0218	0.6871	7.04616	5.76251	5.37287	4.71576	4.09520	3.63698	3.14131	2.75753
0.0148	0.8004	8.17429	6.93014	6.28666	5.40600	4.68912	4.12077	3.58411	3.01981
0.0079	0.8885	8.01848	7.28597	6.46401	5.44742	4.67617	4.11355	3.61436	3.00576
					$z\,(x_1/x_3) = 0.32$				
0.2155	0.1011	-21.1772	-18.0247	-15.2467	-12.4659	-8.72186	-6.61008	-5.04435	-3.80064
0.1943	0.2003	-19.8937	-16.3408	-13.1615	-10.8567	-7.61940	-5.71637	-4.25039	-3.16532
0.1701	0.3018	-15.8056	-12.6066	-9.96418	-7.92118	-5.98051	-4.30039	-3.07848	-2.24099
0.1453	0.3996	-10.4152	-7.96803	-6.31261	-5.03253	-3.96992	-2.69669	-1.80821	-1.39515
0.1206	0.4967	-4.71315	-3.35717	-2.60835	-2.07366	-1.72019	-1.05401	-0.70896	-0.56024
0.0972	0.6011	0.55013	0.88265	0.81738	0.75158	0.67056	0.55908	0.32039	0.22918
0.0729	0.6998	4.57295	4.07464	3.57437	3.18936	2.86064	2.00992	1.24307	1.00143
0.0486	0.7999	6.88458	5.94866	5.32721	4.66174	4.36076	3.42384	2.21079	1.77007
0.0245	0.9036	6.75853	6.05240	5.37539	4.77017	4.44974	4.10694	3.20326	2.55739
					$z\,(x_1/x_3) = 5.03$				
0.7478	0.0998	-67.7788	-57.9078	-44.5740	-34.3678	-25.5414	-18.8040	-13.8995	-10.1508
0.6677	0.2015	-52.5080	-45.2801	-34.6689	-26.6699	-19.6475	-14.3260	-10.2376	-7.70426
0.5679	0.2980	-39.0560	-33.9951	-26.0565	-19.9003	-14.5417	-10.3491	-7.30656	-5.54592
0.5009	0.3997	-33.1242	-29.1222	-22.4338	-17.2203	-12.6112	-8.78903	-6.29705	-4.88736
0.4122	0.4957	-26.2336	-23.3822	-18.1924	-14.0153	-10.1763	-7.04140	-5.10277	-3.99606
0.3346	0.6004	-22.3447	-20.2039	-15.9518	-12.1797	-8.85689	-6.23290	-4.56581	-3.55423
0.2496	0.6969	-17.3206	-15.9259	-12.7418	-9.57012	-6.87590	-5.04001	-3.56876	-2.78358
0.1660	0.7954	-12.2301	-11.3629	-9.06513	-6.44791	-4.56509	-3.41719	-2.25791	-1.71881
0.0829	0.8983	-6.70297	-5.86410	-4.28124	-2.50737	-1.68378	-0.97002	-0.57356	-0.27887

Table E-9: Estimated Parameters and Standard Deviation of Cibulka Equation for Viscosity Deviation $\Delta\eta$ of [bheaa] + MEA + water system for Temperature from (303.15 to 343.15) K

T/ K	303.15	313.15	323.15	333.15	343.15
	[bheaa] + MEA + water system				
B_0	-2746.43	-1736.63	-1142.70	-895.215	-774.798
B_1	19442.5	11512.0	6695.74	4025.23	2333.91
B_2	-16696.2	-9775.61	-5553.49	-3130.81	-1560.47
σ	0.30222	0.28703	0.28591	0.22262	0.19516

Table E-10: Estimated Parameters and Standard Deviation of Cibulka Equation for Viscosity Deviation $\Delta\eta$ of [bmim][BF_4] + MEA + water system for Temperature from (303.15 to 353.15) K.

T/ K	293.15	298.15	303.15	313.15	323.15	333.15	343.15	353.15
	[bmim][BF_4] + MEA + water system							
B_0	889.034	753.826	602.656	487.697	378.530	286.104	215.977	171.530
B_1	-3716.23	-3217.21	-2498.76	-1950.33	-1452.27	-1071.73	-781.957	-590.944
B_2	2827.21	2463.40	1896.11	1462.63	1073.74	785.62	565.979	419.413
σ	0.29766	0.29431	0.23667	0.22851	0.22378	0.19746	0.19574	0.16892

APPENDIX F

Table F-1: Calculated refractive index deviation (Δn_D) of systems involving [bheaa] at temperatures from (303.15 to 353.15) K.

[bheaa] + Water System				[bheaa] + MEA System			
x_1	Δn_D	x_1	Δn_D	x_1	Δn_D	x_1	Δn_D
T=303.15K		T=333.15K		T=303.15K		T=333.15K	
0.0000	0.00000	0.0000	0.00000	0.0000	0.00000	0.0000	0.00000
0.0678	0.04740	0.0678	0.04866	0.0678	0.00564	0.0678	0.00650
0.0995	0.05994	0.0995	0.06120	0.0995	0.00837	0.0995	0.00948
0.1432	0.07023	0.1432	0.07117	0.1432	0.00942	0.1432	0.01055
0.2005	0.07576	0.2005	0.07605	0.2005	0.00963	0.2005	0.01064
0.3159	0.07388	0.3159	0.07334	0.3159	0.00937	0.3159	0.01020
0.4659	0.06349	0.4659	0.06311	0.4659	0.00850	0.4659	0.00912
0.6045	0.04977	0.6045	0.05008	0.6045	0.00693	0.6045	0.00751
0.7465	0.03228	0.7465	0.03288	0.7465	0.00492	0.7465	0.00551
0.8700	0.01668	0.8700	0.01749	0.8700	0.00280	0.8700	0.00295
1.0000	0.00000	1.0000	0.00000	1.0000	0.00000	1.0000	0.00000
T=313.15K		T=343.15K		T=313.15K		T=343.15K	
0.0000	0.00000	0.0000	0.00000	0.0000	0.00000	0.0000	0.00000
0.0678	0.04754	0.0678	0.05010	0.0678	0.00609	0.0678	0.00638
0.0995	0.06007	0.0995	0.06265	0.0995	0.00880	0.0995	0.00982
0.1432	0.07029	0.1432	0.07235	0.1432	0.00978	0.1432	0.01083
0.2005	0.07567	0.2005	0.07658	0.2005	0.00995	0.2005	0.01099
0.3159	0.07354	0.3159	0.07357	0.3159	0.00953	0.3159	0.01049
0.4659	0.06307	0.4659	0.06350	0.4659	0.00856	0.4659	0.00944
0.6045	0.04984	0.6045	0.05026	0.6045	0.00702	0.6045	0.00772
0.7465	0.03244	0.7465	0.03294	0.7465	0.00497	0.7465	0.00550
0.8700	0.01671	0.8700	0.01775	0.8700	0.00266	0.8700	0.00297

1.0000	0.00000	1.0000	0.00000	1.0000	0.00000	1.0000	0.00000
T=323.15K		T=353.15K		T=323.15K		T=353.15K	
0.0000	0.00000	0.0000	0.00000	0.0000	0.00000	0.0000	0.00000
0.0678	0.04790	0.0678	0.05088	0.0678	0.00614	0.0678	0.00672
0.0995	0.06047	0.0995	0.06364	0.0995	0.00917	0.0995	0.01042
0.1432	0.07065	0.1432	0.07337	0.1432	0.01019	0.1432	0.01145
0.2005	0.07561	0.2005	0.07716	0.2005	0.01022	0.2005	0.01161
0.3159	0.07330	0.3159	0.07381	0.3159	0.00985	0.3159	0.01103
0.4659	0.06302	0.4659	0.06354	0.4659	0.00871	0.4659	0.00997
0.6045	0.04984	0.6045	0.05053	0.6045	0.00717	0.6045	0.00817
0.7465	0.03240	0.7465	0.03326	0.7465	0.00512	0.7465	0.00589
0.8700	0.01683	0.8700	0.01792	0.8700	0.00260	0.8700	0.00317
1.0000	0.00000	1.0000	0.00000	1.0000	0.00000	1.0000	0.00000

Table F-2: Calculated refractive index deviation (Δn_D) of systems involving [bmim][BF_4] at temperatures from (293.15 to 353.15) K.

[bmim][BF_4] + Water System				[bmim][BF_4] + MEA System			
x_1	Δn_D	x_1	Δn_D	x_1	Δn_D	x_1	Δn_D
T=293.15K		T=323.15K		T=293.15K		T=323.15K	
0.0000	0.00000	0.0000	0.00000	0.0000	0.00000	0.0000	0.00000
0.1000	0.03689	0.1000	0.03411	0.0999	-0.00427	0.0999	-0.00351
0.2000	0.04437	0.2000	0.04180	0.2001	-0.00636	0.2001	-0.00579
0.2950	0.04443	0.2950	0.04151	0.2994	-0.00764	0.2994	-0.00717
0.4016	0.04092	0.4016	0.03793	0.4004	-0.00803	0.4004	-0.00765
0.5002	0.03599	0.5002	0.03349	0.4999	-0.00772	0.4999	-0.00740
0.5963	0.03023	0.5963	0.02781	0.5994	-0.00678	0.5994	-0.00638
0.6997	0.02288	0.6997	0.02127	0.7005	-0.00550	0.7005	-0.00512
0.8014	0.01545	0.8014	0.01457	0.7992	-0.00398	0.7992	-0.00364
0.8988	0.00870	0.8988	0.00738	0.9002	-0.00203	0.9002	-0.00179
1.0000	0.00000	1.0000	0.00000	1.0000	0.00000	1.0000	0.00000
T=298.15K		T=333.15K		T=298.15K		T=333.15K	
0.0000	0.00000	0.0000	0.00000	0.0000	0.00000	0.0000	0.00000
0.1000	0.03651	0.1000	0.03358	0.0999	-0.00406	0.0999	-0.00333
0.2000	0.04407	0.2000	0.04081	0.2001	-0.00617	0.2001	-0.00561
0.2950	0.04385	0.2950	0.04066	0.2994	-0.00750	0.2994	-0.00707
0.4016	0.04027	0.4016	0.03728	0.4004	-0.00794	0.4004	-0.00757
0.5002	0.03552	0.5002	0.03289	0.4999	-0.00761	0.4999	-0.00733
0.5963	0.02960	0.5963	0.02762	0.5994	-0.00667	0.5994	-0.00628
0.6997	0.02259	0.6997	0.02098	0.7005	-0.00541	0.7005	-0.00501
0.8014	0.01532	0.8014	0.01442	0.7992	-0.00389	0.7992	-0.00353
0.8988	0.00846	0.8988	0.00721	0.9002	-0.00194	0.9002	-0.00170
1.0000	0.00000	1.0000	0.00000	1.0000	0.00000	1.0000	0.00000
T=303.15K		T=343.15K		T=303.15K		T=343.15K	
0.0000	0.00000	0.0000	0.00000	0.0000	0.00000	0.0000	0.00000

0.1000	0.03596	0.1000	0.03321	0.0999	-0.00388	0.0999	-0.00324
0.2000	0.04358	0.2000	0.04017	0.2001	-0.00604	0.2001	-0.00542
0.2950	0.04305	0.2950	0.03996	0.2994	-0.00737	0.2994	-0.00693
0.4016	0.03953	0.4016	0.03702	0.4004	-0.00787	0.4004	-0.00750
0.5002	0.03500	0.5002	0.03264	0.4999	-0.00755	0.4999	-0.00726
0.5963	0.02895	0.5963	0.02739	0.5994	-0.00657	0.5994	-0.00616
0.6997	0.02214	0.6997	0.02097	0.7005	-0.00530	0.7005	-0.00491
0.8014	0.01503	0.8014	0.01424	0.7992	-0.00373	0.7992	-0.00344
0.8988	0.00815	0.8988	0.00717	0.9002	-0.00190	0.9002	-0.00159
1.0000	0.00000	1.0000	0.00000	1.0000	0.00000	1.0000	0.00000
T=313.15K		T=353.15K		T=313.15K		T=353.15K	
0.0000	0.00000	0.0000	0.00000	0.0000	0.00000	0.0000	0.00000
0.1000	0.03479	0.1000	0.03284	0.0999	-0.00369	0.0999	-0.00311
0.2000	0.04264	0.2000	0.03942	0.2001	-0.00590	0.2001	-0.00528
0.2950	0.04209	0.2950	0.03930	0.2994	-0.00729	0.2994	-0.00688
0.4016	0.03856	0.4016	0.03680	0.4004	-0.00777	0.4004	-0.00743
0.5002	0.03409	0.5002	0.03236	0.4999	-0.00750	0.4999	-0.00716
0.5963	0.02835	0.5963	0.02720	0.5994	-0.00650	0.5994	-0.00602
0.6997	0.02173	0.6997	0.02097	0.7005	-0.00526	0.7005	-0.00478
0.8014	0.01480	0.8014	0.01431	0.7992	-0.00371	0.7992	-0.00337
0.8988	0.00781	0.8988	0.00726	0.9002	-0.00185	0.9002	-0.00153
1.0000	0.00000	1.0000	0.00000	1.0000	0.00000	1.0000	0.00000

Table F-3: Estimated Parameter and Standard Deviation of the Redlich-Kister Equation for Refractive Index Deviation Δn_D of systems involving [bheaa] for Temperature from (303.15 to 353.15) K.

T/K	A_0	A_1	A_2	A_3	A_4	A_5	σ
[bheaa] (1) - Water (2) System							
303.15	0.24388	-0.18375	0.14034	-0.21952	0.19073	-0.01957	2.46E-05
313.15	0.24285	-0.17848	0.14517	-0.23411	0.18785	-0.01269	1.33E-05
323.15	0.24283	-0.17595	0.13887	-0.24445	0.20620	-0.00620	5.26E-05
333.15	0.24309	-0.17367	0.14071	-0.24429	0.21968	-0.01247	1.28E-05
343.15	0.24434	-0.17474	0.12929	-0.23915	0.25649	-0.03555	5.74E-05
353.15	0.24572	-0.17334	0.13491	-0.25039	0.26547	-0.04263	0.000107
[bheaa] (1) - MEA (2) System							
303.15	0.03734	-0.01091	0.00663	-0.02534	0.01189	0.01926	1.20E-05
313.15	0.03776	-0.01338	0.00956	-0.01700	0.00876	0.00366	4.54E-06
323.15	0.03847	-0.01462	0.01408	-0.01710	-0.00096	0.00652	4.38E-05
333.15	0.04005	-0.01518	0.01361	-0.01231	0.00529	0.00034	2.65E-05
343.15	0.04172	-0.01463	0.01516	-0.02802	0.00043	0.02298	3.04E-05
353.15	0.04383	-0.01537	0.01816	-0.02920	-0.00251	0.02474	4.66E-05

Table F-4: Estimated Parameter and Standard Deviation of the Redlich-Kister Equation for Refractive Index Deviation Δn_D of systems involving [bmim][BF_4] for Temperature from (293.15 to 353.15) K.

T/K	A_0	A_1	A_2	A_3	A_4	σ
[bmim][BF4] (1) - Water (2) System						
293.15	0.14552	-0.10370	0.06169	-0.14089	0.16776	0.00024
298.25	0.14322	-0.10374	0.06229	-0.13704	0.16104	0.00025
303.15	0.13907	-0.10048	0.07145	-0.13957	0.14005	0.00037
313.15	0.13569	-0.09836	0.07897	-0.13617	0.12031	0.00024
323.15	0.13356	-0.09995	0.08247	-0.12791	0.10909	0.00024
333.15	0.13241	-0.09846	0.08338	-0.12658	0.10074	0.00023
343.15	0.13132	-0.08678	0.05445	-0.13778	0.14240	0.00041
353.15	0.12999	-0.08743	0.06194	-0.13359	0.12709	0.00038
[bmim][BF4] (1)- MEA (2) System						
293.15	-0.03083	0.01177	-0.00120	0.00453	-0.00831	6.36E-05
298.25	-0.03040	0.01171	-0.00087	0.00331	-0.00572	6.69E-05
303.15	-0.03015	0.01216	0.00126	0.00153	-0.00670	5.19E-05
313.15	-0.02988	0.01207	0.00094	0.00013	-0.00373	5.16E-05
323.15	-0.02937	0.01238	0.00063	-0.00152	-0.00147	5.04E-05
333.15	-0.02908	0.01267	0.00201	-0.00302	-0.00071	5.42E-05
343.15	-0.02878	0.01244	0.00389	-0.00299	-0.00155	7.73E-05
353.15	-0.02836	0.01312	0.00392	-0.00519	-0.00002	9.37E-05

Table F-5: Fitting Parameter of A_n (Table F-3) vs T (eq. 4.21) and Errors for the Correlation of Refractive Index Deviation Δn_D of systems involving [bheaa] for Temperature from (303.15 to 353.15) K.

	$\Delta\eta$			
	B_0	B_1	B_2	σ
	[bheaa] + Water system			
A_0	0.55944	-0.00197	3.06E-06	0.00011
A_1	-0.88525	0.00414	-6.03E-06	0.00075
A_2	-0.10995	0.00173	-2.95E-06	0.00376
A_3	1.42832	-0.00970	1.40E-05	0.00462
A_4	2.21759	-0.01391	2.38E-05	0.00688
A_5	-3.45019	0.02150	-3.36E-05	0.00455
	[bheaa] + MEA system			
A_0	0.23276	-0.00131	2.20E-06	0.00009
A_1	0.31354	-0.00193	2.82E-06	0.00042
A_2	-0.27827	0.00157	-2.06E-06	0.00104
A_3	-2.08703	0.01276	-1.96E-05	0.00358
A_4	0.47993	-0.00265	3.64E-06	0.00295
A_5	3.12057	-0.01922	2.96E-05	0.00545

Table F-6: Fitting Parameter of A_n (Table F-4) vs T (eq. 4.21) and Errors for the Correlation of Refractive Index Deviation Δn_D of systems involving [bmim][BF_4] for Temperature from (293.15 to 353.15) K.

	$\Delta\eta$				
	B_0	B_1	B_2	B_3	σ
	[bmim][BF_4] + Water system				
A_0	4.66627	-0.04019	0.00012	-1.18E-07	0.00040
A_1	-1.96261	0.01808	-0.00006	6.48E-08	0.00248
A_2	-13.1985	0.11583	-0.00033	3.19E-07	0.00643
A_3	2.19678	-0.02457	0.00008	-9.57E-08	0.00345
A_4	24.9002	-0.21480	0.00062	-5.89E-07	0.01012
	[bmim][BF_4] + MEA system				
A_0	-0.05930	0.00015	-1.67E-07	-	0.00008
A_1	0.01023	-0.00001	4.17E-08	-	0.00017
A_2	-0.00969	-0.00001	1.45E-07	-	0.00071
A_3	0.19341	-0.00106	1.40E-06	-	0.00047
A_4	-0.29269	0.00167	-2.39E-06	-	0.00077

Table F-7: Calculated Refractive Index Deviation Δn_D of [bheaa] + MEA + Water System at temperatures from (303.15 to 353.15) K.

T/ K		303.15	313.15	323.15	333.15	343.15	353.15
x_1	x_2						
				$z\ (x_1/\ x_3) = 0.11$			
0.0892	0.1003	0.06017	0.05962	0.05908	0.05851	0.05789	0.05740
0.0790	0.1999	0.05741	0.05683	0.05618	0.05567	0.05514	0.05461
0.0694	0.3002	0.05327	0.05267	0.05201	0.05150	0.05086	0.05042
0.0594	0.3999	0.04808	0.04745	0.04688	0.04617	0.04560	0.04506
0.0495	0.4997	0.04131	0.04075	0.04018	0.03947	0.03890	0.03838
0.0396	0.5997	0.03433	0.03378	0.03324	0.03251	0.03191	0.03134
0.0299	0.7000	0.02660	0.02598	0.02541	0.02472	0.02412	0.02359
0.0199	0.7994	0.01829	0.01777	0.01716	0.01654	0.01593	0.01532
0.0099	0.9007	0.00900	0.00838	0.00800	0.00730	0.00677	0.00616
				$z\ (x_1/\ x_3) = 0.62$			
0.3439	0.0998	0.06548	0.06500	0.06465	0.06455	0.06450	0.06445
0.3064	0.2001	0.05897	0.05859	0.05843	0.05829	0.05814	0.05801
0.2680	0.3000	0.05239	0.05221	0.05211	0.05196	0.05186	0.05180
0.2297	0.4001	0.04569	0.04552	0.04546	0.04533	0.04522	0.04517
0.1915	0.4993	0.03876	0.03856	0.03831	0.03816	0.03794	0.03787
0.1531	0.5999	0.03171	0.03146	0.03135	0.03125	0.03217	0.03211
0.1149	0.6998	0.02442	0.02422	0.02411	0.02399	0.02385	0.02374
0.0760	0.7948	0.01756	0.01739	0.01721	0.01711	0.01695	0.01684
0.0381	0.8974	0.00903	0.00889	0.00875	0.00860	0.00849	0.00842
				$z\ (x_1/\ x_3) = 4.03$			
0.7208	0.0995	0.02802	0.02827	0.02869	0.02904	0.02941	0.02974
0.6405	0.1999	0.02782	0.02820	0.02866	0.02900	0.02938	0.02962
0.5610	0.3001	0.02591	0.02627	0.02672	0.02712	0.02744	0.02771
0.4681	0.3895	0.02454	0.02492	0.02537	0.02572	0.02611	0.02640
0.3989	0.4977	0.02136	0.02176	0.02210	0.02245	0.02282	0.02313
0.3191	0.5972	0.01824	0.01864	0.01898	0.01930	0.01967	0.01998
0.2392	0.6966	0.01555	0.01599	0.01642	0.01672	0.01708	0.01742
0.1594	0.7968	0.01174	0.01223	0.01269	0.01299	0.01336	0.01372
0.0803	0.9011	0.00698	0.00747	0.00787	0.00821	0.00859	0.00889

Table F-8: Calculated Refractive Index Deviation Δn_D of [bmim][BF_4] + MEA + Water System at temperatures from (293.15 to 353.15) K.

T/K		293.15	298.15	303.15	313.15	323.15	333.15	343.15	353.15
x_1	x_2								
					$z\,(x_1/x_3) = 0.08$				
0.0664	0.0998	0.03690	0.03660	0.03627	0.03587	0.03552	0.03523	0.03489	0.03464
0.0592	0.2000	0.03947	0.03930	0.03899	0.03869	0.03840	0.03817	0.03787	0.03760
0.0523	0.3002	0.03951	0.03928	0.03903	0.03873	0.03847	0.03820	0.03787	0.03763
0.0444	0.3999	0.03835	0.03808	0.03786	0.03756	0.03723	0.03687	0.03654	0.03625
0.0359	0.4841	0.03598	0.03561	0.03530	0.03489	0.03452	0.03418	0.03384	0.03344
0.0296	0.5997	0.03037	0.02998	0.02972	0.02930	0.02885	0.02845	0.02805	0.02769
0.0218	0.6871	0.02514	0.02500	0.02466	0.02428	0.02386	0.02346	0.02307	0.02272
0.0148	0.8004	0.01747	0.01755	0.01727	0.01705	0.01674	0.01640	0.01602	0.01558
0.0079	0.8885	0.01058	0.01054	0.01028	0.01015	0.00996	0.00960	0.00922	0.00880
					$z\,(x_1/x_3) = 0.32$				
0.2155	0.1011	0.03934	0.03895	0.03859	0.03824	0.03788	0.03761	0.03730	0.03702
0.1943	0.2003	0.03838	0.03788	0.03752	0.03705	0.03661	0.03619	0.03586	0.03545
0.1701	0.3018	0.03475	0.03432	0.03387	0.03344	0.03299	0.03260	0.03212	0.03170
0.1453	0.3996	0.03071	0.03036	0.02978	0.02934	0.02888	0.02849	0.02803	0.02762
0.1206	0.4967	0.02674	0.02634	0.02587	0.02545	0.02501	0.02468	0.02426	0.02387
0.0972	0.6011	0.02176	0.02133	0.02087	0.02047	0.01999	0.01955	0.01912	0.01870
0.0729	0.6998	0.01706	0.01653	0.01612	0.01569	0.01529	0.01491	0.01451	0.01416
0.0486	0.7999	0.01199	0.01153	0.01122	0.01077	0.01042	0.01008	0.00968	0.00935
0.0245	0.9036	0.00618	0.00586	0.00548	0.00517	0.00497	0.00467	0.00431	0.00407
					$z\,(x_1/x_3) = 5.03$				
0.7478	0.0998	0.00997	0.00979	0.00963	0.00949	0.00935	0.00923	0.00911	0.00899
0.6677	0.2015	0.00755	0.00733	0.00709	0.00689	0.00671	0.00647	0.00627	0.00606
0.5679	0.2980	0.00536	0.00511	0.00483	0.00454	0.00435	0.00413	0.00389	0.00366
0.5009	0.3997	0.00128	0.00106	0.00085	0.00065	0.00045	0.00024	0.00006	-0.00013
0.4122	0.4957	-0.00084	-0.00100	-0.00118	-0.00132	-0.00146	-0.00164	-0.00178	-0.00195
0.3346	0.6004	-0.00232	-0.00248	-0.00263	-0.00276	-0.00291	-0.00308	-0.00319	-0.00335
0.2496	0.6969	-0.00262	-0.00277	-0.00294	-0.00308	-0.00320	-0.00334	-0.00345	-0.00358
0.1660	0.7954	-0.00216	-0.00230	-0.00248	-0.00257	-0.00272	-0.00287	-0.00295	-0.00307
0.0829	0.8983	-0.00127	-0.00140	-0.00152	-0.00162	-0.00171	-0.00181	-0.00191	-0.00198

Table F-9: Estimated Parameters and Standard Deviation of Cibulka Equation for Refractive Index Deviation Δn_D of [bheaa] + MEA + water system for Temperature from (303.15 to 353.15) K

T/ K	303.15	313.15	323.15	333.15	343.15	353.15
	[bheaa] + MEA + water system					
B_0	1.60041	1.59878	1.60133	1.60965	1.61948	1.62742
B_1	-0.51570	-0.49173	-0.46388	-0.43963	-0.43009	-0.41405
B_2	-1.06266	-1.08510	-1.11560	-1.14839	-1.16795	-1.19211
σ	0.01355	0.01324	0.01292	0.01266	0.01238	0.01216

Table F-10: Estimated Parameters and Standard Deviation of Cibulka Equation for Refractive Index Deviation Δn_D of [bmim][BF_4] + MEA + water system for Temperature from (293.15 to 353.15) K.

T/ K	293.15	298.15	303.15	313.15	323.15	333.15	343.15	353.15
	[bmim][BF_4] + MEA + water system							
B_0	-0.08057	-0.07460	-0.07051	-0.06747	-0.06453	-0.06352	-0.06281	-0.06132
B_1	-0.78411	-0.77477	-0.76382	-0.75274	-0.73810	-0.72719	-0.71357	-0.70261
B_2	0.90257	0.88692	0.87139	0.85674	0.83866	0.82616	0.81122	0.79822
σ	0.01532	0.01526	0.01521	0.01513	0.01505	0.01500	0.01493	0.01487